C5-1819/3111

CR 73068

STUDIES IN PREDICTOR DISPLAY TECHNIQUE

FINAL REPORT
UNDER CONTRACT NAS2-2166A

Autonetics A DIVISION OF NORTH AMERICAN AVIATION, INC., ANAHEIM, CALIFORNIA

9

STUDIES IN PREDICTOR DISPLAY TECHNIQUE

FINAL REPORT
UNDER CONTRACT NAS2-2166A

OCTOBER 1965

Prepared By:
J. S. Sweeney
N. C. Todd
E. C. Heaton
Display Systems Section

Approved By:

James S Sweeney

J. S. Sweeney
Chief
Display Systems Section

Autonetics, A DIVISION OF NORTH AMERICAN AVIATION, INC., ANAHEIM, CALIFORNIA

ABSTRACT

A series of studies were conducted at Autonetics, NAA covering the utility of the predictor display in: (1) manual control of altitude and (2) in monitoring the performance of an automatic flight control system in the pitch axis.

The effect of prediction time ahead of the aircraft in the pitch axis was examined by analytical and simulation study.

Results are presented indicating that while the predictor display is an effective means for monitoring AFCS flight and for manual flight control in the pitch axis, the mechanization complexity is a formidable barrier to practical realization of the concept. An alternate synthetic prediction system is discussed.

SUMMARY

The predictor display system concept proposes to use fast-time computation of vehicular future position in parallel with the real-time vehicular response to provide a vehicle operator with the information necessary for optimum vehicular control whether in manual or automatic flight control modes.

A series of studies were conducted to evaluate the effect of prediction time ahead of the vehicle on manual altitude control and automatic altitude control.

The analytical investigation indicated that for an assumed transfer function of $\frac{a}{Ts + 1}$ for the pilot, the system employed would be borderline stable for a 5-second prediction period due to the gain required of the human operator.

The simulation study conducted with pilots-in-the-loop supported this finding; the 5-second prediction period tended to instability unless the pilot supplied a lead term.

Simulation effort on monitoring performance for automatic flight control modes indicated that the predictor fast-time computation must include the dynamics of the automatic flight control system for optimum operation.

The basic principle of the system -- the provision of a parallel fast-time analog of the vehicle -- poses a monumental mechanization problem where complex vehicular dynamics exist. It appears doubtful that such a mechanization could be achieved. A synthetic prediction system was derived which depends solely on vehicular derivative measurement for generation of the prediction. Initial testing indicates quite satisfactory performance.

CONTENTS

CONTENTS (Cont)

ILLUSTRATIONS

ILLUSTRATIONS (Cont)

TABLES

I. INTRODUCTION

The fundamental concept of the predictor display involves the prediction of a future vehicular parameter (position, attitude, velocity, etc). The fundamental technique consists of developing a model of the vehicle of interest that will perform in the same way as the real vehicle but in a much shorter time period. The predictor display concept was advanced by Paynter and Ziebolz[1] and more recently by Kelley[2].

If the model space is carefully adjusted to represent the vehicular space, the motion of the model will represent the future condition of the vehicle assuming that the vehicle does not change path. Since vehicles tend to change path frequently, the model must provide a prediction of the outcome of the maneuver at frequent intervals. The required prediction frequency depends upon the rapidity of response of the vehicle (gain and bandwidth), the prediction range, and the vehicular disturbing functions (gusts, terrain, etc).

Kelley[2] has hypothesized that this display mode is an optimum means to allow a vehicular operator to evaluate the outcome of his control motions in terms of vehicular conditions; it would have the property of allowing the human operator considerable flexibility in adjusting vehicular condition relative to the environmental properties. In this way, maximum use could be made of the human operator's adaptive control properties.

The achievement of accurate stable manual control of a vehicle in a fluid medium is difficult to achieve. The current best technique employs the command steering or quickened displays in which the human is treated as a simple gain element. This technique relieves the operator of the necessity to provide lead prediction of the outcome of the control motion, at which the human operator is notoriously deficient. The conventional command steering system, however, precludes adaptive control by the human operator. The predictor display would, theoretically, overcome this deficiency and do so without disorienting the operator since the model space and the vehicle space are identical.

The predictor display would appear to be an excellent means of monitoring the performance of an automatic flight control system if the display could include the environmental elements upon which vehicle control is predicated.

The operator could view the future vehicular condition and initiate changes desired or necessary. Use of the display would eliminate the necessity to view and store the data on the dynamic vehicular status information displays and estimate the future condition.

Current automatic flight control systems are designed to be sluggish, so that the pilot can monitor the performance effectively. If a rapidly responding automatic system were employed, the pilot could not extract the information from the current instrument complex rapidly enough to maintain effective monitoring.

The condition then occurs that the pilot is imposing a performance limit upon the automatic flight control system due to his limited bandwidth in extracting information.

It has been postulated that the use of a predictor display could eliminate this condition and provide effective communication of the dynamic status of the flight control system relative to the vehicular environment.

The studies to be reported were undertaken to evaluate the utility of the predictor display in manual vehicular control and monitoring vehicular performance under full automatic control.

A. STUDY APPROACH

The study was conducted using simplified aircraft pitch axis equations of motion as the vehicle model.

A simplified analysis of the stability of the predictor display was conducted using a relatively simple transfer function term for the human operator.

A more complex analysis was then attempted using the complex equations of motion and incorporating the equations of a representative pitch axis, automatic flight control system, and stability augmentation system.

In parallel with the analytical approach, a simulation evaluation was conducted using simplified aircraft pitch axis equations of motion. The simulation was conducted on an analog computer in conjunction with a dynamic photoformer stimulus generator, and a pilot's control console. These efforts are described in succeeding sections of this report.

II. GENERAL DESCRIPTION OF A PREDICTOR DISPLAY SYSTEM

The general model of a predictor display generation system is shown in Figure II-1. The real time equations of motion are replicated with a gain change in the fast-time equation of motion. The fast-time derivative values must be alined with the real-time derivative values at the initiation of the prediction cycle.

The prediction interval is the time taken to generate the prediction. The prediction time span is the period for which vehicular motion is predicted. The predictor time span is dependent upon the forward gain of the fast-time loop and the prediction interval. The prediction interval is determined primarily by display memory properties.

The required forward gain of the fast-time element is related to the prediction time interval by:

$$V_{of} = V_{if} (G_{(s)}) \ (G_f) + V_{or}$$

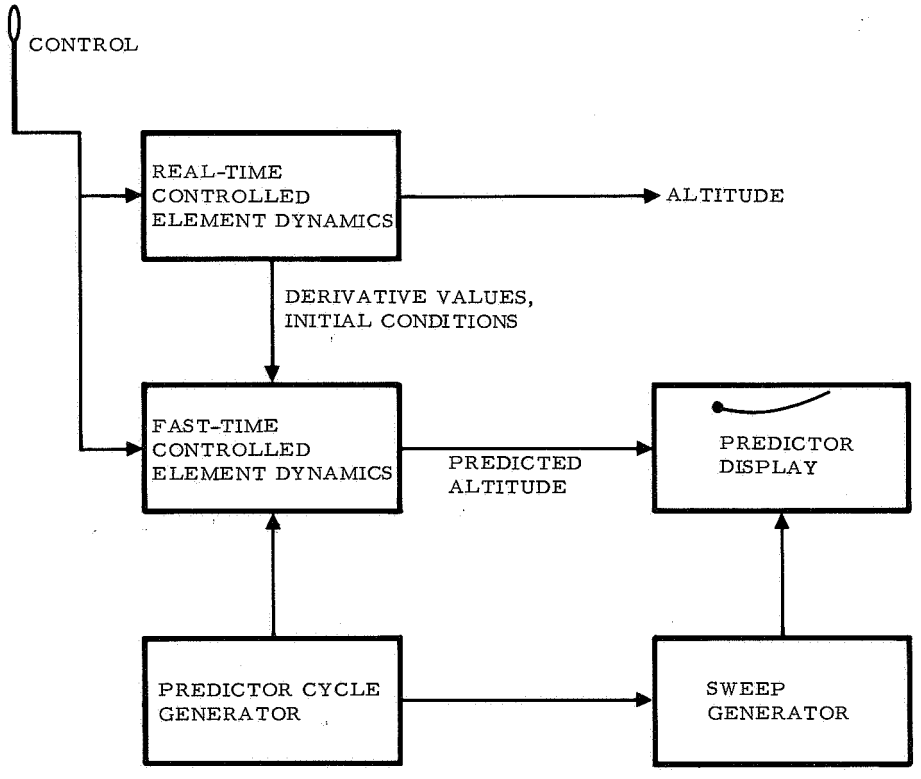

Figure II-1. Predictor Display Generation System Model

where

$$G_{(f)} = \frac{\text{Prediction}}{\text{Prediction Interval}} .$$

Thus, if it is desired that a prediction be made every 1/10 of a second of the value of a variable 10 seconds hence, the forward gain required is 10/0.1 = 100. A 20-second prediction would require a gain of 200 and so on.

Considering that these gains are cascaded, the fast-time analog loop for a third order equation would reach:

$$V_{of} = V_i \, (100 \, G_{(s)}1) \, (100 \, G_{(s)}2) \, (100 \, G_{(s)}3)$$

$$= 10^6 \, (G_{(s)}1) \, (G_{(s)}2) \, (G_{(s)}3)$$

for a 10-second prediction at 10 predictions per second.

A 20-second prediction would result in a gain factor of 8×10^6.

It is quite apparent that the straightforward application of the fast-time prediction would be restricted to those equations in which the real-time forward gain is extremely low.

Scaling the fast-time analog by reducing both the forward gain and the value of the initial conditions by a constant will reduce the value of the absolute gain (Figure II-2). It would appear, however, that scaling limits of the order of 10/1 reductions would be the useful limit, due to the contribution of computational noise.

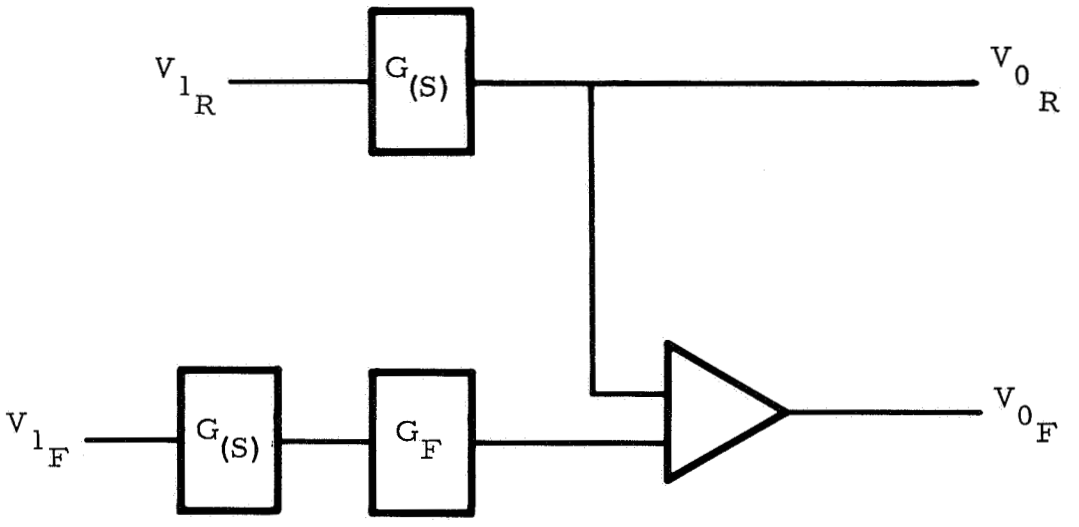

$$V_{0_F} = V_{1_F} (G_{(S)}) (G_F) + V_{0_R}$$

$G_{(S)}$ = DYNAMIC STAGE GAIN FROM REAL-TIME EQUATION

G_F = FAST-TIME GAIN MULTIPLIER

Figure II-2. Fast-Time Element Configuration

III. SIMPLIFIED ANALYTICAL STUDY OF PITCH AXIS PREDICTION

In order to analyze overall stability of aircraft response to an altitude change command originating from and being updated by a combination pilot and altitude prediction system, a simplified

$$\frac{B}{S^3}$$

open loop aircraft was assumed for verification of approach. The predictor model had a

$$\frac{B K^3}{S^3}$$

open loop characteristic; simulated pilot dynamics were represented by

$$\frac{A}{TS + 1} .$$

The predictor model gain constant K is a function of desired prediction time. A block diagram of the system is given in Figure III-4. It is readily seen that the predictor is initialized with the current values of the dynamic variables $\dot{\theta}$, θ, and H_o, at the beginning of each prediction period.

A. ANALYTICAL APPROACH

As indicated a closed loop modified Z transfer function

$$\left(\frac{H_o(Z)}{H_i(Z)} = F(Z) \right.$$

was derived for the system of Figure III-4 in which the pilot time constant was set at 0.5 seconds and the sampling period at 0.1 seconds.

The characteristic equation determined from this Z transfer function was used in a root locus stability analysis for each of three prediction times, 7.5, 10, and 20 seconds. The generalized gain constant AB appeared as a parameter in the root locus analysis.

After determination of the region of stability for each of the specified prediction times, two digital time response studies were made for the 20-second prediction case using gains of 0.003, and 0.0057. These gains were selected from the root locus plot to represent a stable system and a marginally stable system, respectively, for further interpretation of the root locus results.

After completion of the above efforts, a generalized predictor model was developed which could be adapted to, and used in conjunction with any specified aircraft having an autopilot and more complete system dynamics. This model incorporated predicted rate, position and altitude feedback, thereby presenting a more realistic output for pilot utilization.

B. ANALYTICAL METHODOLOGY

The following paragraphs demonstrate the development of the open loop system transfer function of the block diagram depicted in Figure III-4. This open loop transfer function was required to analytically evaluate the stability of the given system for a step input.

Although this development was begun in the S plane, anticipation of the ultimately required Z plane transformation prompted the immediate Z transformation of the numerator of the

$$\frac{1 - e^{Ts}}{S}$$

zero order hold to the equivalent hybrid expression

$$\frac{Z-1}{SZ} .$$

This accounts for the appearance of Z terms at the beginning of the development.

When the open loop transfer function had been determined symbolically in Equation (22) application of an appropriate set of S to Z transforms yields the desired Z transfer function. On the basis of this Z function, a general expression for the characteristic equation of the system was written

$$\frac{k_i \; AB \; (Z + Z_1) \; (Z - Z_2) \; (\dot{Z} - X \pm jY)}{Z \; (Z - 1)^3 \; (Z - .8187)} = -1$$

in which k_i is a gain factor depending upon the desired prediction time; A is the stick gain; and B is the velocity of the vehicle. This expression was used to determine root loci as a function of the gain AB for various prediction periods.

$$\delta = (H_i - H_d)^* \frac{Z - L}{Z} \frac{A}{S(TS + 1)} \tag{1}$$

$$\dot{\theta} = \delta \frac{1}{S} \tag{2}$$

$$\dot{\theta}' = \delta \frac{K}{S} \tag{3}$$

$$\theta = \dot{\theta} \frac{1}{S} \tag{4}$$

$$\theta' = \dot{\theta}' \frac{K}{S} + (\dot{\theta} - \dot{\theta}')^* \frac{Z - 1}{Z} \frac{K}{S^2} \tag{5}$$

$$H_o = \theta \frac{B}{S} \tag{6}$$

$$H' = \theta' \frac{BK}{S} + (\theta - \theta')^* \frac{Z - 1}{Z} \frac{BK}{S^2} \tag{7}$$

$$H_d = H' + (H_o - H')^* \frac{Z - 1}{Z} \frac{1}{S} \tag{8}$$

$$H_o = \delta \frac{B}{S^3} = (H_i - H_d)^* \frac{Z - 1}{Z} \frac{AB}{S^4(TS + 1)} \tag{9}$$

$$H_d = \theta' \frac{BK}{S} + (\theta - \theta') * \frac{Z-1}{Z} \frac{BK}{S^2} + \left[H_o - \theta' \frac{BK}{S} - (\theta - \theta') * \frac{Z-1}{Z} \frac{BK}{S^2}\right] * \frac{Z-1}{Z} \frac{1}{S}$$

$$= \dot{\theta}' \frac{BK^2}{S^2} + (\dot{\theta} - \dot{\theta}') * \frac{Z-1}{Z} \frac{BK^2}{S^3} + \left[\dot{\theta} \frac{1}{S} - \dot{\theta}' \frac{K}{S} - (\dot{\theta} - \dot{\theta}') * \frac{Z-1}{Z} \frac{K}{S^2}\right] * \frac{Z-1}{Z} \frac{BK}{S^2}$$

$$+ \left\{H_o - \dot{\theta}' \frac{BK^2}{S^2} - (\dot{\theta} - \dot{\theta}') * \frac{Z-1}{Z} \frac{BK^2}{S^3} - \left[\dot{\theta} \frac{1}{S} - \dot{\theta}' \frac{K}{S} - (\dot{\theta} - \dot{\theta}') * \frac{Z-1}{Z} \frac{K}{S^2}\right] * \right.$$

$$\left. \frac{Z-1}{Z} \frac{BK}{S^2}\right\} * \frac{Z-1}{Z} \frac{1}{S} \qquad (10)$$

$$H_d = \delta \frac{BK^3}{S^3} + (\delta \frac{1}{S} - \delta \frac{K}{S}) * \frac{Z-1}{Z} \frac{BK^2}{S^3} + \left[\delta \frac{1}{S^2} - \delta \frac{K^2}{S^2} - (\delta \frac{1}{S} - \delta \frac{K}{S}) * \frac{Z-1}{Z} \frac{K}{S^2}\right] * \frac{Z-1}{Z} \frac{BK}{S^2}$$

$$+ \left\{H_o - \delta \frac{BK^3}{S^3} - (\delta \frac{1}{S} - \delta \frac{K}{S}) * \frac{Z-1}{Z} \frac{BK^2}{S^3} - \left[\delta \frac{1}{S^2} - \delta \frac{K^2}{S^2} - \left(\delta \frac{1}{S} - \delta \frac{K}{S}\right) * \frac{Z-1}{Z} \frac{BK}{S^2}\right] * \frac{Z-1}{Z} \frac{BK}{S^2}\right\} * \frac{Z-1}{Z} \frac{1}{S}$$

$$H_d = (H_i - H_d) * \frac{Z-1}{Z} \frac{ABK^3}{S^4 (TS+1)} + \left[(H_i - H_d) * \frac{Z-1}{Z} \frac{AB(1-K)}{S^2 (TS+1)}\right] * \frac{Z-1}{Z} \frac{K^2}{S^3} + \left\{(H_i - H_d) * \right.$$

$$\left. \frac{Z-1}{Z} \frac{AB(1-K^2)}{S^3 (TS+1)}\right. \qquad (11)$$

$$- \left[(H_i - H_d)^* \frac{Z-1}{Z} \frac{AB}{S^2} \frac{(1-K)}{(TS+1)}\right]^* \frac{Z-1}{Z} \frac{K}{S^2} \Bigg]^* \frac{Z-1}{Z} \frac{K}{S^2} + \left(H_o - (H_i - H_d)^* \frac{Z-1}{Z} \frac{ABK^3}{S^{4(TS+1)}}\right.$$

$$- \left[(H_i-H_d)^* \frac{Z-1}{Z} \frac{AB(1-K)}{S^{2(TS+1)}}\right]^* \frac{Z-1}{Z} \frac{K^2}{S^3} - \left\{(H_i-H_d)^* \frac{Z-1}{Z} \frac{AB(1-K^2)}{S^{3(TS+1)}} - \left[(H_i-H_d)^* \frac{Z-1}{Z} \frac{AB(1-K)}{S^{2(TS+1)}}\right]^*\right.$$

$$\left.\left.\frac{Z-1}{Z} \frac{K}{S^2}\right] \frac{Z-1}{Z} \frac{K}{S^2}\right) \frac{Z-1}{Z} \frac{1}{S}\Bigg)$$

$$H_d = (H_i-H_d)^* \frac{Z-1}{Z} \left(\frac{ABK^3}{S^{4(TS+1)}} + \left[\frac{AB(1-K)}{S^{2(TS+1)}}\right]^* \frac{Z-1}{Z} \frac{K^2}{S^3} + \left\{\frac{AB(1-K^2)}{S^{3(TS+1)}} - \left[\frac{AB(1-K)}{S^{2(TS+1)}}\right]^* \frac{Z-1}{Z} \frac{K}{S^2}\right] \frac{Z-1}{Z} \frac{K}{S^2}\right.$$

$$+ \left[- \frac{ABK^3}{S^{4(TS+1)}} - \left(\frac{AB(1-K)}{S^{2(TS+1)}}\right)^* \frac{Z-1}{Z} \frac{K^2}{S^3} - \left\{\frac{AB(10K^2)}{S^{3(TS+1)}} - \left[\frac{AB(1-K)}{S^{2(TS+1)}}\right]^* \frac{Z-1}{Z} \frac{K}{S^2}\right\}^* \frac{Z-1}{Z} \frac{K}{S^2}\right]^* \frac{Z-1}{Z} \frac{1}{S}\Bigg)$$

$$+ H_o^* \frac{Z-1}{Z} \frac{1}{S}$$

(12)

$$H_o^* = (H_i-H_d)^* \frac{Z-1}{Z} \left[\frac{AB}{S^{4(TS+1)}}\right]^*$$

$$H_d^* = (H_i-H_d)^* \frac{Z-1}{Z} \left\{\left[\frac{ABK^3}{S^{4(TS+1)}}\right]^m + \left[\frac{AB(1-K)}{S^{2(TS+1)}}\right]^* \frac{Z-1}{Z} \left[\frac{K^2}{S^3}\right]^m + \left[\frac{AB(1-K^2)}{S^{3(TS+1)}}\right]^* \frac{Z-1}{Z} \left[\frac{K}{S^2}\right]^m\right.$$

(13)

$$- \left[\frac{AB(1-K)}{S^{2(TS+1)}}\right]^{*} \frac{Z-1}{Z}\left[\frac{K}{S^2}\right]^{*} \frac{Z-1}{Z}\left[\frac{K}{S^2}\right]^{m} - \left[\frac{ABK^3}{S^{4(TS+1)}}\right]^{*} \frac{Z-1}{Z}\left[\frac{1}{S}\right]^{m} - \left[\frac{AB(1-K)}{S^{2(TS+1)}}\right]^{*} \frac{Z-1}{Z}\left[\frac{K^2}{S^3}\right] \frac{Z-1}{Z}\left[\frac{1}{S}\right]^{m}$$

$$- \left[\frac{AB(1-K^2)}{S^{3(TS+1)}}\right]^{*} \frac{Z-1}{Z}\left[\frac{K}{S^2}\right]^{*} \frac{Z-1}{Z}\left[\frac{1}{S}\right]^{m} = \left[\frac{AB(1-K)}{S^{2(TS+1)}}\right]^{*} \frac{Z-1}{Z}\left[\frac{K}{S^2}\right]^{*} \frac{Z-1}{Z}\left[\frac{K}{S^2}\right]^{*} \frac{Z-1}{Z}\left[\frac{1}{S}\right]^{m}$$

$$+ H_o^{*} \frac{Z-1}{Z}\left[\frac{1}{S}\right]^{m} \tag{14}$$

where superscript * denotes normal Z transforms and superscript ^{m} denotes modified Z transforms with m - 1.

The above equations are of the form:

$$H_o^{*} = (H_i - H_d)^{*} P \tag{15}$$

$$H_d^{*} = (H_i - H_d)^{*} Q + H_o^{*} R \tag{16}$$

therefore

$$H_d^{*} = \frac{H_i H_i^{*} P - H_o^{*}}{P} = \frac{H_i^{*} Q + H_o^{*} R}{1 + Q} \tag{17}$$

and

$$H_o^* = \frac{P}{1 + Q + PR} H_i^* \tag{18}$$

where

$$P = \frac{Z - 1}{Z} \left[\frac{AB}{S^{4(TS+1)}}\right]^*$$

$$Q = \left[\frac{ABK^3}{S^{4(TS+1)}}\right]^m \frac{Z-1}{Z} - \left[\frac{ABK^3}{S^{4(TS+1)}}\right]^* \frac{(Z-1)^2}{Z^2} \left[\frac{1}{S}\right]^m + \left[\frac{AB}{S^{3(TS+1)}}\right]^* \left\{\frac{(1-K^2)(Z-1)^2}{Z^2} \left[\frac{K}{S^2}\right]^m \right.$$

$$\left. - \frac{(1-K^2)(Z-1)^3}{Z^3} \left[\frac{K}{S^2}\right]^* \left[\frac{1}{S}\right]^m \right\} + \left[\frac{AB}{S^{2(TS+1)}}\right]^* \left\{\frac{(1-K)(Z-1)^2}{Z^2} \left[\frac{K^2}{S^3}\right]^m \right.$$

$$\left. - \frac{(1-K)(Z-1)^3}{Z^3} \left[\frac{K}{S^2}\right]^* \left[\frac{K}{S^2}\right]^m - \frac{(1-K)(Z-1)^3}{Z^3} \left[\frac{K^2}{S^3}\right]^* \left[\frac{1}{S}\right]^m \right\} \tag{19}$$

$$+ \frac{(1-K)(Z-1)^4}{Z^4} \left[\frac{K}{S^2}\right]^* \left[\frac{K}{S^2}\right]^* \left[\frac{1}{S}\right]^m \Bigg\} \tag{20}$$

$$R = \frac{Z - 1}{Z} \left[\frac{1}{S}\right]^m \tag{21}$$

The open loop transfer function becomes

$$Q + PR = \left[\frac{ABK^3}{S^4(TS+1)}\right]^m \frac{Z-1}{Z} + \left[\frac{AB(1-K^3)}{S^4(TS+1)}\right] * \frac{(Z-1)^2}{Z^2} \left[\frac{1}{S}\right]^m$$

$$+ \left[\frac{AB(1-K^2)}{S^3(TS+1)}\right] * \frac{(Z-1)^2}{Z^2} \left\{ \left[\frac{K}{S^2}\right]^m - \frac{Z-1}{Z} \left[\frac{K}{S^2}\right] * \left[\frac{1}{S}\right]^m \right\}$$

$$+ \left[\frac{AB(1-K)}{S^2(TS+1)}\right] * \frac{(Z-1)^2}{Z^2} \left[\frac{K^2}{S^3}\right]^m - \frac{Z-1}{Z} \left[\frac{K}{S^2}\right] * \left[\frac{K}{S^2}\right]^m - \frac{Z-1}{Z} \left[\frac{K^2}{S^3}\right] * \left[\frac{1}{S}\right]^m$$

$$+ \frac{(Z-1)^2}{Z^2} \left[\frac{K}{S^2}\right] * \left[\frac{K}{S^2}\right] * \left[\frac{1}{S}\right]^m$$

(22)

After partial fraction expansion of Equation (23), application of the appropriate S to Z transform pairs found in "Digital and Sampled Data Control Systems," by Julius T. Tou, results in the open loop transfer function expressed in terms of Z, k, T, t, AB, and m, where T is the pilot time constant and t is the sampling period. Setting T = 0.5 seconds, t = 0.1 seconds, and m = 1, this expression may be simplified, factored, and set equal to -1, producing the characteristic equation given in Equation (24). The term k_i is determined by the desired prediction time. When a specific value of k_i is substituted into Equation (24), a root locus analysis can be made yielding the desired stability criterion.

C. RESULTS

The root locus plots for the 7.5; 10-and 20-second prediction times are presented in Figures III-1, III-2, III-3, respectively. As indicated in these plots, each case has a region for the gain constant AB in which stable operation (all poles lie within the unit circle) may be expected. All three plots also indicate instability for extremely small gains. It may also be noticed that higher gains are required for stable operation as the prediction time is decreased. On the basis of these figures, it may be concluded that stable operation may be achieved with the simplified system of Figure III-4, if the gains are maintained in the required region.

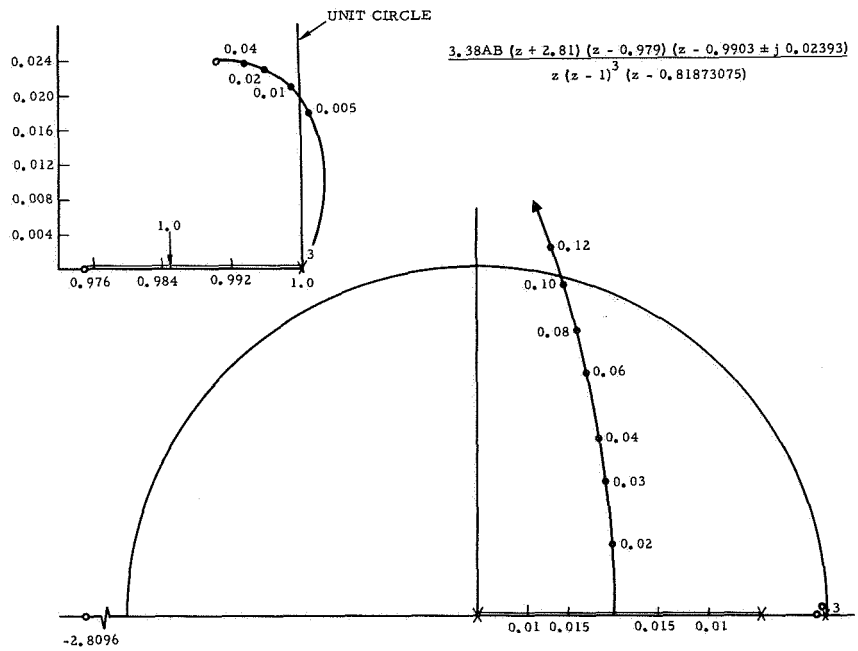

Figure III-1. Root Locus for 7.5-Second Prediction Time

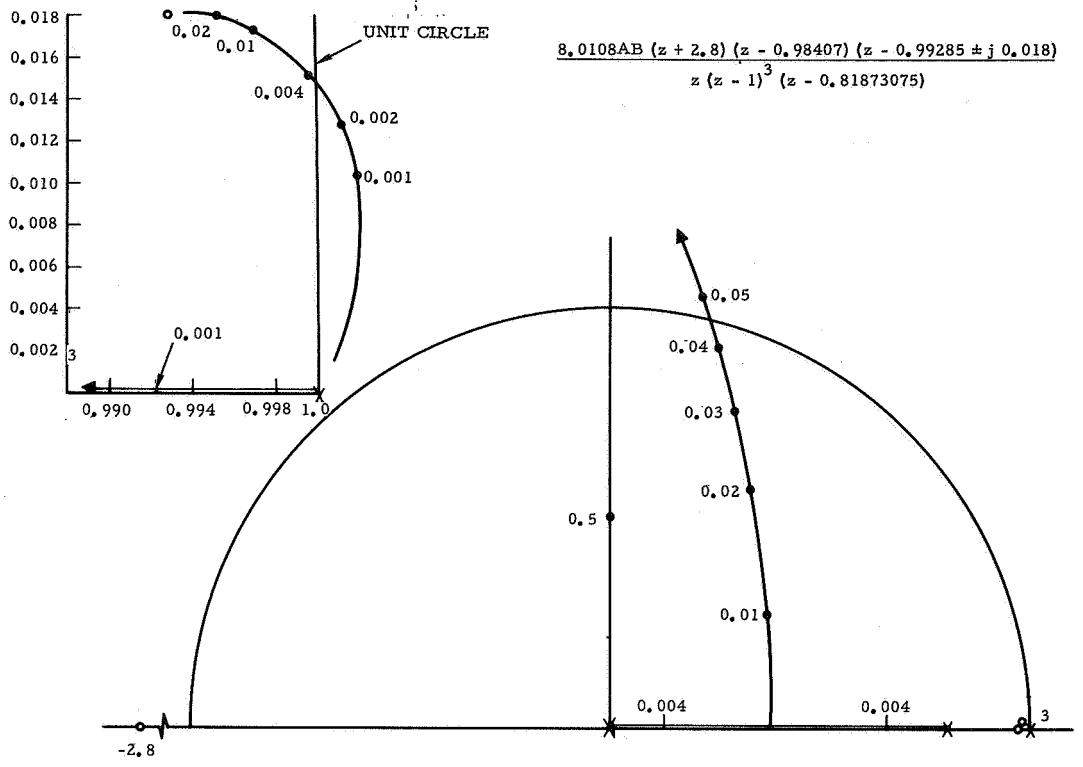

Figure III-2. Root Locus for 10-Second Prediction Time

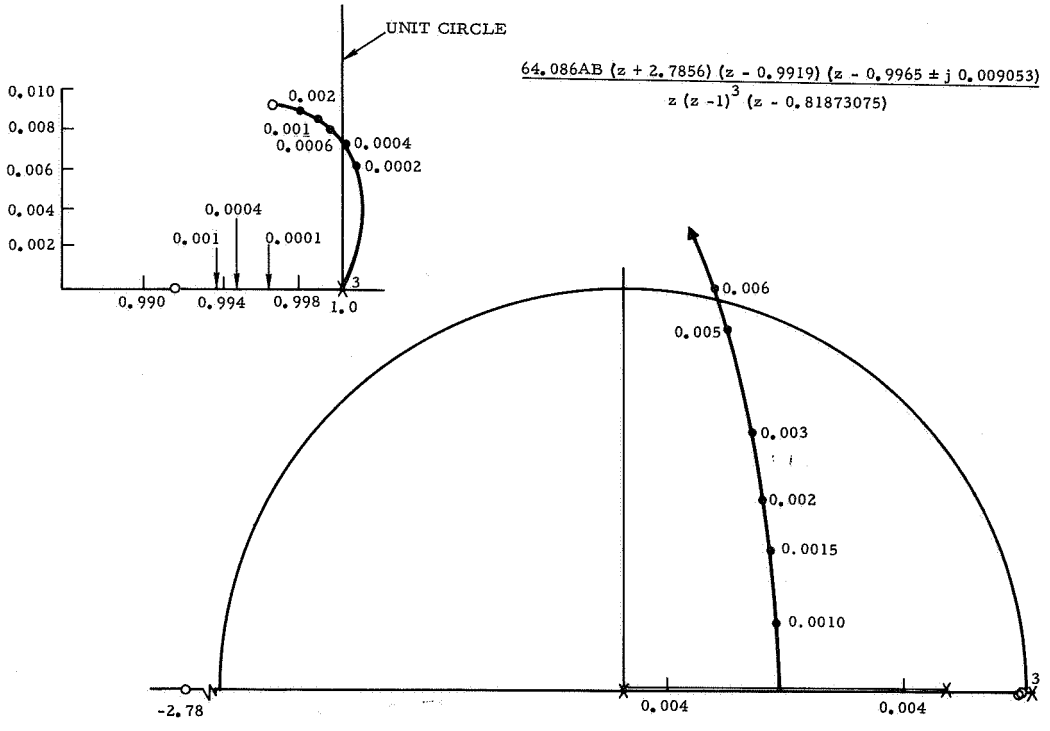

Figure III-3. Root Locus for 20-Second Prediction Time

A digital time response study was made of the 20-second prediction time case for gains AB of 0.003 and 0.0057, respectively. Examination of Figure III-3 indicates a gain of 0.003 should produce completely stable operation, while operation with a gain of 0.0057 should display marginal stability. Figures III-5 and III-6 present the results of the simulation study and verify the predictions based on the root locus plot. The results plotted in Figures III-5 and III-6 give the system response for a desired change of h/B feet. In Figure III-6, it may be noted from the frequency of the response that the three poles near Z = 1 are dominant during the first 100 plus seconds of change, and then the pair of complex poles just outside the unit circle dominate and cause a high frequency oscillation of increasing amplitude exhibiting instability.

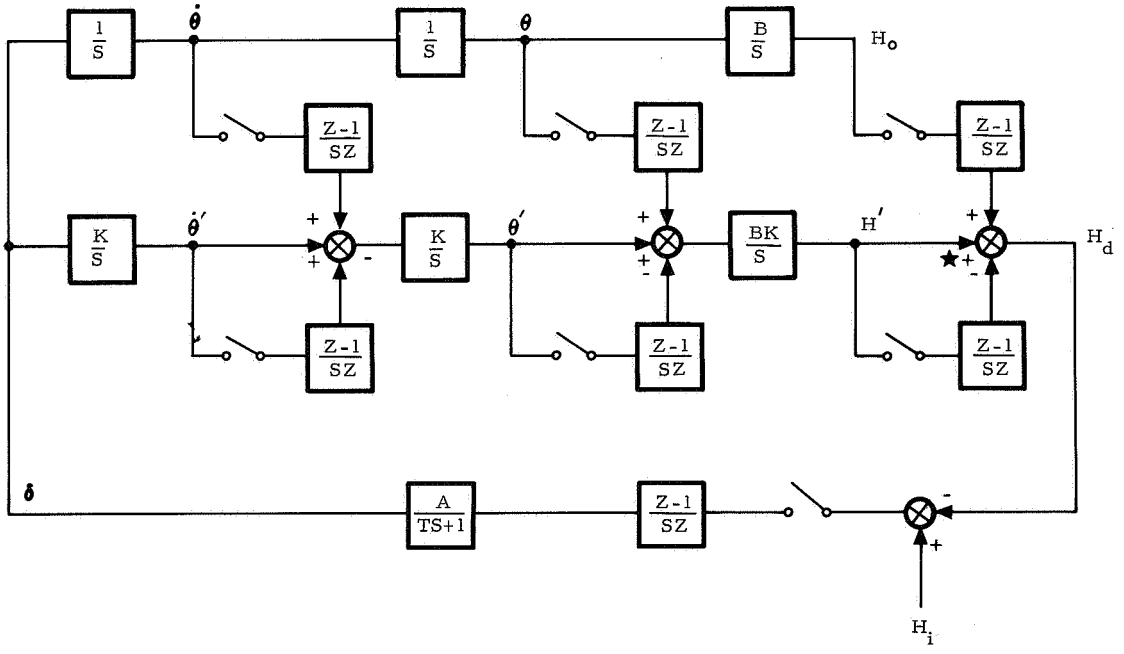

Figure III-4. Block Diagram of Simplified Systems with $\frac{BK^3}{S^3}$ Predicter Model

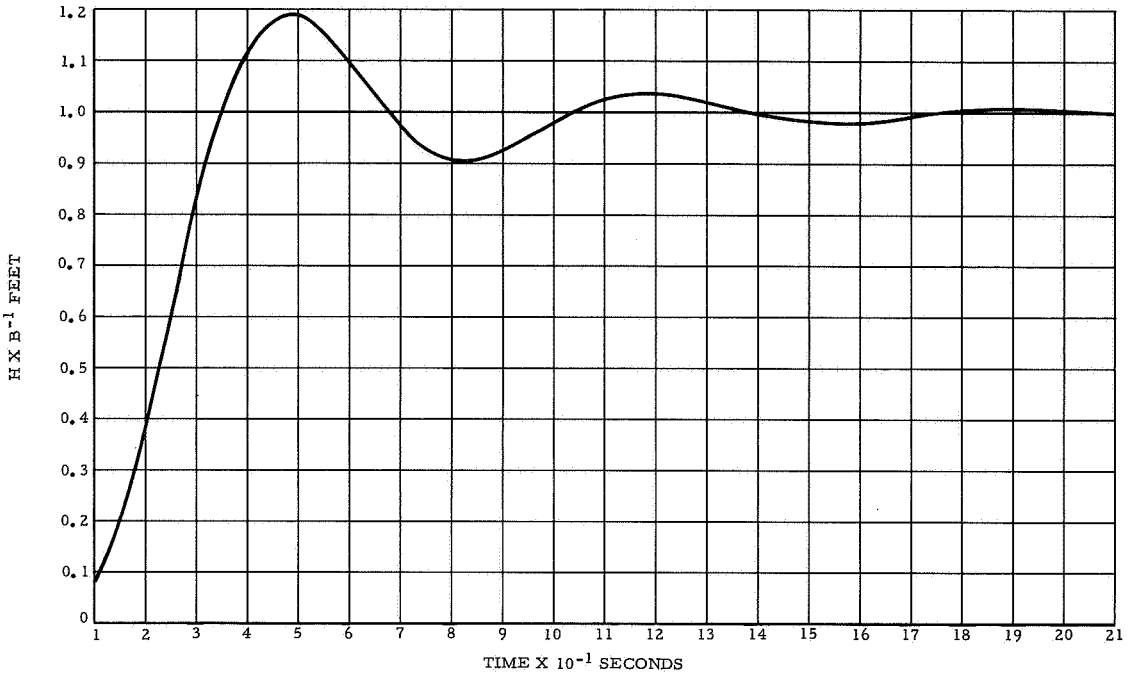

Figure III-5. Time Response for 20-Second Prediction Period - Gain AB = 0.003

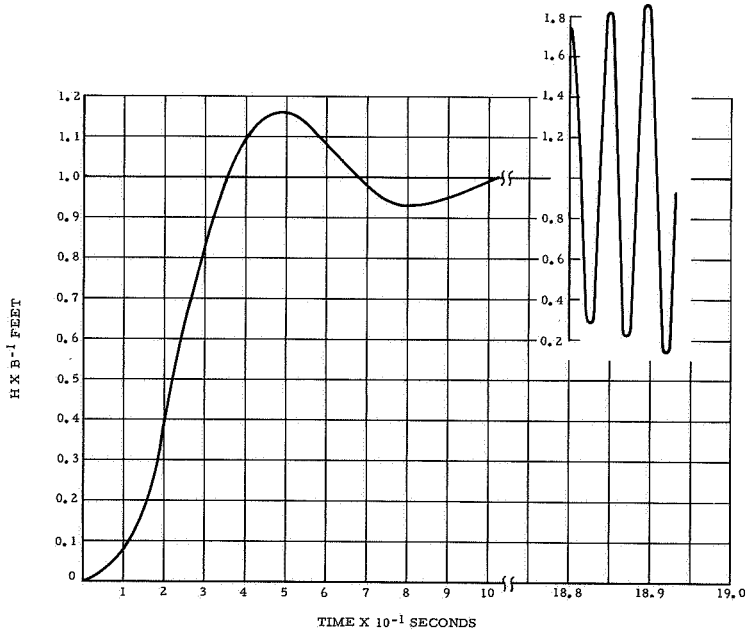

Figure III-6. Time Response for 20-Second Prediction Period - Gain AB = 0.0057

IV. COMPLEX ANALYTICAL STUDY OF PITCH AXIS PREDICTION

Having demonstrated the feasibility of mathematically determining the stability characteristics of a pilot-predictor altitude control system for a simulated B/S^3 open loop aircraft and a $P\alpha/S+\alpha$ simulated pilot characteristic, it was decided to attempt to apply the same technique for a stability analysis of an actual aircraft. Both analyses were constrained by the assumption of constant aircraft velocity and the linearizing assumption of small angles, angular rates, and no yaw or roll motion. These assumptions do not introduce appreciable error in the results for routine altitude changes of moderate performance aircraft.

A. ANALYTICAL APPROACH

The analysis was begun using the system block diagram of Figure IV-1. The symbols which may not be clear are defined as follows:

a = aircraft velocity in feet per second

M_{δ_e} = the moment stability parameter associated with elevator deflection

M_q = the moment stability parameter associated with pitch rate

$P(S)$ = pilot transfer function

$R(S)$ = elevator actuator-servo transfer functions

Inspection of Figure IV-1 shows the upper half of the figure to comprise a general block diagram for an aircraft including the basic elements for an altitude hold system, except for the altitude feedback loop. This loop has been removed as the pilot is to perform the altitude control function.

The middle section of Figure IV-1 comprises the general block diagram for the predictor model of the aircraft dynamics and control system. The predictor is initialized at each reset by the sensed or true aircraft variables. The effect of change in angle of attack has not been included in the predictor model as this variable is difficult to sense accurately, and the addition of this effect would make the already complex predictor model even more complex. Omission of the angle of attack effect in the predictor will increase slightly the required time for a given

altitude change, but will not affect the accuracy of the pilot-predictor control system.

The bottom loop in Figure IV-1 represents the predictor display and pilot response to the display signal.

In performing the stability analysis of the given system, a closed loop Z plane transfer function of the type $h(Z)/h_c(Z)$ must be obtained because of the reset mechanism in the predictor model and because the control function is of a discrete nature. In developing the desired transfer function, the approach was to keep all blocks completely general until such time as specific constants and transfer functions had to be inserted in order to continue the analysis.

The first and by far the most complex part of the analysis consisted in determining h'^* as a function of $(h_c^* - h'^*)$ and $[h]^m$ where $[\ ]^*$ refers to the Z transform and $[^c\ ]^m$ refers to the modified Z transform. Modified Z transformations were required since the term $(h_c^* - h'^*)$ was to reflect the difference between the predicted and commanded altitudes at the sampling instant. Because of the reset mechanism in the predictor resetting simultaneously with the error sampler, the use of ordinary Z transforms would have provided $(h_c^* - h^*)$ which information was not desired.

B. ANALYTICAL PROCEDURE

The open loop transfer function for h' may be written directly from Figure IV-1 and is seen to be

$$
\begin{aligned}
k' = h + \frac{\alpha K\theta}{S} - \left[\frac{\alpha K\theta}{S}\right]^* \frac{Z-1}{ZS} + \frac{\alpha K^2\dot{\theta}}{S^2} - \left[\frac{K\dot{\theta}}{S}\right]^* \frac{Z-1}{Z}\left(\frac{\alpha K}{S^2} - \left[\frac{\alpha K}{S^2}\right]^* \frac{Z-1}{ZS}\right) \\
- \left[\frac{K^2\theta}{S^2}\right]^* \frac{Z-1}{ZS} + \frac{\alpha K^3\delta m}{S^3} - \left[\frac{K^2\delta m}{S^2}\right]^* \frac{Z-1}{Z}\left(\frac{\alpha K}{S^2} - \left[\frac{\alpha K}{S^2}\right]^* \frac{Z-1}{ZS}\right) \\
- \left[\frac{\alpha K^3}{S^3}\delta m\right]^* \frac{Z-1}{ZS} + \left[\frac{K\delta m}{S}\right]^* \left(-\frac{(Z-1)}{Z}\frac{\alpha K^2}{S^3} + \frac{(Z-1)^2}{Z^2}\left[\frac{K}{S^2}\right]^* \frac{\alpha K}{S^2}\right. \\
\left. - \frac{(Z-1)^3}{Z^3}\left[\frac{K}{S^2}\right]^* \left[\frac{\alpha K}{S^2}\right]^* \frac{1}{S} + \frac{(Z-1)^2}{Z^2}\left[\frac{\alpha K^2}{S^3}\right]^* \frac{1}{S}\right) \qquad \text{(I-1)}
\end{aligned}
$$

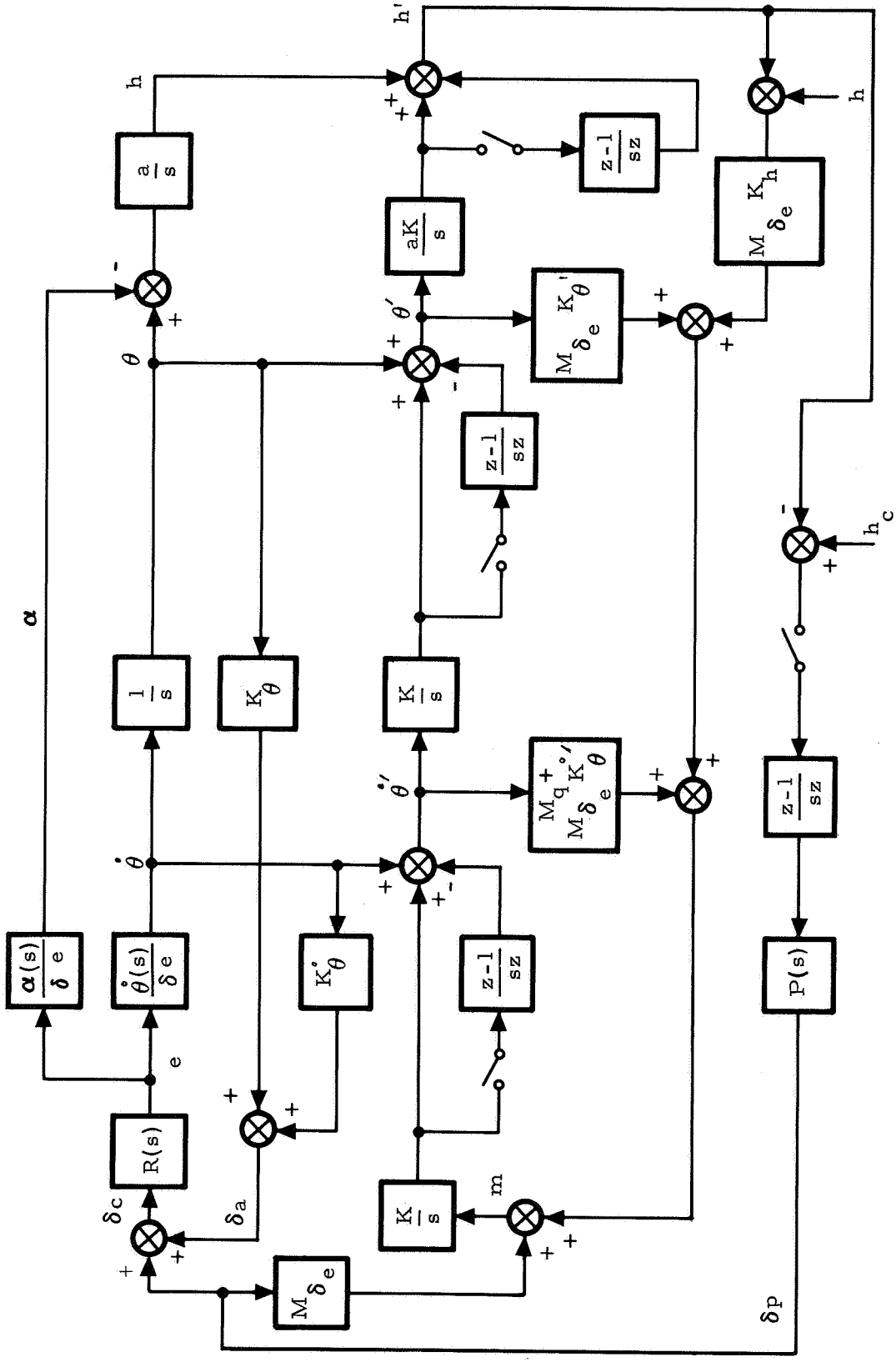

Figure IV-1. System Block Diagram

In Equation (I-1), h' is expressed in terms of the sensed aircraft variables, and δ_m, the error signal to the predictor system. As may be noted, δ_m which is a time varying quantity appears in several different Z-transformed terms as well as in an S plane function. Z-transforms can only be obtained when the functions to be transformed are known. Thus, the terms

$$\frac{\delta m}{S^3}, \quad \left[\frac{\delta m}{S^3}\right]^*, \quad \left[\frac{\delta m}{S^2}\right]^* \text{ and } \left[\frac{\delta m}{\delta}\right]^*$$

must be determined explicitly in terms of known or measurable quantities.

δ_m may be written in the form

$$\delta_m = b\delta p - A\dot{\theta}' - B\theta' - c(h - h') \qquad \text{(I-2)}$$

where

$$b = m_{\delta_e}$$

$$A = \left|m_q + M_{\delta_e} K\dot{\theta}\right|$$

$$B = \left|M_{\delta_e} K\theta\right|$$

$$C = \left|M_{\delta_e} Kh\right|$$

Elimination of $\dot{\theta}'$ and $\dot{\theta}$ in Equation (I-2) yields

$$\delta_m = b\delta p - B\theta - \frac{acK\theta}{S} + c\left[\frac{aK\theta}{S}\right]^* \frac{Z-1}{ZS} - A\dot{\theta} - \frac{BK\dot{\theta}}{S} - \frac{acK^2\theta}{S^2}$$

$$+ B\left[\frac{K\dot{\theta}}{S}\right]^* \frac{Z-1}{ZS} + c\left[\frac{K\dot{\theta}}{S}\right]^* \frac{Z-1}{Z}\left[\frac{aK}{S^2}\right] - \left[\frac{aK}{S^2}\right]^* \frac{Z-1}{ZS}\Bigg)$$

$$+ c\left[\frac{aK^2\dot{\theta}}{S^2}\right]^* \frac{Z-1}{ZS} - \frac{A\delta_m K}{S} - \frac{BK^2\delta_m}{S^2} - \frac{acK^3\delta_m}{S^3}$$

$$+ A\left[\frac{K\delta m}{S}\right]^* \frac{Z-1}{ZS} - B\left[\frac{K\delta m}{S}\right]^* \left(\frac{(Z-1)^2}{Z^2}\left[\frac{K}{S^2}\right]^* \frac{1}{S} - \frac{Z-1}{Z}\frac{K}{S^2}\right)$$

$$- c\left[\frac{K\delta m}{S}\right]^* \left(-\frac{(Z-1)}{Z}\frac{aK^2}{S^3} + \frac{(Z-1)^2}{Z^2}\left[\frac{K}{S^2}\right]^* \frac{aK}{S^2} - \frac{(Z-1)^3}{Z^3}\left[\frac{K}{S^2}\right]^* \left[\frac{aK}{S^2}\right]^* \frac{1}{S}\right.$$

$$+ \frac{(Z-1)^2}{Z^2}\left[\frac{aK^2}{S^3}\right]^* \frac{1}{S} + B\left[\frac{K^2\delta m}{S^2}\right]^* \frac{Z-1}{ZS} + c\left[\frac{K^2\delta m}{S^2}\right]^* \frac{Z-1}{Z}\left(\frac{aK}{S^2} - \left[\frac{aK}{S^2}\right]^* \frac{Z-1}{ZS}\right)$$

$$+ c\left[\frac{aK^3\delta m}{S^3}\right]^* \frac{Z-1}{ZS} \qquad \text{(I-3)}$$

Manipulation of Equation (I-3) gives

$$\frac{\delta m}{S^3} = \frac{b\delta p}{\$_6} - \frac{\$_4\theta}{\$S_6} + c\left[\frac{aK\theta}{\delta}\right]^* \frac{Z-1}{Z}\frac{1}{S\$_6} - \frac{\$_5\dot{\theta}}{S^2\$_6} + \left[\frac{K\dot{\theta}}{S}\right]^* \frac{Z-1}{Z}\frac{\$_4}{S^2\$_6}$$

$$- \left[\frac{K\dot{\theta}}{S}\right]^* \frac{(Z-1)^2}{Z^2}\left[\frac{aK}{S^2}\right]^* \frac{c}{S\$_6} + \left[\frac{aK^2\dot{\theta}}{S^2}\right]^* \frac{Z-1}{Z}\frac{c}{S\$_6} + \left[\frac{K\delta m}{S}\right] \frac{Z-1}{Z}\frac{\$^5}{S^3\$_6}$$

$$-\left[\frac{K\delta m}{S}\right]^* \frac{(Z-1)^2}{Z^2}\left[\frac{K}{S^2}\right]^* \frac{\$_4}{S^2\$_6} + \left[\frac{K\delta m}{S}\right]^* \frac{(Z-1)^3}{Z^3}\left[\frac{K}{S^2}\right]^* \left[\frac{aK}{S^2}\right]^* \frac{c}{S\$_6}$$

$$- \left[\frac{K\delta m}{S}\right]^* \frac{(Z-1)^2}{Z^2}\left[\frac{aK^2}{S^3}\right]^* \frac{c}{S\$_6} + \left[\frac{K^2\delta m}{S^2}\right]^* \frac{Z-1}{Z}\frac{\$_4}{S^2\$_6}$$

$$- \left[\frac{K^2\delta m}{S^2}\right]^* \frac{(Z-1)^2}{Z^2}\left[\frac{aK}{S^2}\right]^* \frac{c}{S\$_6} + \left[\frac{aK^3\delta m}{S^3}\right]^* \frac{Z-1}{Z}\frac{c}{S\$_6} \qquad (I-4)$$

where

$$\$_4 = BS + acK$$

$$\$_5 = AS^2 + BKS + acK^2$$

$$\$_6 = S^3 + AKS^2 + BK^2S + acK^3$$

The starred (z) transform of Equation (I-4) gives

$$\left[\frac{\delta_m}{S^3}\right]^* = Z_1\left[\frac{b\delta p}{\$_6}\right]^* - Z_1\left[\frac{\$_4\theta}{S\$_6}\right]^* + Z_1\left[\frac{K\theta}{S}\right]\frac{Z-1}{Z}\left[\frac{ac}{S\$_6}\right]^* - Z_1\left[\frac{\$_5\dot{\theta}}{S^2\$_6}\right]^*$$

$$+ Z_1\left[\frac{K\dot{\theta}}{S}\right]^*\frac{Z-1}{Z}\left[\frac{\$_4}{S^2\$_6}\right]^* - Z_1\left[\frac{K\dot{\theta}}{S}\right]^*\frac{(Z-1)^2}{Z^2}\left[\frac{K}{S^2}\right]^*\left[\frac{ac}{S\$_6}\right]^*$$

$$+ Z_1\left[\frac{K^2\dot{\theta}}{S^2}\right]^*\frac{Z-1}{Z}\left[\frac{ac}{S\$_6}\right]^* + Z_1\left[\frac{K\delta m}{S}\right]^*\frac{Z-1}{Z}\left[\frac{\$_5}{S^3\$_6}\right]^* - Z_1\left[\frac{K\delta m}{S}\right]^*\frac{(Z-1)^2}{Z^2}\left[\frac{K}{S^2}\right]^*$$

$$\left[\frac{\$_4}{S^2\$_6}\right]^* + Z_1\left[\frac{K\delta m}{S}\right]^*\frac{(Z-1)^3}{Z^3}\left[\frac{K}{S^2}\right]^*\left[\frac{K}{S^2}\right]^*\left[\frac{ac}{S\$_6}\right]^* - Z_1\left[\frac{K\delta m}{S}\right]^*\frac{(Z-1)^2}{Z^2}\left[\frac{K^2}{S^3}\right]^*$$

$$\left[\frac{ac}{S\$_6}\right]^* + Z_1\left[\frac{K^2\delta m}{S^2}\right]^*\frac{Z-1}{Z}\left[\frac{\$_4}{S^2\$_6}\right] - Z_1\left[\frac{K^2\delta m}{S^2}\right]\frac{(Z-1)^2}{Z^2}\left[\frac{K}{S^2}\right]^*\left[\frac{ac}{S\$_6}\right]^*$$

$$\text{with } Z_1 = \frac{1}{1 - \dfrac{Z-1}{Z}\left[\dfrac{acK^3}{S\$_6}\right]^*}$$

Equation (I-4) and (I-5) give δ_m/S^3 and $\left[\delta_m/S^3\right]^*$ in terms of sensed variables, known constants, and the remaining undetermined terms $\left[\delta_m/S^2\right]^*$ and $\left[\delta_m/S\right]^*$. The results of Equations (I-4) and (I-5) may be substituted into Equation (I-1) to give

$$h' = \frac{abK^3\delta_p}{\phi_6} + h + \left(\frac{aK}{S} - \frac{a\phi_4K^3}{S\phi_6}\right)\theta + \left[\frac{K\theta}{S}\right]^* \frac{Z-1}{Z}\left(\frac{a^2cK^3}{S\phi_6} - \frac{a}{S}\right)$$

$$+\left(\frac{aK^2}{S^2} - \frac{a\phi_5K^3}{S^2\phi_6}\right)\theta + \left[\frac{K\theta}{S}\right]^* \frac{Z-1}{Z}\left(\frac{aK^3\phi_4}{S^2\phi_6} - \frac{aK}{S^2}\right) + \left[\frac{K\theta}{S}\right]^* \frac{(Z-1)^2}{Z^2}\left[\frac{K}{S^2}\right]^*$$

$$\left(\frac{a}{S} - \frac{a^2cK^3}{S\phi_6}\right) + \left[\frac{K^2\theta}{S^2}\right]^* \frac{Z-1}{Z}\left(\frac{A^2cK^3}{S\phi_6} - \frac{a}{S}\right) + \left[\frac{K\delta_m}{S}\right]^* \frac{Z-1}{Z}\left(\frac{aK^3\phi_5}{S^3\phi_6} - \frac{aK^2}{S^3}\right)$$

$$+\left[\frac{K\delta_m}{S}\right]^* \frac{(Z-1)^2}{Z^2}\left[\frac{K}{S^2}\right]^*\left(\frac{aK}{S^2} - \frac{aK^3\phi_4}{S^2\phi_6}\right) + \left[\frac{K\delta_m}{S}\right]^* \frac{(Z-1)^3}{Z^3}\left[\frac{K}{S^2}\right]^*\left[\frac{K}{S^2}\right]^*$$

$$\left(\frac{a^2cK^3}{S\phi_6} - \frac{a}{S}\right) + \left[\frac{K\delta_m}{S}\right]^* \frac{(Z-1)^2}{Z^2}\left[\frac{K^2}{S^3}\right]^*\left(\frac{a}{S} - \frac{a^2cK^3}{S\phi_6}\right)$$

$$+\left[\frac{K^2\delta_m}{S^2}\right]^* \frac{Z-1}{Z}\left(\frac{aK^3\phi_4}{S^2\phi_6} - \frac{aK}{S^2}\right) + \left[\frac{K^2\delta_m}{S^2}\right]^* \frac{(Z-1)^2}{Z^2}\left[\frac{K}{S^2}\right]^*\left(\frac{a}{S} - \frac{a^2cK^3}{S\phi_6}\right)$$

$$+\left[\frac{\delta_p}{\$_6}\right]^* bK^3Z_1\ \frac{Z-1}{Z}\left(\frac{a^2cK^3}{S\$_6}-\frac{a}{S}\right)-\left[\frac{\$_4\theta}{S\$_6}\right]^* K^3Z_1\ \frac{Z-1}{Z}\left(\frac{a^2cK^3}{S\$_6}-\frac{a}{S}\right)$$

$$+\left[\frac{K\theta}{S}\right]^* \frac{(Z-1)^2}{Z^2}\left[\frac{acK^3}{S\$_6}\right]^* Z_1\left(\frac{a^2cK^3}{S\$_6}-\frac{a}{S}\right)-\left[\frac{\$_5\theta}{S^2\$_6}\right]^* K^3Z_1\ \frac{Z-1}{Z}\left(\frac{a^2cK^3}{S\$_6}-\frac{a}{S}\right)$$

$$+\left[\frac{K\theta}{S}\right]^* Z_1\ \frac{(Z-1)^2}{Z^2}\left[\frac{\$_4K^3}{S^2\$_6}\right]^*\left(\frac{a^2cK^3}{S\$_6}-\frac{a}{S}\right)-\left[\frac{K\theta}{S}\right]^* Z_1\ \frac{(Z-1)^3}{Z^3}\left[\frac{K}{S^2}\right]^*\left[\frac{acK^3}{S\$_6}\right]^*$$

$$\left(\frac{a^2cK^3}{S\$_6}-\frac{a}{S}\right)+\left[\frac{K^2\dot{\theta}}{S^2}\right]^* Z_1\ \frac{(Z-1)^2}{Z^2}\left[\frac{acK^3}{S\$_6}\right]^*\left(\frac{a^2cK^3}{S\$_6}-\frac{a}{S}\right)$$

$$+\left[\frac{K\delta_m}{S}\right]^* Z_1\ \frac{(Z-1)^2}{Z^2}\left[\frac{\$_5K^3}{S^3\$_6}\right]^*\left(\frac{a^2cK^3}{S\$_6}-\frac{a}{S}\right)-\left[\frac{K\delta_m}{S}\right]^* Z_1\ \frac{(Z-1)^3}{Z^3}\left[\frac{K}{S^2}\right]^*\left[\frac{\$_4K^3}{S^2\$_6}\right]^*$$

$$\left(\frac{a^2cK^3}{S\$_6}-\frac{a}{S}\right)+\left[\frac{K\delta_m}{S}\right]^* Z_1\ \frac{(Z-1)^4}{Z^4}\left[\frac{K}{S^2}\right]^*\left[\frac{K}{S^2}\right]^*\left[\frac{acK^3}{S\$_6}\right]^*\left(\frac{a^2cK^3}{S\$_6}-\frac{a}{S}\right)$$

$$-\left[\frac{K\delta_m}{S}\right]^* Z_1\ \frac{(Z-1)^3}{Z^3}\left[\frac{K^2}{S^3}\right]^*\left[\frac{acK^3}{S\$_6}\right]^*\left(\frac{a^2cK^3}{S\$_6}-\frac{a}{S}\right)+\left[\frac{K^2\delta_m}{S^2}\right]^* Z_1\ \frac{(Z-1)^2}{Z^2}$$

$$\left[\frac{\$_4K^3}{S^2\$_6}\right]^*\left(\frac{a^2cK^3}{S\$_6}-\frac{a}{S}\right)-\left[\frac{K^2\delta_m}{S^2}\right]^* Z_1\ \frac{(Z-1)^3}{Z^3}\left[\frac{K}{S^2}\right]^*\left[\frac{acK^3}{S\$_6}\right]^*\left(\frac{a^2cK^3}{S\$_6}-\frac{a}{S}\right)$$

(I-6)

Equation (I-4) may be differentiated and Z-transformed to symbolically produce $\left[\delta_m/S^2\right]^*$ in terms of sensed variables, known constants and $\left[\delta_m/S\right]^*$. A second differentiation of Equation (I-4) and the symbolic Z-transformation yields $\left[\delta_m/S\right]^*$. Both of these very complex terms are then appropriately substituted into Equation (I-6) to produce h' as a function of sensed variables, known constants and pilot input. h' then becomes

$$h' = \frac{abK^3\delta_p}{\$_6} + \left[\frac{S^2\delta_p}{\$_6}\right]^* \left[\frac{Z_3}{Z_2}\ bKX\left(\frac{aK^3\$_5}{S^3\$_6} - \frac{aK^2}{S^3}\right) + \frac{Z_3}{Z}\ bK^2X^2Y_2\left(\frac{aK}{S^2} - \frac{aK^3S_1}{S^2\$_6}\right)\right.$$

$$\left. + b\ \frac{Z_1Z_3Z_9}{Z}\left(\frac{a^2cK^3}{S\$_6} - \frac{a}{S}\right) + b\ Z_3Z_4K^2X\left(\frac{aK^3\$_4}{S^2\$_6} - \frac{aK}{S^2}\right) + b\ Z_1Z_3Z_4Z_{10}\left(\frac{a}{S} - \frac{a^2cK^3}{S\$_6}\right)\right]$$

$$+ \left[\frac{S\delta_p}{\$_6}\right]^* \left[b\ Z_3Z_5KX\left(\frac{aK^3\$_5}{S^3\$_6} - \frac{aK^2}{S^3}\right) + b\ Z_3Z_5X^2K^2Y_2\left(\frac{aK}{S^2} - \frac{aK^3\$_4}{S^2\$_6}\right)\right.$$

$$+ b\ Z_1Z_3Z_5Z_9\left(\frac{a^2cK^3}{S\$_6} - \frac{a}{S}\right) + b\frac{Z_2}{Z_1}\ K^2X\left(\frac{aK^3\$_4}{S^2\$_6} - \frac{aK}{S^2}\right) + b\ Z_2Z_{10}\left(\frac{a}{S} - \frac{a^2cK^3}{S\$_6}\right)$$

$$\left. + b\ Z_2Z_3Z_4Z_5K^2X\left(\frac{aK^3S_4}{S^2\$_6} - \frac{aK}{S^2}\right) + b\ Z_1Z_2Z_3Z_4Z_5Z_{10}\left(\frac{a}{S} - \frac{a^2cK^3}{S\$_6}\right)\right]$$

$$+ \left[\frac{\delta_p}{\$_6}\right]^* \left[bK^3XZ_1\left(\frac{a^2cK^3}{S\$_6} - \frac{a}{S}\right) + bZ_3Z_6KX\left(\frac{aK^3\$_5}{S^3\$_6} - \frac{aK^2}{S^3}\right) + bZ_3Z_6K^2X^2Y_2\left(\frac{aK}{S^2}\right.\right.$$

$$- \frac{aK^3\$_4}{S^2\$_6}\Bigg) + bZ_1Z_3Z_6Z_9\left(\frac{a^2cK^3}{S\$_6} - \frac{a}{S}\right) + bZ_2Z_7K^4X\left(\frac{aK^3S_4}{S^2\$_6} - \frac{aK}{S^2}\right)$$

$$+ bZ_1Z_2Z_7Z_{10}K^2\left(\frac{a}{S} - \frac{a^2cK^3}{S\$_6}\right) + bZ_2Z_3Z_4Z_6K^2X\left(\frac{aK^3}{S^2\$_6} - \frac{aK}{S^2}\right)$$

$$+ bZ_1Z_2Z_3Z_4Z_6Z_{10}\left(\frac{a}{S} - \frac{a^2cK^3}{S\$_6}\right) + h + \theta\left(\frac{aK}{S} - \frac{aK^3\$_4}{S\$_6}\right)$$

$$- \left[\frac{\$_4S_\theta}{\$_6}\right]^*\left[\frac{Z_3}{Z_5}KX\left(\frac{aK^3\$_5}{S^3\$_6} - \frac{aK^2}{S^3}\right) + \frac{Z_3}{Z_2}K^2X^2Y_2\left(\frac{aK}{S^2} - \frac{aK^3\$_4}{S^2\$_6}\right)\right.$$

$$\left. + \frac{Z_1Z_3Z_9}{Z_2}\left(\frac{a^2cK^3}{S\$_6} - \frac{a}{S}\right) + Z_3Z_4K^2X\left(\frac{aK^3\$_4}{S^2\$_6} - \frac{aK}{S^2}\right) + Z_1Z_3Z_4Z_{10}\left(\frac{a}{S} - \frac{a^2cK^3}{S\$_6}\right)\right]$$

$$- \left[\frac{\$_4\theta}{\$_6}\right]^*\left[Z_3Z_5KX\left(\frac{aK^3\$_5}{S^3\$_6} - \frac{aK^2}{S^3}\right) + Z_3Z_5K^2X^2Y_2\left(\frac{aK}{S^2} - \frac{aK^3\$_4}{S^2\$_6}\right)\right.$$

$$\left. + Z_1Z_3Z_5Z_9\left(\frac{a^2cK^3}{S\$_6} - \frac{a}{S}\right) + \frac{Z_2}{Z_1}K^2X\left(\frac{aK^3\$_4}{S^2\$_6} - \frac{aK}{S^2}\right) + Z_2Z_{10}\left(\frac{a}{S} - \frac{a^2cK^3}{S\$_6}\right)\right.$$

$$+ Z_2Z_3Z_4Z_5K^2X\left(\frac{aK^3\$_4}{S^2\$_6} - \frac{aK}{S^2}\right) + Z_1Z_2Z_3Z_4Z_5Z_{10}\left(\frac{a}{S} - \frac{a^2cK^3}{S\$_6}\right)\Bigg]$$

$$- \left[\frac{\$_4\theta}{S\$_6}\right]^* \Bigg[K^3XZ_1\left(\frac{a^2cK^3}{S\$_6} - \frac{a}{S}\right) + Z_3Z_6KX\left(\frac{aK^3\$_5}{S^3\$_6} - \frac{aK^2}{S^3}\right) + Z_3Z_6K^2X^2Y_2\left(\frac{aK}{S^2}$$

$$- \frac{aK^3\$_4}{S^2\$_6}\right) + Z_1Z_3Z_6Z_9\left(\frac{a^2cK^3}{S\$_6} - \frac{a}{S}\right) + Z_2Z_7K^4X\left(\frac{aK^3\$_4}{S^2\$_6} - \frac{aK}{S^2}\right) + Z_1Z_2Z_7Z_{10}K^2\left(\frac{a}{S}$$

$$- \frac{a^2cK^3}{S\$_6}\right) + Z_2Z_3Z_4Z_6K^2X\left(\frac{aK^3\$_4}{S^2\$_6} - \frac{aK}{S^2}\right) + Z_1Z_2Z_3Z_4Z_6Z_{10}\left(\frac{a}{S} - \frac{a^2cK^3}{S\$_6}\right)\Bigg]$$

$$+ \left[\frac{\theta}{S}\right]^* \Bigg[KXZ_1\left(\frac{a^2cK^3}{S\$_6} - \frac{a}{S}\right) + \frac{Z_3Z_6X}{K}\left(\frac{aK^3\$_5}{S^3\$_6} - \frac{aK^2}{S^3}\right) + Z_3Z_6X^2Y_2\left(\frac{aK}{S^2} - \frac{aK^3\$_4}{S^2\$_6}\right)$$

$$+ \frac{Z_1Z_3Z_6Z_9}{K^2}\left(\frac{a^2cK^3}{S\$_6} - \frac{a}{S}\right) + Z_2Z_7K^2X\left(\frac{aK^3\$_4}{S^2\$_6} - \frac{aK}{S^2} + Z_1Z_2Z_7Z_{10}\left(\frac{a}{S} - \frac{a^2cK^3}{S\$_6}\right)\right.$$

$$+ Z_2Z_3Z_4Z_6X\left(\frac{aK^3\$_4}{S^2\$_6} - \frac{aK}{S^2}\right) + \frac{Z_1Z_2Z_3Z_4Z_6Z_{10}}{K^2}\left(\frac{a}{S} - \frac{a^2cK^3}{S\$_6}\right) + \dot{\theta}\left(\frac{aK^2}{S^2} - \frac{aK^3\$_5}{S^2\$_6}\right)\Bigg]$$

$$- \left[\frac{\$_5\theta}{S\$_6}\right]^* \Bigg[Z_3Z_5KX\left(\frac{aK^3\$_5}{S^3\$_6} - \frac{aK^2}{S^3}\right) + Z_3Z_5K^2X^2Y_2\left(\frac{aK}{S^2} - \frac{aK^3\$_4}{S^2\$_6}\right)$$

$$+ Z_1Z_3Z_5Z_9\left(\frac{a^2cK^3}{S\$_6} - \frac{a}{S}\right) + \frac{Z_2}{Z_1}K^2X\left(\frac{aK^3\$_4}{S^2\$_6} - \frac{aK}{S^2}\right) + Z_2Z_{10}\left(\frac{a}{S} - \frac{a^2cK^3}{S\$_6}\right)$$

$$+ Z_2Z_3Z_4Z_5K^2X\left(\frac{aK^3\$_4}{S^2\$_6} - \frac{aK}{S^2}\right) + Z_1Z_2Z_3Z_4Z_5Z_{10}\left(\frac{a}{S} - \frac{a^2cK^3}{S\$_6}\right)\Bigg]$$

$$- \left[\frac{\$_5\dot{\theta}}{S^2\$_6}\right]^* \Bigg[K^3XZ_1\left(\frac{a^2cK^3}{S\$_6} - \frac{a}{S}\right) + Z_3Z_6KX\left(\frac{aK^3\$_5}{S^3\$_6} - \frac{aK^2}{S^3}\right) + Z_3Z_6K^2X^2Y_2\left(\frac{aK}{S^2} -$$

$$\frac{aK^3\$_4}{S^2\$_6}\right) + Z_1Z_3Z_6Z_9\left(\frac{a^2cK^3}{S\$_6} - \frac{a}{S}\right) + Z_2Z_7K^4X\left(\frac{aK^3\$_4}{S^2\$_6} - \frac{aK}{S^2}\right) + Z_1Z_2Z_7Z_{10}K^2\left(\frac{a}{S}\right.$$

$$\left. - \frac{a^2cK^3}{S\$_6}\right) + Z_2Z_3Z_4Z_6K^2X\left(\frac{aK^3\$_4}{S^2\$_6} - \frac{aK}{S^2}\right) + Z_1Z_2Z_3Z_4Z_6Z_{10}\left(\frac{a}{S} - \frac{a^2cK^3}{S\$_6}\right)\Bigg]$$

$$- \left[\frac{\$_5\dot{\theta}}{\$_6}\right]^* \Bigg[\frac{Z_3}{Z_2}KX\left(\frac{aK^3\$_5}{S^3\$_6} - \frac{aK^2}{S^3}\right) + \frac{Z_3}{Z_2}K^2X^2Y_2\left(\frac{aK}{S^2} - \frac{aK^3\$_4}{S^2\$_6}\right) + \frac{Z_1Z_3Z_9}{Z_2}\left(\frac{a^2cK^3}{S\$_6}\right.$$

$$\left. - \frac{a}{S}\right) + Z_3Z_4K^2X\left(\frac{aK^3\$_4}{S^2S_6} - \frac{aK}{S^2}\right) + Z_1Z_3Z_4Z_{10}\left(\frac{a}{S} - \frac{a^2cK^3}{S\$_6}\right) + \left[\frac{\dot{\theta}}{S}\right]^*\Bigg]\Bigg[KX\left(\frac{aK^3\$_4}{S^2\$_6}\right.$$

$$\left. - \frac{aK}{S^2}\right) + K^2X^2Y_2Z_1\left(\frac{a}{S} - \frac{a^2cK^3}{S\$_6}\right) - K^4X^2Y_6Z_1\left(\frac{a}{S} - \frac{a^2cK^3}{S\$_6}\right) + Z_3Z_5X\left(\frac{aK^3S_5}{S^3\$_6}\right.$$

$$\left. - \frac{aK^2}{S^3}\right) + Z_3Z_5KX^2Y_2\left(\frac{aK}{S^2} - \frac{aK^3\$_4}{S^2\$_6}\right) + \frac{Z_1Z_3Z_5Z_9}{K}\left(\frac{a^2cK^3}{S\$_6} - \frac{a}{S}\right) + Z_2Z_8K^2X\left(\frac{aK^3\$_4}{S^2\$_6}\right.$$

$$\left. - \frac{aK}{S^2}\right) + Z_1Z_2Z_8Z_{10}\left(\frac{a}{S} - \frac{a^2cK^3}{S\$_6}\right) + Z_2Z_3Z_4Z_5KX\left(\frac{aK^3\$_4}{S^2\$_6} - \frac{aK}{S^2}\right) + \frac{Z_1Z_2Z_3Z_4Z_5Z_{10}}{K}\left(\frac{a}{S}\right.$$

$$\left. - \frac{a^2cK^3}{S\$_6}\right)\Bigg] + \left[\frac{\dot{\theta}}{S^2}\right]^* \Bigg[K^2XZ_1\left(\frac{a^2cK^3}{S\$_6} - \frac{a}{S}\right) + Z_3Z_6X\left(\frac{aK^3\$_5}{S^3\$_6} - \frac{aK^2}{S^3}\right)$$

$$+ Z_3Z_6KX^2Y_2\left(\frac{aK}{S^2} - \frac{aK^3\$_4}{S^2\$_6}\right) + \frac{Z_1Z_3Z_6Z_9}{K}\left(\frac{a^2cK^3}{S\$_6} - \frac{a}{S}\right) + Z_2Z_7K^3X\left(\frac{aK^3\$_4}{S^2\$_6}\right.$$

$$\left. - \frac{aK}{S^2}\right) + Z_1Z_2Z_7Z_{10}K\left(\frac{a}{S} - \frac{a^2cK^3}{S\$_6}\right) + Z_2Z_3Z_4Z_6KX\left(\frac{aK^3\$_4}{S^2\$_4} - \frac{aK}{S^2}\right)$$

$$+ \frac{Z_1Z_2Z_3Z_4Z_6Z_{10}}{K}\left(\frac{a}{S} - \frac{a^2cK^3}{S\$_6}\right)\Bigg] \qquad \text{(I-7)}$$

where the following definitions have been used:

$$X = \left[\frac{Z-1}{Z}\right] \qquad Y_5 = \left[\frac{1}{\$_6}\right]^* \qquad Y_9 = \left[\frac{\$_4}{\$_6}\right]^*$$

$$Y_1 = \left[\frac{1}{S}\right]^* \qquad Y_6 = \left[\frac{S_4}{S^2\$_6}\right]^* \qquad Y_{10} = \left[\frac{\$_5}{S\$_6}\right]^*$$

$$Y_2 = \left[\frac{1}{S^2}\right]^* \qquad Y_7 = \left[\frac{1}{S\$_6}\right]^* \qquad Y_{11} = \left[\frac{\$_5}{S^2\$_6}\right]^*$$

$$Y_3 = \left[\frac{1}{S^3}\right]^* \qquad Y_8 = \left[\frac{S}{\$_6}\right]^* \qquad Y_{12} = \left[\frac{\$_5}{S^3\$_6}\right]^*$$

$$Y_4 = \left[\frac{S_4}{S\$_6}\right]^*$$

$$\frac{Z_2}{Z_1} = \frac{1 - acK^3XY_7}{1 - acK^3XY_7 - K^2XY_4 + acK^5X^2Y_9Y_7 + acK^3X^2Y_2Y_5 - acK^5X^2Y_5Y_6}$$

$$\frac{Z_3}{Z_2} = \frac{1 - acK^3XY_2 - K^2XY_4 + acK^5X^2Y_4Y_7 + acK^3X^2Y_2Y_5 - acK^5X^2Y_5Y_6}{1 - acK^3XY_7 - K^2XY_4 + acK^5X^2Y_4Y_7 + acK^3X^2Y_2Y_5 - acK^5X^2Y_5Y_6}$$

$$-KXY_{10} + acK^4X^2Y_7Y_{10} + K^3X^2Y_4Y_{10} - acK^6X^3Y_4Y_7Y_{10} - acK^4X^3Y_2Y_5Y_{10}$$

$$+ acK^6X^3Y_5Y_6Y_{10} - K^3X^2Y_9Y_{11} + acK^6X^3Y_7Y_9Y_{11} + acK^5X^3Y_3Y_5Y_9$$

$$- acK^6X^3Y_5Y_9Y_{12} + K^2X^2Y_2Y_9 - acK^5X^3Y_2Y_7Y_9 + acK^4X^3Y_2Y_8Y_{11}$$

$$-acK^6X^3Y_6Y_8Y_{11} - acK^3X^3Y_2Y_2Y_8 + acK^3X^2Y_3Y_8 - acK^5X^3Y_3Y_4Y_8$$

$$- acK^4X^2Y_8Y_{12} + acK^6X^3Y_4Y_8Y_{12} + acK^5X^3Y_2Y_6Y_8$$

$$Z_4 = KXY_{11} - acK^4X^2Y_7Y_{11} - K^2X^2Y_2Y_4 + acK^5X^3Y_2Y_4Y_7 + acK^3X^3Y_2Y_2Y_5 - acK^3X^2Y_3Y_5 + acK^4X^2Y_5Y_{12} - acK^5X^3Y_2Y_5Y_6$$

$$Z_5 = K^2XY_9 - acK^5X^2Y_7Y_9 - acK^3X^2Y_2Y_8 + acK^5X^2Y_6Y_8$$

$$Z_6 = acK^5X^2Y_5Y_9 + acK^3XY_8 - acK^5X^2Y_4Y_8$$

$$Z_7 = acKXY_5$$

$$Z_8 = KXY_4 - acK^4X^2Y_4Y_7 - acK^2X^2Y_2Y_5 + acK^4X^2Y_5Y_6$$

$$Z_9 = K^3X^3Y_2Y_2 - K^3X^2Y_3 - K^5X^3Y_2Y_6 + K^4X^2Y_{12}$$

$$Z_{10} = K^3X^2Y_2 - K^5X^2Y_6$$

Now using approximate transfer functions for the C-141 flying at 550 feet per second at sea level, and neglecting the effect of the elevator actuator-servo transfer function because of its relatively short time constant, specific values may be inserted for the sensed aircraft variables and constants. For this particular aircraft the following constants were used:

$M_{\delta_e} = -14.0$ $\qquad$ $K_\theta = 2.36$

$M_q = -3.0$ $\qquad$ $K_h = 0.01$

$K_{\dot{\theta}} = 0.465$

From these values, the constants A, B, and C may be determined.

$A = 3 + 6.5 = 9.5$

$B = 33$

$C = 0.14$

The following aircraft transfer functions are also used:

$$\frac{\alpha}{\delta_e}(S) = \frac{-0.2\,(S + 73)}{S^2 + 6S + 21}$$

$$\frac{\dot{\theta}}{\delta_e}(S) = \frac{-13.8\,(S + 1.81)}{S^2 + 6\,S + 21}$$

$$\frac{\theta}{\delta_p}(S) = \frac{-13.8\,(S + 1.81)}{S^3 + 12.42\,S^2 + 65.2\,S + 59}$$

$$\frac{h}{\delta_p} = \frac{110\,(S^2 + 4\,S - 125)}{S\,(S^3 + 12.42\,S^2 + 65.2\,S + 59)}$$

Additional functions appearing in later equations are defined by:

$$E_1' = -1/K$$

$$E_2' = -\frac{S + 9.5K}{K^2}$$

$$E_3' = -\frac{S^2 + 9.5\,KS + 33\,K^2}{77\,K^3}$$

$$E_5 = 110\,(S^2 + 4\,S - 125)$$

$$E_6 = -13.8\,(S + 1.81)$$

$$E_7 = \left[-13.8\,(S + 1.81)\right]\ \left[33\,S + 77K\right]$$

$$E_8 = \left[-13.8\,(S + 1.81)\right]\left[9.5\,S^2 + 33\,KS + 77\,K^2\right]$$

$$\$_6 = S^3 + 9.5K\,S^2 + 33\,K^2\,S + 77\,K^3$$

$$\$_7 = S^3 + 12.42\,S^2 + 65.2S + 59$$

$$\$_8 = (S^3 + 12.42\,S^2 + 65.2\,S + 59)(S^3 + 9.5K\,S^2 + 33K^2\,S + 77K^3)$$

From the preceding relationships, the following equations may be derived.

$$h^* = \left[\frac{E_S P(S)}{S^2 \$_7}\right]^* X\,(h_c - h'^*). \quad \left[\frac{\theta}{S}\right]^* = \left[\frac{\dot{\theta}}{S^2}\right]^* = \left[\frac{E_6 P(S)}{S^2 \$_7}\right]^* X\,(h_c^* - h'^*)$$

$$\left[\frac{\$_4\theta}{S\$_6}\right]^* = \left[\frac{E_7P(S)}{S^2\$_8}\right]^* X\,(h_c^* - h'^*) \qquad \left[\frac{\dot{\theta}}{S}\right]^* = \left[\frac{E_6P(S)}{S\$_7}\right]^* X\,(h_c^* - h'^*)$$

$$\left[\frac{\$_4 S\theta}{\$_6}\right]^* = \left[\frac{E_7P(S)}{\$_8}\right]^* X\,(h_c^* - h'^*)$$

$$\left[\frac{\$_4\theta}{\$_6}\right]^* = \left[\frac{E_7P(S)}{S\$_8}\right]^* X\,(h_c^* - h'^*)$$

$$\left[\frac{\$_5\dot{\theta}}{S^2\$_6}\right]^* = \left[\frac{E_8P(S)}{S^2\$_8}\right]^* X\,(h_c^* - h'^*)$$

$$\left[\frac{\$_5\dot{\theta}}{S\$_6}\right]^* = \left[\frac{E_8P(S)}{S\$_8}\right]^* X\,(h_c^* - h'^*)$$

$$\left[\frac{\$_5\dot{\theta}}{\$_6}\right]^* = \left[\frac{E_8P(S)}{\$_8}\right]^* X\,(h_c^* - h'^*)$$

Simplification of Equation (I-7), substitution of the above expressions where appropriate and taking the modified Z transform of the resulting expression, yields Equation (1) of the text as the resulting expression for h'*. Because of the length of that equation, it will not be repeated here.

Now it is time for the long and tedious process of substituting the appropriate expressions for the subscripted Z and y terms in order to simplify the expression for h'*. This is a very time consuming exercise and much care must be used to avoid error during the process.

After the above substitution and simplification, the expression for h'* becomes

$$
\begin{aligned}
h'^* = (h_c^* - h'^*) &\left[\left[\frac{E_3'}{\$_6}\right]^* - \left[\frac{E_3'}{\$_6}\right]^m\right] \left\{\left[\frac{S\,P(S)}{\$_6}\right]^* \left\{\frac{abK^3X}{Z_{11}}\left[\left[\frac{SE_2'}{\$_6}\right]^* \left[\frac{E_1'}{\$_6}\right]^* - \left[\frac{SE_1'}{\$_6}\right]^* \left[\frac{E_2'}{\$_6}\right]^*\right]\right\}\right. \\
&+ \left[\frac{P(S)}{\$_6}\right]^* \left\{\frac{abK^3X}{Z_{11}} \left[\left[\frac{S^2E_1'}{\$_6}\right]^* \left[\frac{E_2'}{\$_6}\right]^* - \left[\frac{\$_4}{\$_6}\right]^* \left[\frac{E_1'}{\$_6}\right]^*\right]\right\} \\
&+ \left[\frac{P(S)}{S\$_6}\right]^* \left\{\frac{abK^3X}{Z_{11}} \left[\left[\frac{SE_1'}{\$_6}\right]^* \left[\frac{\$_4}{\$_6}\right]^* - \left[\frac{S^2E_1'}{\$_6}\right]^* \left[\frac{SE_2'}{\$_6}\right]^*\right]\right\} - \left[\frac{E_7P(S)}{\$_8}\right]^* \left\{\frac{aK^3X}{Z_{11}}\right. \\
&\left.\left[\left[\frac{SE_2'}{\$_6}\right]^* \left[\frac{E_1'}{\$_6}\right]^* - \left[\frac{SE_1'}{\$_6}\right]^* \left[\frac{E_2'}{\$_6}\right]^*\right]\right\} - \left[\frac{E_7P(S)}{S^2\$_8}\right]^* \left\{\frac{aK^3X}{Z_{11}} \left[\left[\frac{SE_1'}{\$_6}\right]^* \left[\frac{\$_4}{\$_6}\right]^*\right.\right. \\
&\left.\left. - \left[\frac{S^2E_1'}{\$_6}\right]^* \left[\frac{SE_2'}{\$_6}\right]^*\right]\right\} + \left[\frac{E_6P(S)}{S^2\$_7}\right]^* \left\{\frac{aKX(1+K)}{Z_{11}} \left[\left[\frac{SE_1'}{\$_6}\right]^* \left[\frac{\$_4}{\$_6}\right]^* - \left[\frac{S^2E_1'}{\$_6}\right]^* \left[\frac{SE_2'}{\$_6}\right]^*\right]\right\} \\
&+ \left[\frac{E_6P(S)}{\$_9S}\right]^* \left\{\frac{aK^2X}{Z_{11}} \left[\left[\frac{S^2E_1}{\$_6}\right]^* \left[\frac{E_2'}{\$_{11}}\right]^* - \left[\frac{\$_4}{\$_6}\right]^* \left[\frac{E_1'}{\$_6}\right]^*\right]\right\} - \left[\frac{E_8P(S)}{S^2\$_8}\right]^* \left\{\frac{aK^3X}{Z_{11}}\right. \\
&\left.\left[\left[\frac{SE_1'}{\$_6}\right]^* \left[\frac{\$_4}{\$_6}\right]^* - \left[\frac{S^2E_1'}{\$_6}\right]^* \left[\frac{SE_2'}{\$_6}\right]^*\right]\right\} - \left[\frac{E_8P(S)}{S\$_8}\right]^* \left\{\frac{aK^3X}{Z_{11}} \left[\left[\frac{S^2E_1'}{\$_6}\right]^* \left[\frac{E_2'}{\$_6}\right]^*\right.\right. \\
&\left.\left. - \left[\frac{\$_4}{\$_6}\right]^* \left[\frac{E_1'}{\$_6}\right]^*\right]\right\} - \left[\frac{E_8P(S)}{\$_8}\right]^* \left\{\frac{ac^3X}{\$_{11}} \left[\left[\frac{SE_2'}{\$_6}\right]^* \left[\frac{E_1'}{\$_6}\right]^* - \left[\frac{SE_1'}{\$_6}\right]^* \left[\frac{E_2'}{\$_6}\right]^*\right]\right\} \\
&\left. - \left[\frac{E_7P(S)}{S\$_8}\right]^* \left\{\frac{aK^2X}{Z_{11}} \left[\left[\frac{S^2E_1'}{\$_6}\right]^* \left[\frac{E_2'}{\$_6}\right]^* - \left[\frac{\$_4}{\$_6}\right]^* \left[\frac{E_1'}{\$_6}\right]^*\right]\right\}\right\} + h^*
\end{aligned}
$$

(I-8)

where

$$Z_{11} = \left[\frac{S}{\$_6}\right]^* \left\{ \left[\frac{SE_2'}{\$_6}\right]^* \left[\frac{E_1'}{\$_6}\right]^* - \left[\frac{SE_1'}{\$_6}\right]^* \left[\frac{E_2'}{\$_6}\right]^* \right\}$$

$$+ \left[\frac{1}{\$_6}\right]^* \left\{ \left[\frac{S^2 E_1'}{\$_6}\right]^* \left[\frac{E_2'}{\$_6}\right]^* - \left[\frac{\$_1}{\$_6}\right]^* \left[\frac{E_1'}{\$_6}\right]^* \right\}$$

$$+ \left[\frac{E_3'}{\$_6}\right]^* \left\{ \left[\frac{SE_1'}{\$_6}\right]^* \left[\frac{\$_4}{\$_6}\right]^* - \left[\frac{S^2 E_1'}{\$_6}\right]^* \left[\frac{SE_2'}{\$_6}\right]^* \right\}$$

Examination of the common terms $\left[\left[\frac{E_3'}{\$_6}\right]^* - \left[\frac{E_3'}{\$_6}\right]^m\right]$

demonstrates it to have the constant value

$$-\frac{1}{acK^3} = -\frac{1}{77K^3} .$$

After substitution of this value into Equation (I-8), the remaining indicated Z-transformed expressions must be actually transformed and combined to produce an explicit value for h'^* in the form given in Equation (2) of the text:

$$h'^* = (h_c^* - h'^*)\, G(Z, 1) + h^* \qquad \text{(I-9)}$$

It may be readily seen from the number of Z transformations and combinations that must be made in Equation (I-8), that a high degree of precision must be used in order to obtain an accurate final expression for h'^*. As pointed out in the text, a small change in the coefficients of the number of the open loop transfer function $\frac{h(Z)}{h_c(Z)}$ could very easily change the location of the open loop zeros, and consequently, the region of stability indicated by the root locus analysis. When the general transfer function referred to above had been obtained, specific aircraft transfer functions and constants had to be obtained to proceed with the computation of the Z transformations. Typical transfer functions

for a C-141 flying at sea level at a velocity of 550 feet per second were used in the final transformations to replace the symbols θ, $\dot{\theta}$, η, etc., that had hitherto been used. After substitution, the transfer function had the form

$$
\begin{aligned}
h'^{*} = {} & (h_c^{*} - h'^{*}) \left\{ \left[\frac{SP(S)}{\$_6}\right]^{*} \left\{ abK^4X^2 \frac{Z_3}{Z_2} \left[\frac{E_1'}{\$_6}\right]^{*} + \left[abK^5X^2 Z_3Z_4 - abK^5X^3y_2 \frac{Z_3}{Z_2} \right] \left[\frac{E_2'}{\$_6}\right]^{*} \right.\right. \\
& \left.\left. + \left[a^2bcK^3X \left(\frac{Z_1Z_3Z_9}{Z_2} - Z_1Z_3Z_4Z_{10} \right) \right] \left[\frac{E_3'}{\$_6}\right]^{m} \right\} + \left[\frac{P(S)}{\$_6}\right]^{*} \left\{ abK^4X^2 Z_3Z_5 \left[\frac{E_1'}{\$_6}\right]^{*} \right. \\
& + \left[abK^5X^2 \left(\frac{Z_2}{Z_1} + Z_2Z_3Z_4Z_5 \right) - abK^5X^3 y_2Z_3Z_5 \right] \left[\frac{E_2'}{\$_6}\right]^{*} + \left[a^2bcK^3X (Z_1Z_3Z_5Z_9 \right. \\
& \left. \left. - Z_1Z_2Z_3Z_4Z_5Z_{10} - Z_2Z_{10}) \right] \left[\frac{E_3'}{\$_6}\right]^{m} \right\} + \left[\frac{P(S)}{S\$_6}\right]^{*} \left\{ abK^3X + abK^4X^2 Z_3Z_6 \left[\frac{E_1'}{\$_6}\right]^{*} \right. \\
& + \left[abK^5X^2 Z_2Z_3Z_4Z_6 + abK^7X^2 Z_2Z_7 - abK^5X^3 y_2Z_3Z_6 \right] \left[\frac{E_2'}{\$_6}\right]^{*} + \left[a^2bcK^3X (Z_1Z_3Z_6Z_9 \right. \\
& \left. \left. + K^3XZ_1 - K^2 Z_1Z_2Z_7Z_{10} - Z_1Z_2Z_3Z_4Z_6Z_{10}) \right] \left[\frac{E_3'}{\$_6}\right]^{m} \right\} - \left[\frac{E_7P(S)}{\$_8}\right]^{*} \left\{ aK^4X^2 \frac{Z_3}{Z_2} \left[\frac{E_1'}{\$_6}\right]^{*} \right. \\
& + \left[aK^5X^2 Z_3Z_4 - aK^5X^3 y_2 \frac{Z_3}{Z_2} \right] \left[\frac{E_2'}{\$_6}\right]^{*} + \left[a^2cK^3X \left(\frac{Z_1Z_3Z_9}{Z_2} - Z_1Z_3Z_4Z_{10} \right) \right] \left[\frac{E_3'}{\$_6}\right]^{m} \left. \right\} \\
& - \left[\frac{E_7P(S)}{S\$_8}\right]^{*} \left\{ aK^4X^2 Z_3Z_5 \left[\frac{E_1'}{\$_6}\right]^{*} + \left[aK^5X^2 \left(\frac{Z_2}{Z_1} + Z_2Z_3Z_4Z_5 \right) - aK^5X^3 y_2Z_3Z_5 \right] \left[\frac{E_2'}{\$_6}\right]^{*} \right.
\end{aligned}
$$

$$+\left[a^2cK^3X\left(Z_1Z_3Z_5Z_9 - Z_2Z_{10} - Z_1Z_2Z_3Z_4Z_5Z_{10}\right)\right]\left[\frac{E_3'}{\$_6}\right]^m\Bigg\} - \left[\frac{E_7P(S)}{S^2\$_8}\right]^*\Bigg\{aK^3X$$

$$+ aK^4X^2\,Z_3Z_6\left[\frac{E_1'}{\$_6}\right]^* + \left[aK^7X^2\,Z_2Z_7 + aK^5X^2\,Z_2Z_3Z_4Z_6 - aK^5X^3\,y_2Z_3Z_6\right]\left[\frac{E_2'}{\$_6}\right]^*$$

$$+\left[a^2cK^6X^2\,Z_1 + a^2cK^3X\left(Z_1Z_3Z_6Z_9 - Z_1Z_2Z_3Z_4Z_6Z_{10}\right) - a^2cK^5X\,Z_1Z_2Z_7Z_{10}\right]\left[\frac{E_3'}{\$_6}\right]^m\Bigg\}$$

$$+\left[\frac{E_6P(S)}{S^2\$_7}\right]^*\Bigg\{aKX\,(1+K) + \left[aK^2X^2\,Z_3Z_6\,(1+K)\right]\left[\frac{E_1'}{\$_6}\right]^* + \left[aK^5X^2\,Z_2Z_7\,(1+K)\right.$$

$$\left.+ aK^3X^2\,Z_2Z_3Z_4Z_6\,(1+K) - aK^3X^3\,Y_2Z_3Z_6\,(1+K)\right]\left[\frac{E_2'}{\$_6}\right]^* + \left[a^2cK^4X^2\,Z_{1(1+K)}\right.$$

$$\left.+ a^2cKX\,Z_1Z_3Z_6Z_9\,(1+K) - a^2cK^3X\,Z_1Z_2Z_7Z_{10}\,(1+K) - a^2cKX\,Z_1Z_2Z_3Z_4Z_6Z_{10}\,(1+K)\right]$$

$$\left[\frac{E_3'}{\$_6}\right]^m\Bigg\} - \left[\frac{E_8P(S)}{S^2\$_8}\right]^*\Bigg\{aK^3X + aK^4X^2\,Z_3Z_6\left[\frac{E_1'}{\$_6}\right]^* + \left[aK^7X^2\,Z_2Z_7 + aK^5X^2\,Z_2Z_3Z_4Z_6\right.$$

$$\left.- aK^5X^3\,Y_2Z_3Z_6\right]\left[\frac{E_2'}{\$_6}\right]^* + \left[a^2cK^3X\left(Z_1Z_3Z_6Z_9 - Z_1Z_2Z_3Z_4Z_6Z_{10}\right) + a^2cK^6X^2\,Z_1\right.$$

$$\left.- a^2cK^5\,Z_1Z_2Z_7Z_{10}\right]\left[\frac{E_3'}{\$_6}\right]^m\Bigg\} - \left[\frac{E_8P(S)}{S\$_8}\right]^*\Bigg\{aK^4X^2\,Z_3Z_5\left[\frac{E_1'}{\$_6}\right]^* + \left[aK^5X^2\left(\frac{Z_2}{Z_1}\right.\right.$$

$$\left.\left.+ Z_2Z_3Z_4Z_5\right) - aK^5X^3\,y_2Z_3Z_5\right]\left[\frac{E_2'}{\$_6}\right]^* + \left[a^2cK^3X\left(Z_1Z_3Z_5Z_9 - Z_1Z_2Z_3Z_4Z_5Z_{10} - Z_2Z_{10}\right)\right]$$

$$\left[\frac{E_3'}{\$_6}\right]^m\Bigg\} - \left[\frac{E_8P(S)}{\$_8}\right]^*\Bigg\{aK^4X^2\,\frac{Z_3}{Z_2}\left[\frac{E_1'}{\$_6}\right]^* + \left[aK^5X^2\,Z_3Z_4 - aK^5X^3\,y_2\,\frac{Z_3}{Z_2}\right]\left[\frac{E_2'}{\$_6}\right]^*$$

$$+\left[a^2cK^3X\left(\frac{Z_1Z_3Z_9}{Z_2} - Z_1Z_3Z_4Z_{10}\right)\right]\left[\frac{E_3'}{\$_6}\right]^m\Bigg\} + \left[\frac{E_6P(S)}{S\$_9}\right]^*\Bigg\{aK^3X^2\,Z_3Z_5\left[\frac{E_1'}{\$_6}\right]^*$$

$$+\left[aK^4X^2 - aK^4X^3\,y_2Z_3Z_5 + aK^5X^2\,Z_2Z_8 + aK^4X^2\,Z_2Z_3Z_4Z_5\right]\left[\frac{E_2'}{\$_6}\right]^*$$

$$+\left[a^2cK^7X^3\,Z_1\left[\frac{E_2'}{\$_6}\right]^* + a^3cK^2X\,Z_1Z_3Z_5Z_9 - a^2cK^3X\,Z_1Z_2Z_8Z_{10} - a^2cK^2X\,Z_1Z_2Z_3Z_4Z_5Z_{10}\right]$$

$$\left[\frac{E_3'}{\$_6}\right]^m\Bigg\}\Bigg\} + h^* \qquad (1)$$

where the subscripted Z's are not related to the complex variable Z. Equation (1) may be rewritten in the form

$$h'^* = (h_c^* - h'^*)\, G(Z, 1) + h^* \tag{2}$$

where G(Z, 1) includes all the terms in the brackets $\{\ \}$ in equation (1).

The open loop transfer function for h* may also be written as:

$$h^* = \left[\frac{E_5 P(S)}{S^2 \$_7}\right]^* X\,(h_c^* - h'^*) \tag{3}$$

where $\left[\frac{E_5 P(S)}{S^2 \$_7}\right]^*$ is the Z transform of the open loop transfer function for h. Combining and manipulating Equations (2) and (3) eliminate h'* yielding the desired closed loop transfer function

$$\frac{h^*}{h_c^*} = \frac{h(Z)}{h_c(Z)} = \frac{\left[\frac{E_5 P(S)}{S^2 \$_7}\right]}{1 + G(Z, 1) + \left[\frac{E_5 P(S)}{S^2 \$_7}\right]^* X} \tag{4}$$

The characteristic equation of the closed loop system is seen from Equation (4) to be

$$1 + G(Z, 1) + \left[\frac{E_5 P(S)}{S^2 \$_7}\right] X = 0 \tag{5}$$

from which the root locus analysis was made.

C. RESULTS

After making substitution of the proper values for the symbols in Equation (1) and using a sampling time of 0.1 seconds, a prediction

period of 10 seconds, and a pilot transfer function of the nature,

$$P(S) = \frac{-2P}{S+2} \tag{6}$$

where P is the combination pilot-stick gain, the necessary Z transformations were obtained to determine the values of

$$G(Z,\ 1) \text{ and } \left[\frac{E_5 P(S)}{S^2 \$_7}\right] \quad X \ .$$

The open loop transfer function was then determined to be

$$\frac{18.38\ P\,(Z + .039)(Z - .302 \pm j\ .283)(Z - 1.159 \pm j.540)}{Z\,(Z-1)\,(Z-.8937)(Z-\ .8187)\,(Z-.511 \pm j.249)} \tag{7}$$

The root locus is plotted in Figure IV-2.

Comparison of this root locus with the previously determined simplified version for a 10-second prediction period indicates a less stable system for the actual aircraft. This does not seem reasonable because of the stabilization built into the aircraft dynamics and because of the stability augmentation outer loops included both in the aircraft control system and the predictor model. This tendency to instability stems from the pair of complex zeros in the open loop transfer function.

These results are only tentative because there was insufficient time to calculate root loci for more than one prediction period or to do a computer simulation for the prediction period which was studied. In addition, determination of accurate Z transformations of complex S plane functions require a high degree of precision in the computation, particularly in a case such as this where many such transforms had to be combined sometimes resulting in small differences of large numbers. A slight change in the numerator coefficients of the open loop transfer function could conceivably change the position of the open loop zeros to produce a very different region of stability.

$$\frac{18.38p\ (z + 0.039)\ (z - 0.302 \pm j\ 0.283)\ (z - 1.159 \pm j\ 0.540)}{z\ (z - 1)\ (z - 0.8937)\ (z - 0.8187)\ (z - 0.511 \pm j\ 0.249)}$$

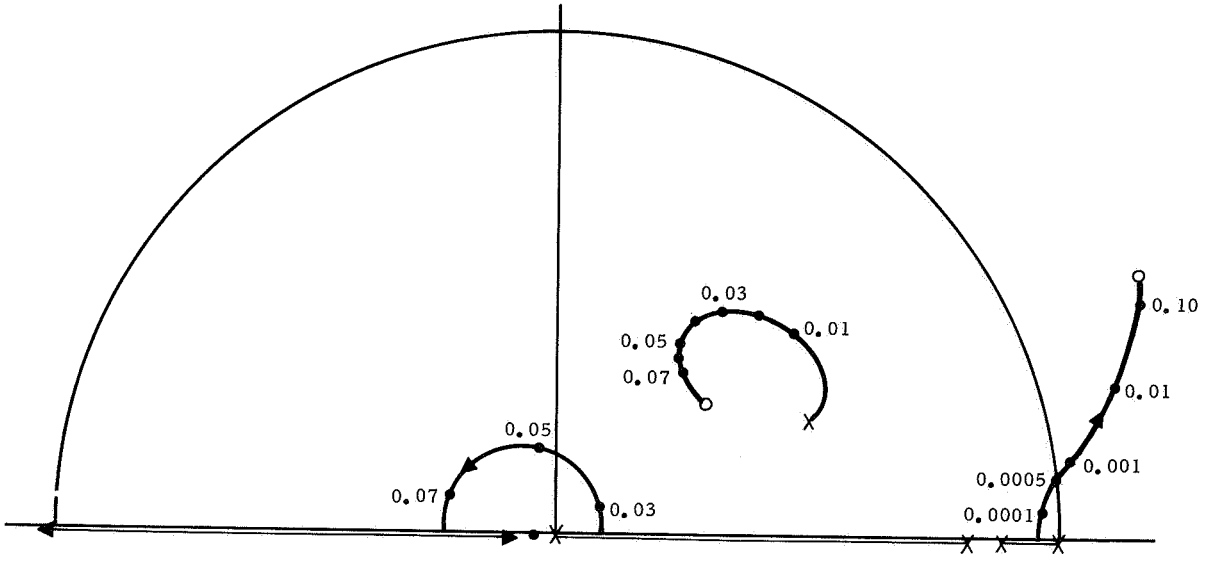

Figure IV-2. Root Locus for 10-Second Prediction Period

V. SIMULATION STUDY OF PITCH AXIS MANUAL CONTROL USING PREDICTOR DISPLAY CONFIGURATIONS

A. INTRODUCTION

A general simplified pitch axis analog computer simulation was developed to evaluate the applicability of the analytical results and to develop predictor display technique in general.

The basic elements of the simulation consist of:

1. AD 64 Analog Computer, programmed to provide:
    a. Real-time pitch axis equations of motion
    b. Fast-time equations of motion
    c. Automatic flight control equations of motion
    d. Stability augmentation equations of motion
    e. Predictor display timing and sweep generation functions
    f. Altitude error measurement
2. Dynamic Photoformer — generates terrain, flight path profile, etc.
3. Aircraft Display Console:
    a. Predictor display
    b Radar altitude
    c. Rate of climb
    d. Pitch attitude (roll, bank and turn displays were in place but not driven)
    e. Flight control stick
4. Experimenter's Console
5. Recording Equipment

B. COMPUTER PROGRAM

1. Real- and Fast-Time Equations of Motion

The real- and fast-time equations of motion are shown in block diagram form in Figure V-1 and in computer mechanization form in Figure V-2.

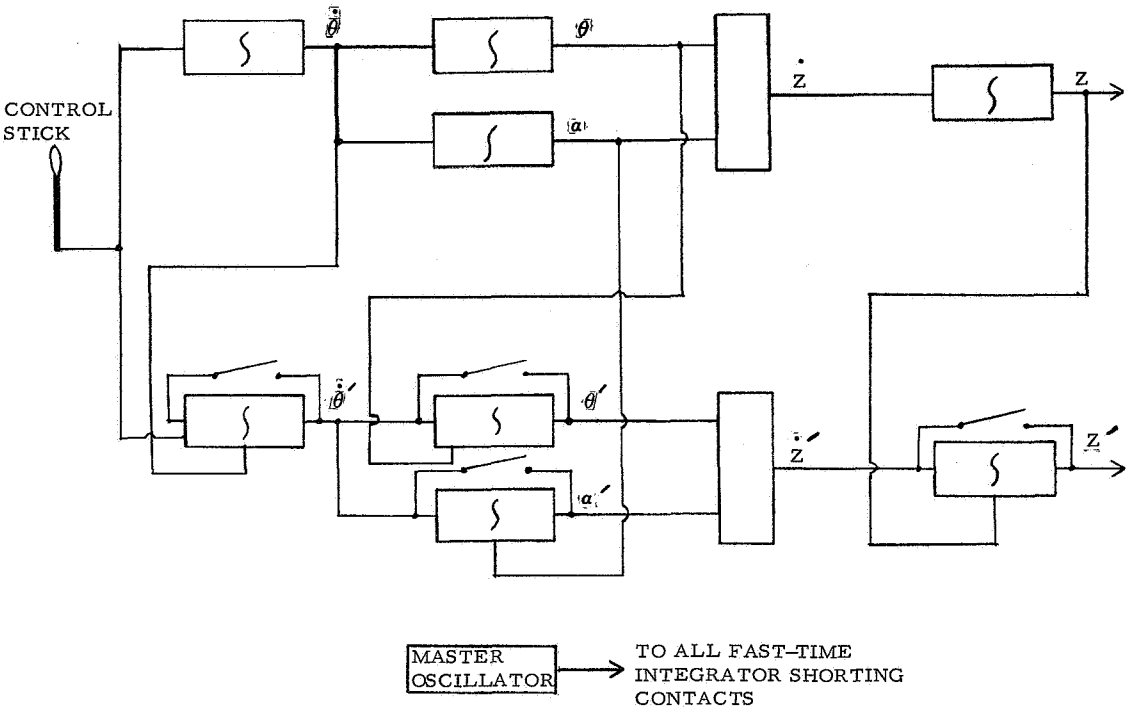

Figure V-1. Simplified Block Diagram, Real- and Fast-Time Equations of Motion

The real-time equation is generated straightforwardly to obtain Z, $\dot{Z}$, θ, $\dot{\theta}$ and α, a function of elevator position (stick position).

The notation is given in Table V-1 and the equation coeficients in Table V-2.

The fast-time equation is generated similarly but each integrator is shorted by a dry reed relay driven by the predictor timing generator.

When the timing generator recycles, the integrator is driven to the zero condition. The output of each fast-time section in the reset condition is the value of the real time derivative, Figure V-3.

Since each of the fast-time sections is cascaded (Figure V-3), the only output of the fast-time section during reset and at the initiation of the computing cycle is the altitude term.

During the fast-time computing epoch, the value of the fast-time derivatives changes dynamically to provide the altitude profile for the predictor time span (Figure V-4).

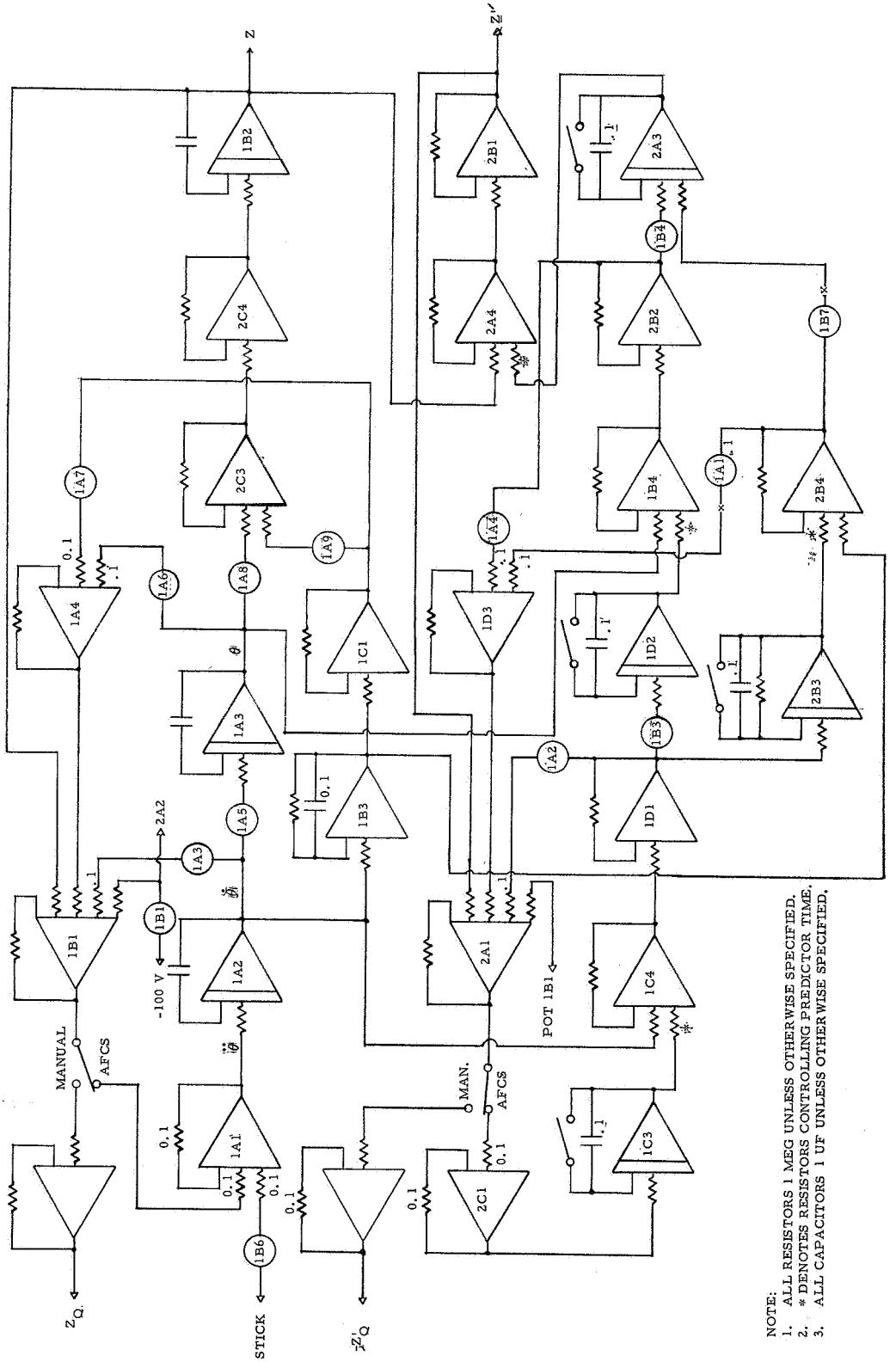

Figure V-2. Real- and Fast-Time Analog Computer Program for Nonlinear Predictor Display Study

Table V-1. Notation

α = Angle of attack

α' = Fast-time angle of attack

θ = Pitch angle

θ' = Fast-time pitch angle

$\dot{\theta}$ = Rate of change of pitch angle

$\dot{\theta}'$ = Fast-time rate of change of pitch angle

$\ddot{\theta}$ = Pitch angle accelleration

$\ddot{\theta}'$ = Fast-time pitch angle accelleration

$\dot{Z}$ = Climb rate

$\dot{Z}'$ = Fast time climb rate

Z = Altitude

Z' = Fast-time altitude

ZQ = Altitude steering signal

$Z'Q$ = Fast-time altitude steering signal

β = Flight path vector angle

V = Flight path velocity vector magnitude

The predictor time span is changed by changing the forward gain of the fast-time equation. In the simulation performed, three values of the predictor time span were used: 5, 10 and 20 seconds (i.e., aircraft altitude for the next 5 seconds, 10 seconds, etc).

The determination of gain for each section was discussed in an earlier section.

The output of the fast-time equation is displayed on a two-gun Dumont 322A oscilloscope as a vertical deflection of one gun.

Table V-2. Real- and Fast-Time Loop Coefficients

Term	Real-Time		Fast-Time	
	Pot	Value	Pot	Value
$\dot{\theta}$	1A5	0.720	1B3	0.720
θ	1A8	0.500	1B4	0.500
α	1A9	0.150	1B7	0.150
$\dot{\theta}$ fdbK	1A3	0.100	1A2	0.100
θ fdbK	1A6	0.400	1A4	0.400
α fdbK	1A7	0.440	1A1	0.440

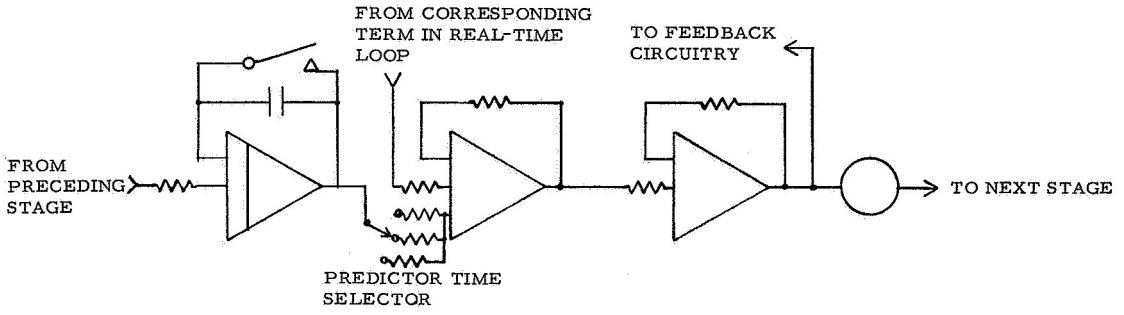

Figure V-3. Fast-Time Computing Section

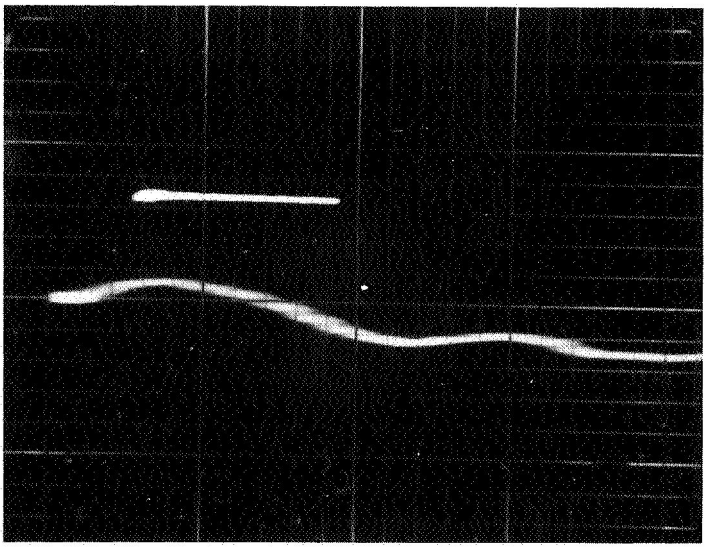

Figure V-4. Prediction of Altitude Flight Path Profile for Next 10 Seconds

2. Time Generation Functions

a. Prediction Cycle Generator

The master oscillator program consists of an integrator inverter and limiter connected in a closed loop, Figure V-5.

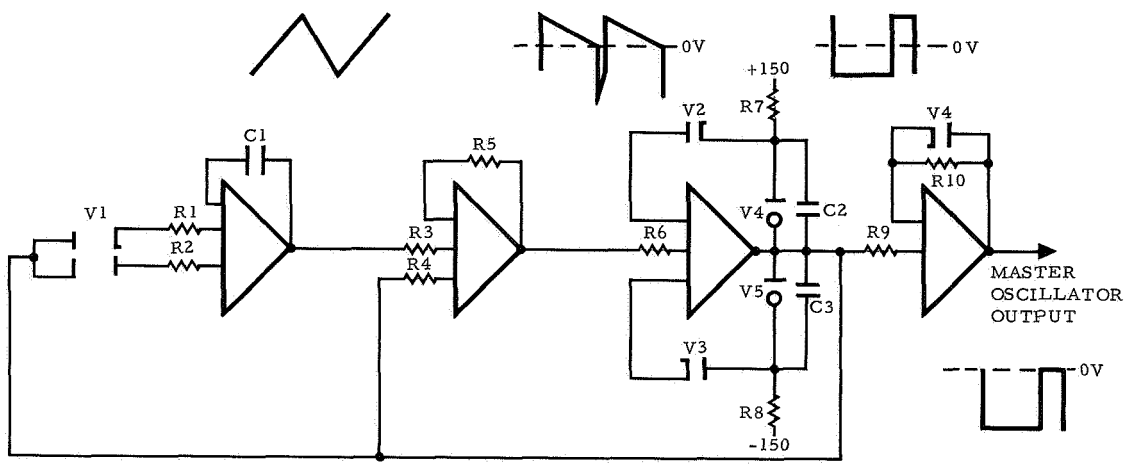

Figure V-5. Prediction Cycle Generator

The output amplitude is a precisely regulated square wave. The amplitude is a function of the voltage regulating element (V4 and V5). The frequency of oscillation is governed by the forward gain in the loop, primarily by the integrator elements, R1, R2 and C2.

The duty cycle is determined by the ratio of R1, R2 and the polarity of the diodes in V1.

The output square wave is used to drive the sweep generator and the fast-time reset switches. The reset switches used are dry reed components to minimize contact closure time and resistance since transients and pickup in the high gain, fast-time loop (8×10^6) can be exceedingly difficult to eliminate.

b. Sweep Generator Program

The sweep generator program consists of an operational amplifier connected as an integrator with a dual triode connected from input to output to short the integrator into reset whenever the master oscillator goes positive. The incoming square wave has been clipped such that grid potential remains below zero dc (Figure V-6).

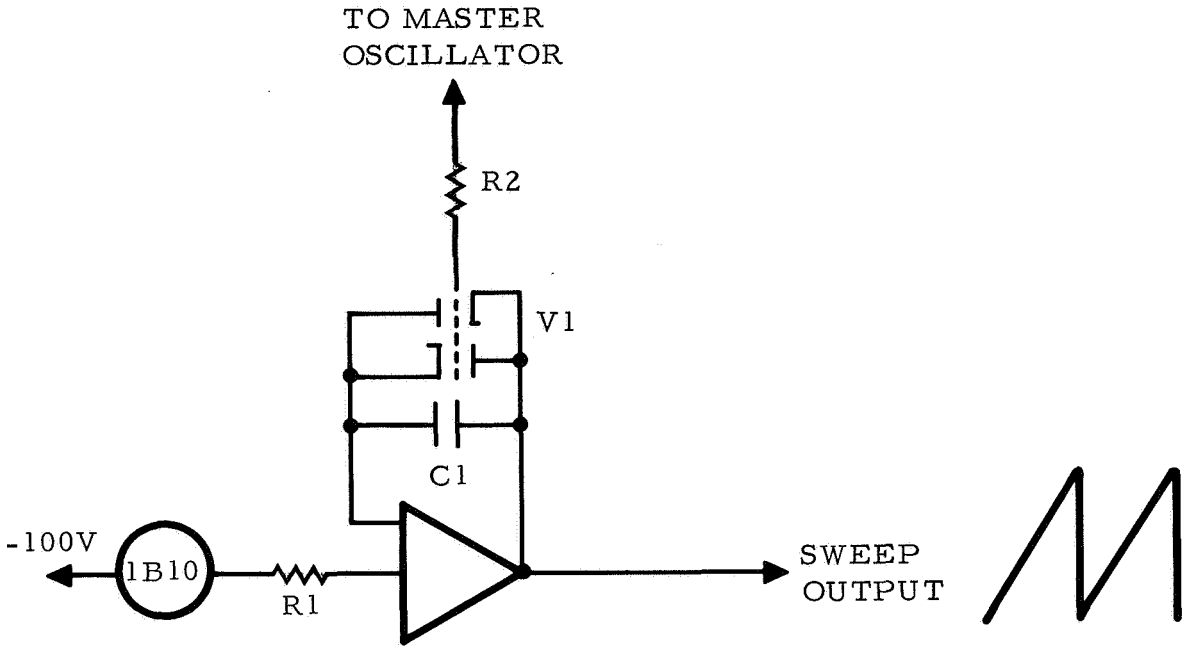

Figure V-6. Sweep Generator Program

The resulting sweep waveform has a period equal to the on period of the master oscillator. The output of the sweep generator is fed to the predictor display horizontal drive and to the dynamic photoformer horizontal drive.

3. Altitude Above Terrain Measurement

The measurement of altitude above the terrain consists of sampling the terrain data at a predetermined point on the horizontal sweep by coincidence gating of a track and hold circuit.

The coincidence detector and track and hold circuits are shown in Figures V-7 and V-8. The output terrain altitude is summed with computed altitude to develop radar altitude. Two such units are used. One detects terrain altitude ahead of the aircraft as an input driving function for automatic terrain following (ATF). (See Figure V-7.) A second unit is used to provide current radar altitude (Figure V-8).

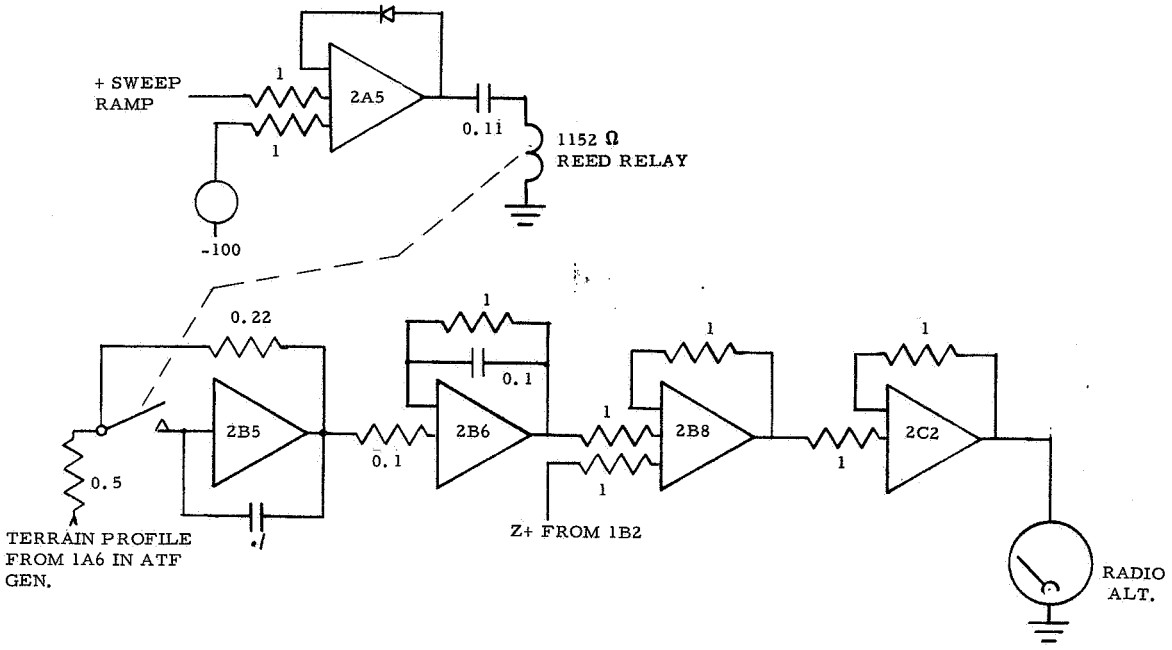

Figure V-7. Radio Altitude Generation

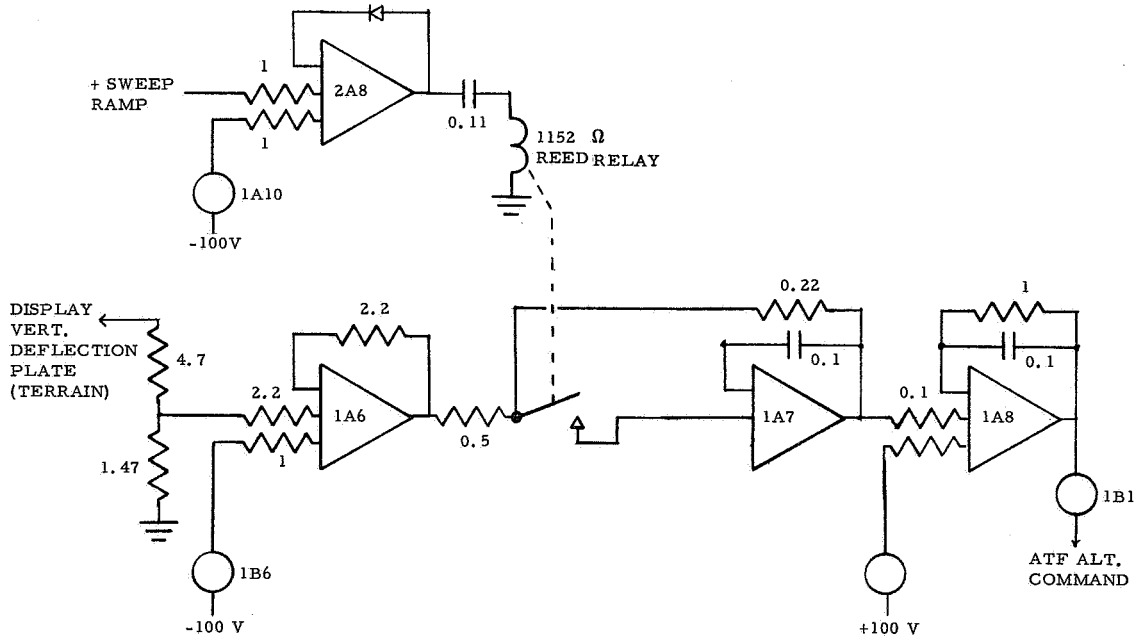

Figure V-8. ATF Generation

4. Dynamic Photoformer

A photoformer was developed to generate terrain contour and glide slope wave shapes through use of a cathode ray tube, photoconductive cell, and film drive mechanism, Figure V-9. A sawtooth voltage was used to sweep the cathode ray tube spot horizontally; a photocell viewing the screen was used to make the spot vary vertically to conform to the terrain contour of a 70-mm film mask (Figure V-10) driven across the cathode ray tube face. Thus, the output voltage wave shape was a replica of the shape of the contour mask use. A blanking pulse was used at the end of each sweep to turn off the cathode ray tube spot during retrace.

The photoformer functions degeneratively so that variations of cathode ray tube brilliance, photoconductive cell sensitivity and the gain of any amplifier employed have negligible effects on the transfer device. However, the photoformer is limited in response time by conventional bandwidth considerations and by the response time of the photoconductive cell used.

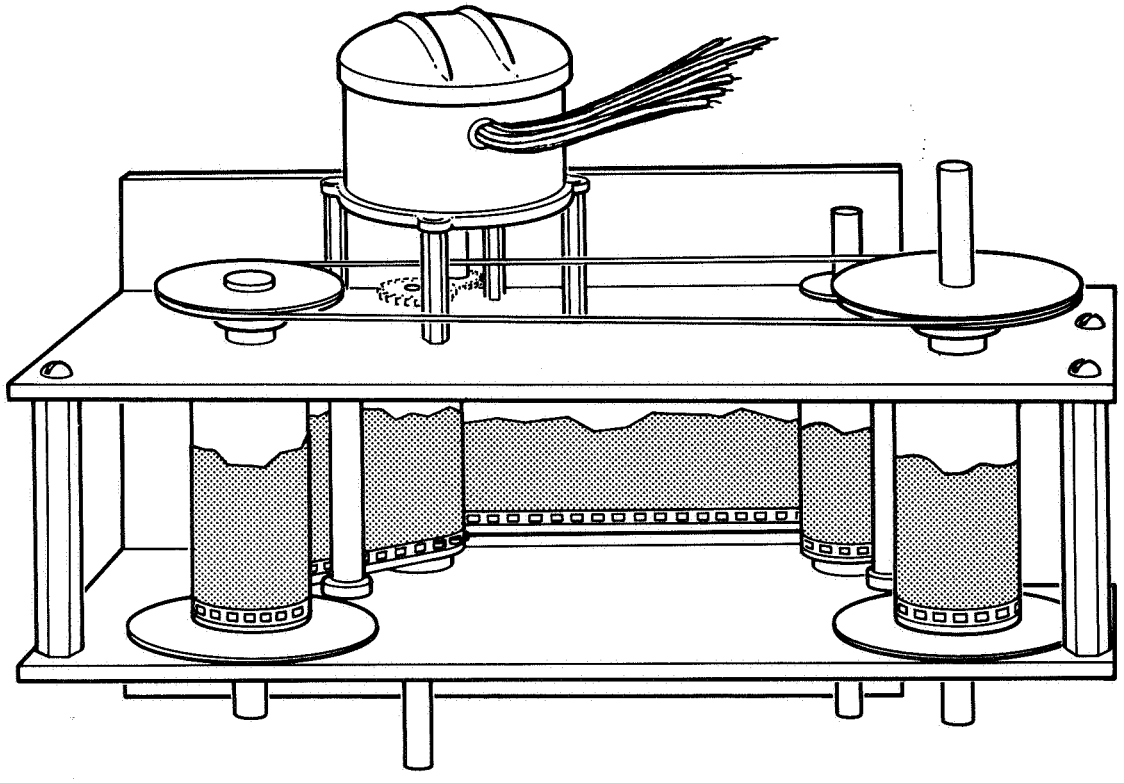

Figure V-9. Photoformer Drive Mechanism

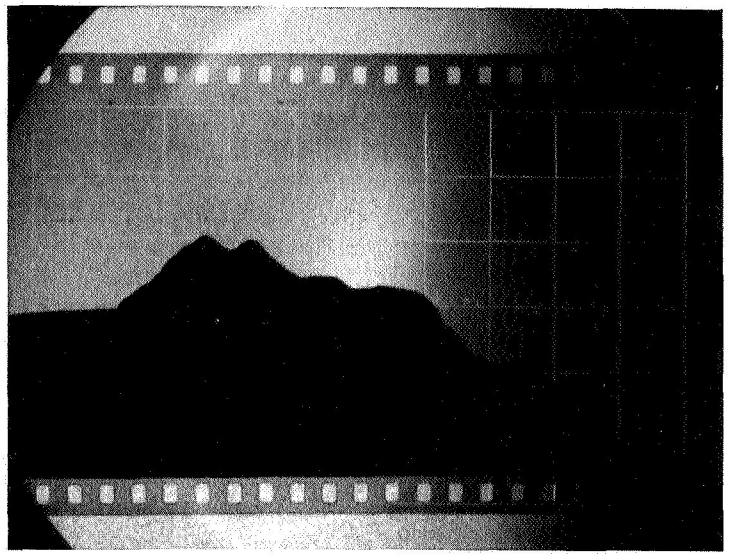

Figure V-10. Sample of 70 MM Film Terrain Profile Used in Photoformer

With further circuit refinements, rise times of less than 20 microseconds were achieved. This was accomplished by analyzing the delay time around the feedback loop. This delay time included the decay time of the phosphor of the cathode ray tube cascaded with the delay time through the amplifiers and photocells. For short output rise times, the total delay time must be short. Phosphors which exhibit short decay time, in order of decreasing persistence, are P1, P11, P5 and P15. By using a P5 phosphor, it was possible to provide rise times, in the output circuit of approximately 10 microseconds, which correspond to a high frequency cutoff of approximately 150 kc.

Another factor considered in the design was the degree of accuracy with which the center of the spot coincided with the mask height. This was determined by an analysis of the gain around the forward loop. It was determined that for loop gains on the order of 40 db or greater, the position of a given portion of the spot generally coincided with the mask displacement to an accuracy of better than 1 percent. The circuitry employed is shown in Figure V-11.

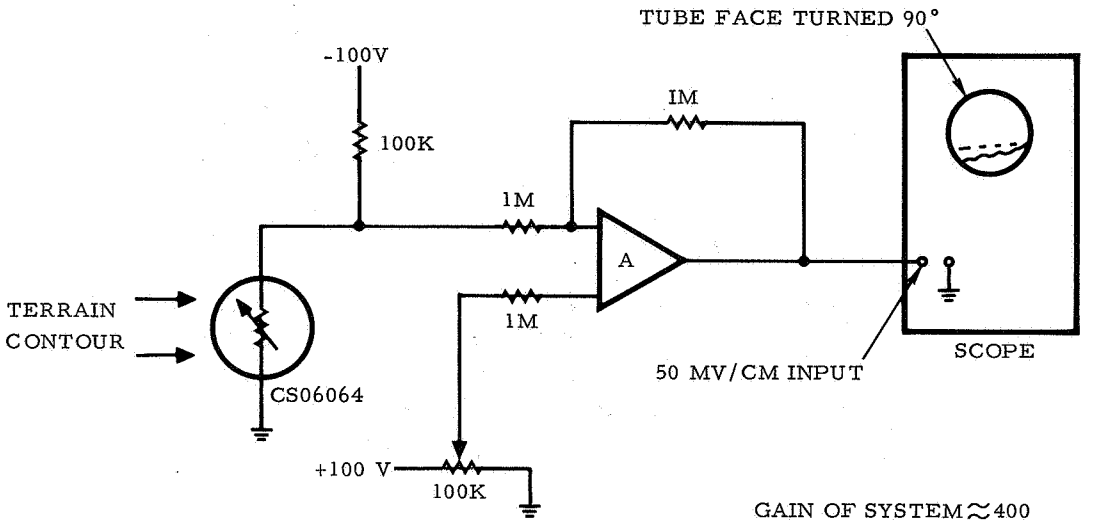

Figure V-11. Electrical Schematic - Photoformer Circuit

C. COCKPIT MOCKUP

A cockpit mockup was constructed to provide radio altitude, pressure altitude, gyro horizon and climb rate. The predictor display was shown on a Dumont 5 inch 322A oscilloscope mounted directly in front of the pilot. A two-axis flight control stick was provided with two-axis potentiometer pickoff. A switch on the handgrip was used to initiate trials. A command altitude control was provided as a 10-turn calibrated potentiometer.

D. EXPERIMENTER - CONTROL CONSOLE

An experimental control console was constructed to simplify experimental operations, Figure V-12. The following controls were included:

1. Predictor time selector - Selects 5-, 10-, or 20-second predictor.

2. Real-time loop control selector - Selects AFCS on manual control mode for real-time loop.

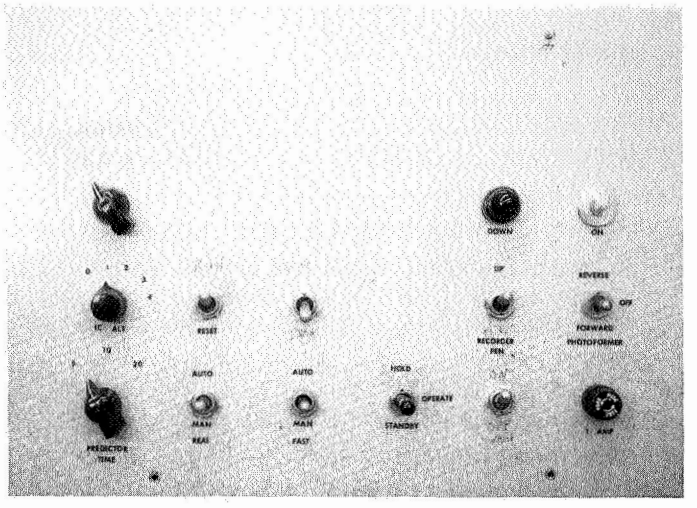

Figure V-12. Experimental Control Panel

3. Fast-time loop selector - Selects AFCS or manual control mode for fast-time loop.

4. Computer control switch - Selects computer function: Hold, Operate, Standby.

5. Sweep switch - Controls display X-axis sweep: ON-OFF.

6. Photoformer control switch - Controls photoformer film drive motor: Forward, Off, Reverse.

7. Recorder pen switch - Selects automatic X-Y recorder pen operation or pen up.

8. Error integrator input switch - Controls input to error integrator: RUN, STOP.

9. Error integration reset switch - Controls error integrator: RUN, RESET.

10. I. C. altitude switch - Selects initial condition altitude: 1, 2, 3, 4 units.

11. Display selector switch - Selects display presented: predictor display, altitude and quickened altitude display (displayed as two dots), altitude dot only.

E. MANUAL ALTITUDE CONTROL

A study was designed and conducted to determine the effect of predictor display prediction time span on altitude changing performance, relative to performance achieved in conventional instrument performance for the same task.

Four altitude levels were used: 100, 200, 300 and 400 feet. Three predictor time spans were employed: aircraft position in 5 seconds, 10 seconds and 20 seconds (Figure V-13). A fourth display condition was employed in which the subject used radio altitude, gyro horizon and climb rate to perform the same task.

The basic control task was to return an offset altitude to a zero reference. The predictor display offset appeared as a level flight indication at one of the altitude offsets. In the conventional case, the offset appeared on the radar altimeter.

The integrated error for the time away from the zero reference for a fixed trial period was obtained. This measure reflects the time taken to zero the error. Each trial was recorded and characterized with respect to flight path performance achieved. A basic latin square experimental design was employed to collect data to minimize position and order effects in condition presentation. A recording was taken of each trial.

In each trial, the pilot-subject would initiate the trial by depressing a switch on the flight control column. He would maneuver the simulated aircraft by manipulation of the flight control column. He would reduce the attitude error in an appropriate maneuver and maintain zero error until the end of the trial. The conditions used are shown in Table V-3.

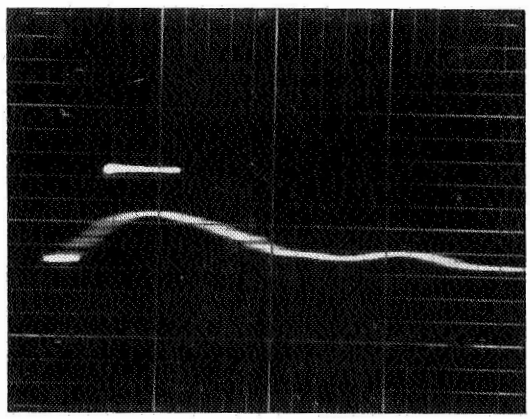

5 SECONDS

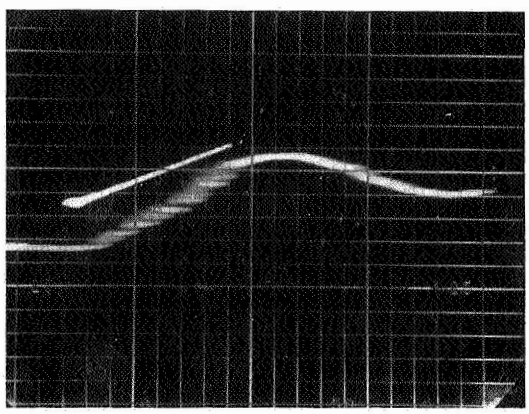

10 SECONDS

APPEARANCE OF PREDICATOR DISPLAY IN 5, 10, & 20 SECOND PREDICTION

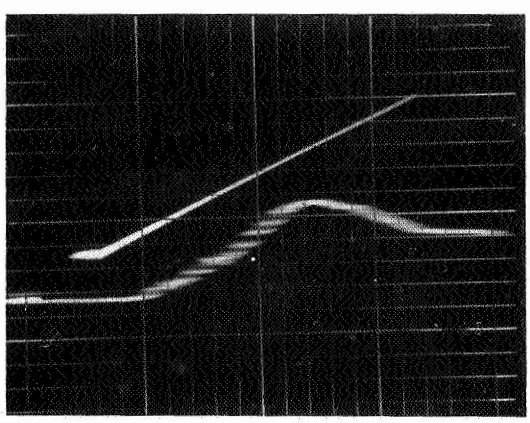

20 SECONDS

Figure V-13. Appearance of Predictor Display in 5-, 10-, and 20-Second Prediction

Table V-3. Experimental Display Conditions

5-Second Predictor		100 Foot Error
10-Second Predictor	X	200 Foot Error
		300 Foot Error
20-Second Predictor		400 Foot Error

1. Results

The experimental results were treated in two different ways: (1) an analysis of variance was performed on the numerical integrated altitude error, and (2) the recordings were characterized by stability of response, time to reduce error and magnitude of overshoot.

a. Analysis of Variance of Altitude Error

The analysis of variance was performed to obtain the significance of overall difference between the display conditions (D), altitude error conditions (A) between subject (B/S_s), and the interactions; altitude by display condition, subjects by altitude (S x A), subjects by displays (S x D), and subjects by displays by altitudes (S x A x D).

The results of the analysis are shown in Table V-4, and the results for each condition and altitude offset are shown in Figure V-14.

(1) Displays. The highly significant difference between displays would tend to confirm the hypothesis that performance with a prediction time of 5 seconds would be different than that for the conventional and 20-second prediction times. Figure V-15 which combines the altitude offset data for each display mode would seem to show that the difference is due to the performance occurring on the 20-second prediction mode.

It is somewhat surprising that this difference appears when the relatively crude average altitude error measure is used as a criterion.

(2) Altitude. The highly significant difference between the altitude offsets is not surprising since the independent variable altitude error is made up of the time integral of altitude. Thus, if the time of response were held constant and the altitude offset increased, the error would

Table V-4. Analysis of Variance Results

Source	D. F.	MS	F
D	3	493.86	23.88
A	3	5210.15	229.62
A x D	9	52.35	N. S. (0.0365)
S x D	15	20.68	
S x A	15	22.69	
S x A x D	45	1431.34	

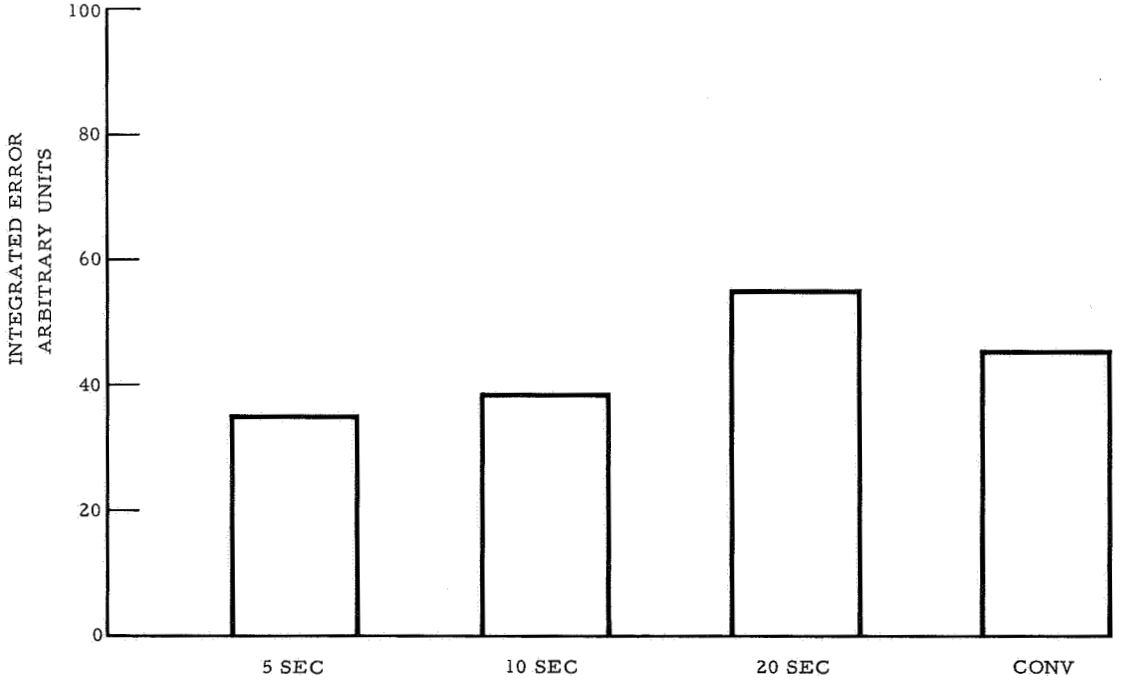

Figure V-14. Display Modes (Data Consolidated for All Altitudes)

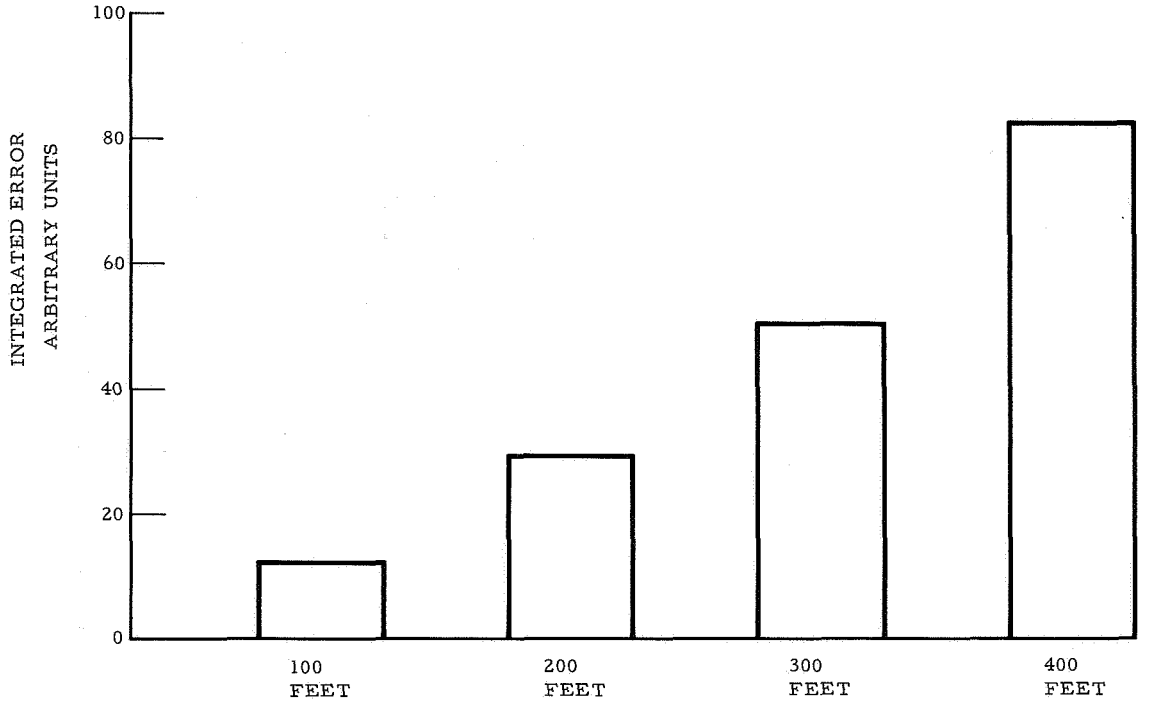

Figure V-15. Altitude Offsets (Data Consolidated for All Display Modes)

increase proportionally. If, however, time of response was associated with altitude offset, the curve would probably rise more steeply. Examination of Figure V-16 indicates that a relatively linear increase seems to occur. This favors the constant-time of response hypothesis but does not prove it.

b. Analysis of Records

A second treatment of the data was made to develop a more fundamental knowledge of the properties of performance of the effect of prediction time relative to the performance on a conventional display system.

Each record was examined to determine: (1) time of response, (2) overshoot or undershoot, and (3) estimated stability.

1. Time of Response. This is measured as the time taken from trial start until the base line is crossed.

2. Overshoot. This measure reflects maximum departure from the reference after crossing the base line whether undershot or overshot.

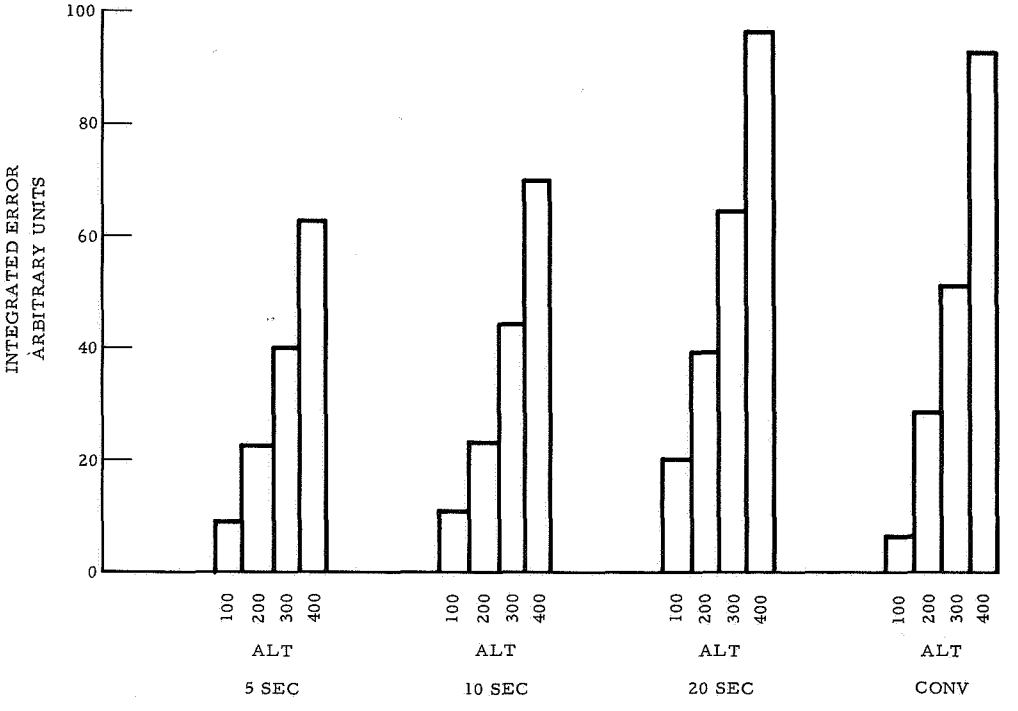

Figure V-16. Display Modes

3. Estimated Stability. This estimate is essentially an opinion rating based on the scale below:

Rank 5 — Smooth curve without oscillation about reference
Rank 4 — Essentially smooth curve with small amplitude oscillation at reference
Rank 3 — Majority of curve smooth with marked oscillation in reference
Rank 2 — Irregularity in major curve and mild oscillation at reference
Rank 1 — Irregularity in major curve and marked oscillation at reference

(1) Results. The time required to cross the baseline for each predictor mode and for the conventional mode increases with predictor time. For all altitude offsets, performance with the conventional display is intermediate, closely paralleling performance with the 10-second predictor.

The results are shown graphically in Figures V-17, V-18, V-19, V-20, V-21 and in tabular form in Table V-5.

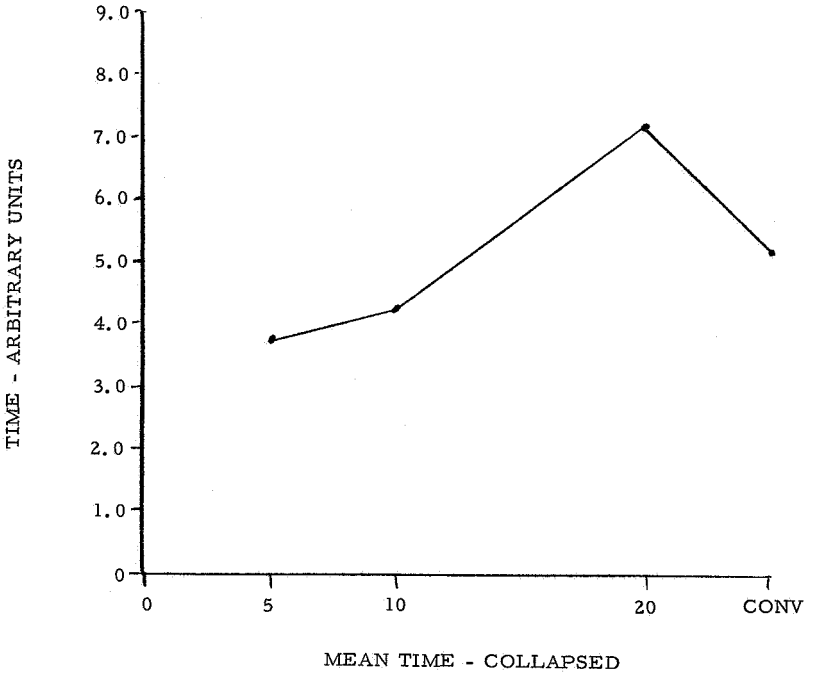

Figure V-17. Mean Time Collapsed

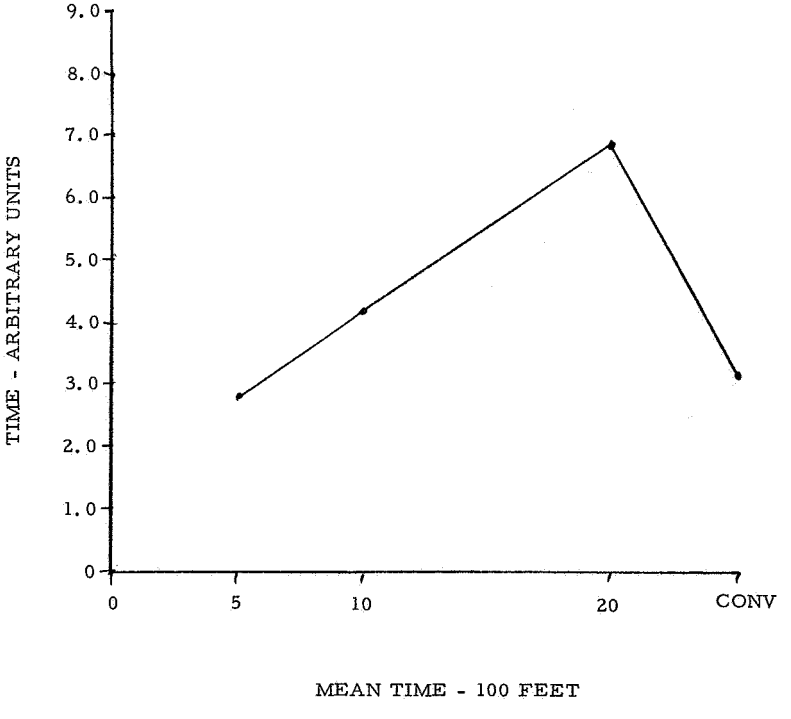

Figure V-18. Mean Time - 100 Feet

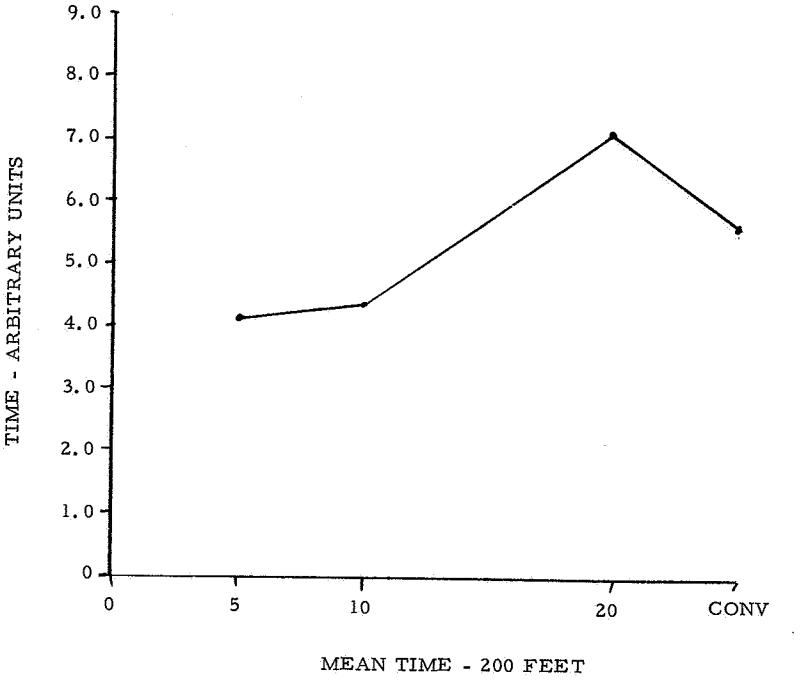

Figure V-19. Mean Time - 200 Feet

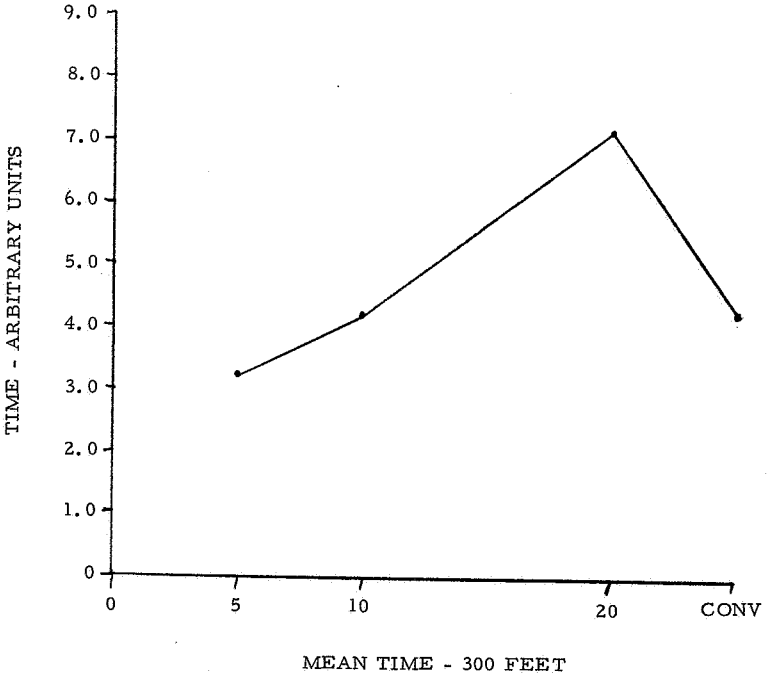

Figure V-20. Mean Time - 300 Feet

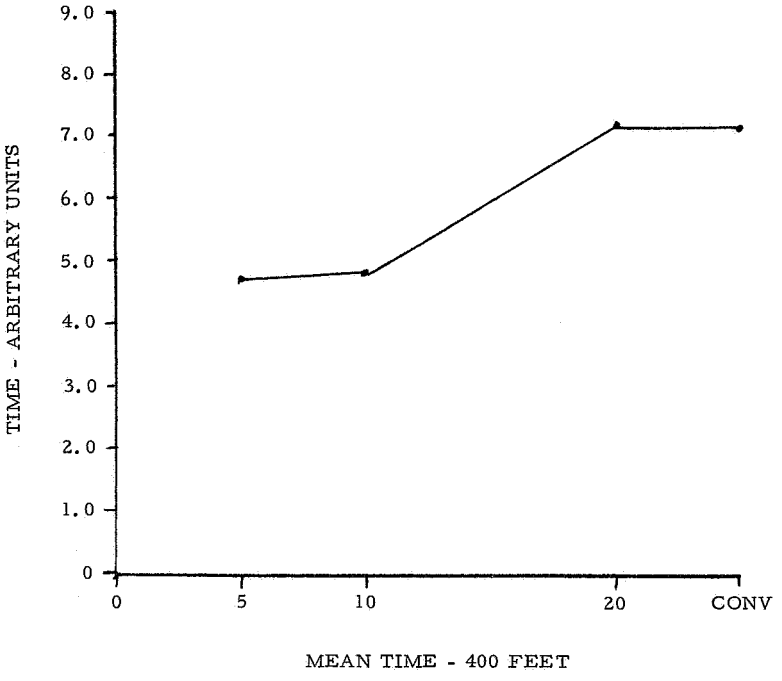

Figure V-21. Mean Time - 400 Feet

Table V-5. Time to Cross Baseline Display Modes

	5 Sec	10 Sec	20 Sec	Conv
All Altitude Mean	3.83	4.38	7.13	5.07
100 Feet				
M	2.85	4.02	6.73	3.17
σ	0.64	0.70	0.48	0.42
200 Feet				
M	3.32	4.28	7.05	4.22
σ	0.72	0.87	0.51	0.41
300 Feet				
M	4.01	4.45	7.35	5.57
σ	1.21	0.81	0.77	0.79
400 Feet				
M	4.70	4.77	7.39	7.31
σ	0.72	0.83	0.97	1.24

(2) Stability. Reference to Figures V-22, V-23, V-24, V-25, and V-26 and Table V-6 indicates that the estimated stability is poorest for the 5-second predictor display and the conventional display. Estimated stability increased with increasing prediction time.

(3) Overshoot. The overshoot resulting from an altitude changing maneuver is greatest for the shortest prediction time (5 seconds) and least for the longest prediction time. Use of the conventional display mode results in the greatest overshoot (Table V-7 and Figures V-27, V-28, V-29, V-30, and V-31).

(4) General Conclusion. The predictor display modes can be characterized as follows for the dynamics employed:

1. Use of the 5-second prediction time is characterized by a short response time, considerable overshoot and was judged unstable.
2. Increasing prediction time was associated with increasing judged stability and lessened overshoot.
3. Use of the conventional display tended to result in poor stability, characteristically longer medium response time, and a large overshoot relative to the predictor display modes.

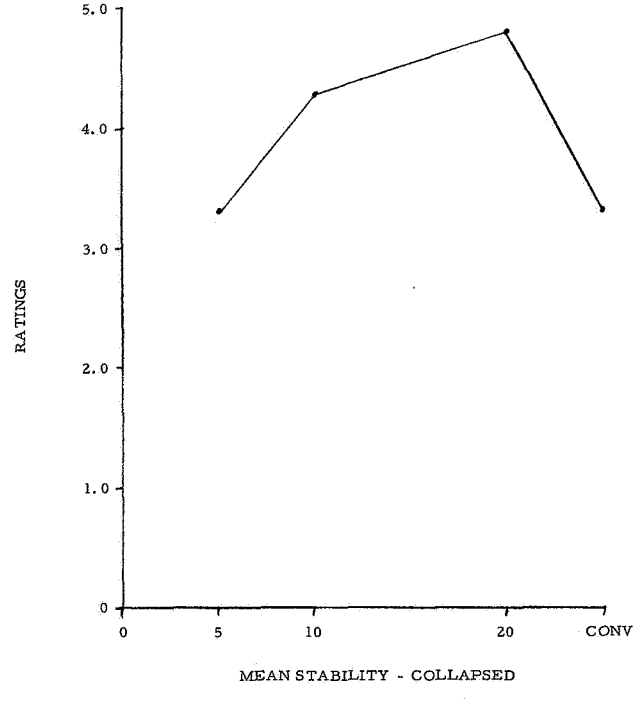

Figure V-22. Mean Stability - Collapsed

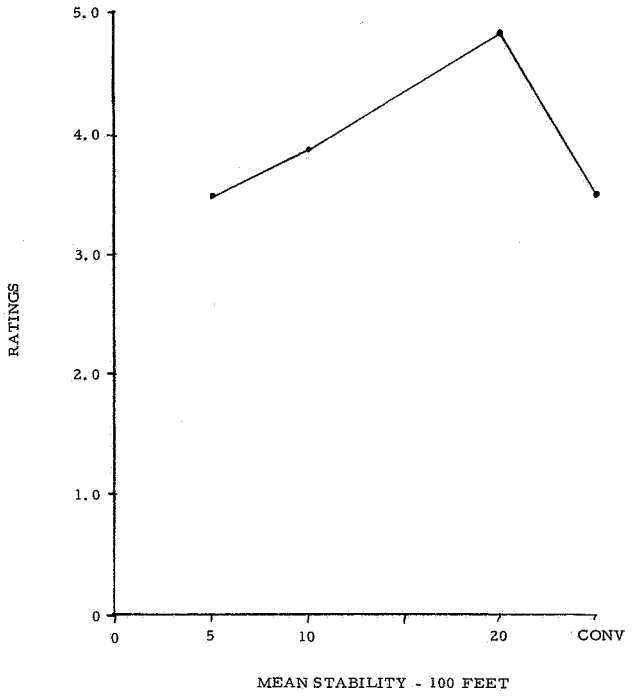

Figure V-23. Mean Stability - 100 Feet

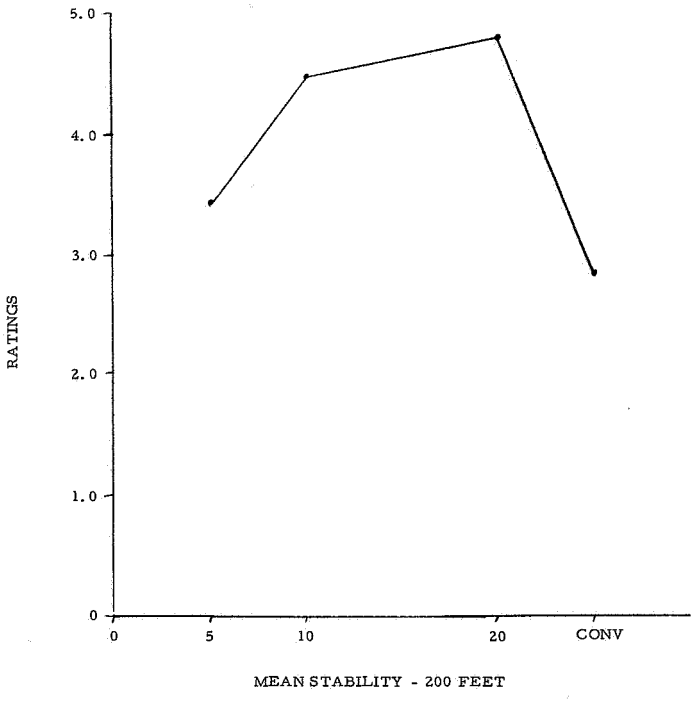

Figure V-24. Mean Stability - 200 Feet

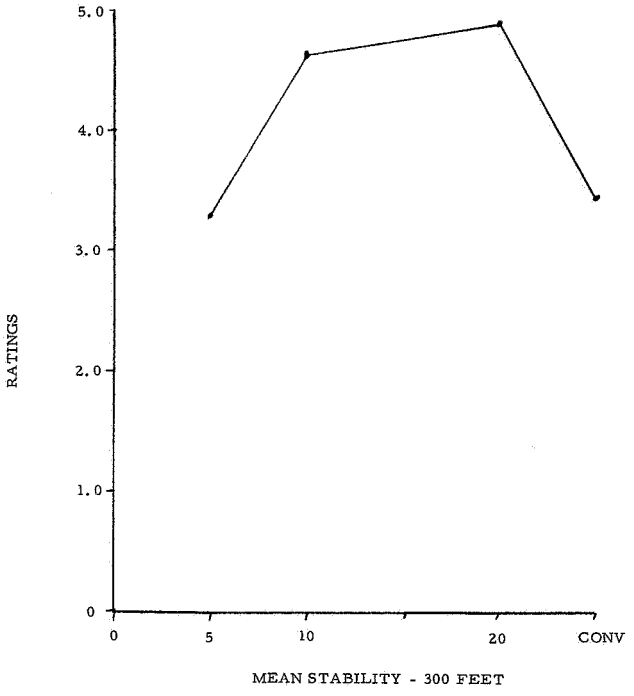

Figure V-25. Mean Stability - 300 Feet

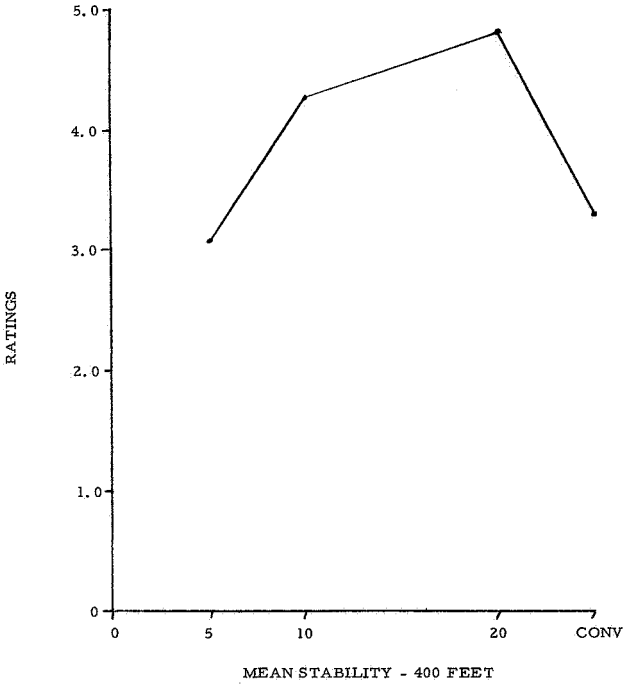

Figure V-26. Mean Stability - 400 Feet

Table V-6. Estimated Stability

		Display Modes		
	5 Sec	10 Sec	20 Sec	Convention
All Altitude Mean	3.40	4.32	4.87	3.29
100 Feet				
M	3.54	3.87	4.88	3.58
σ	0.39	1.05	0.19	0.77
200 Feet				
M	3.46	4.54	4.88	2.84
σ	0.64	0.34	0.19	0.98
300 Feet				
M	3.37	4.67	4.92	3.46
σ	0.43	0.28	0.12	0.96
400 Feet				
M	3.13	4.25	4.83	3.33
σ	0.83	0.35	0.28	0.80

Table V-7. Overshoot (In Feet)

		Display Modes		
	5 Sec	10 Sec	20 Sec	Convention
All Altitude Mean	11.44	7.41	6.27	14.70
100 Feet				
M	7.10	4.54	2.42	14.42
σ	5.28	3.19	1.19	4.51
200 Feet				
M	10.29	5.38	3.75	14.13
σ	6.12	3.73	1.81	7.42
300 Feet				
M	12.08	6.83	5.13	13.58
σ	7.20	3.66	2.47	3.60
400 Feet				
M	16.29	12.88	13.79	16.67
σ	9.99	5.86	8.32	8.67

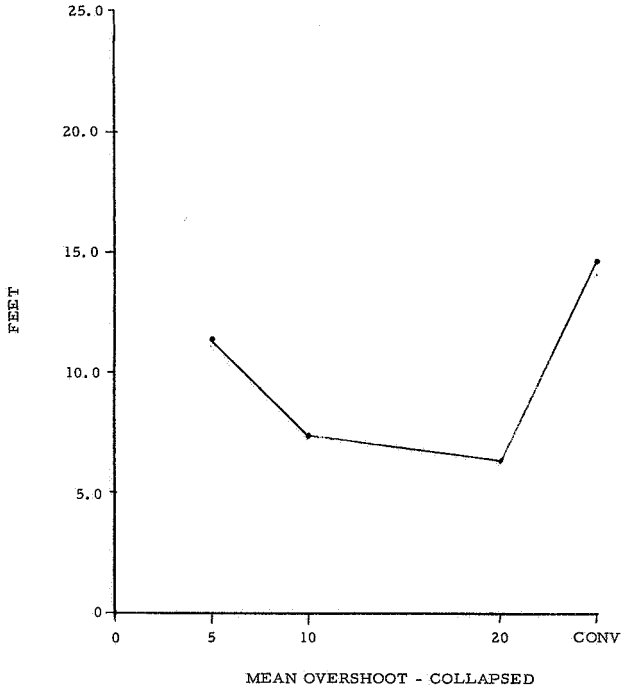

Figure V-27. Mean Overshoot - Collapsed

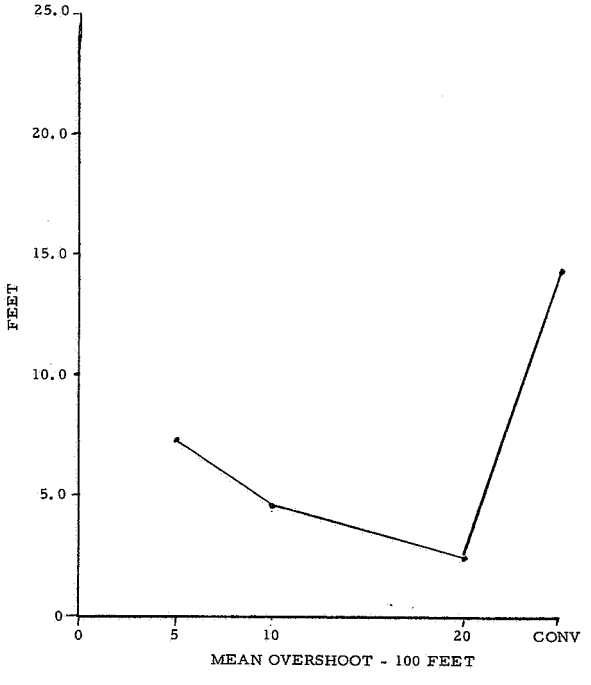

Figure V-28. Mean Overshoot - 100 Feet

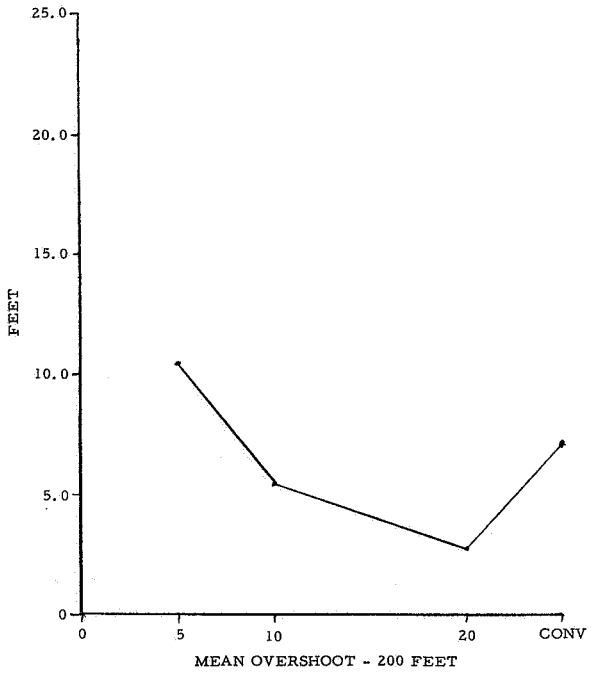

Figure V-29. Mean Overshoot - 200 Feet

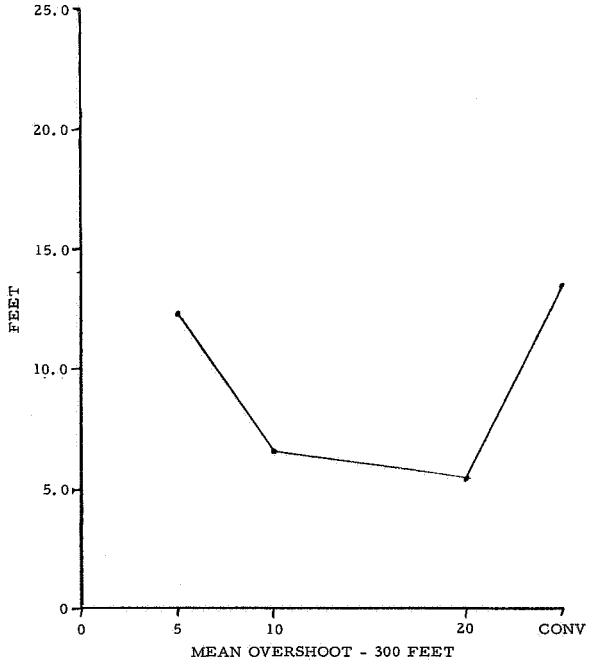

Figure V-30. Mean Overshoot - 300 Feet

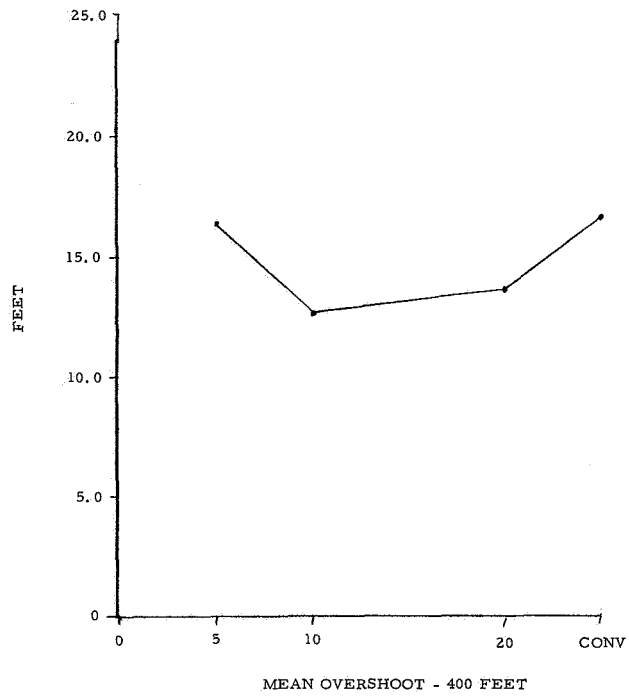

Figure V-31. Mean Overshoot - 400 Feet

F. MONITORING AUTOMATIC FLIGHT CONTROL SYSTEM PERFORMANCE

A series of exploratory studies were undertaken to evaluate the utility of the predictor display in monitoring the performance of an Automatic Flight Control System in a terrain following mode.

No attempt was made to obtain sufficient quantitative data for statistical analysis due to the methodological difficulty of providing sufficient stimulus material extending over a long enough time period to provide a realistic simulation of the monitoring situation in an aircraft. The results of this study were essentially observational.

1. Simulation

The simulation consisted of the presentation of terrain data on the face of a cathode ray tube. The terrain presented is scaled to provide a simulation of an aircraft moving at 400 miles an hour.

The computer program for the AFCS is shown in Figure V-2.

The subject was seated facing the display. Each trial consisted of a 3-minute presentation of one of the predictor display modes (5-second prediction, 10-second prediction, and 20-second prediction) for a conventional predictor and a predictor modified to include a fast-time simulation of the automatic flight control system.

2. Results

a. Conventional Predictor Display

All predictions (5, 10 and 20 seconds) were unsatisfactory. The use of a predictor which does not employ a fast-time model of the Automatic Flight Control System provides a false transient response since the form of the prediction is not related to the closed loop response of the AFCS aircraft system.

b. Predictor Displays with AFCS Fast Time Simulation

In general, the provision of an AFCS fast-time simulation provided an identity of dynamic response between the predictor model and the real-time aircraft equation.

c. Five-Second Prediction

The 5-second prediction was inadequate as a monitor since a clobber could occur before pilot take-over could have an appreciable effect on aircraft altitude.

d. Ten-Second Prediction

The 10-second prediction was judged by all pilots in all cases to be the most satisfactory prediction interval. The lead time was sufficient to provide an adequate pilot take-over for the terrain and aircraft dynamics employed.

e. Twenty-Second Prediction

The 20-second prediction was judged to be satisfactory but generally was ranked behind the 10-second prediction. The pilot group felt that the long prediction tended to provide relatively useless information for the flight configuration employed.

f. Conventional

The conventional indication (parallels current E-scan system) was judged to be satisfactory. Pilot take-over due to uncertainty about a near passage over an obstacle was more frequent than with 10- and 20-second prediction.

g. General Results

The results here suggest that:

1. The predictor display in monitoring AFCS performance must utilize a fast-time simulation of the Automatic Flight Control System.

2. The optimum prediction period will be associated with the aircraft dynamics, flight velocity and the disturbing function parameters.

G. ANALYTICAL RESULTS VERSUS SIMULATION RESULTS

The anlytical results indicate primarily that as prediction time decreases for the dynamics chosen, the gain required of the pilot to maintain stability will increase. The primary assumption in the analysis is that the predictor end point is maintained at the reference indication.

For the assumed nominal gains for the pilot, it is predicted that the 5-second prediction mode will be in a borderline stability state.

The results of the simulation correspond almost exactly with the analytical result. The short response time, the tendency to overshoot, and the poor estimated stability of the 5-second prediction corroborate this analytical finding.

The longest prediction interval (20 seconds) requiring the least pilot gain analytically was characterized in the simulation as "too sensitive" (small control motions resulted in large displacement of the predictor end point).

It is felt that the complex pitch axis analysis represents the most that can be accomplished by a strictly analytical approach. Analysis of the 6-degree-of-freedom case with complex cross-coupling terms would be impractical.

VI. SYNTHETIC PITCH AXIS PREDICTOR DISPLAY

The advantages of the predictor display in manual control and in monitoring automatic flight control system performance as indicated in previous sections would suggest that such a display be mechanized for further testing in a more rigorous environment.

A mechanization analysis conducted in the course of the study clarifies the major problem area — the feasibility of procuring accurate aircraft real-time equations which are valid across a large velocity range and aircraft configurations.

The improbability of achieving these equations and the difficulty of mechanizing the fast-time equations with the exceedingly high gains required in the forward loop, preclude an effective transition from simulation to operational equipment.

Experience has been gained in mechanization of automatic terrain following systems in which a backward calculation of flight path is made using aircraft flight parameters to develop the desired path relative to the measured terrain. This approach has been determined to be exceedingly difficult and prohibitively expensive in equipment and reliability.

Clearly this approach to the development of a display to monitor flight performance to improve flight safety is highly undesirable. A new approach would have to be found.

The approach was provided inadvertently from the comment of a pilot subject who indicated during the course of a trial that he would be happier if the prediction line indicated the line of flight — that the curved flight path was not desirable! Examination of his records revealed that he was attempting to use the predictor display as a transverse attitude indicator since he was making sharp adjustments in pitch rather than a continuous adjustment, as would occur in a track obtained when the predictor end point is maintained on the altitude reference.

The new approach consists of the provision of a display of flight vector velocity referenced to current altitude (Figure VI-1). The simulation mechanization is straight forward (Figure VI-2). Aircraft altitude and angle of attack are combined to yield flight path and

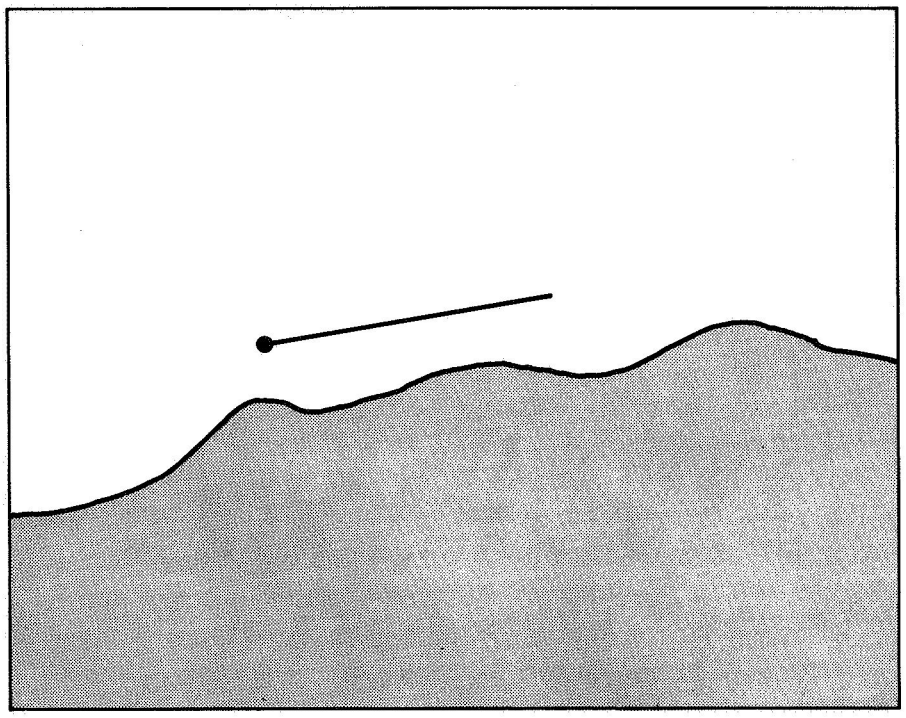

Figure VI-1. Synthetic Predictor Display

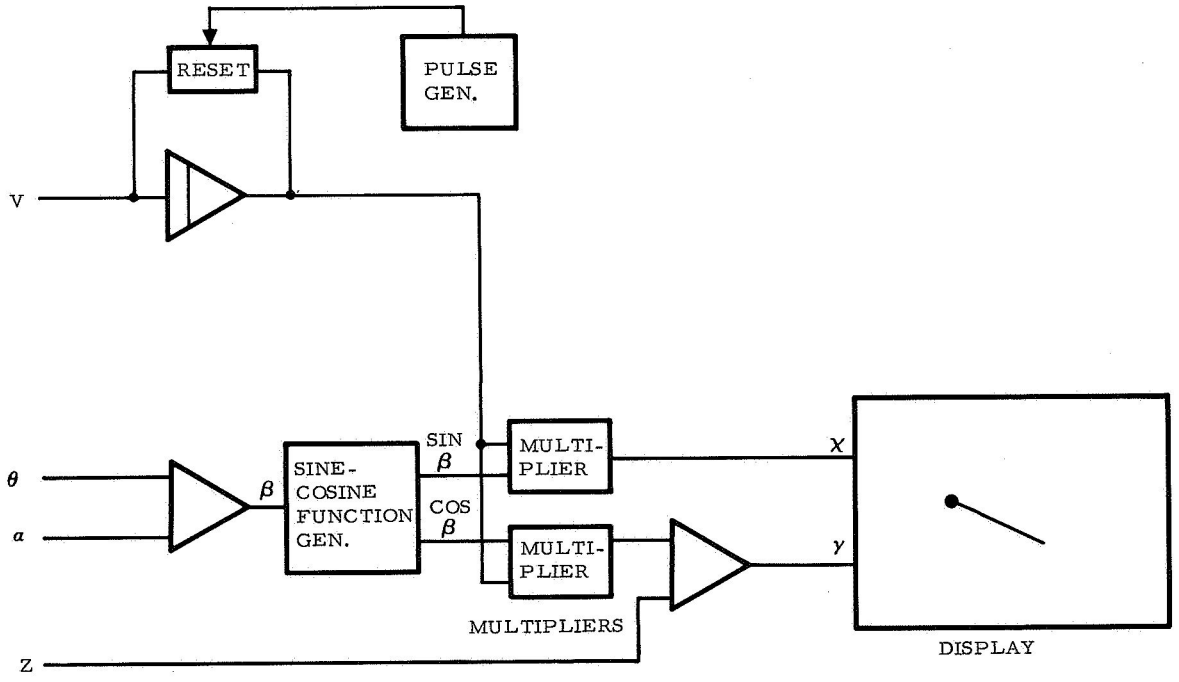

Figure VI-2. Simulation Mechanization

referred to aircraft altitude. True aircraft vector velocity is used to control the period of a sawtooth generator. The X, Y display conversion consists of resolving this vector through the flight path angle developed.

If the display is appropriately scaled, a prediction exists of future position of the aircraft. The aircraft flight path is not provided since the pitch attitude rate term is not provided.

In theory, manual control should be stable and accurate. The lead prediction term required of the pilot is that for pitch rate requiring less than 90° of phase lead, depending upon the aircraft configuration.

The possibility of inducing instability as a function of adjusting flight path per se is eliminated. The display format provides an easily interpreted integration of relatively conventional aircraft display parameters (altitude, attitude, and aircraft velocity). When incorporated with an E Scan (Figure VI-3) or synthetic glide slope, Figure VI-4, the interpretability is quite simple. The velocity indication, when pulling up over a terrain obstacle, should be of considerable help (Figure VI-5) since inadequate power will require adjustment of throttle position.

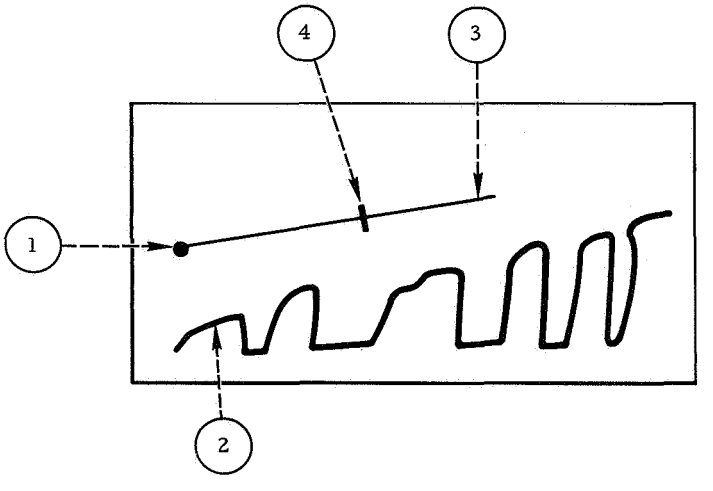

1. CURRENT ALTITUDE
2. RADAR E SCAN DISPLAY (RANGE HEIGHT)
3. FLIGHT VECTOR (LENGTH PROPORTIONAL TO VECTOR VELOCITY)
4. COMMAND VELOCITY (OR REFERENCE STALL SPEED ETC)

Figure VI-3. Synthetic Predictor Display in E Scan Terrain Following

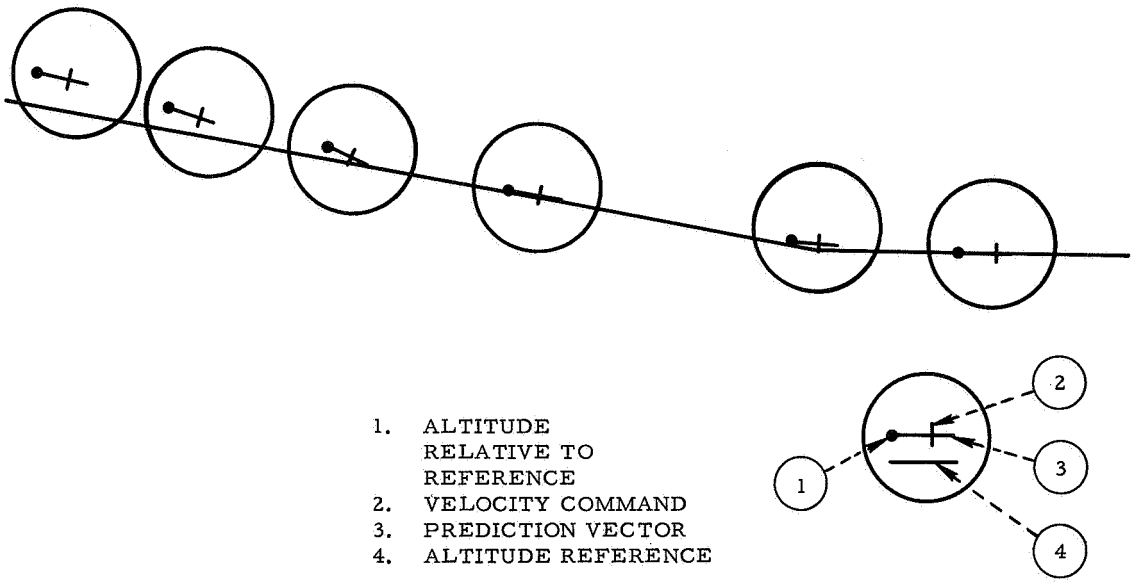

Figure VI-4. Synthetic Predictor Display in ILS Approach

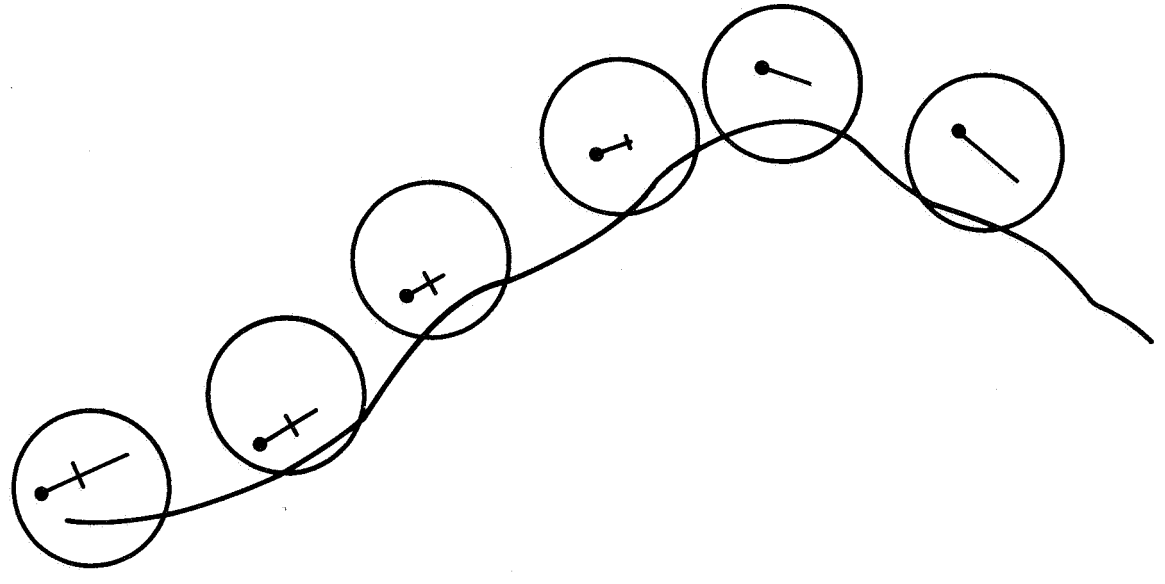

Figure VI-5. Synthetic Predictor Display in Terrain Following

Preliminary testing indicates that this display system would provide a distinct advance in display technology in both manual flight control and in monitoring automatic flight control performance. An extensive evaluation while required is not within the scope of this study.

VII. CONCLUSIONS

A predictor display instrument, when used by experienced pilots in simple manual control of altitude does not provide a distinct advantage over conventional altitude control. Inexperienced subjects (non-pilots) report that altitude changing is "easier" for them when they use the predictor display.

The optimum prediction time is related to: (a) the dynamic response of the aircraft and (b) the bandwidth of the forcing function. For the system studied, long prediction periods raise the display system gain, lower pilot gain, and reduce the forward gain of the overall system. Short prediction times raise the demanded pilot gain, increases the probability of an overshoot and loss of control.

The long prediction time results in an excessively sensitive control movement requirement by the pilot (lowered pilot gain).

Predictor displays used for monitoring automatic flight control system performance, which do not include the fast-time calculation of the automatic flight control system performance, result in less efficient monitoring performance than those predictor displays which utilize fast-time simulation of the automatic flight control system performance.

Predictor display systems utilizing fast-time computation to generate a flight path prediction are extremely sensitive to component drift, and gain changes. Dynamic changes in aircraft equations of motion as a function of the velocity range change in aircraft configuration (stores, flaps, etc) introduce excessively difficult mechanization parameters for maintaining an accurate prediction of flight path.

A synthesized predictor display providing a graphic representation of the flight vector referred to present aircraft altitude appears to yield flight control performance superior to the flight path predictor display and is susceptible to simple and direct mechanization.

VIII. RECOMMENDATIONS

It is recommended that:

1. A simulation evaluation of the synthesized predictor display be undertaken to determine manual aircraft control performance and monitoring performance in automatic flight control modes

2. A mechanization analysis be conducted to establish display design and development parameters

3. A pitch axis synthesized predictor display be constructed to meet flight-worthy specifications

4. A flight test program be conducted to evaluate the display in manual and automatic flight control modes in both terrain following and instrument approach

IX. REFERENCES

1. Ziebolz, H. and Paynter, H. M., "Possibilities of a Two-Time Scale Computing System for Control and Simulation of Dynamic Systems," Proceedings of National Electronic Conference, 9, pp 215-223, 1954.

2. Kelly, Charles R., "Manual Control, Theory and Applications," Office of Naval Research, Washington, D. C., 26 June 1964.

APPENDIX: RECORDS OF SUBJECT TRIALS IN ALTITUDE CHANGING

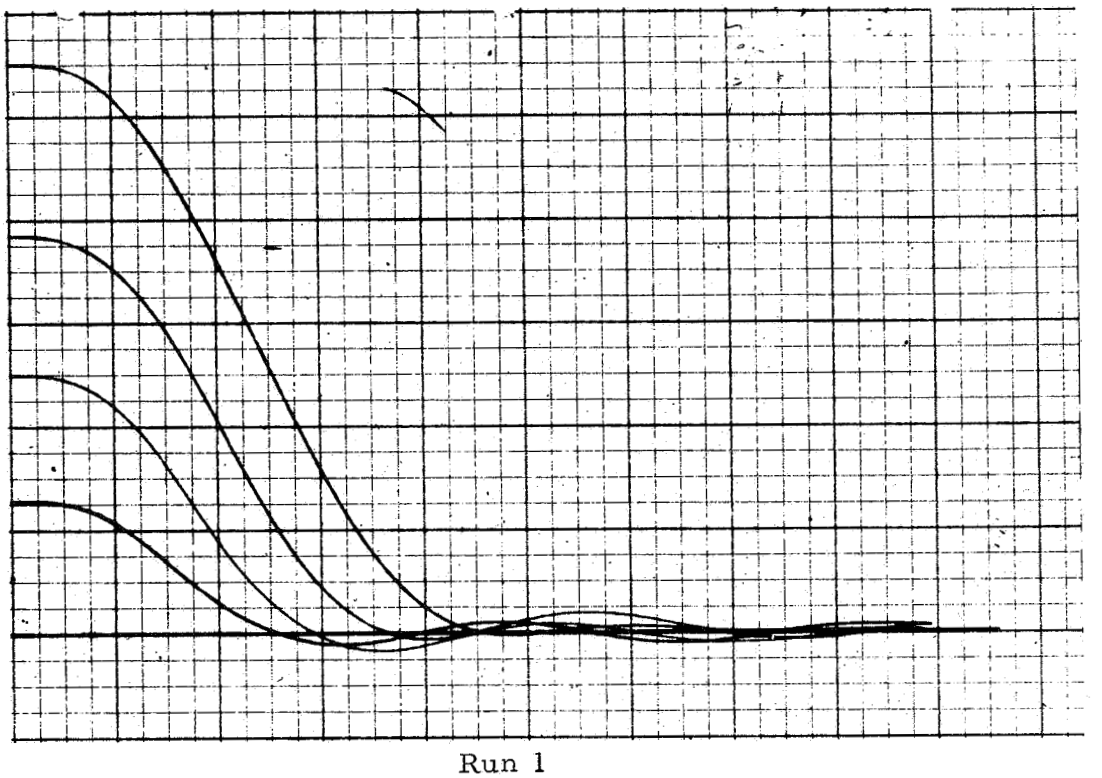

Run 1

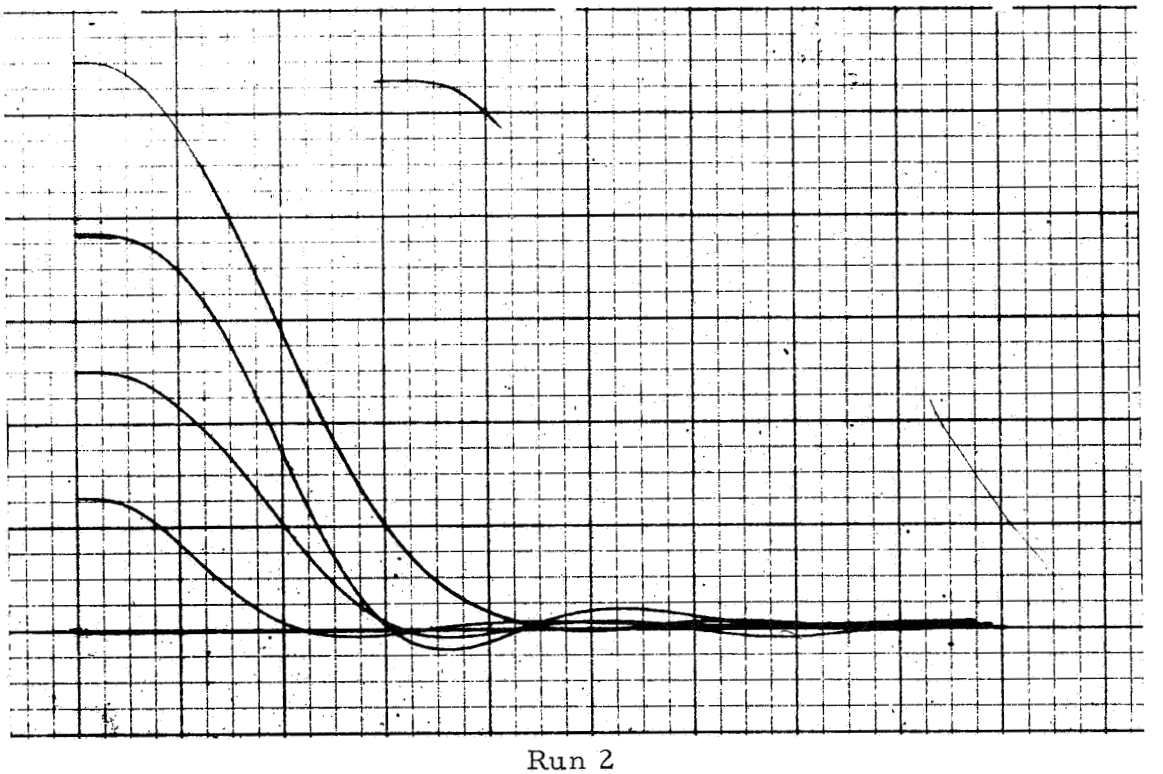

Run 2

Figure A-1. Subject 1 - 5 Seconds

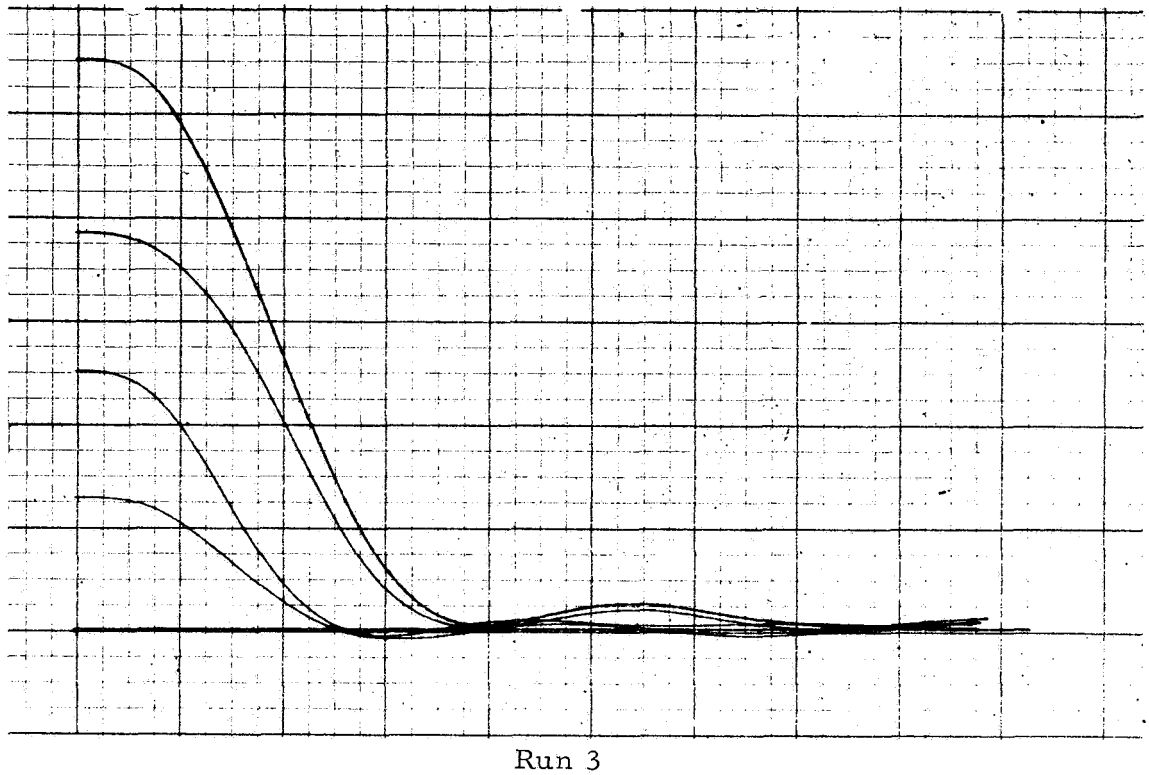

Run 3

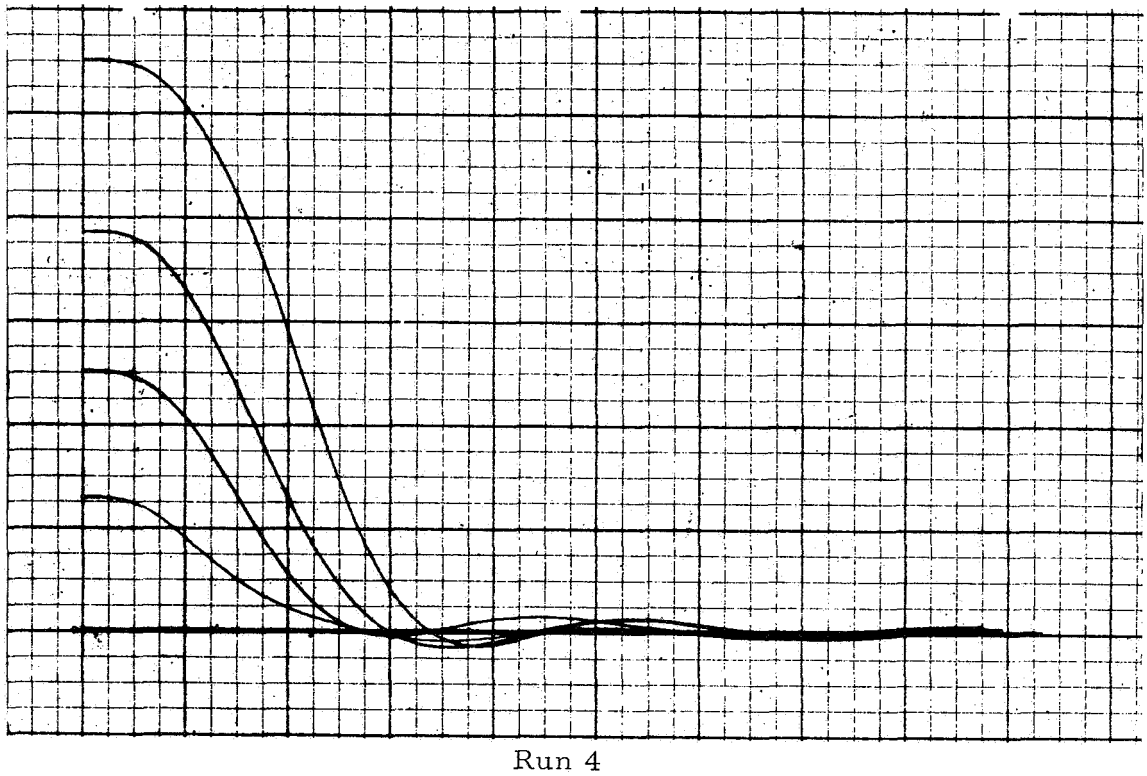

Run 4

Figure A-1 (Cont)

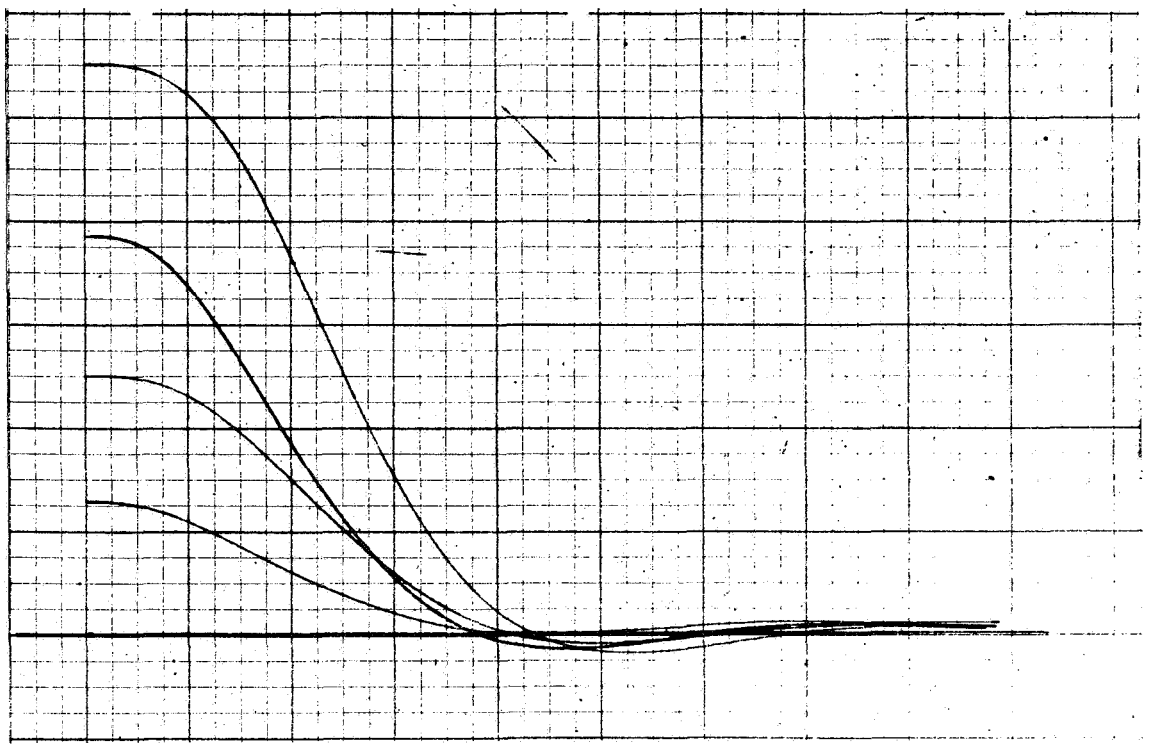

Run 1

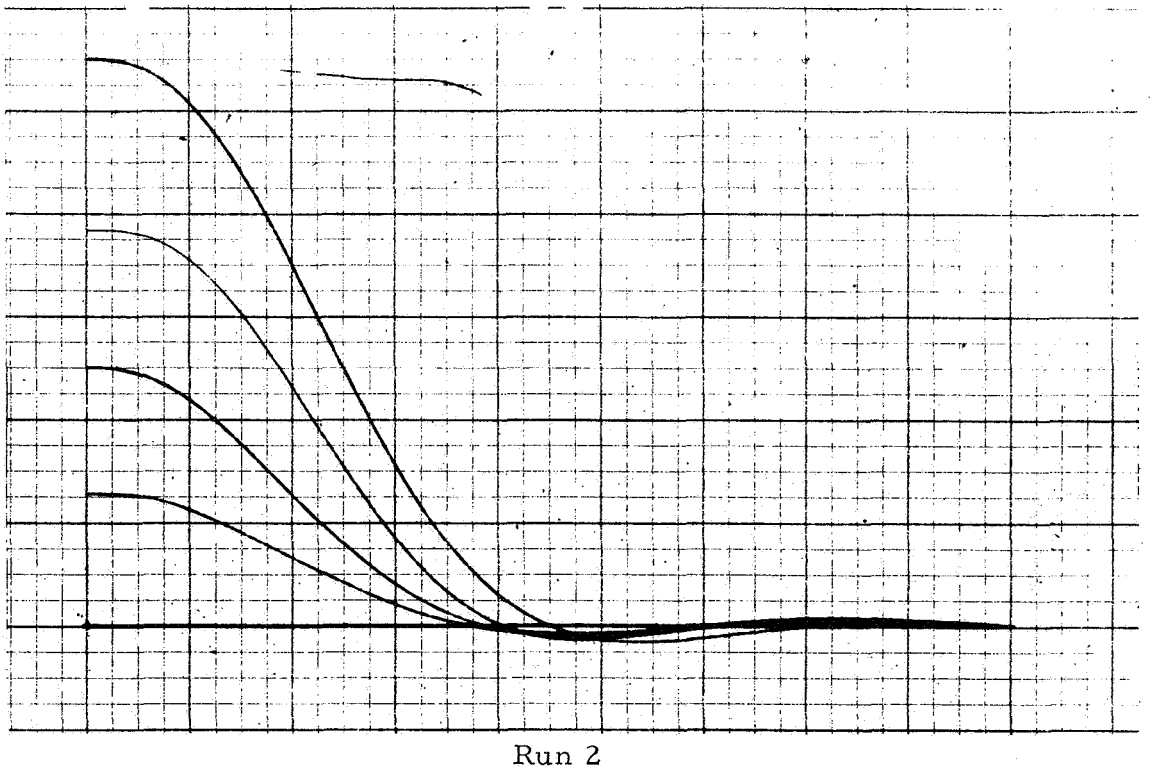

Run 2

Figure A-2. Subject 1 - 10 Seconds

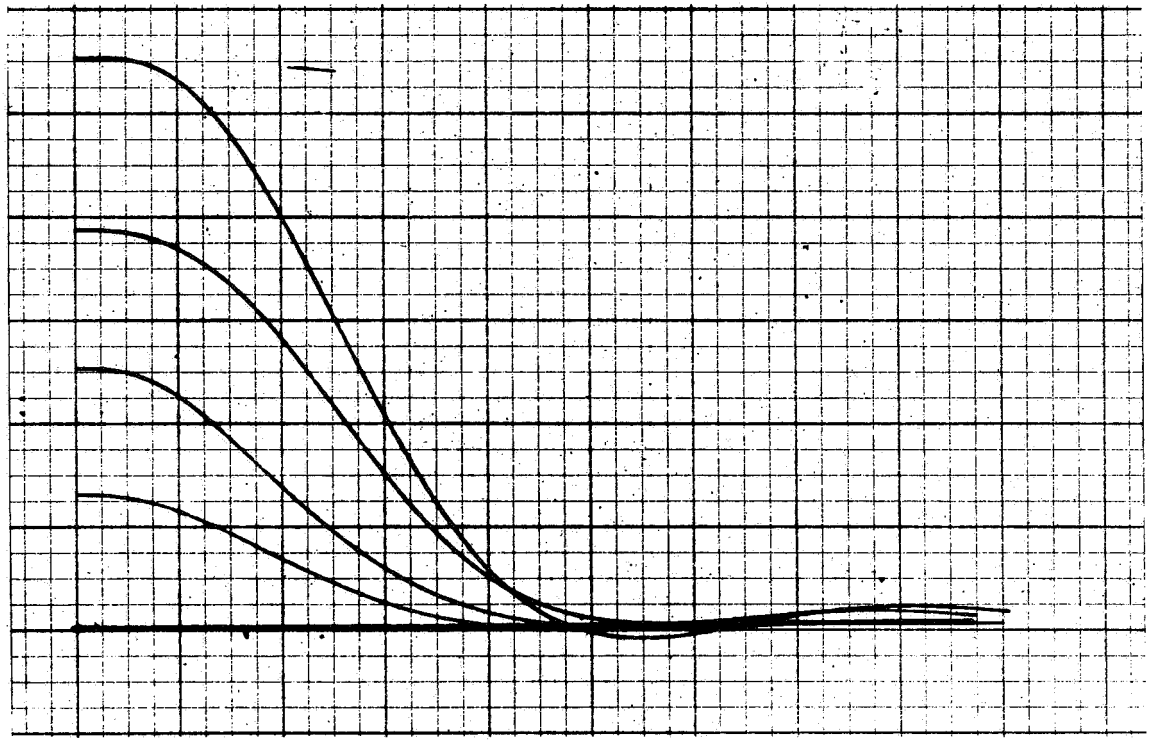

Run 3

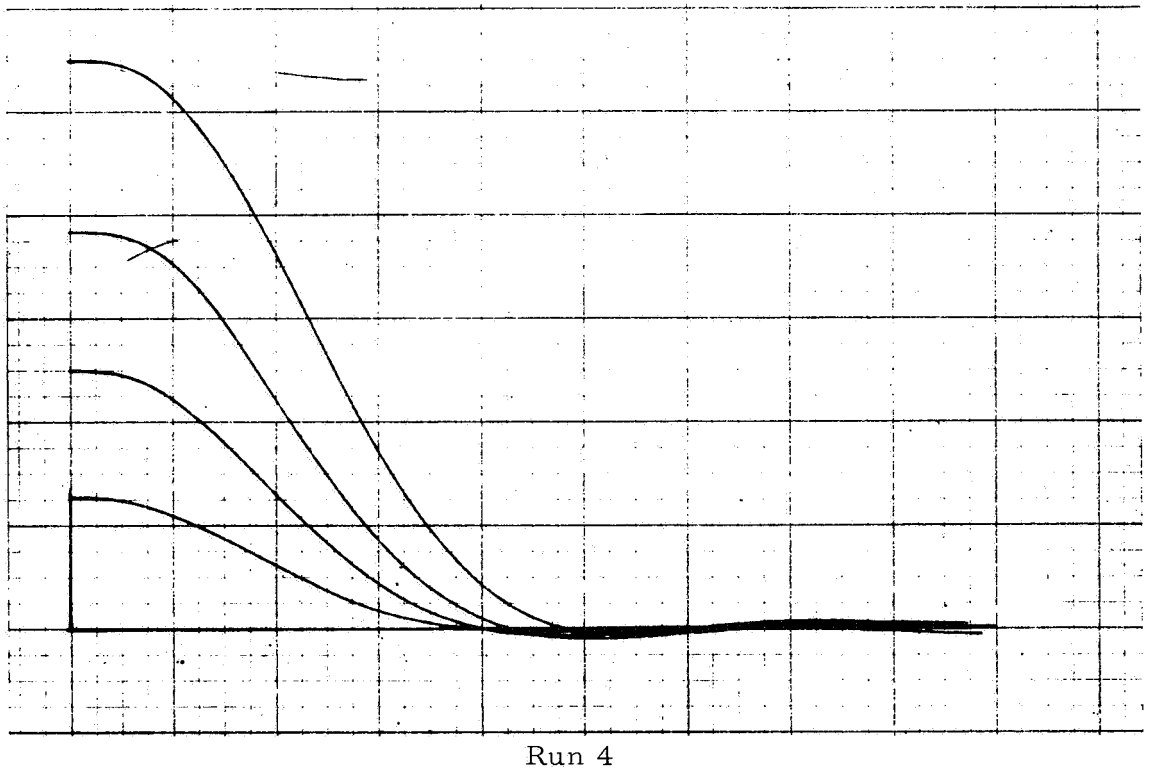

Run 4

Figure A-2. (Cont)

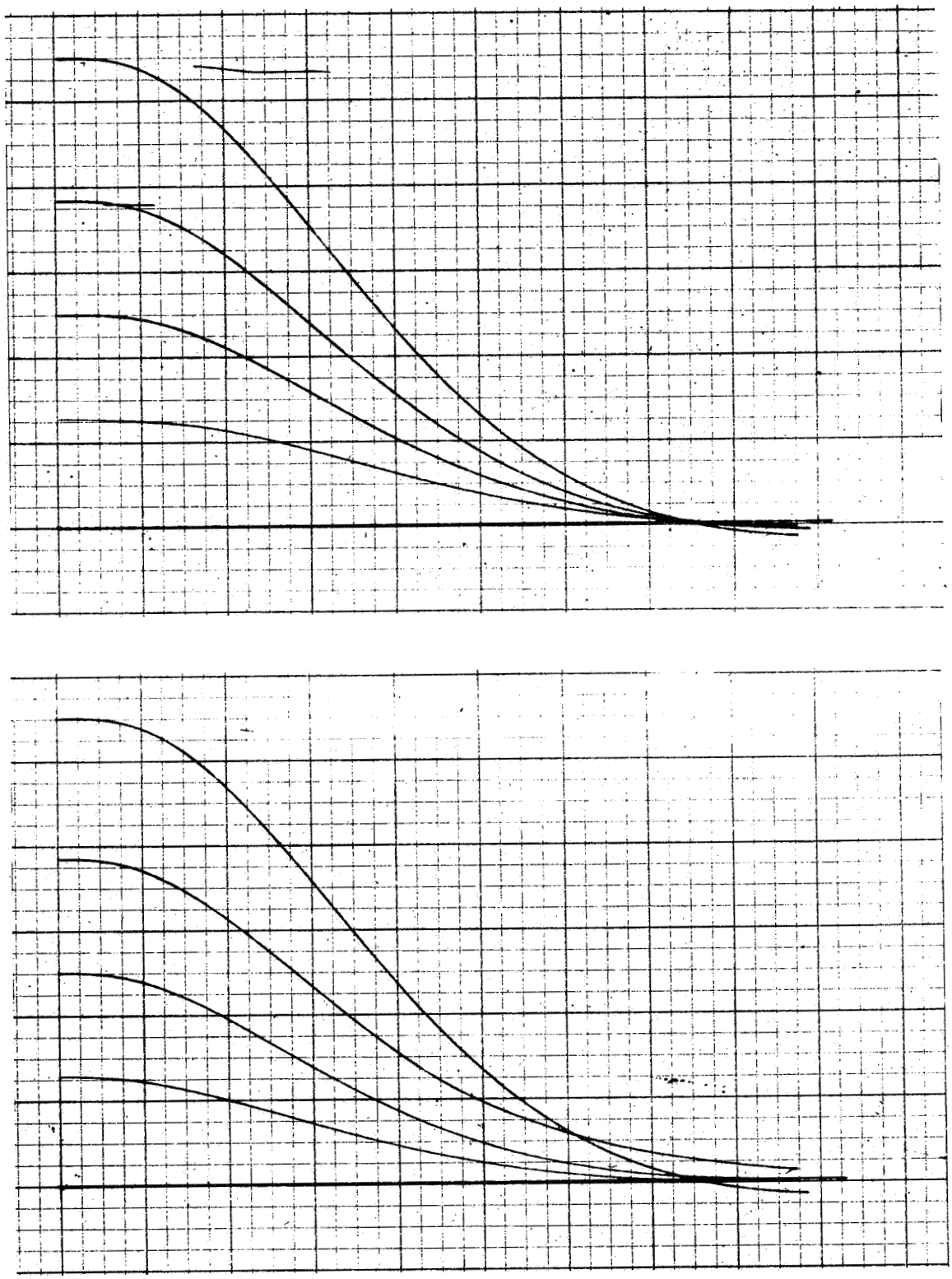

Run 2

Figure A-3. Subject 1 - 20 Seconds

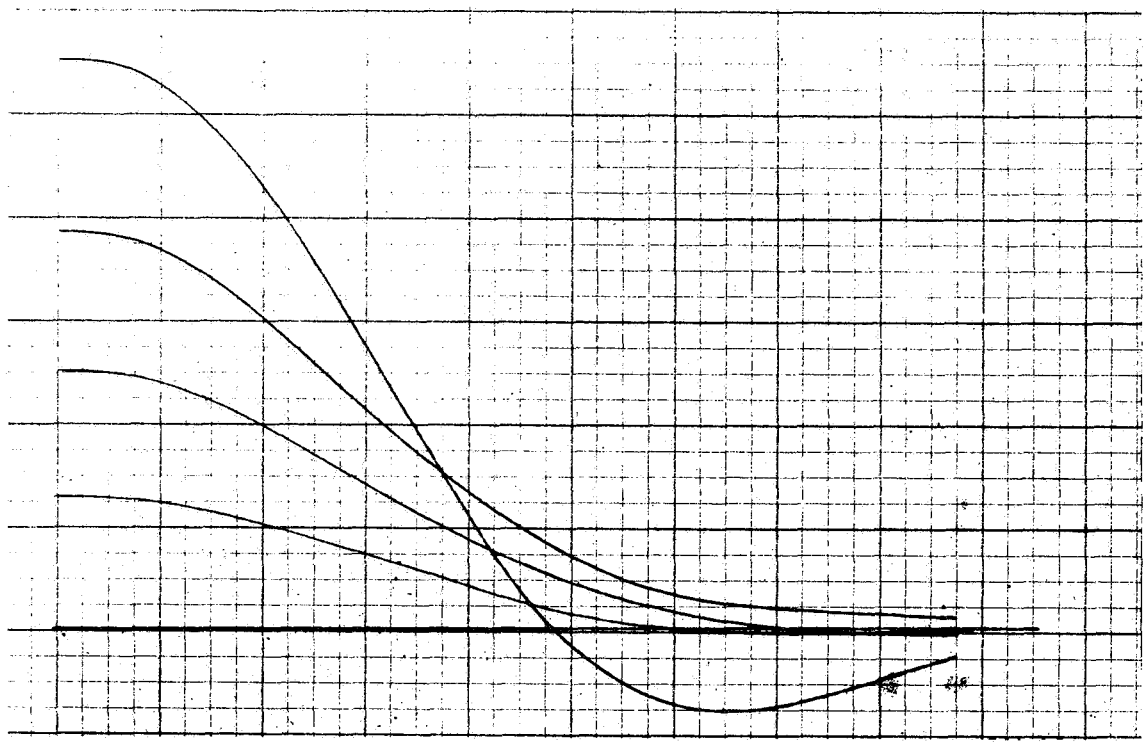

Run 3

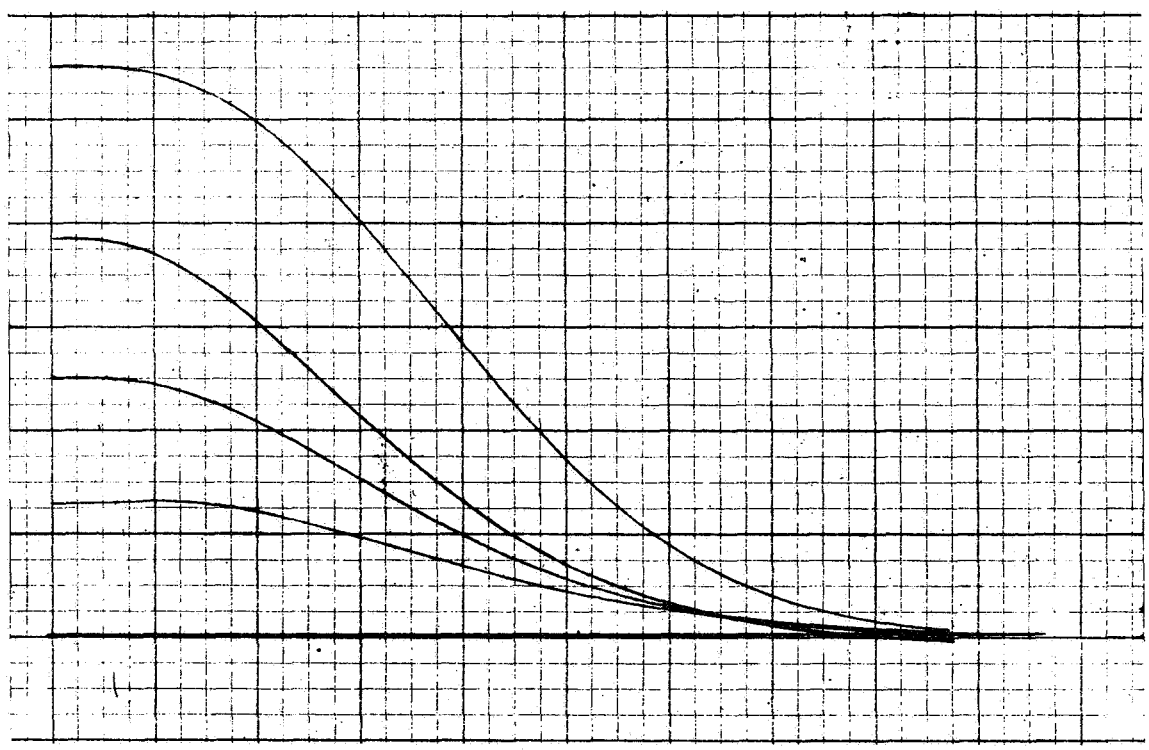

Run 4

Figure A-3. (Cont)

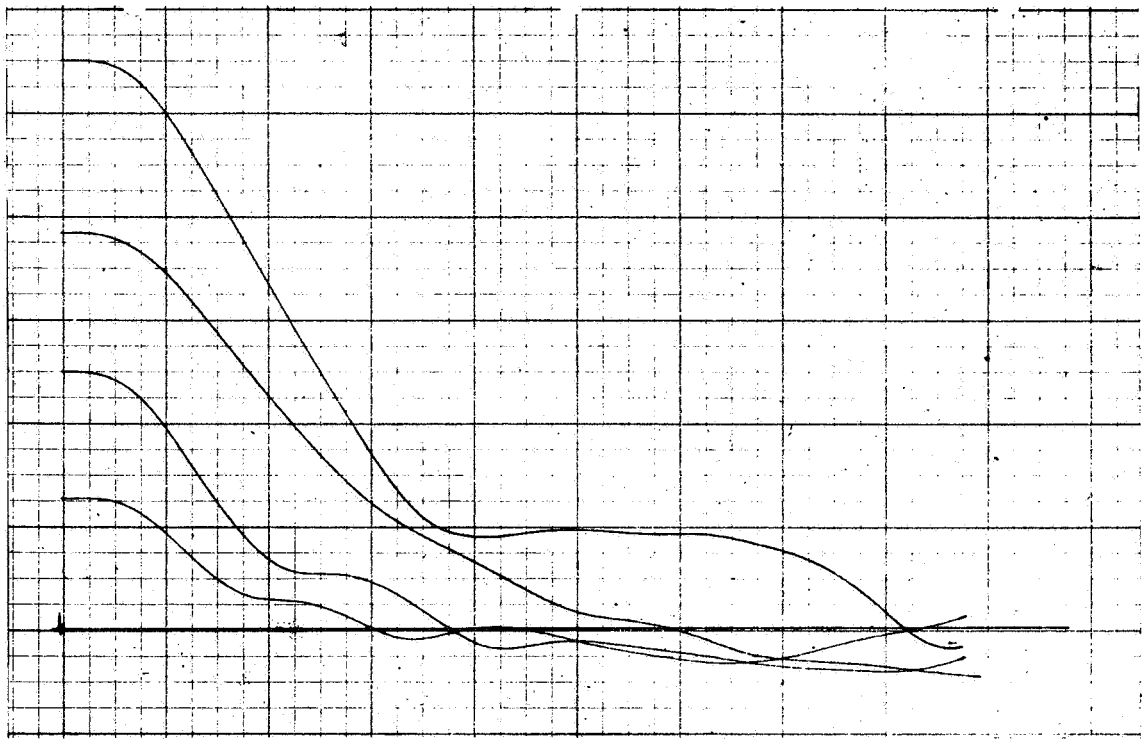

Run 1

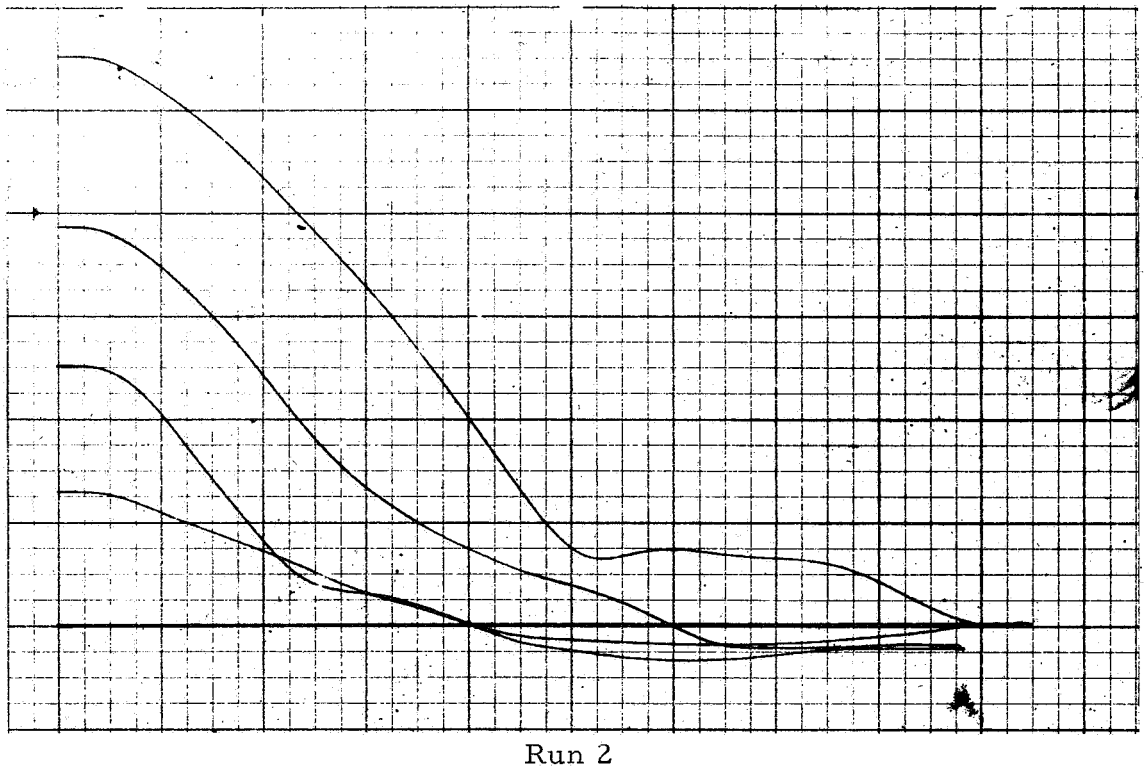

Run 2

Figure A-4. Subject 1 - Conventional

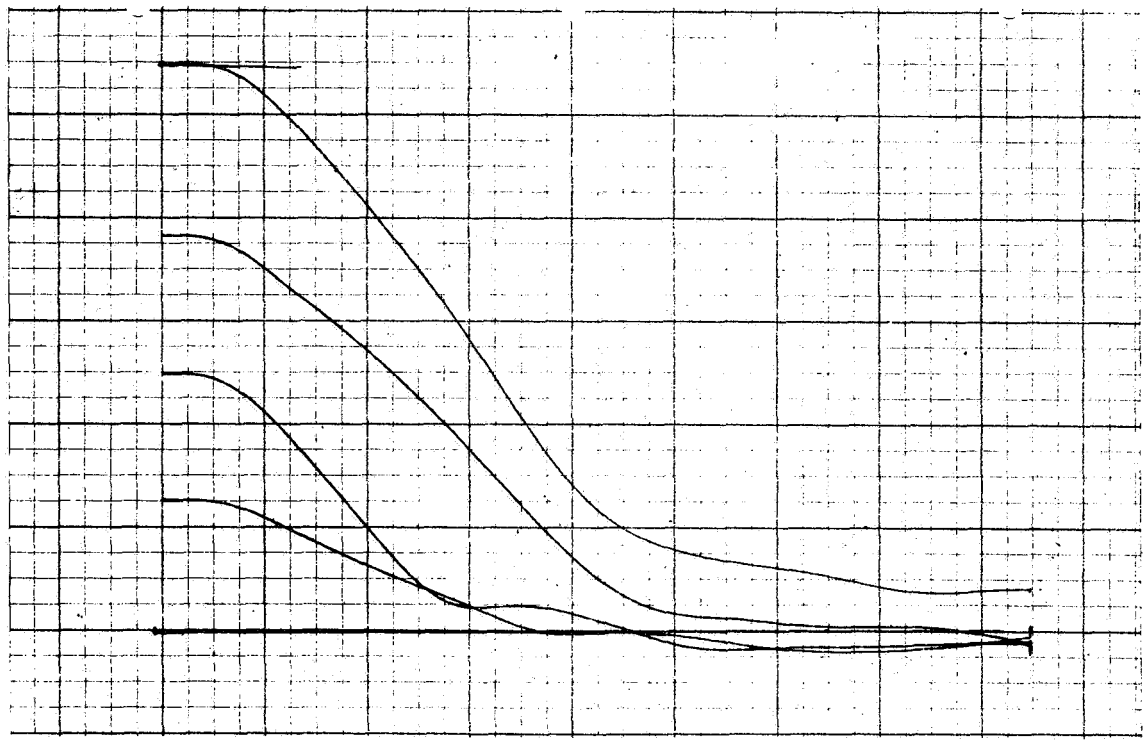

Run 3

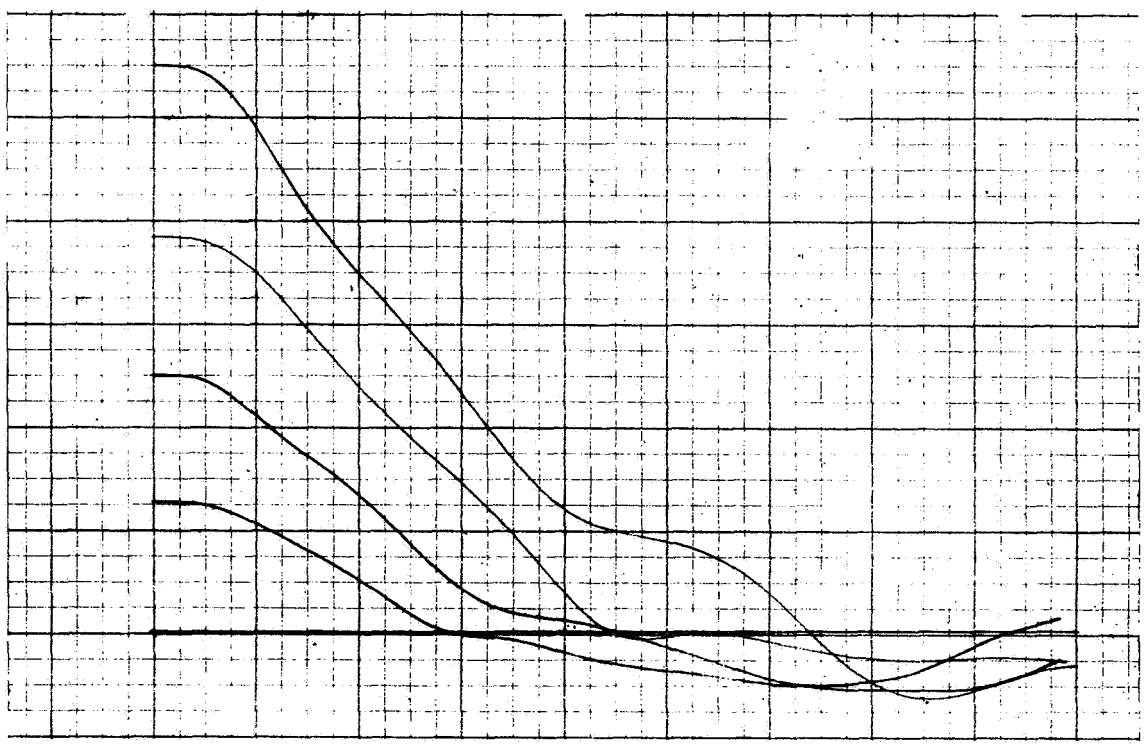

Run 4

Figure A-4. (Cont)

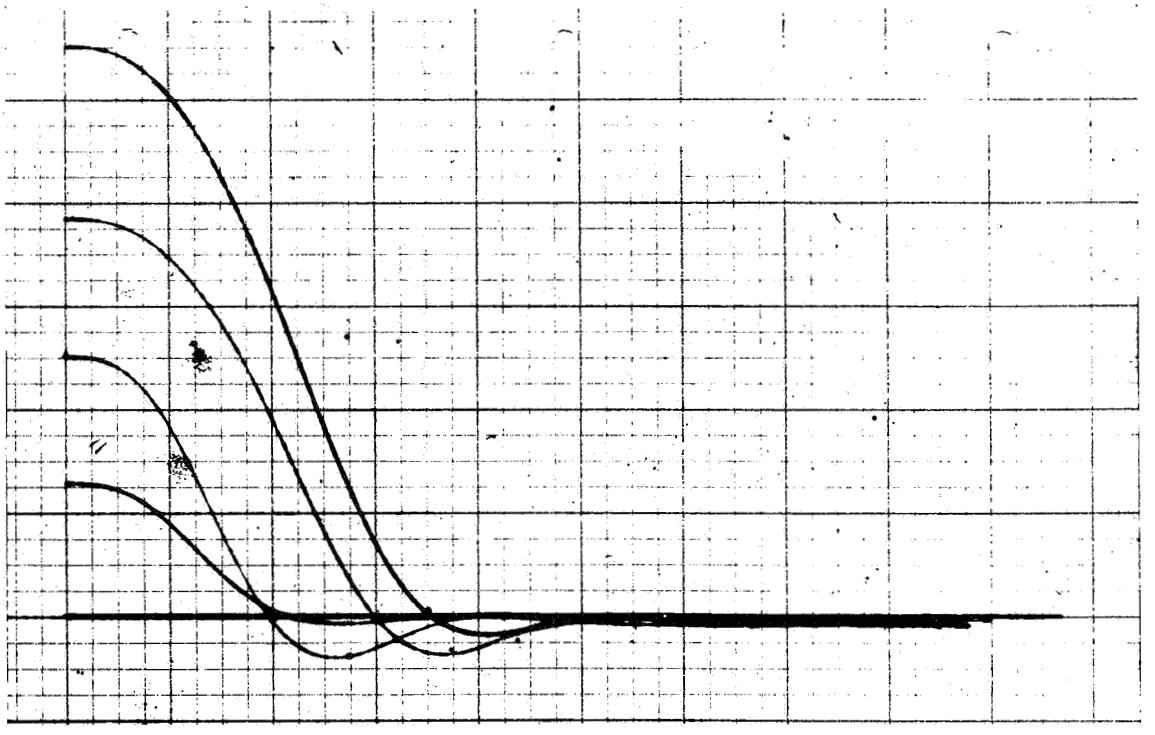

Run 1

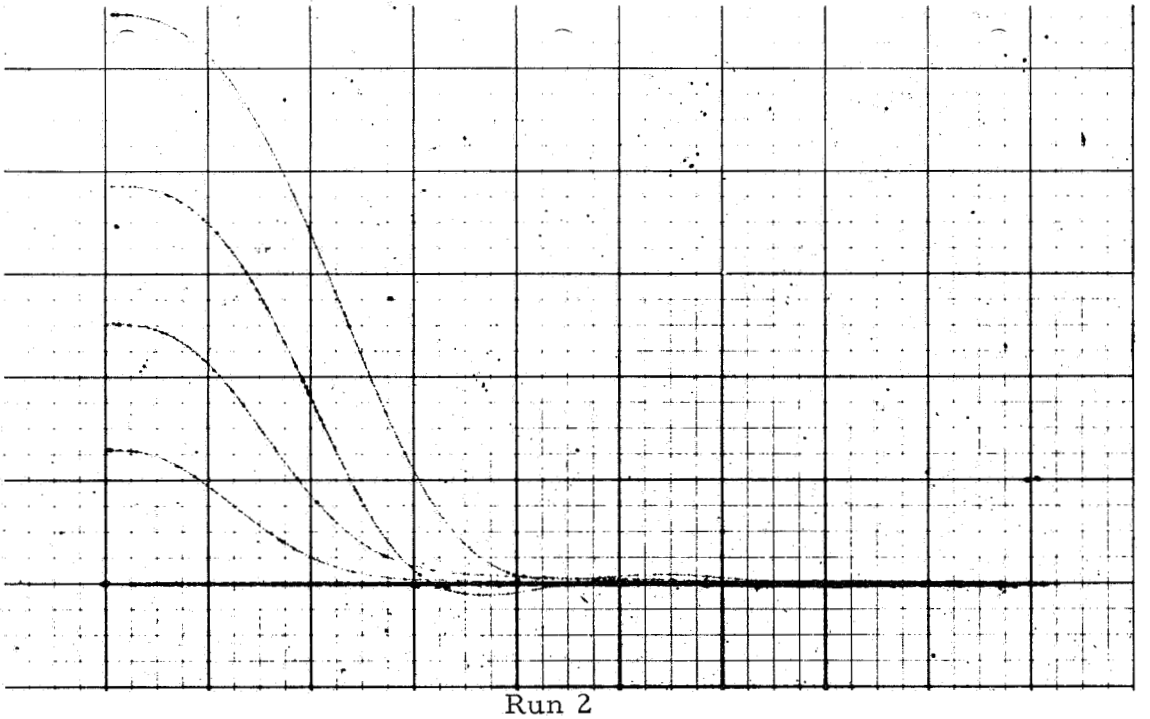

Run 2

Figure A-5. Subject 2 - 5 Seconds

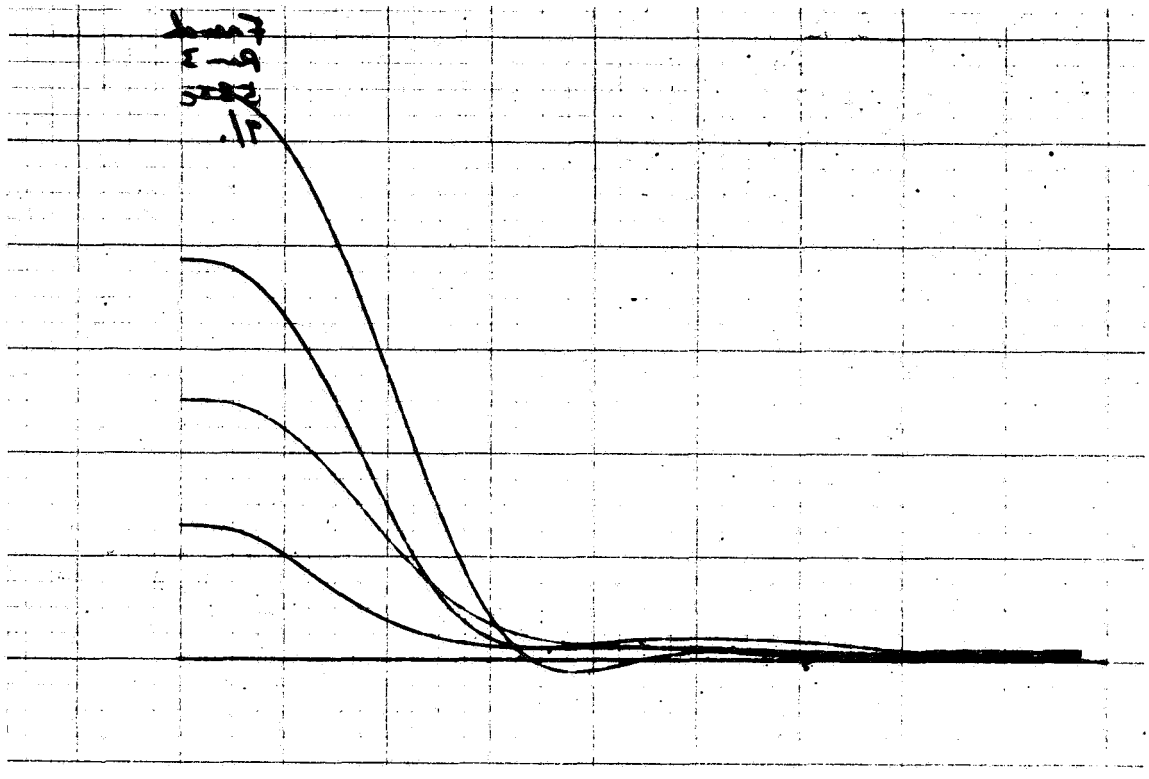

Run 3

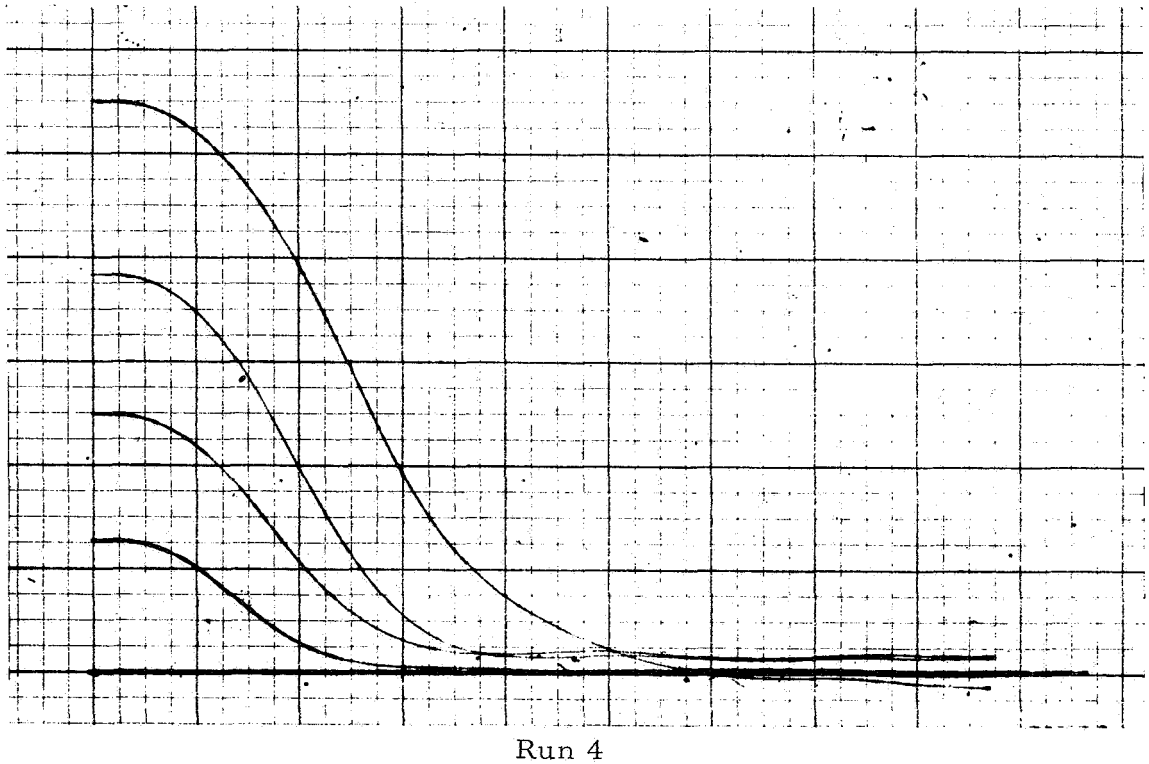

Run 4

Figure A-5. (Cont)

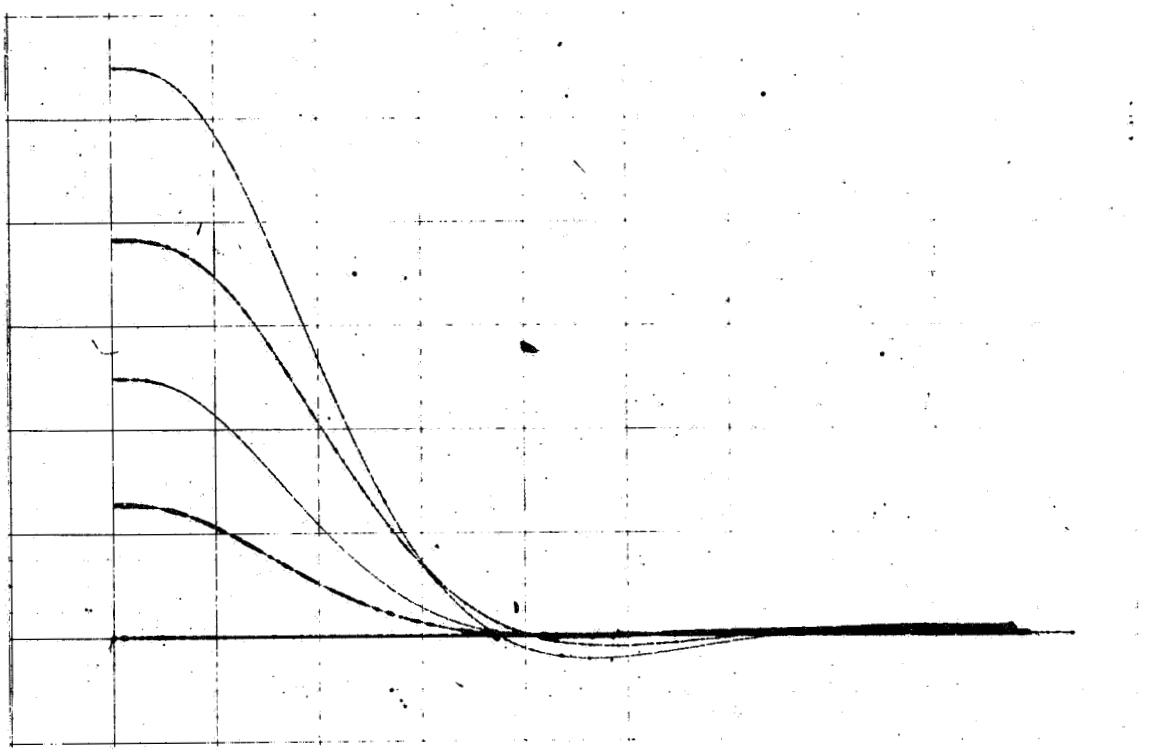

Run 1

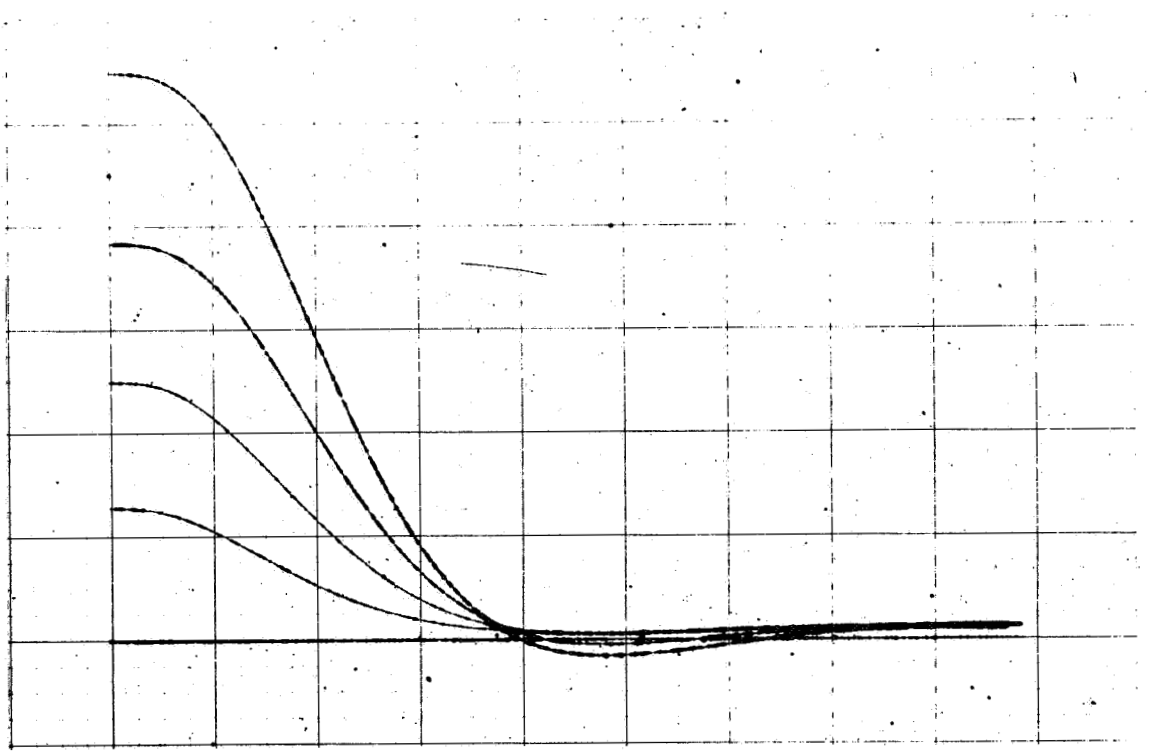

Run 2

Figure A-6. Subject 2 - 10 Seconds

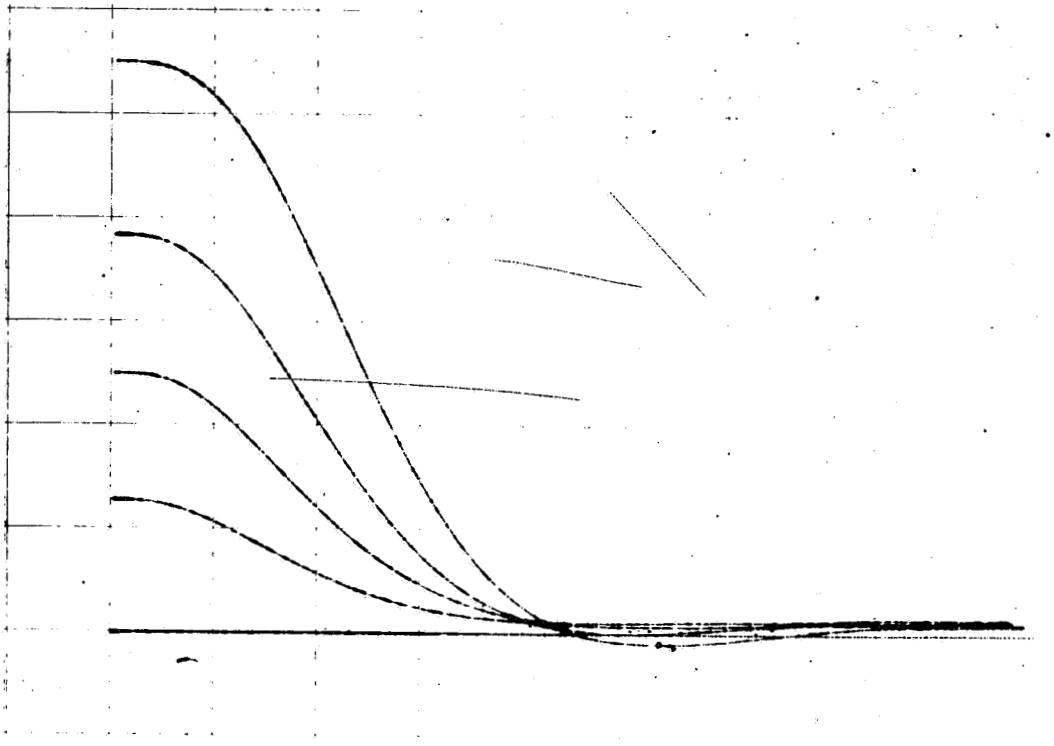

Run 3

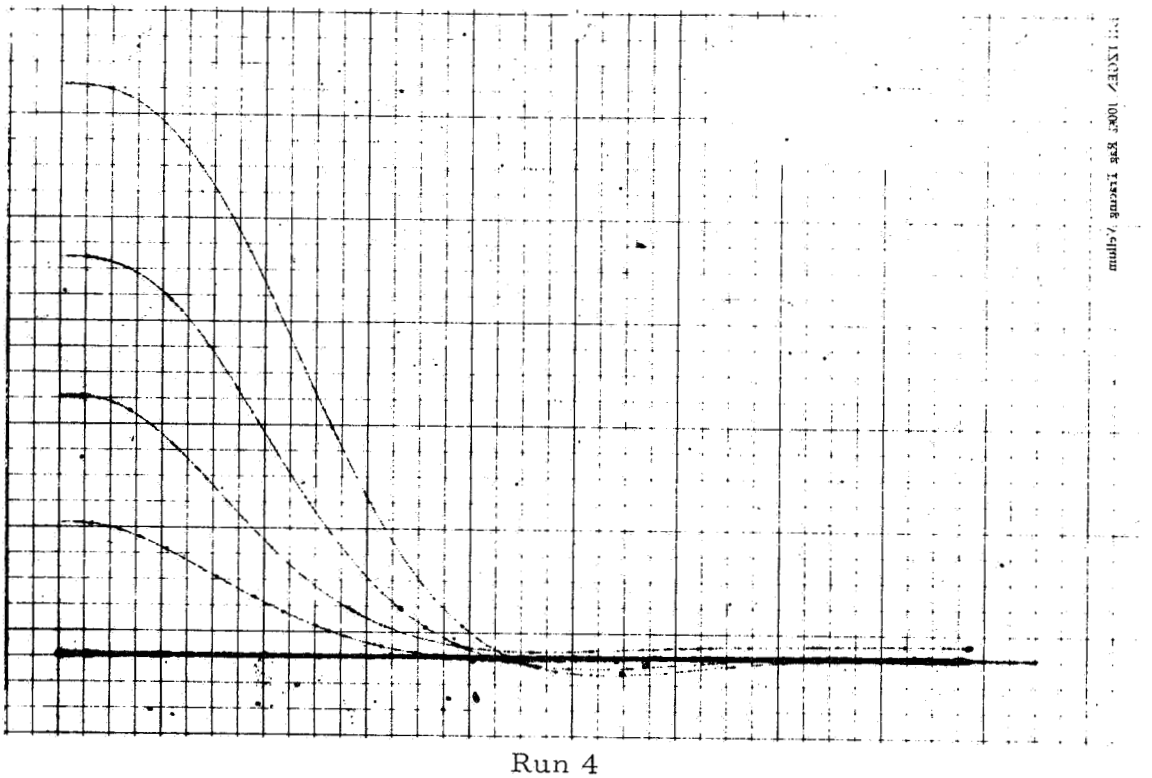

Run 4

Figure A-6. (Cont)

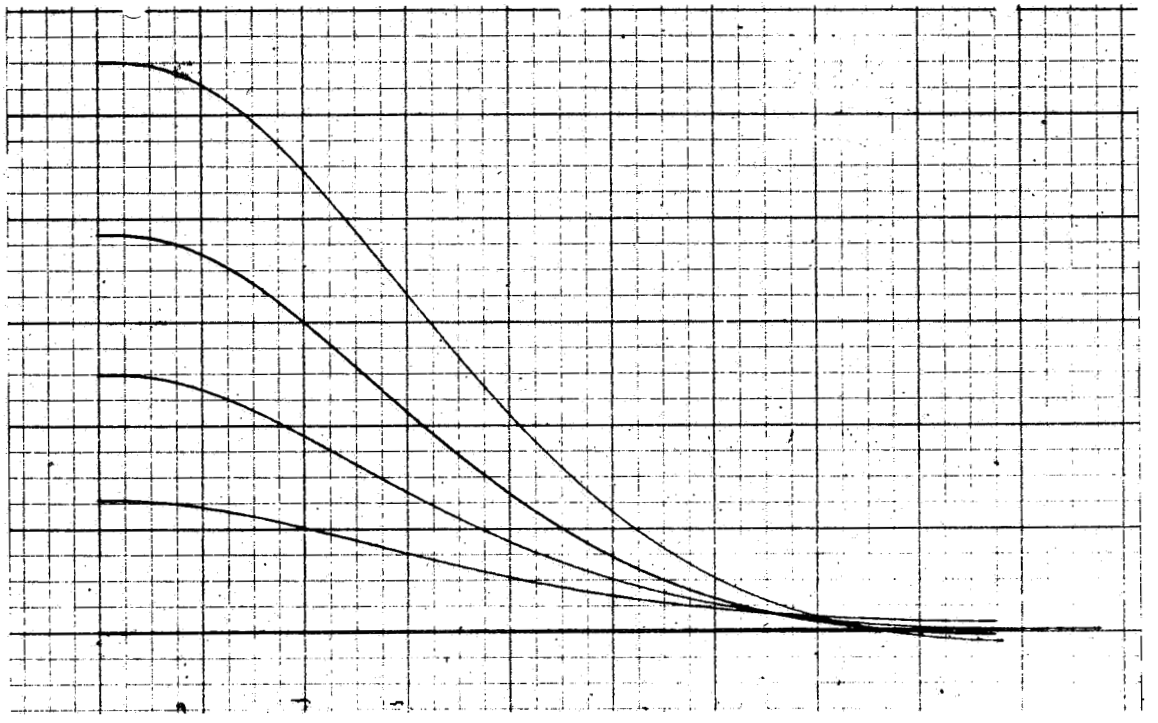

Run 1

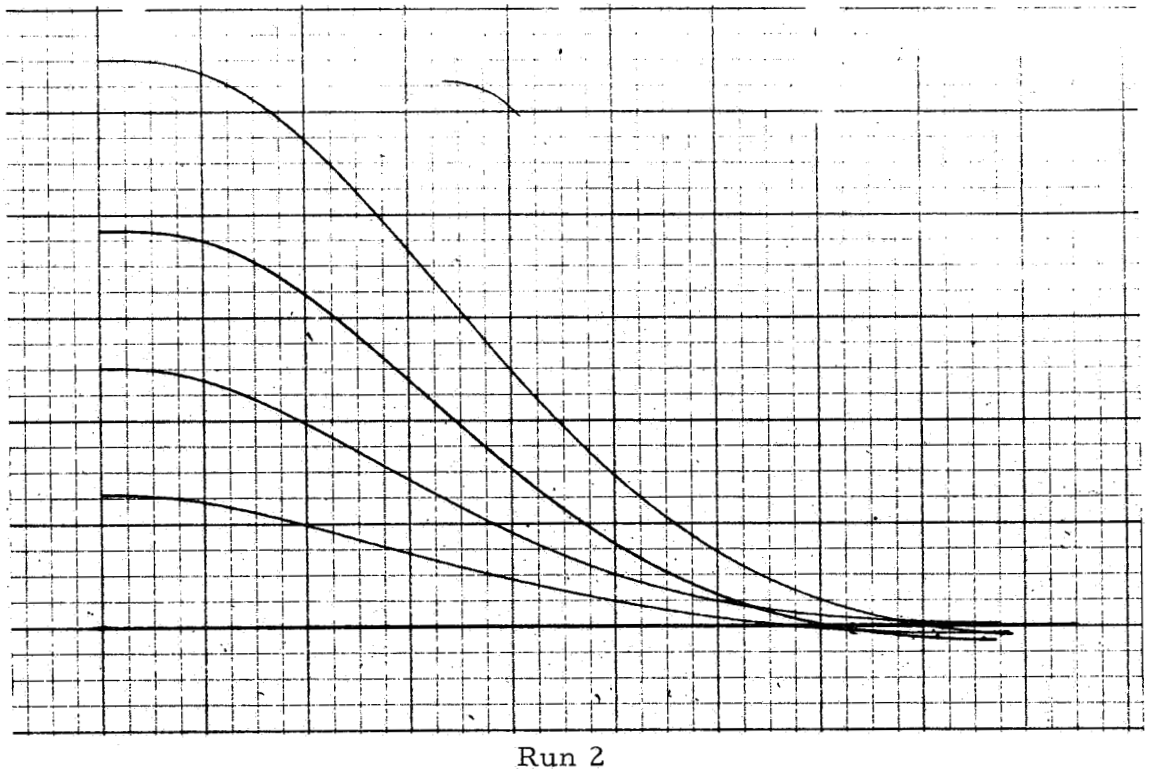

Run 2

Figure A-7. Subject 2 - 20 Seconds

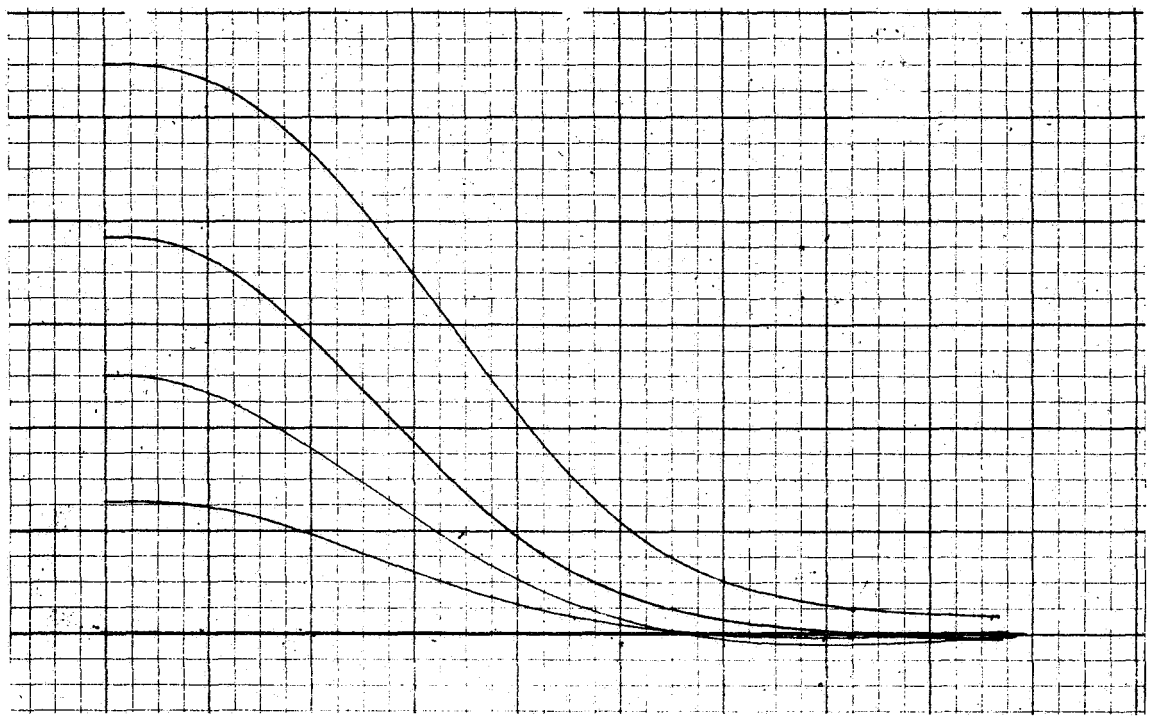

Run 3

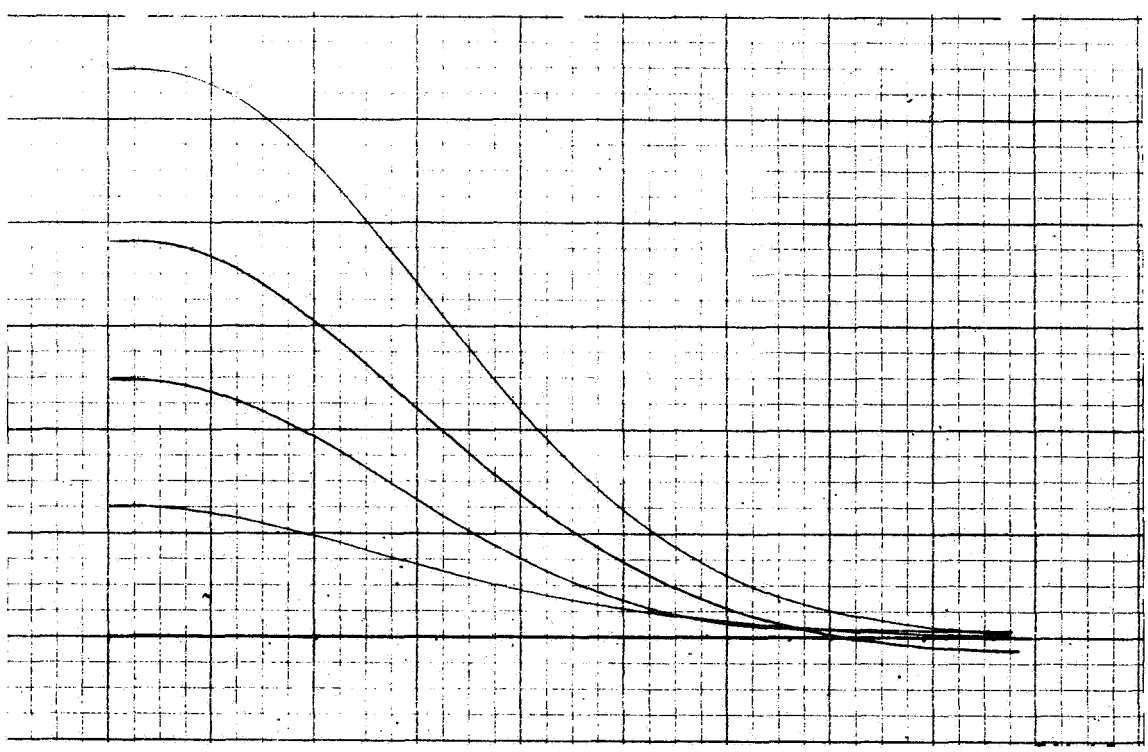

Run 4

Figure A-7. (Cont)

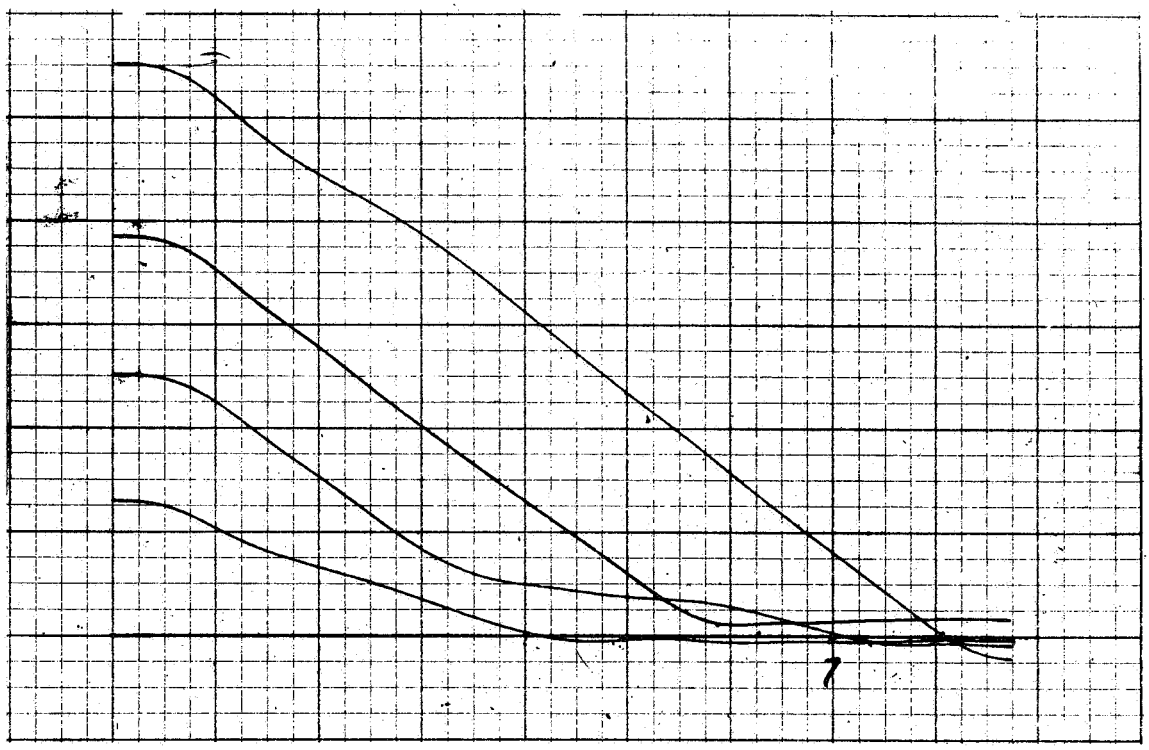

Run 1

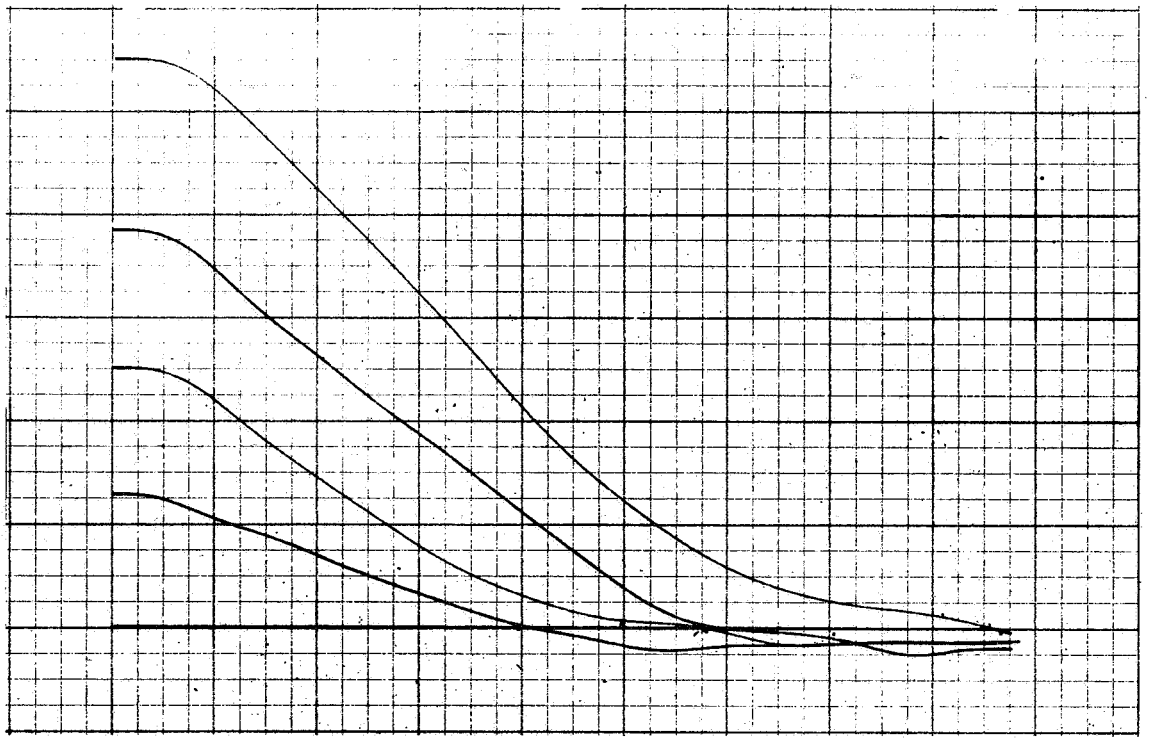

Run 2

Figure A-8. Subject 2 - Conventional

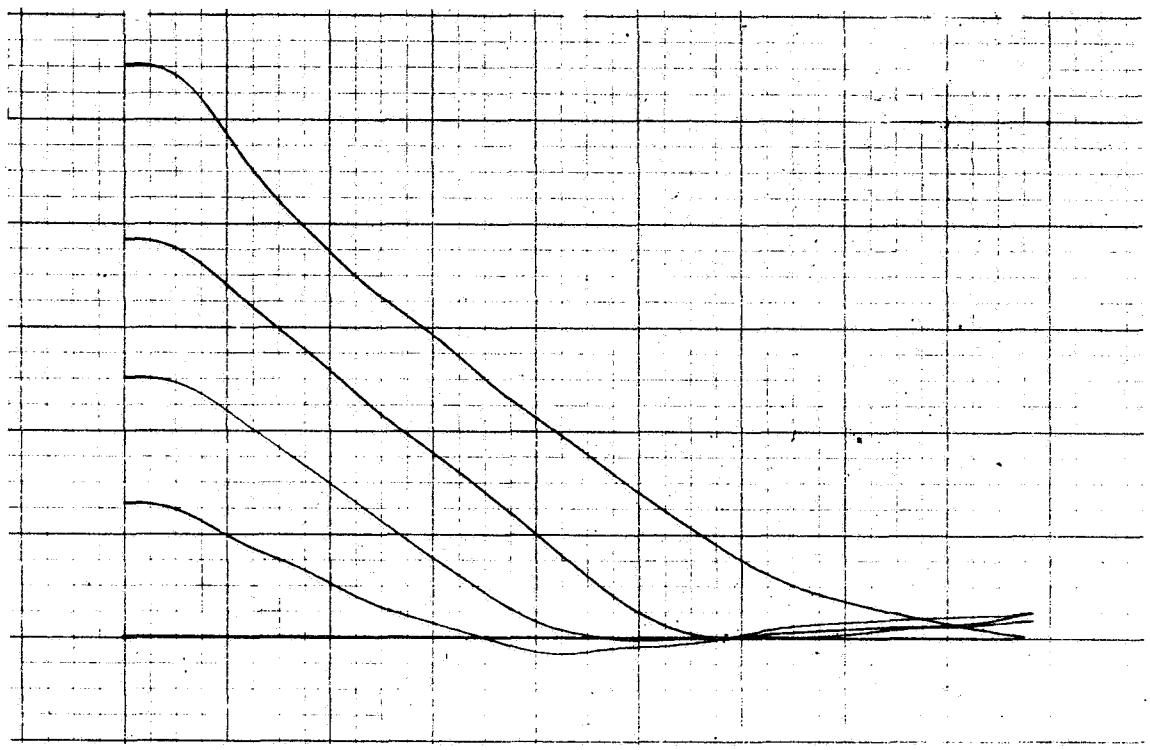

Run 3

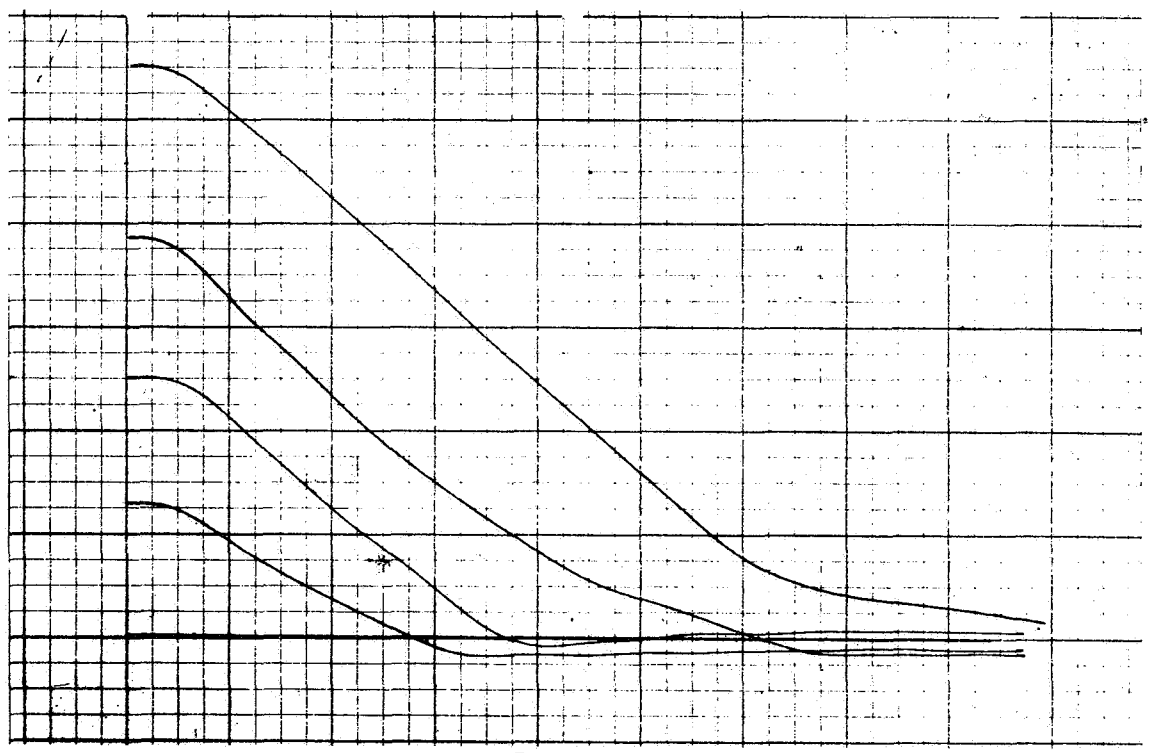

Run 4

Figure A-8. (Cont)

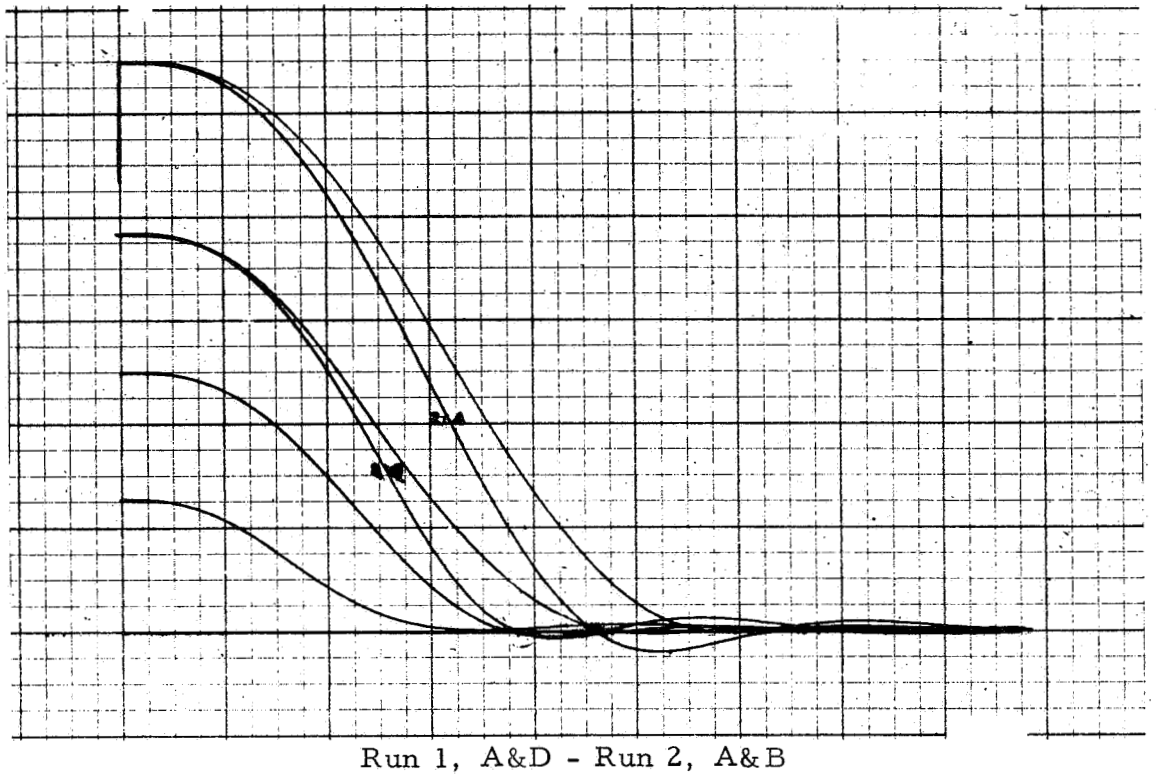

Run 1, A&D - Run 2, A&B

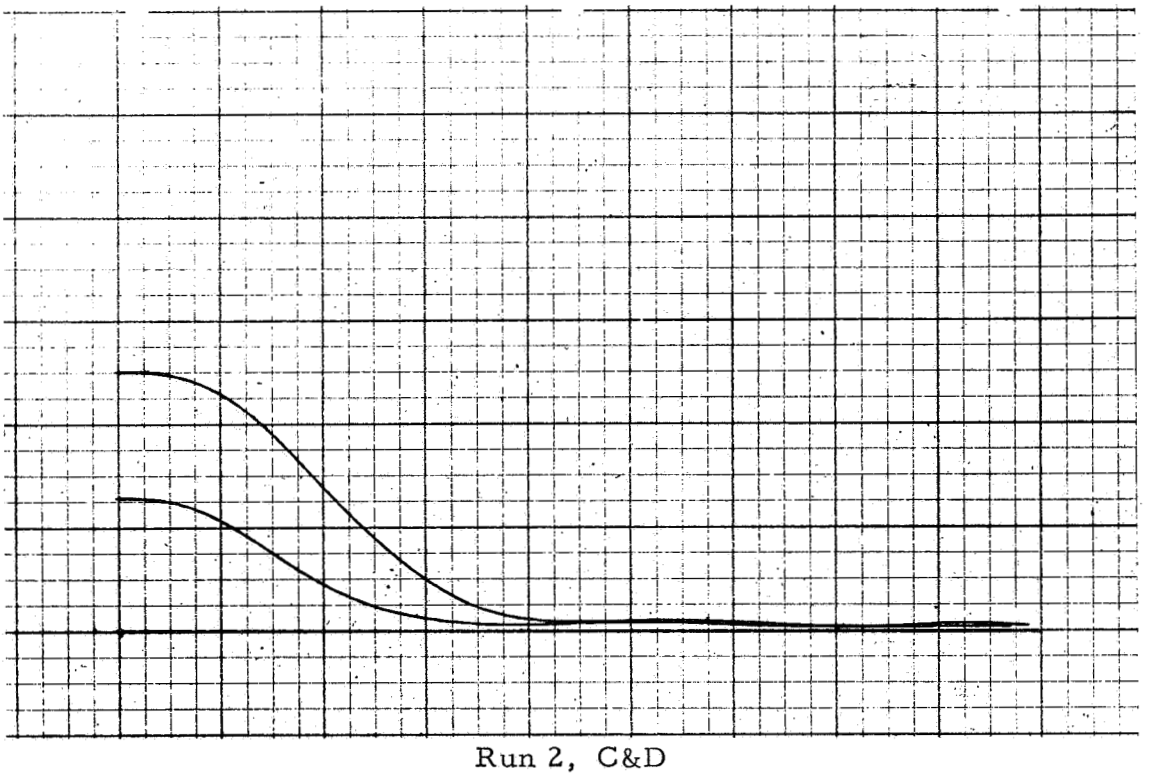

Run 2, C&D

Figure A-9. Subject 3 - 5 Seconds

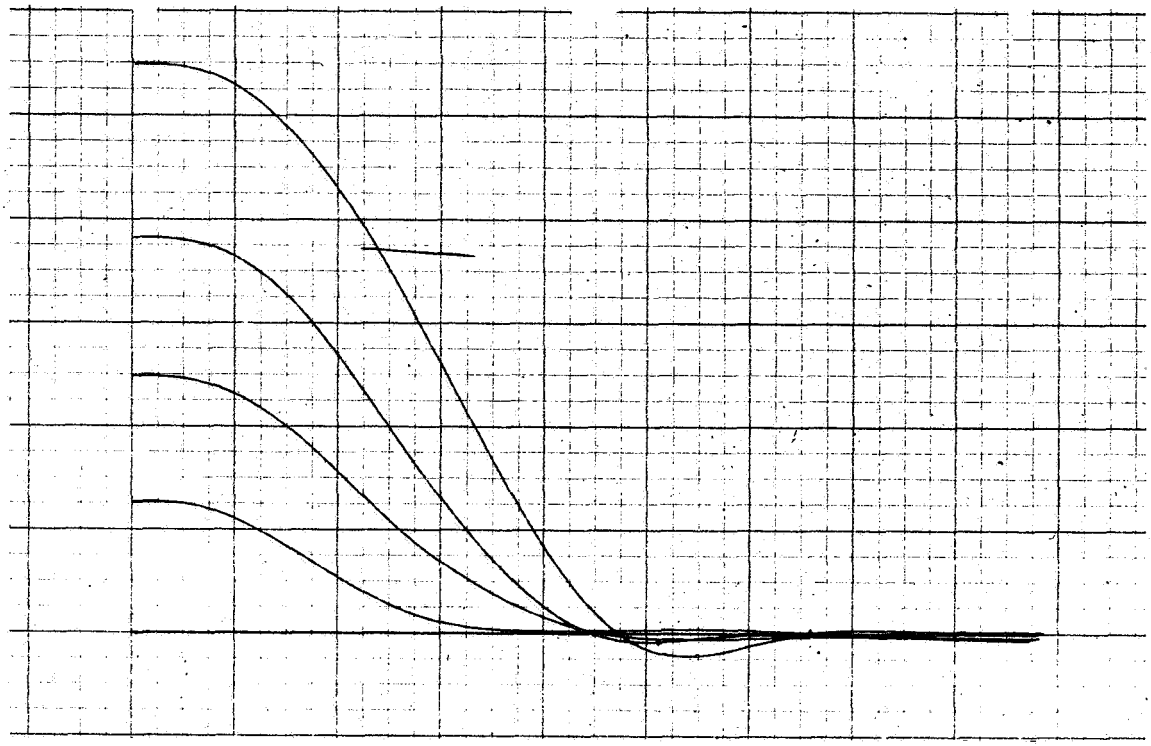

Run 3

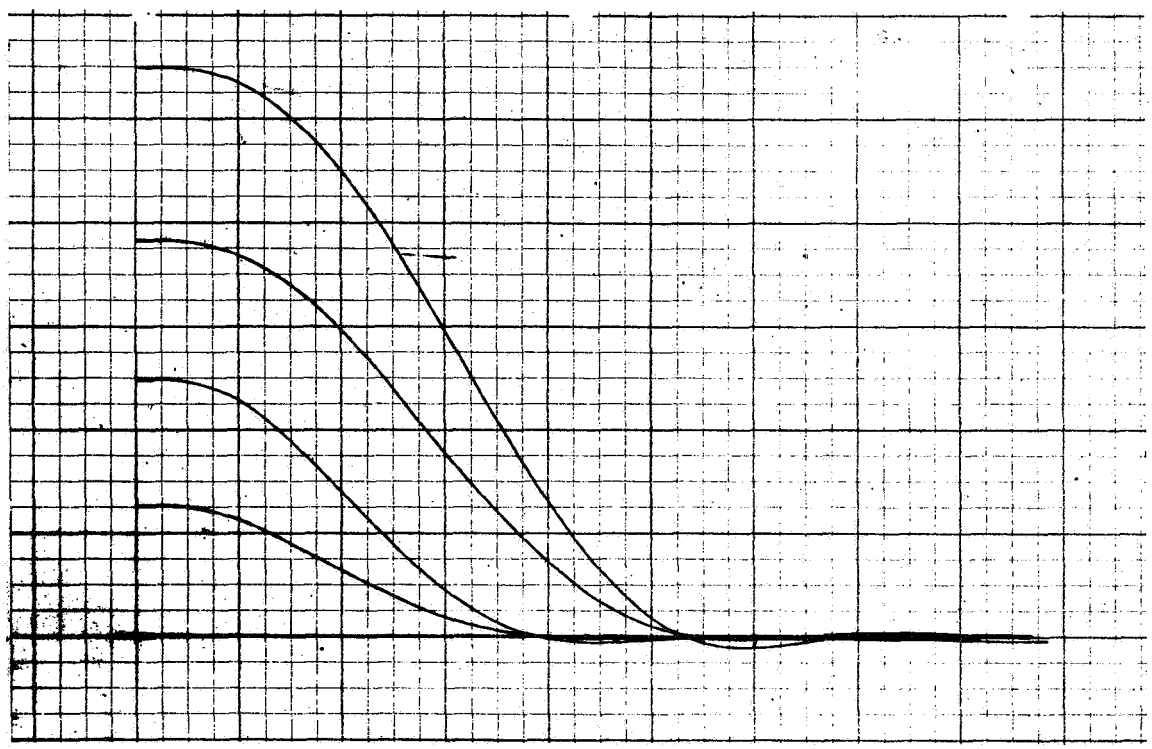

Run 4

Figure A-9. (Cont)

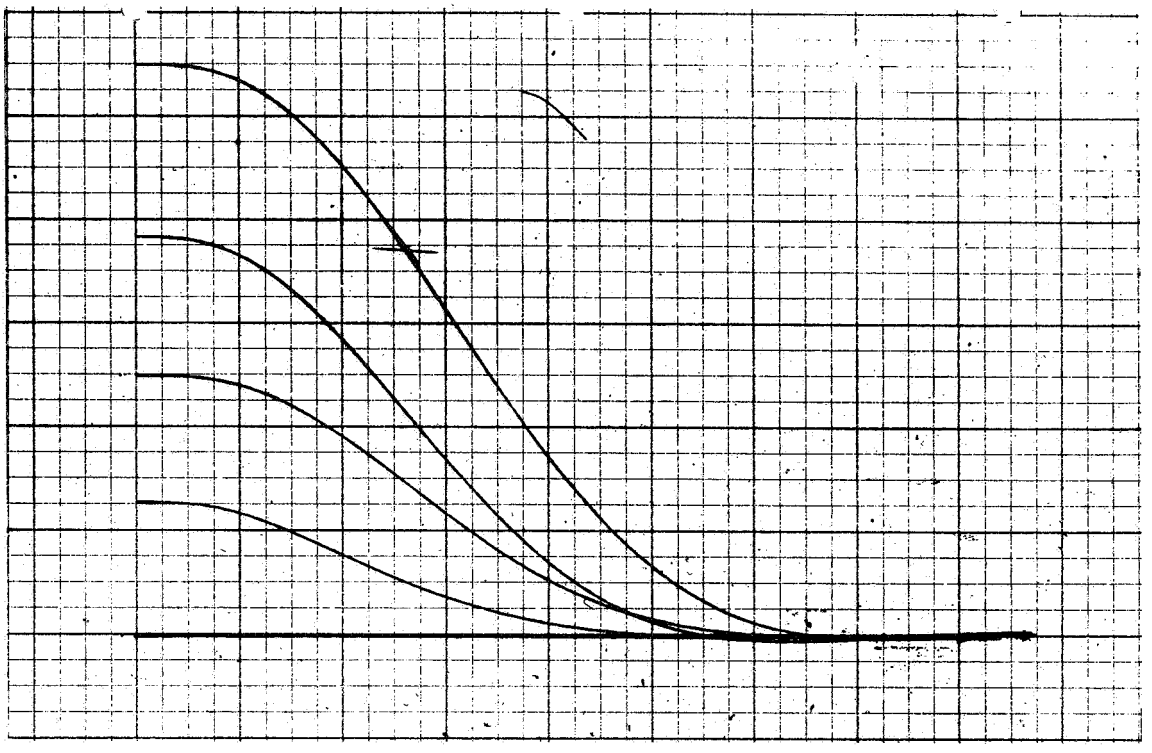

Run 1

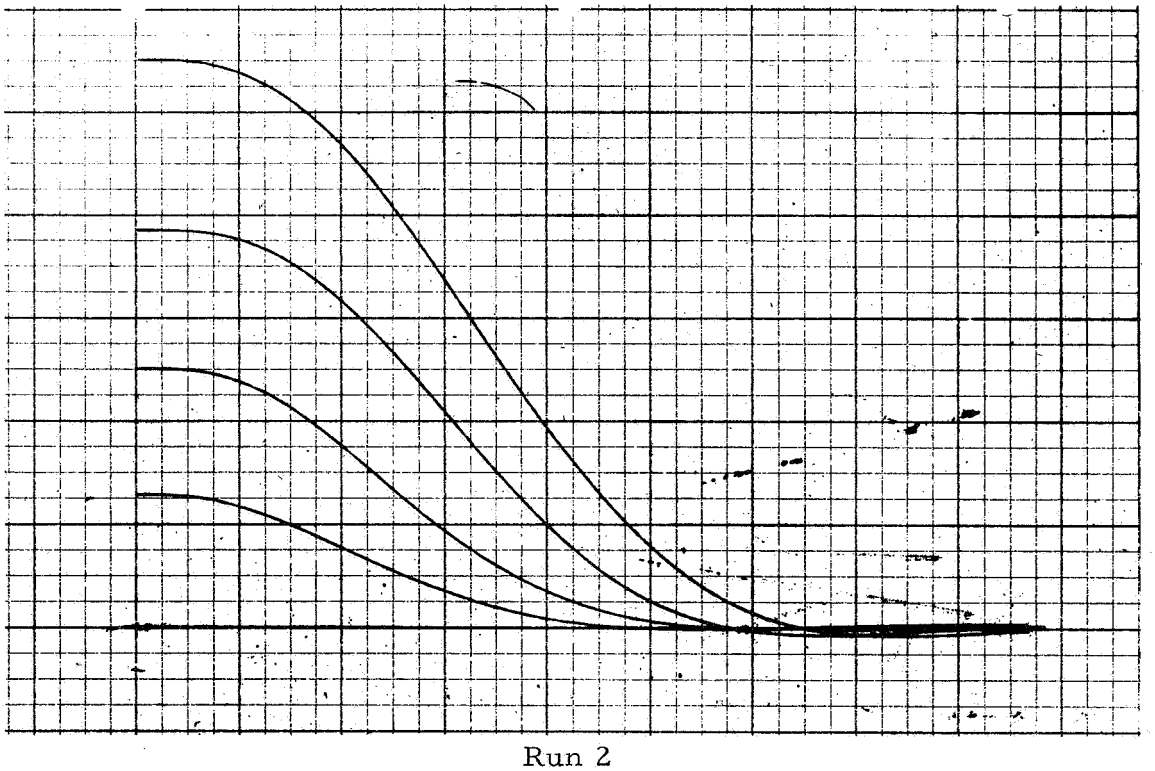

Run 2

Figure A-10. Subject 3 - 10 Seconds

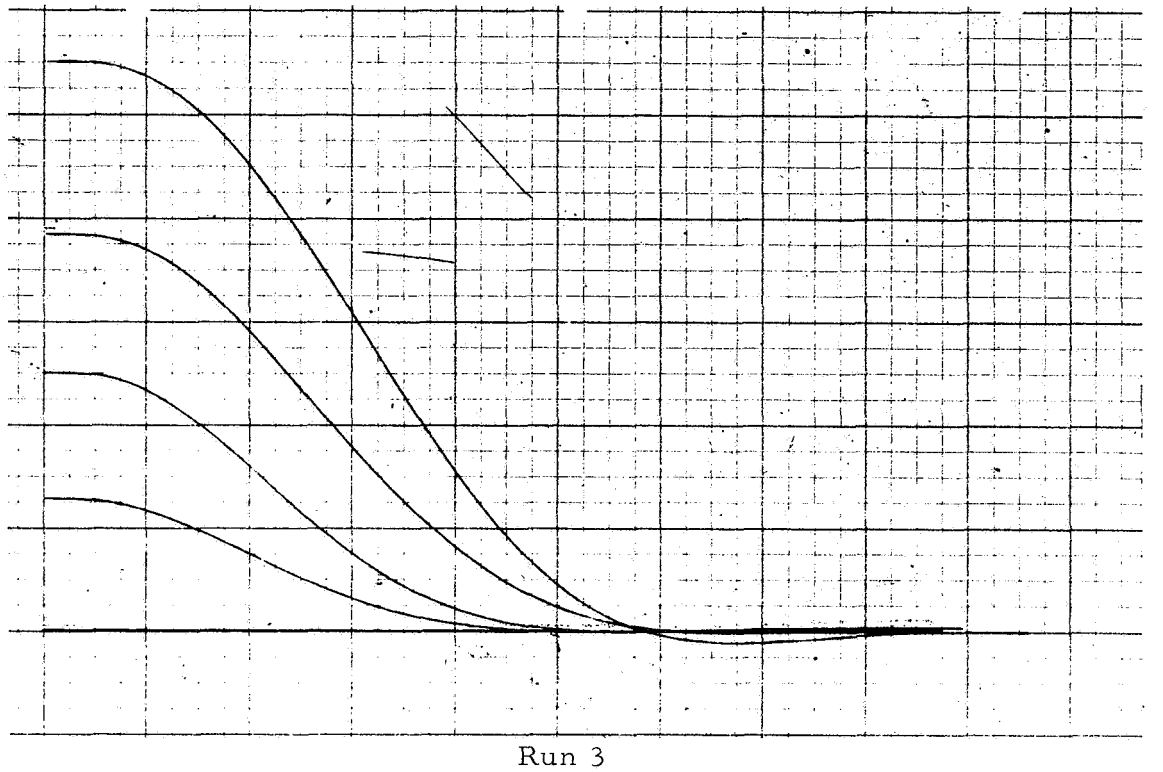

Run 3

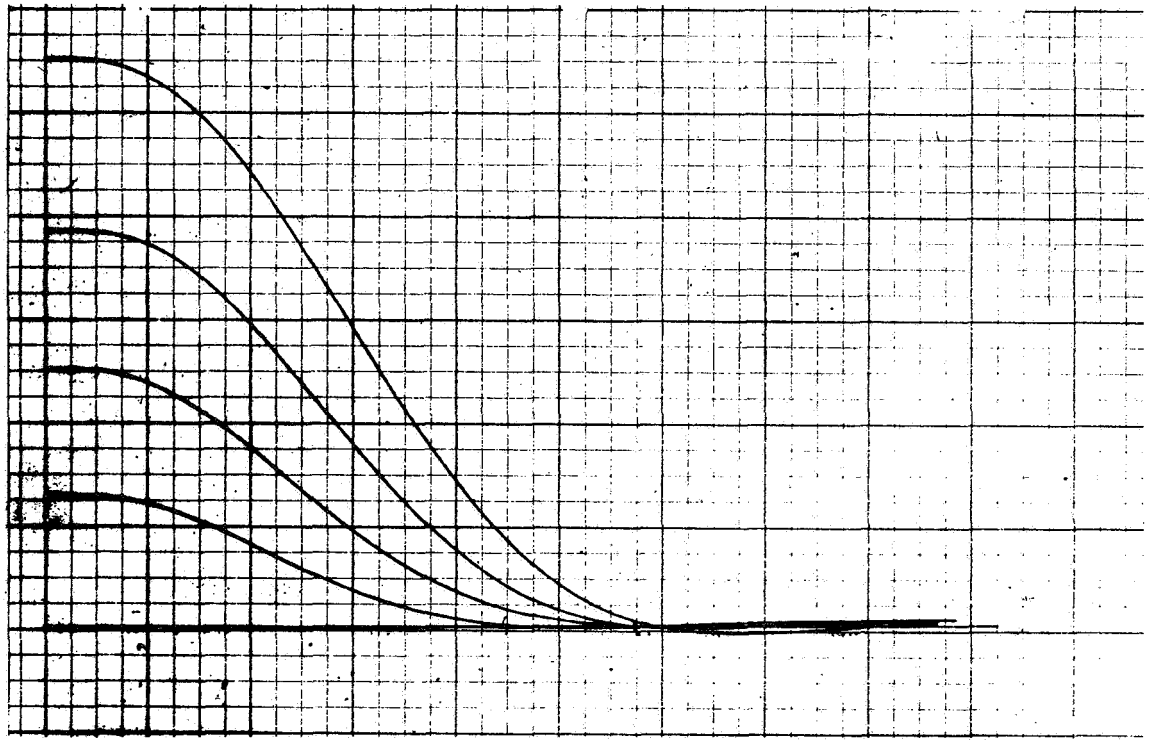

Run 4

Figure A-10. (Cont)

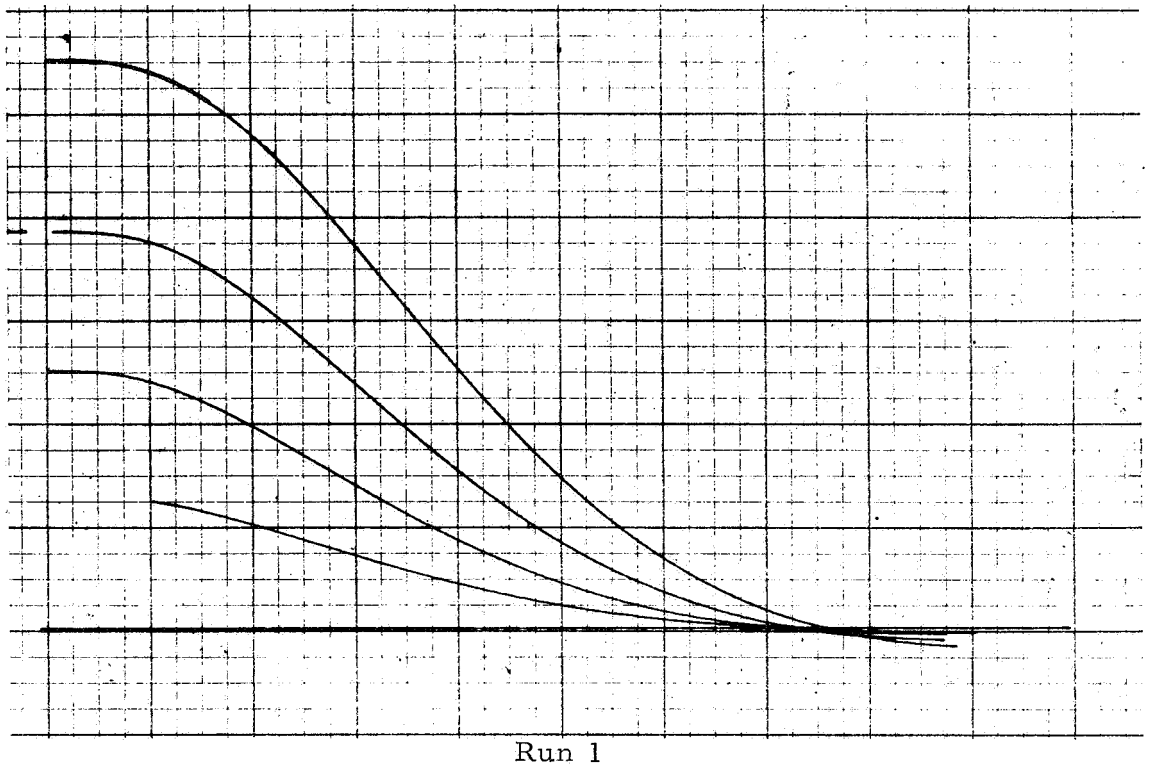

Run 1

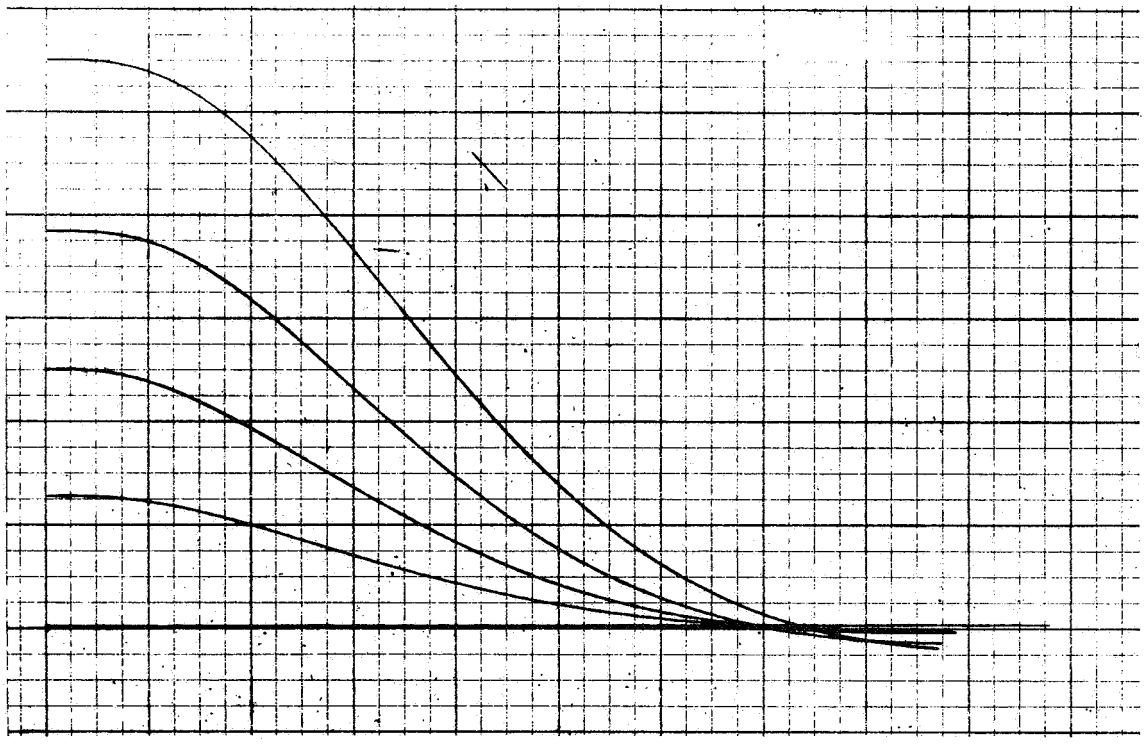

Run 2

Figure A-11. Subject 3 - 20 Seconds

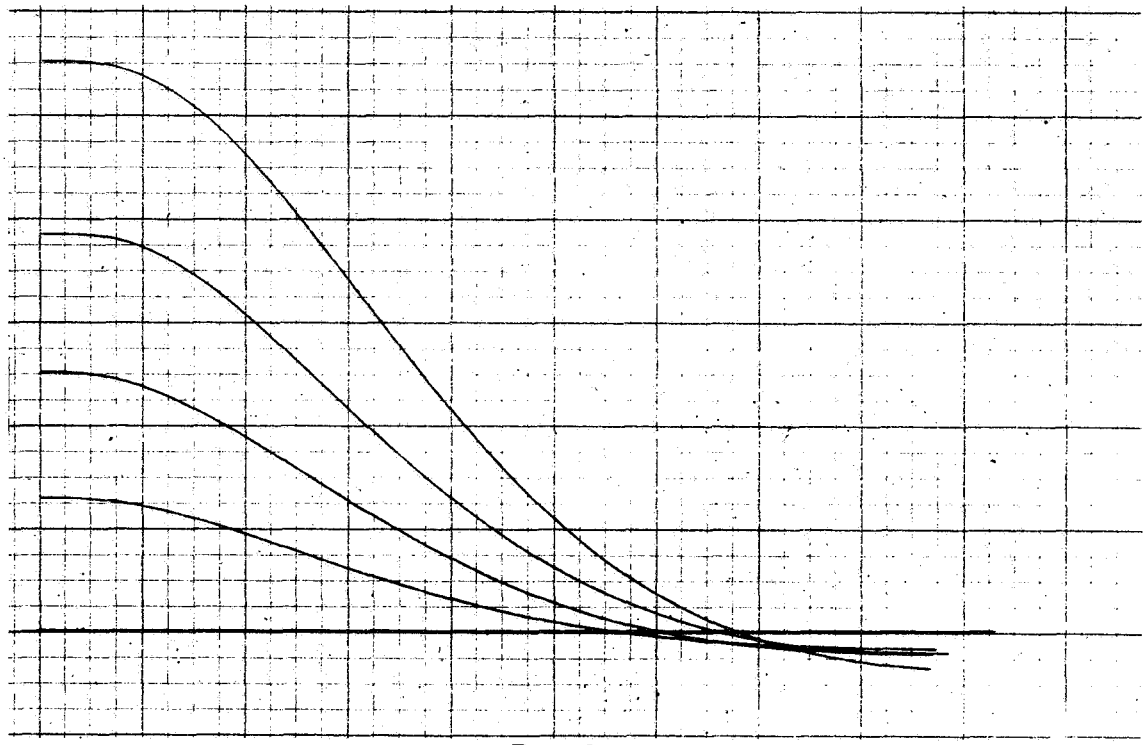

Run 3

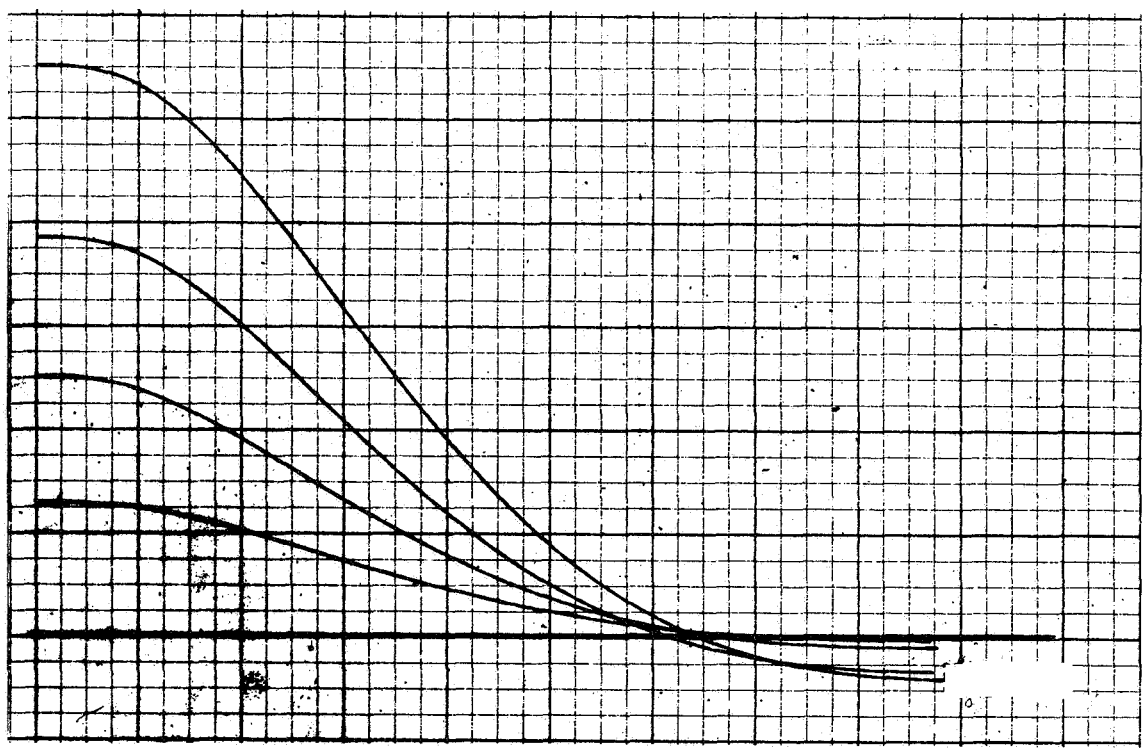

Run 4

Figure A-11. (Cont)

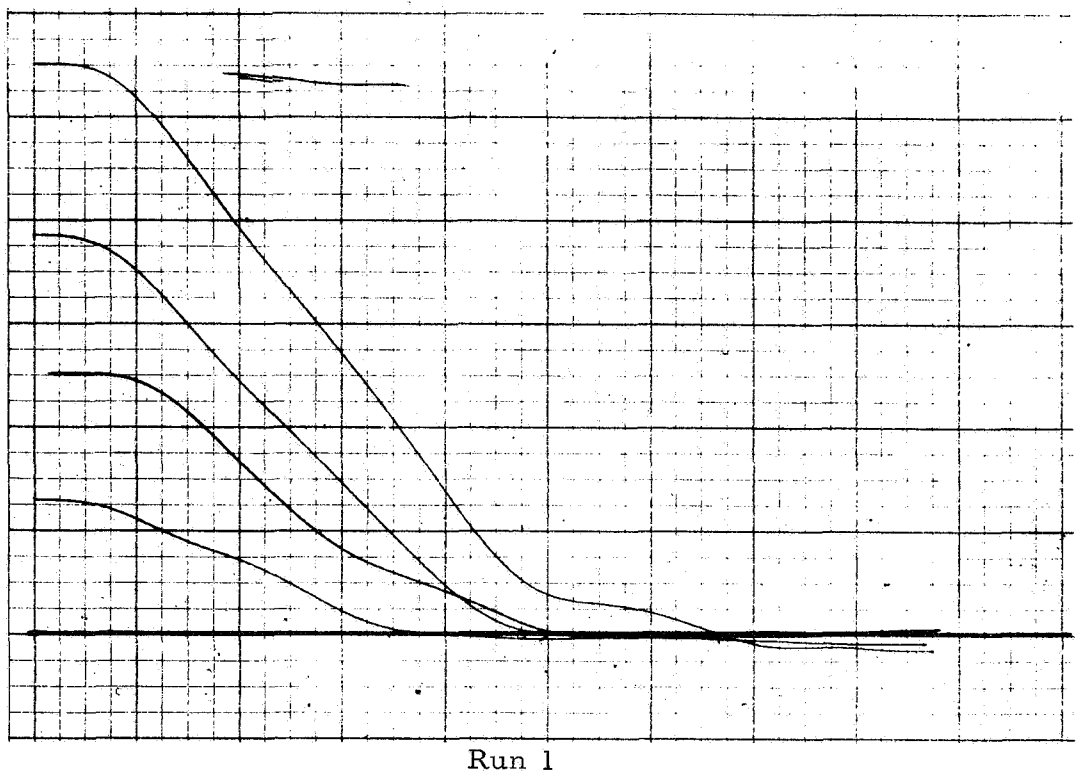

Run 1

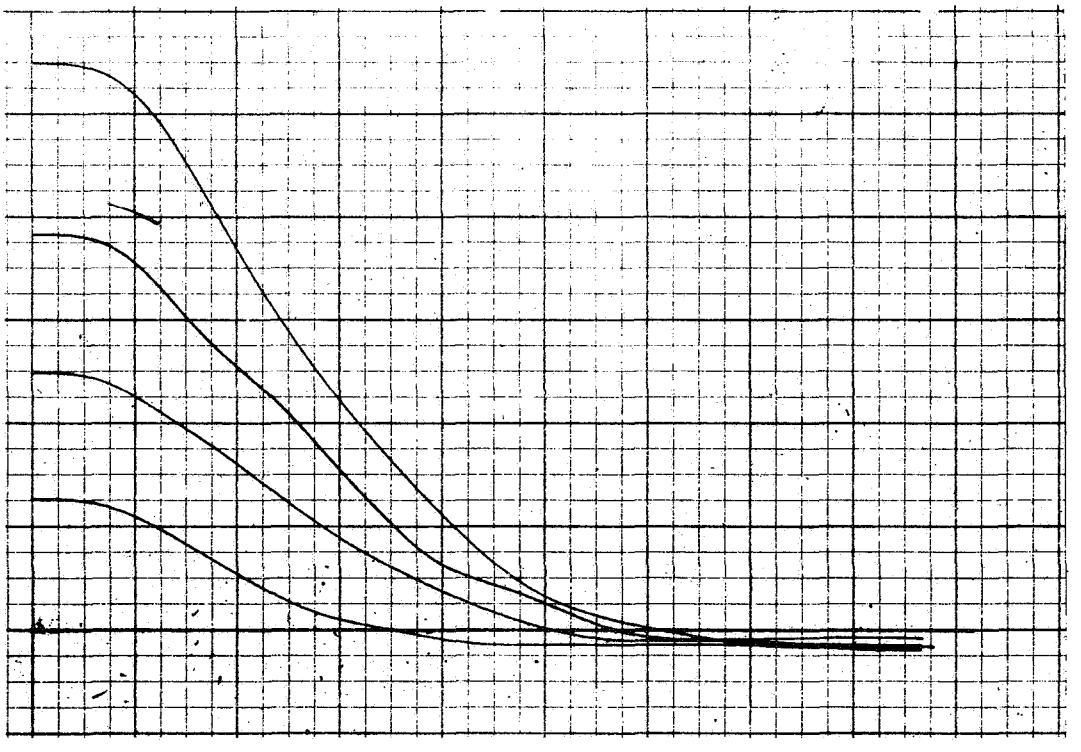

Run 2

Figure A-12. Subject 3 - Conventional

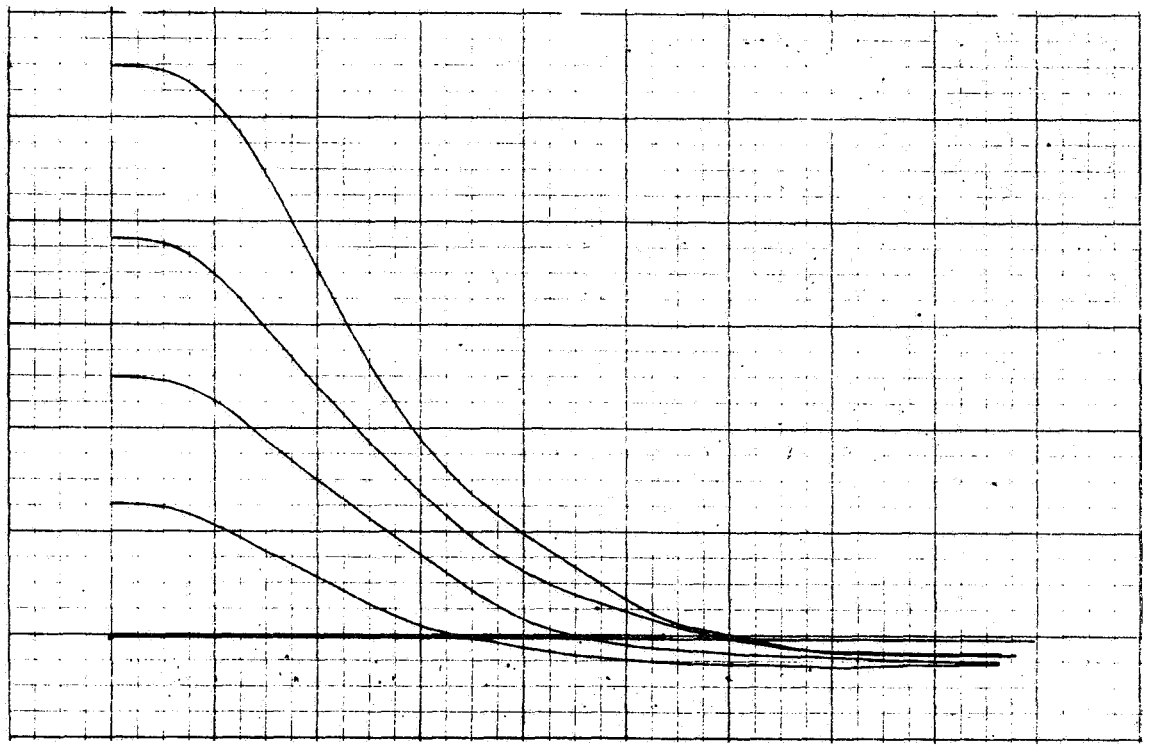

Run 3

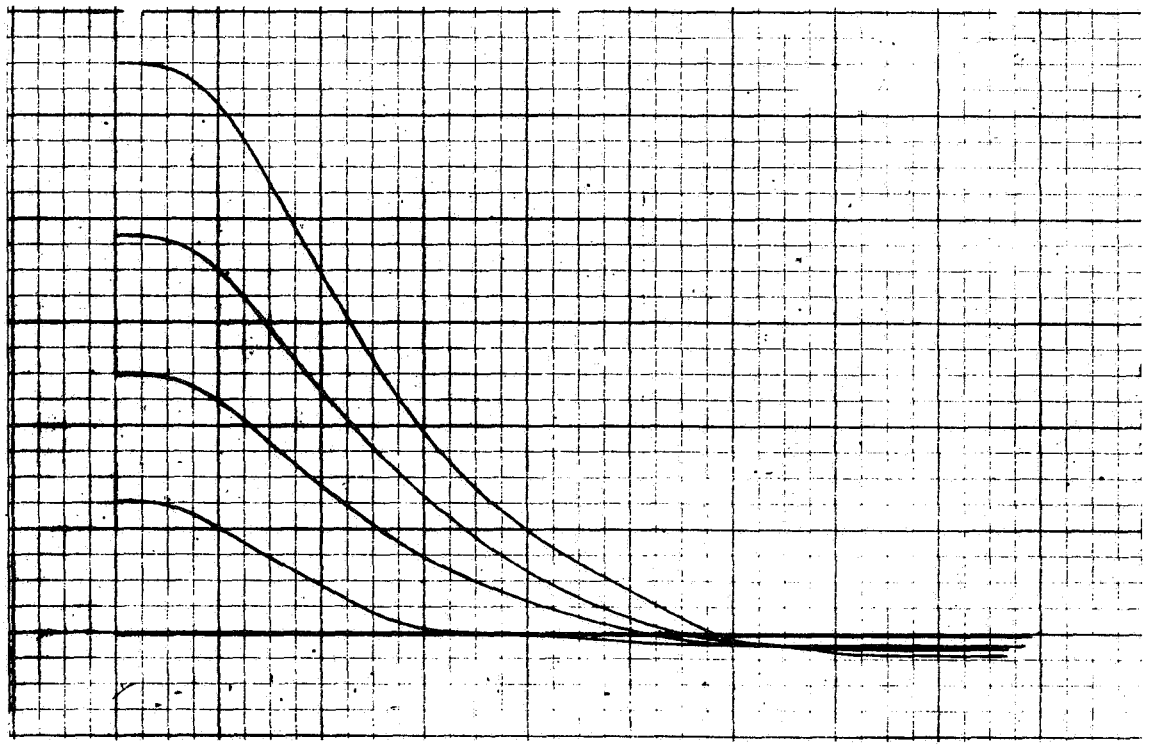

Run 4

Figure A-12. (Cont)

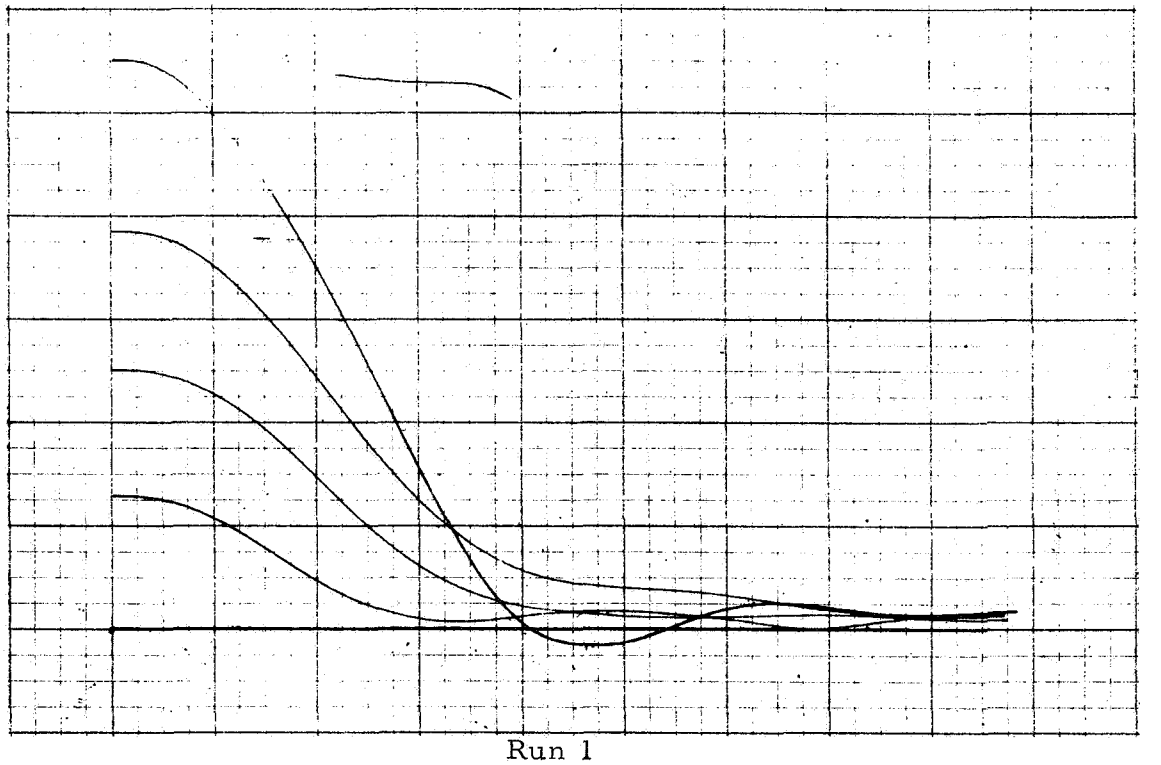

Run 1

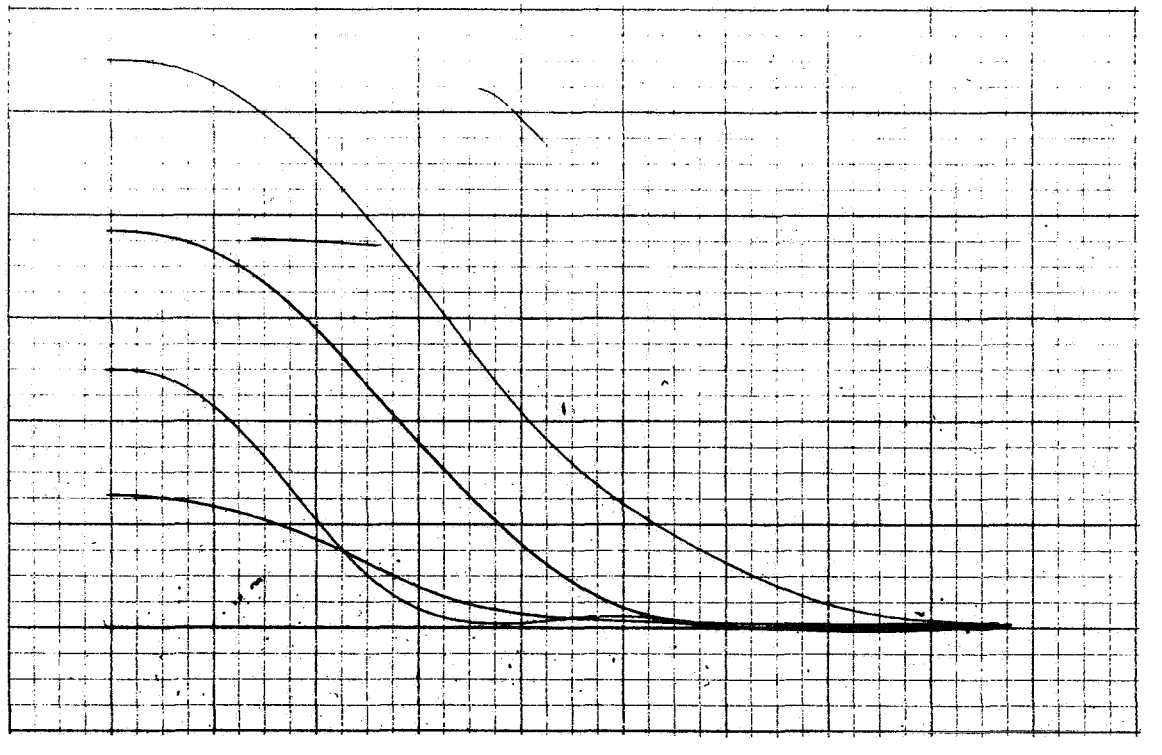

Run 2

Figure A-13. Subject 4 - 5 Seconds

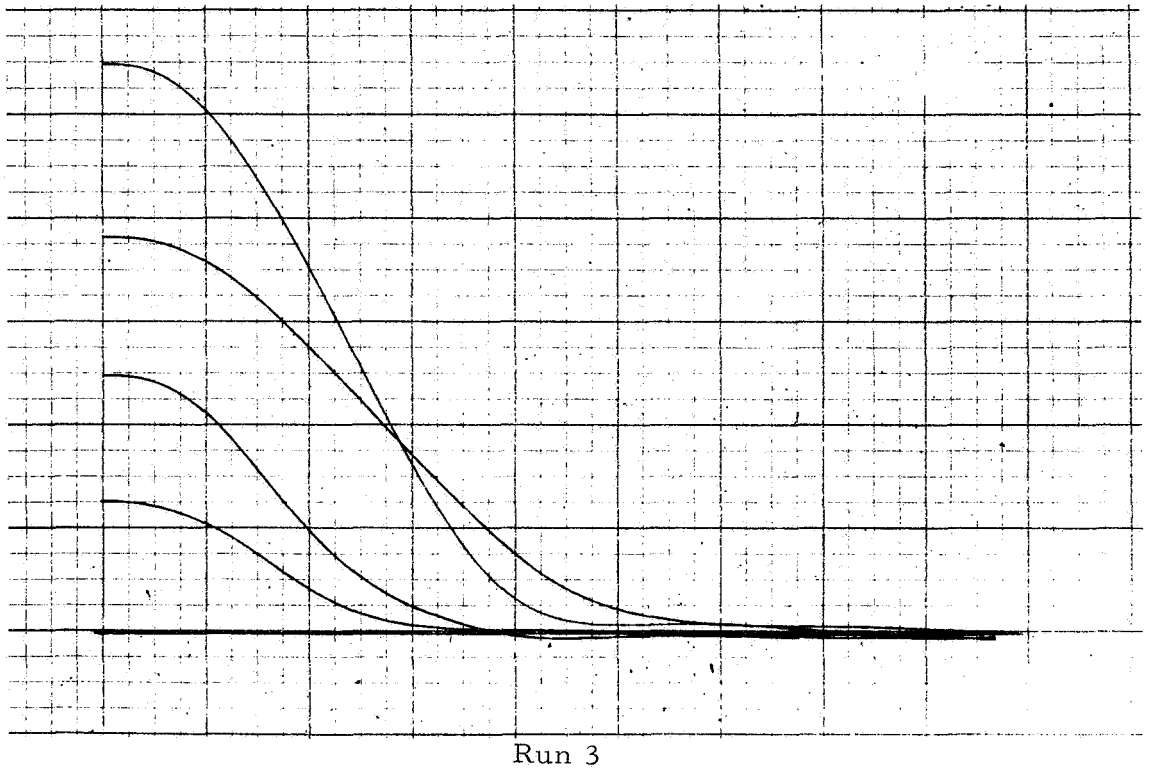

Run 3

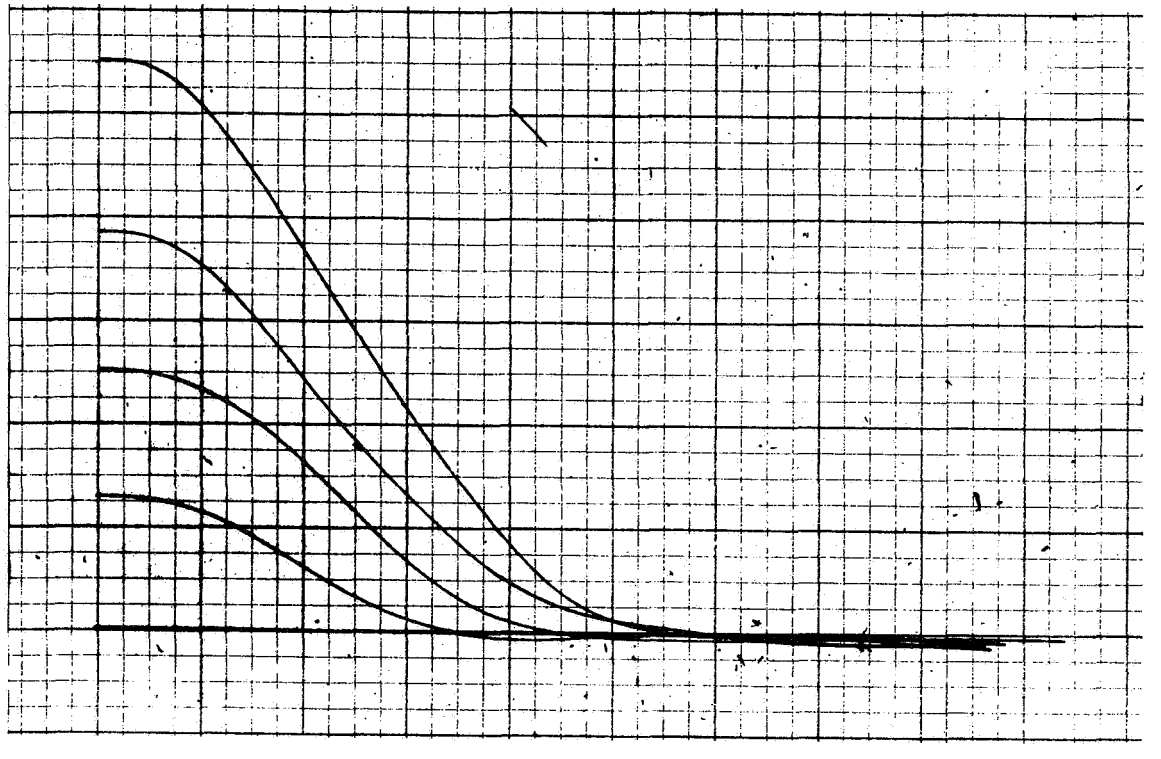

Run 4

Figure A-13. (Cont)

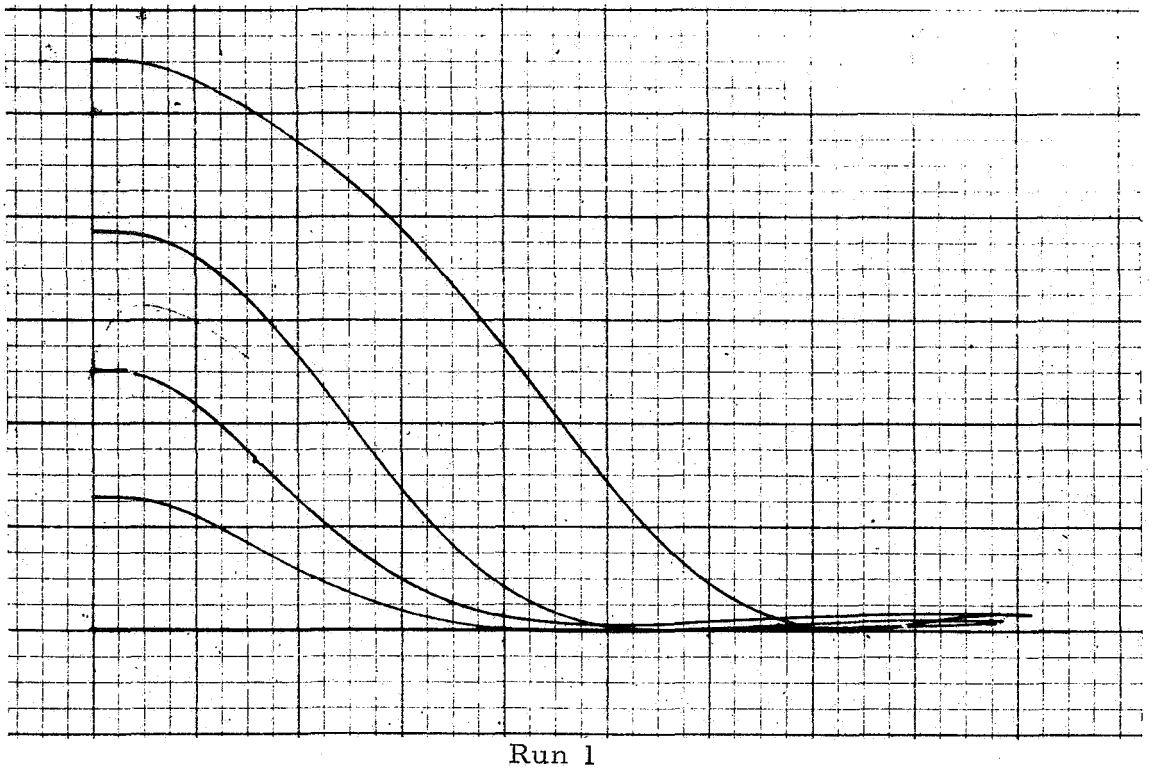

Run 1

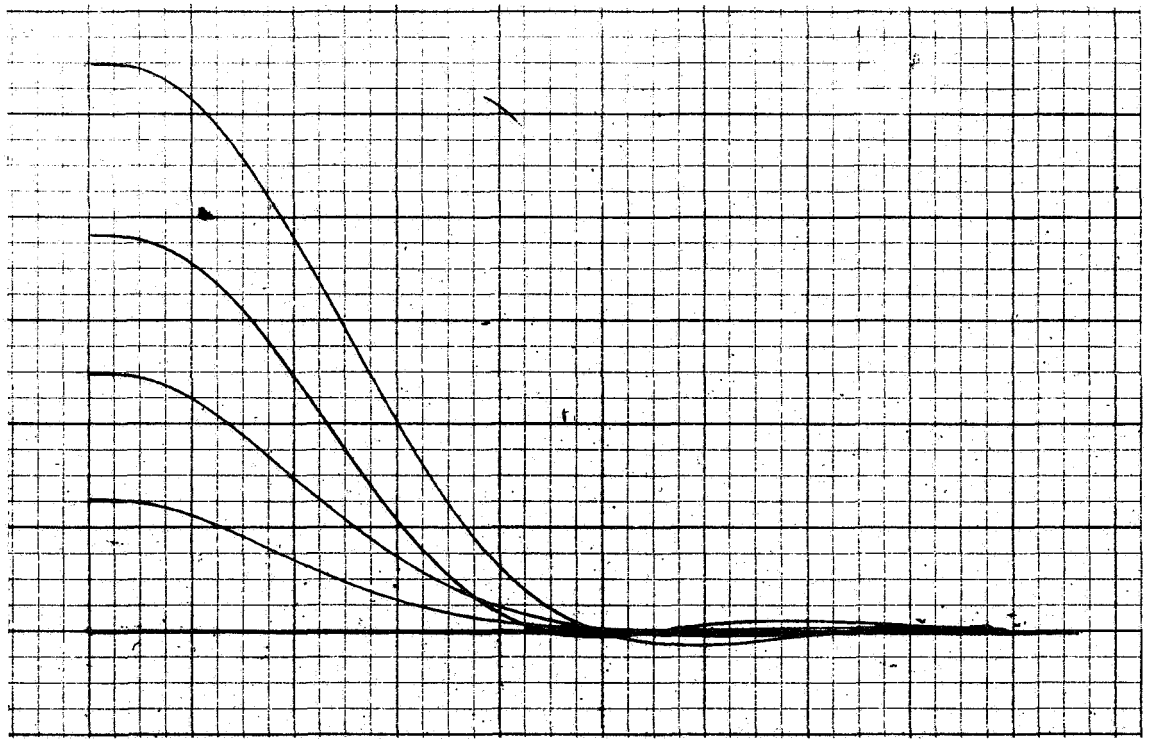

Run 2

Figure A-14. Subject 4 - 10 Seconds

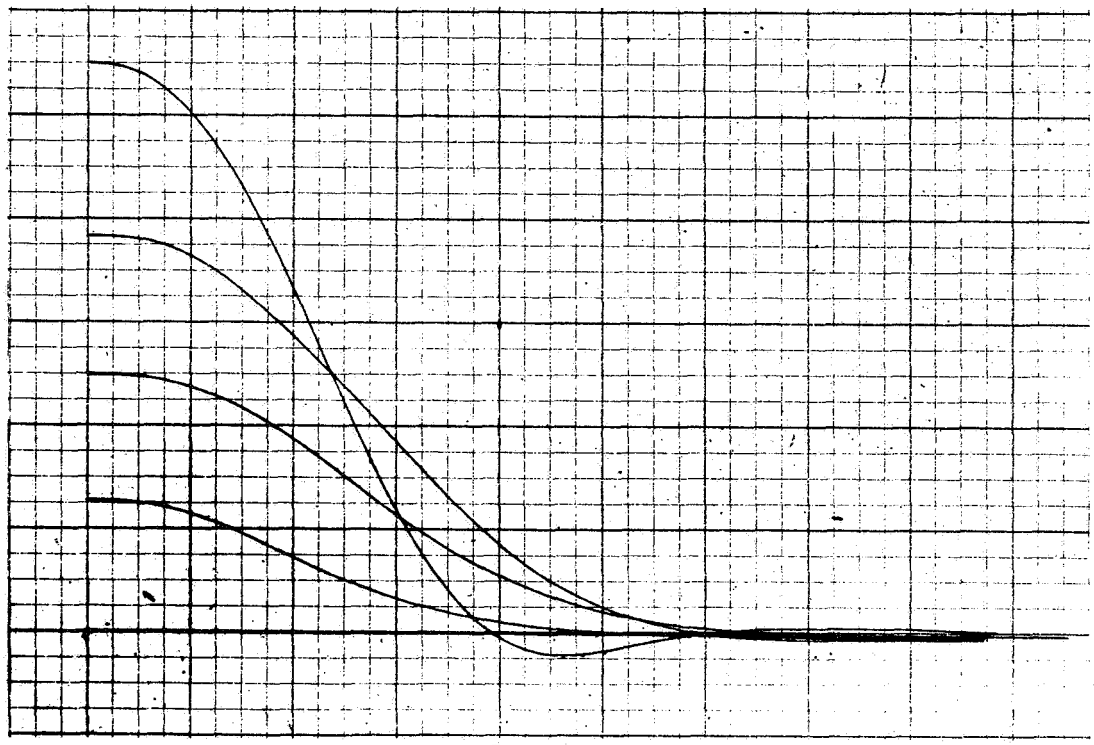

Run 3

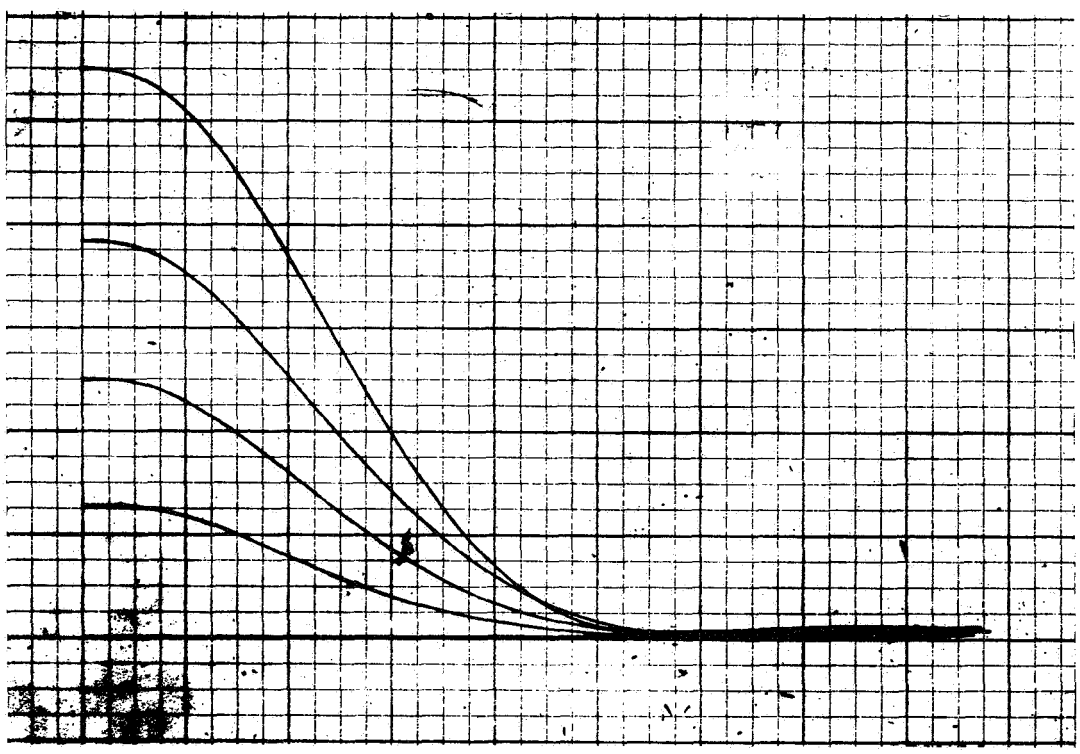

Run 4

Figure A-14. (Cont)

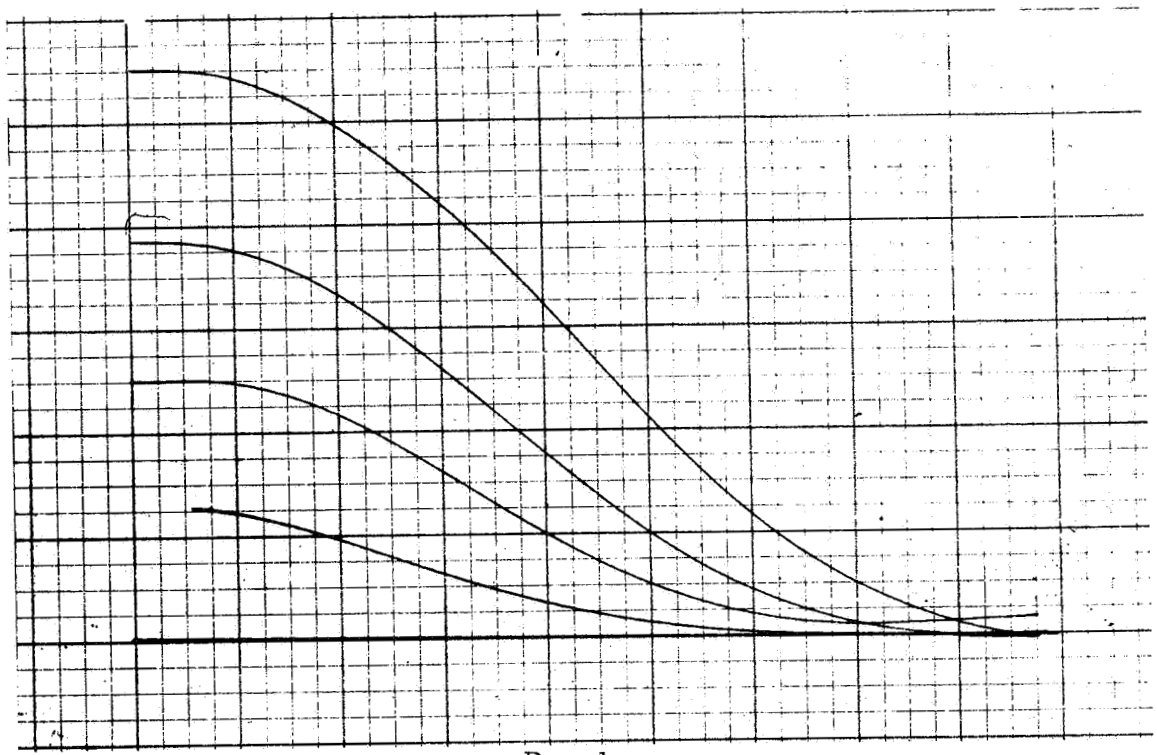

Run 1

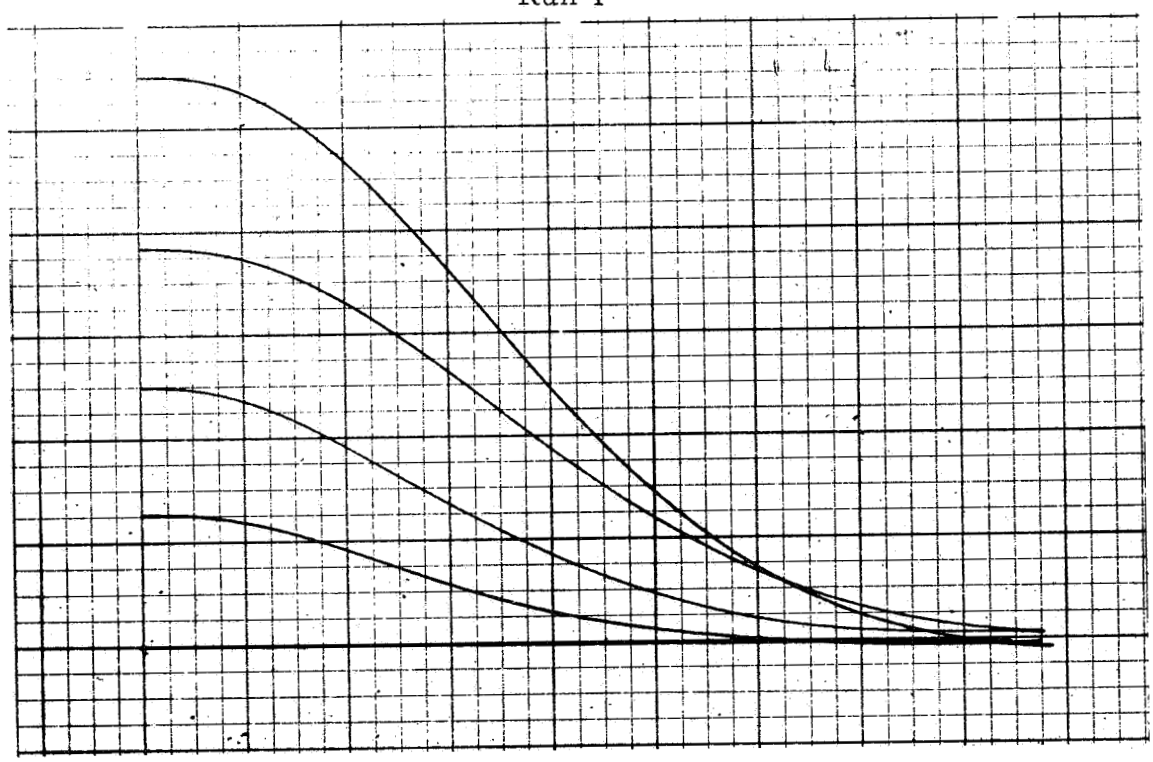

Run 2

Figure A-15. Subject 4 - 20 Seconds

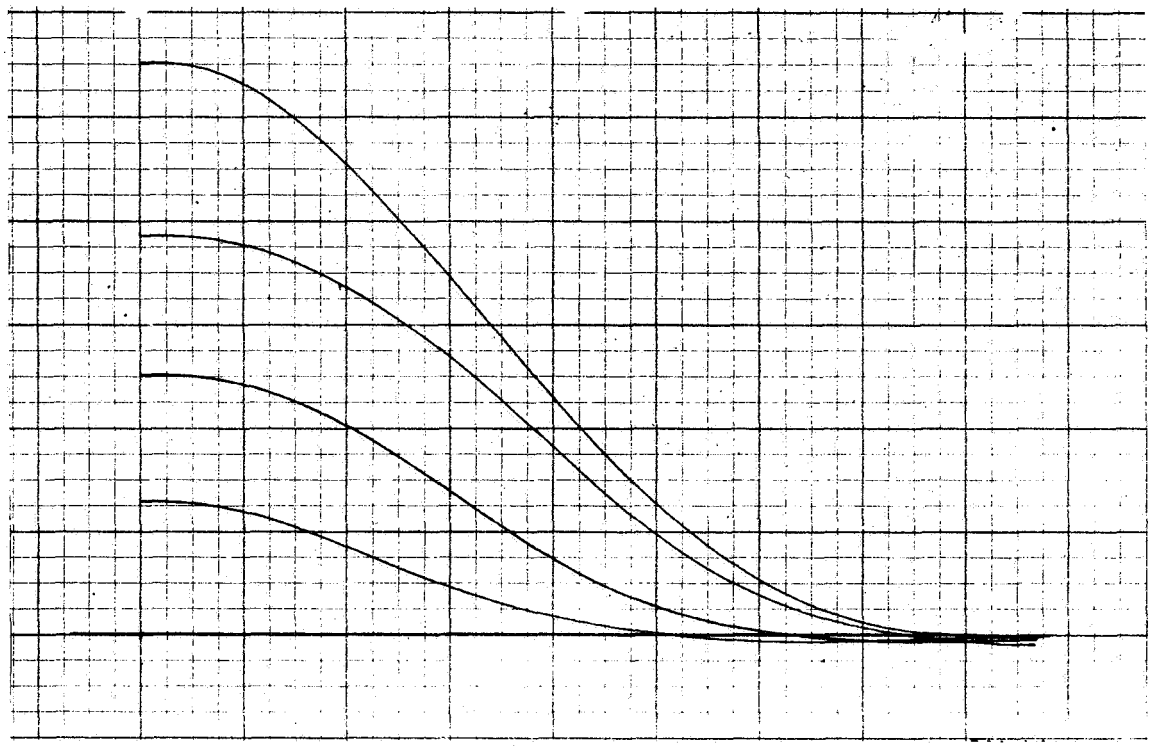

Run 3

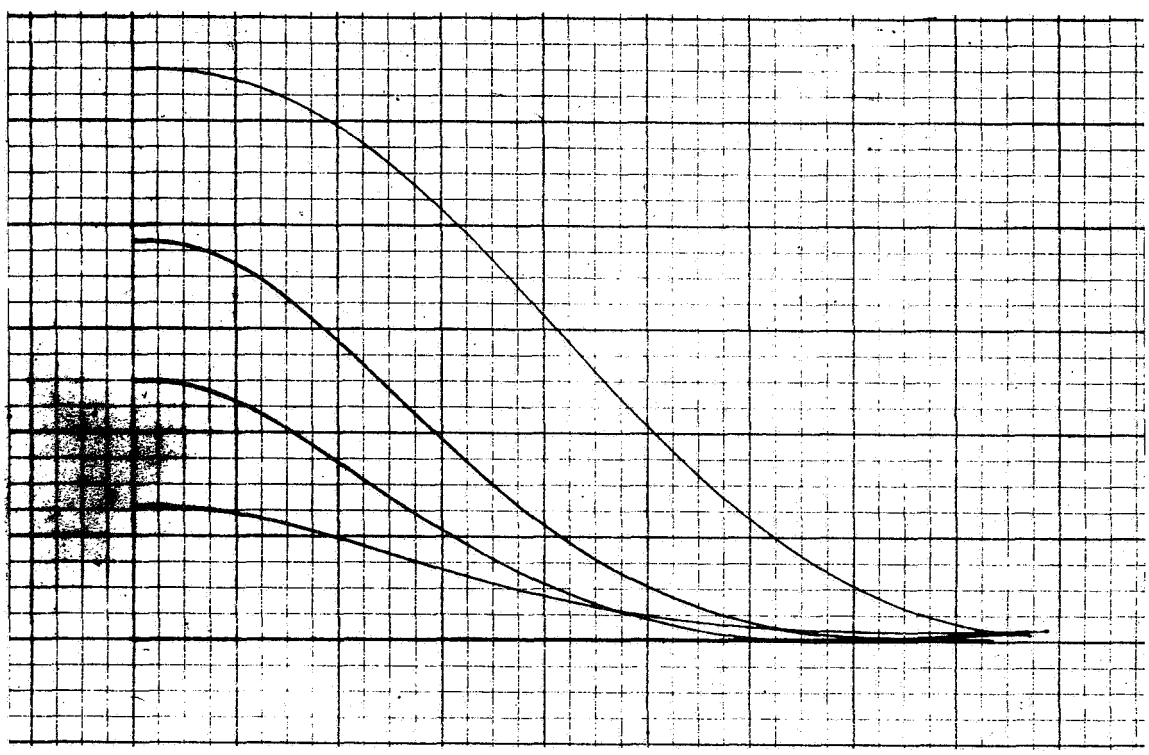

Run 4

Figure A-15. (Cont)

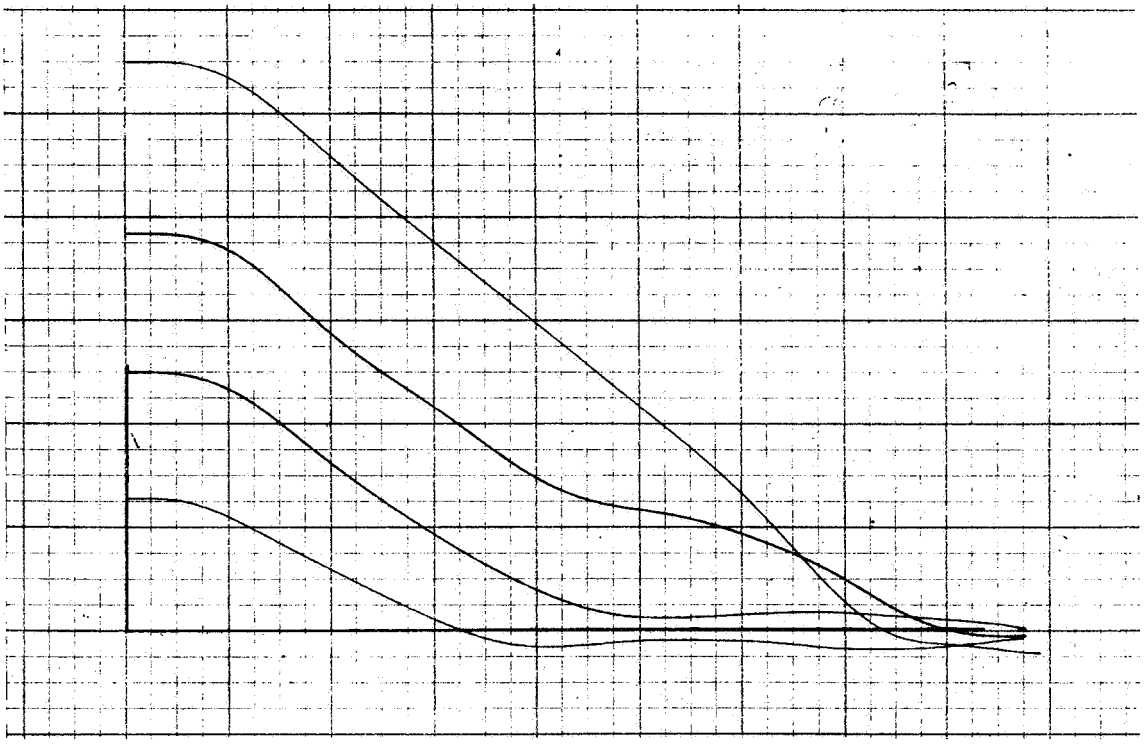

Run 1

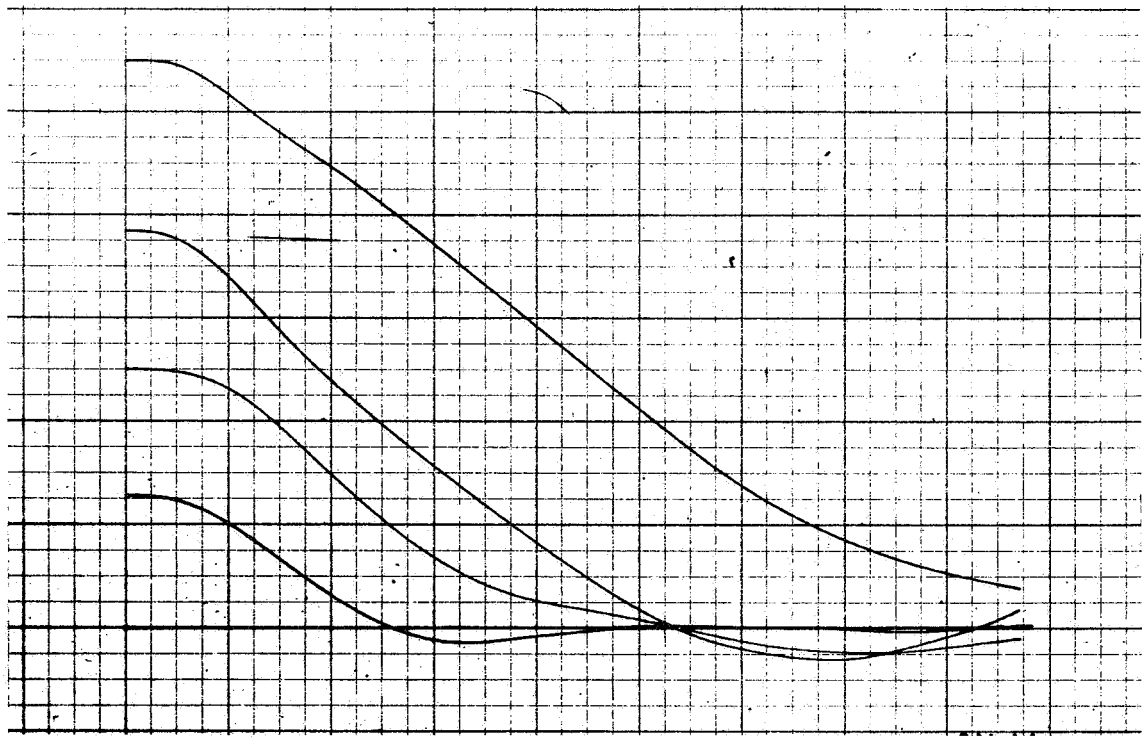

Run 2

Figure A-16. Subject 4 - Conventional

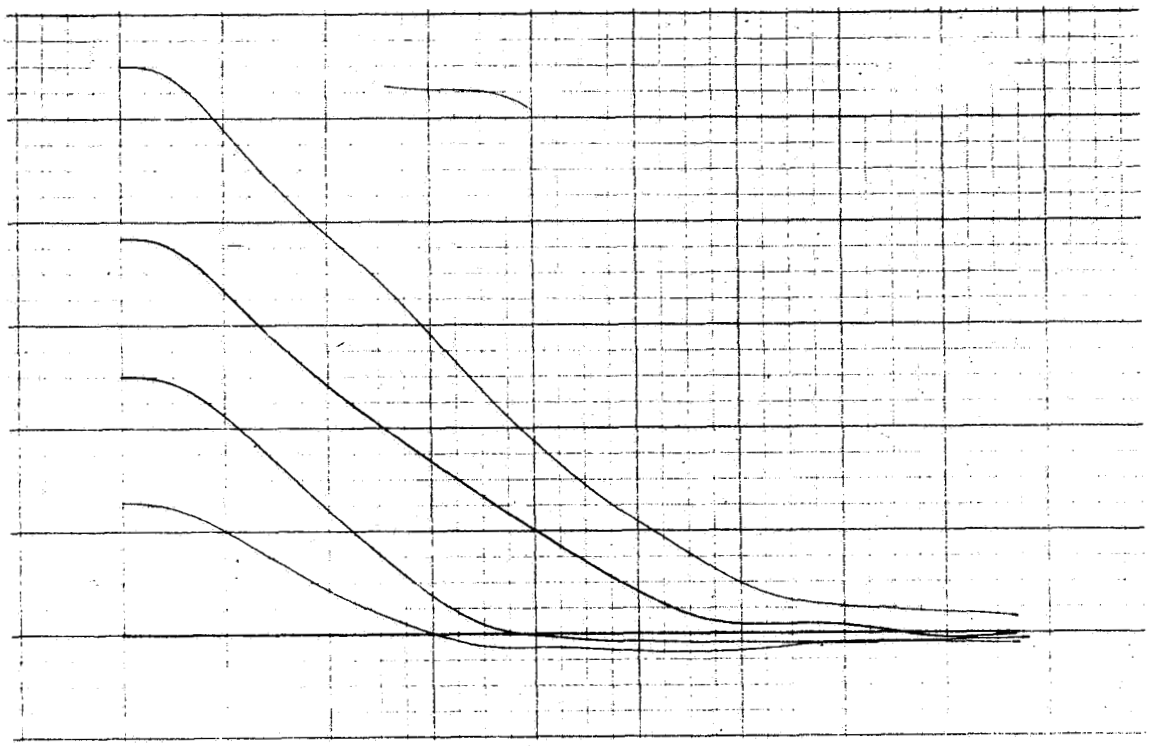

Run 3

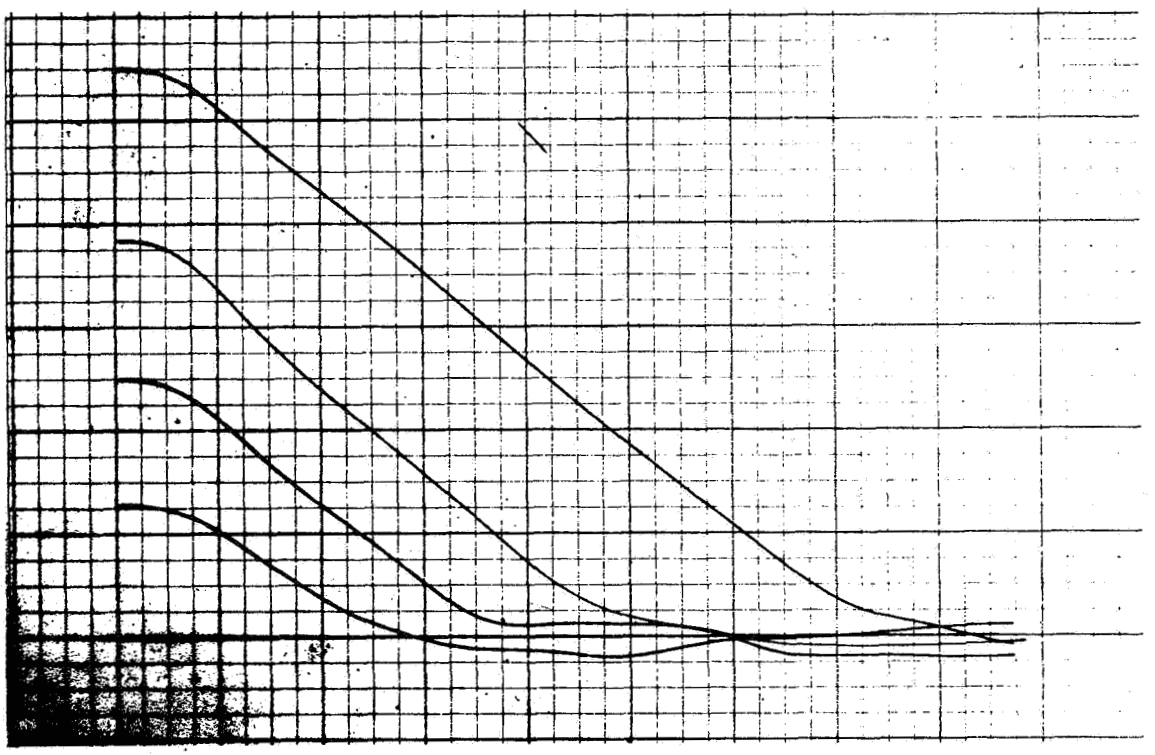

Run 4

Figure A-16. (Cont)

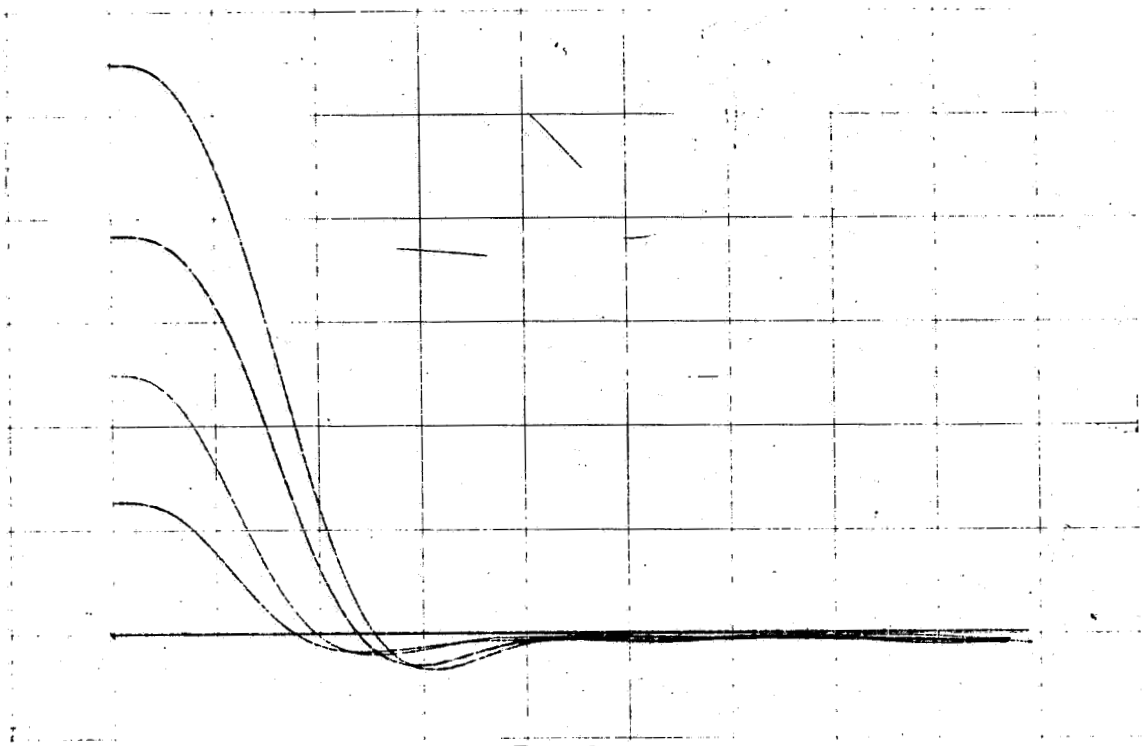

Run 1

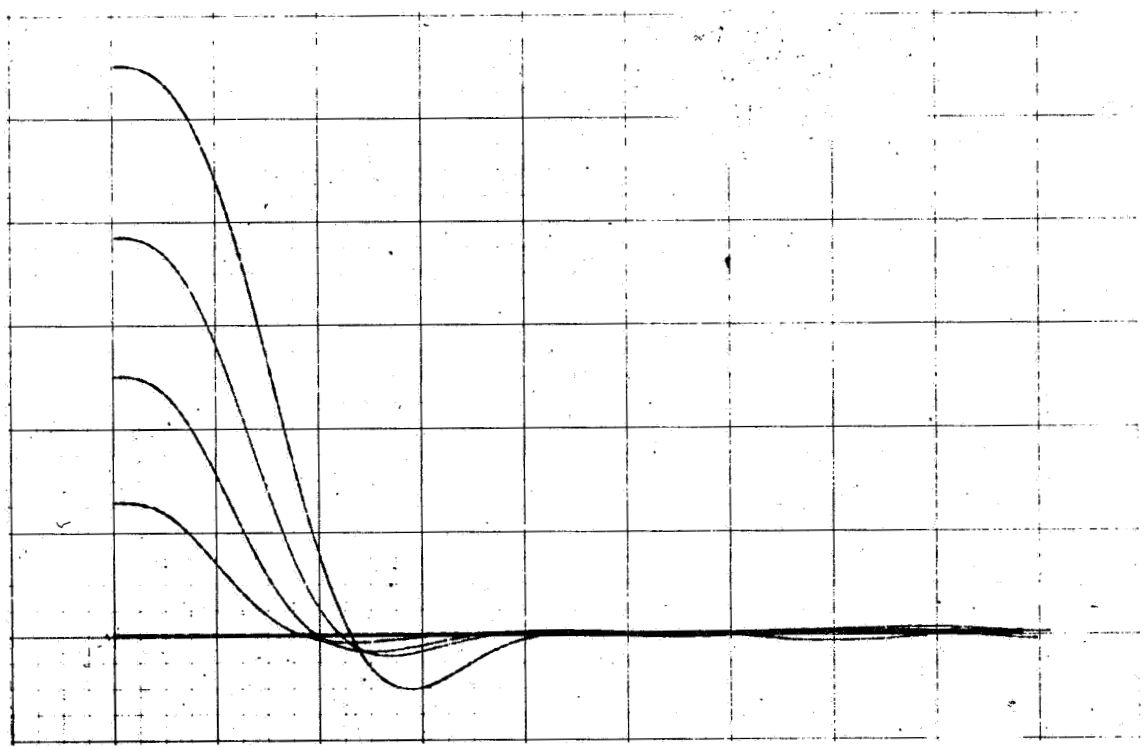

Run 2

Figure A-17. Subject 5 - 5 Seconds

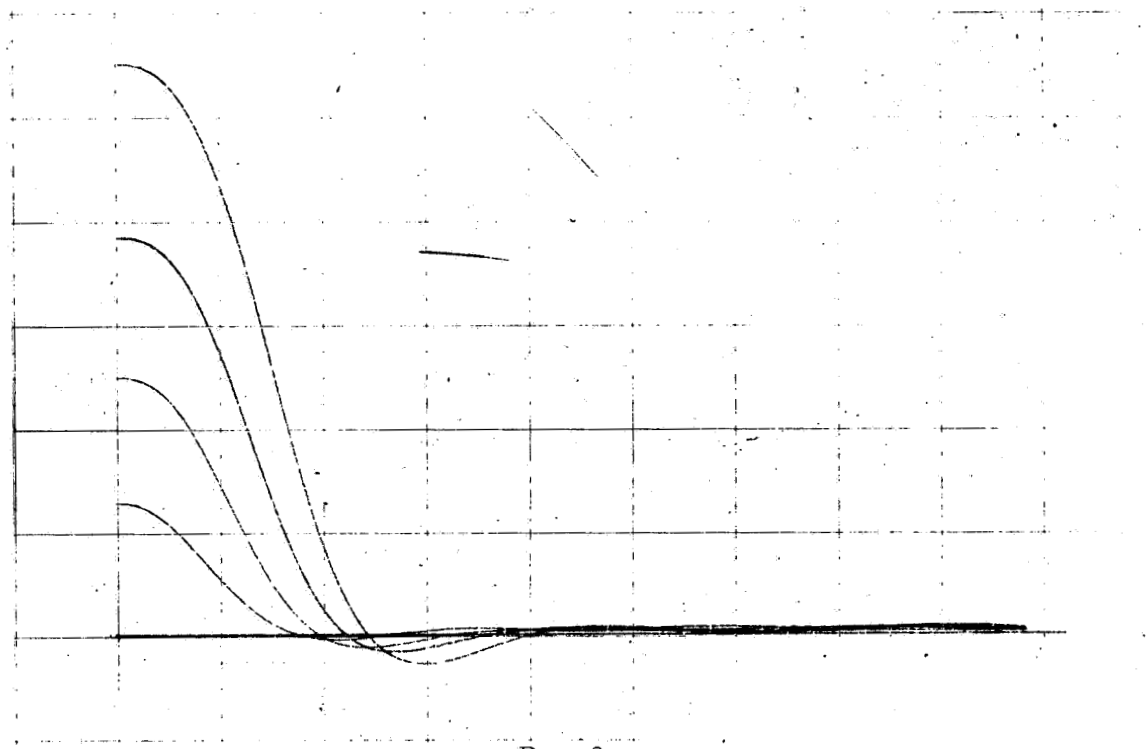

Run 3

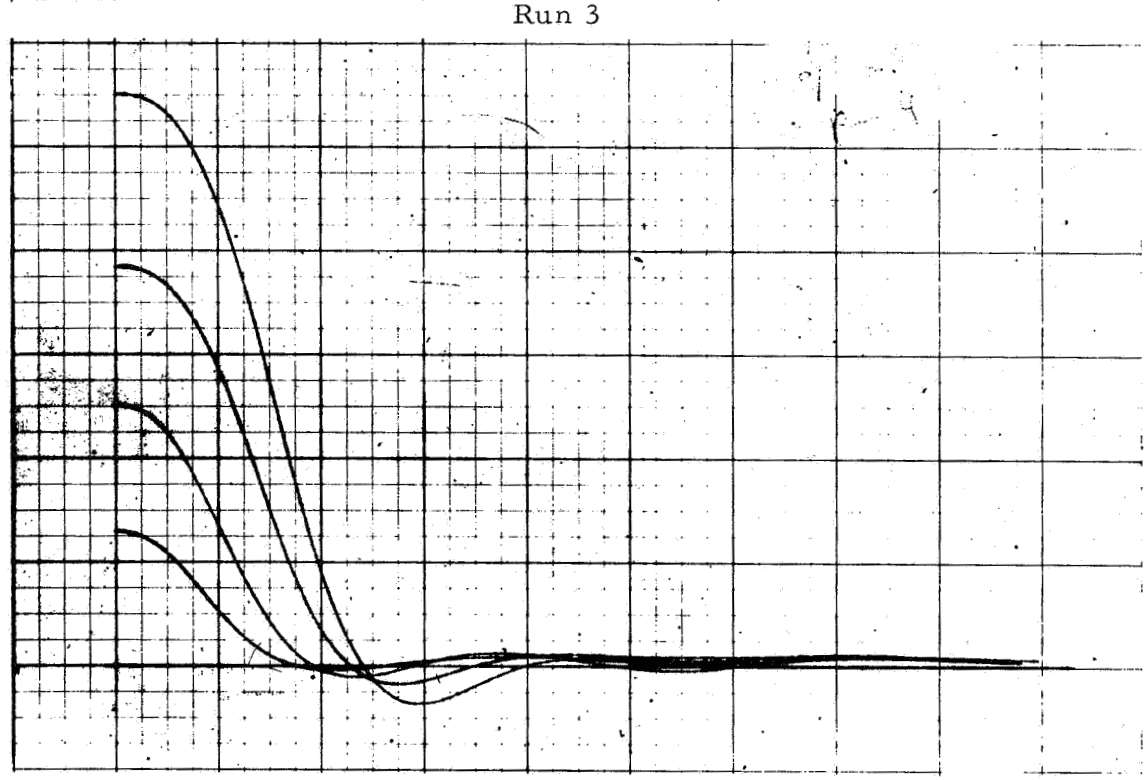

Run 4

Figure A-17. (Cont)

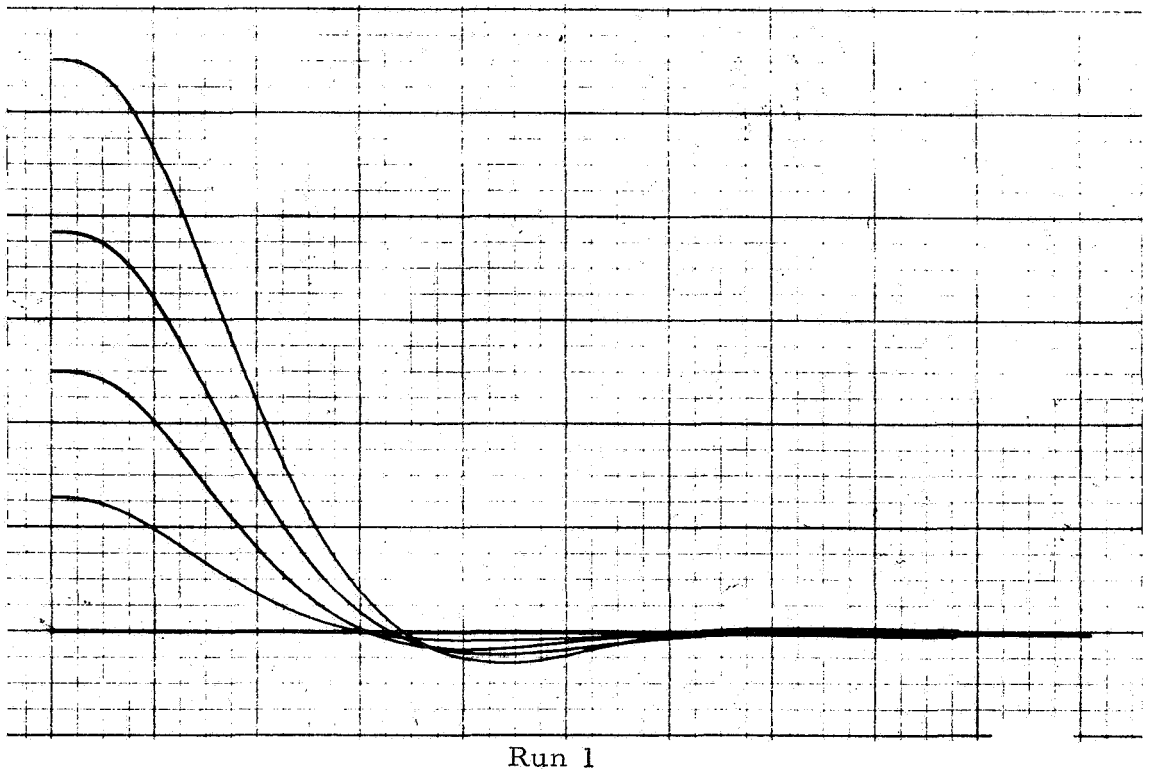

Run 1

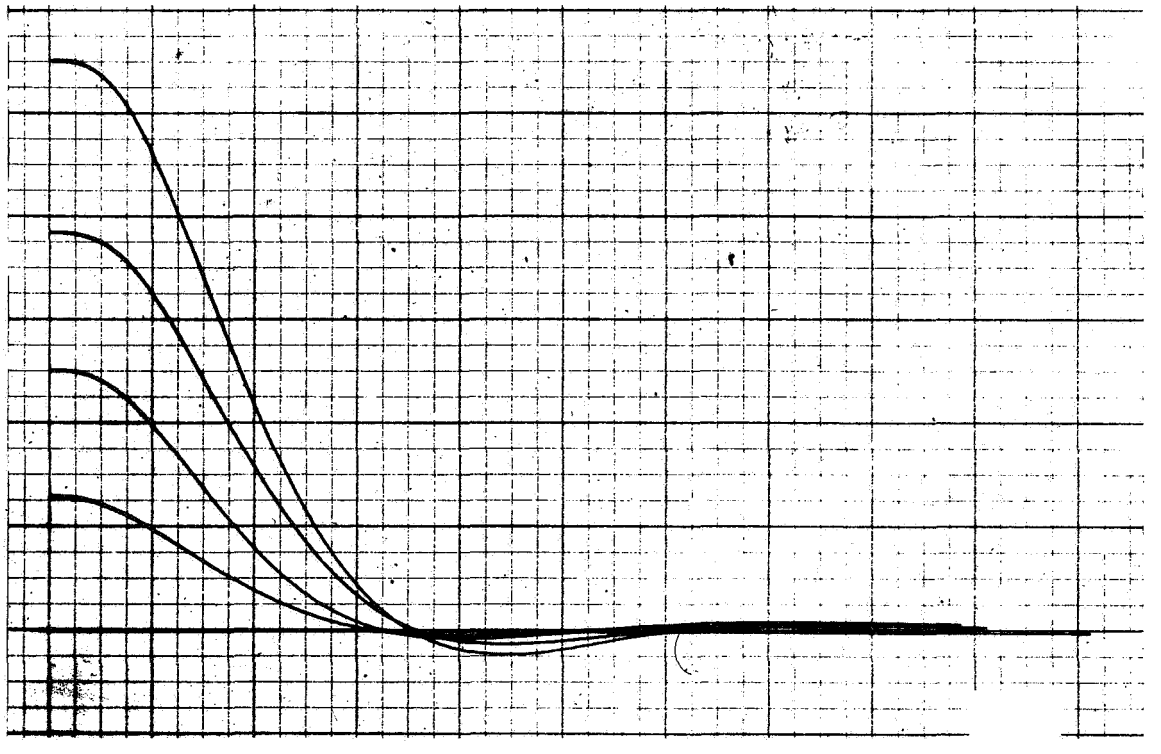

Run 2

Figure A-18. Subject 5 - 10 Seconds

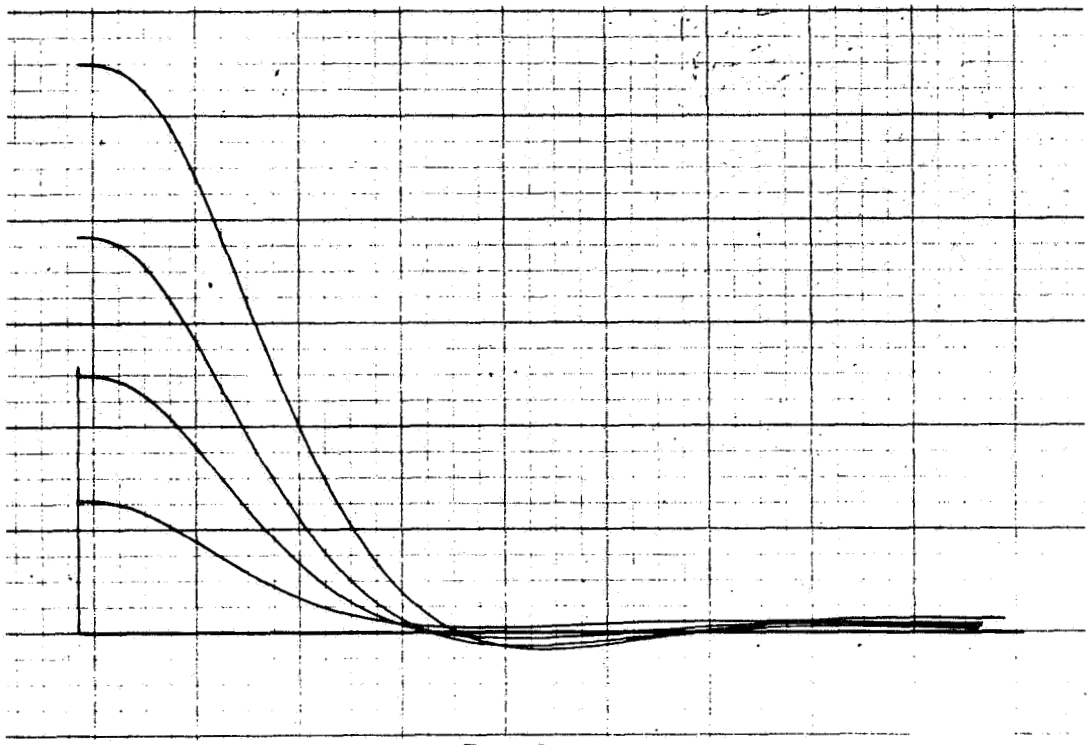

Run 3

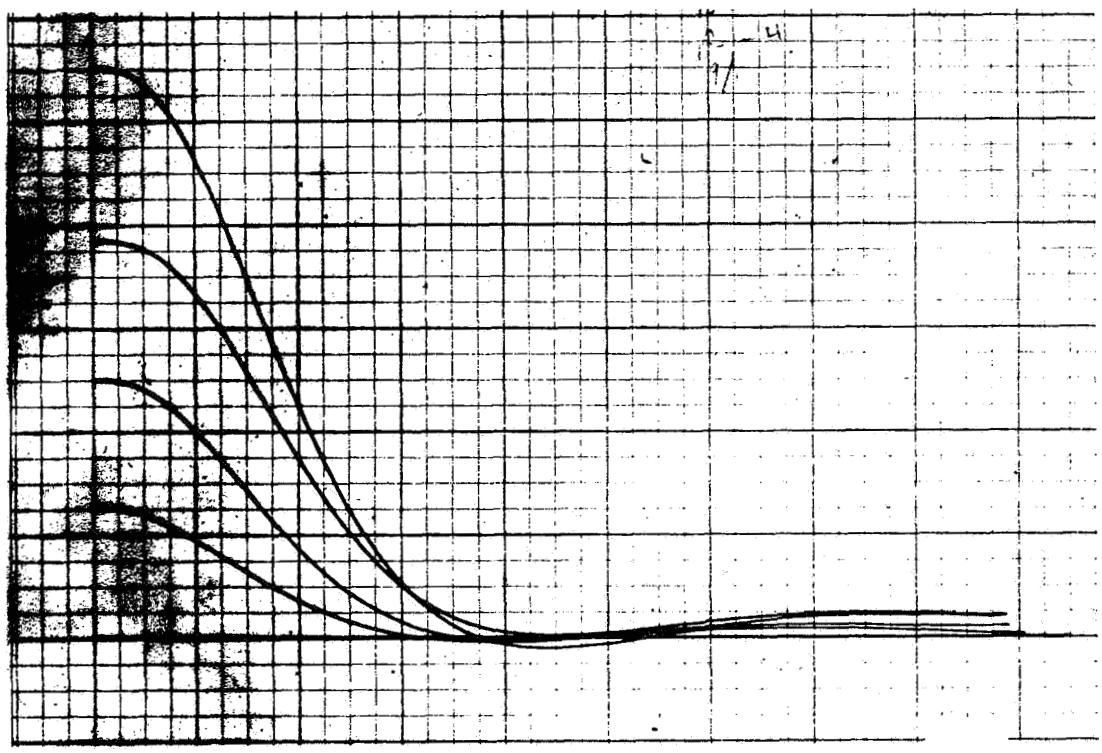

Run 4

Figure A-18. (Cont)

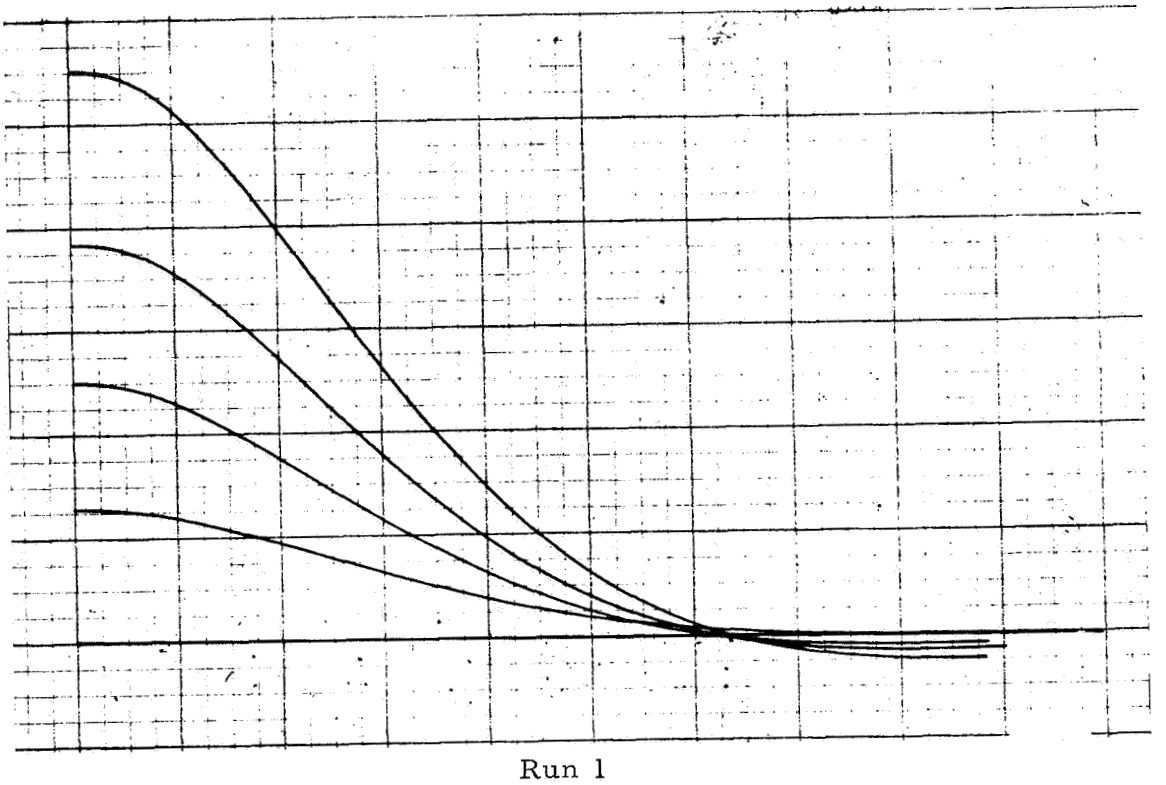

Run 1

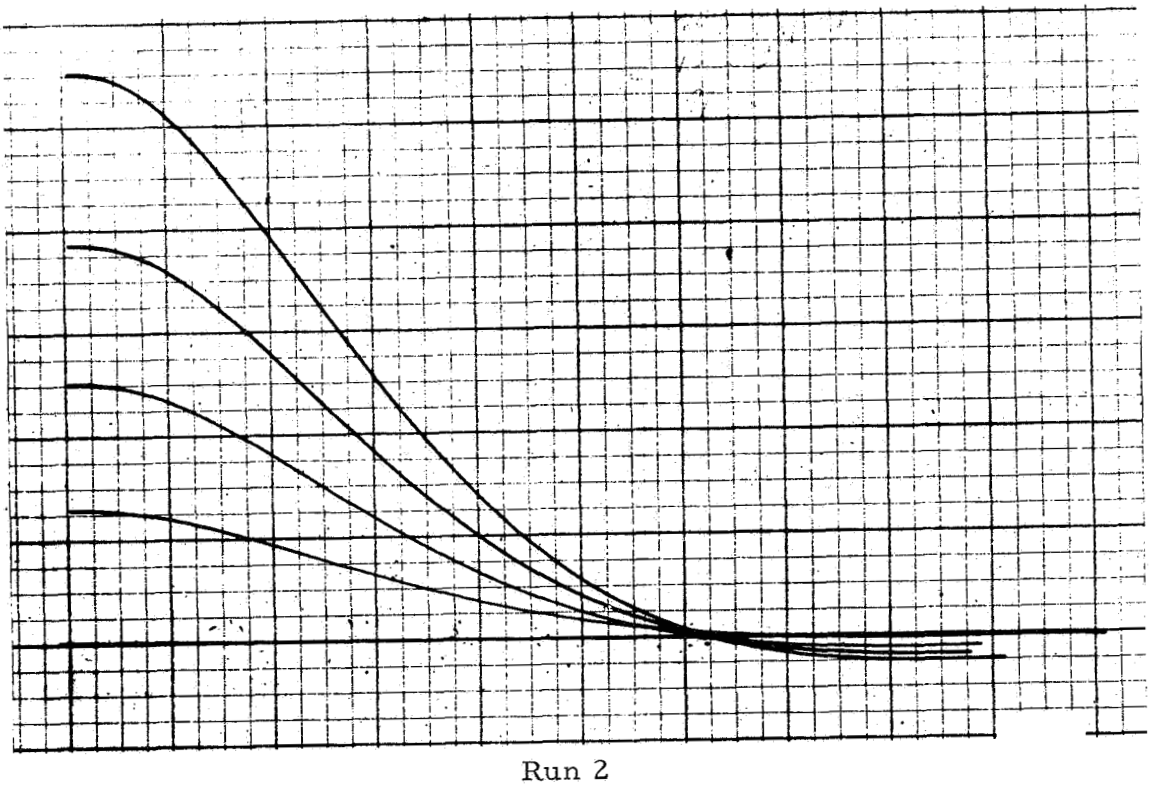

Run 2

Figure A-19. Subject 5 - 20 Seconds

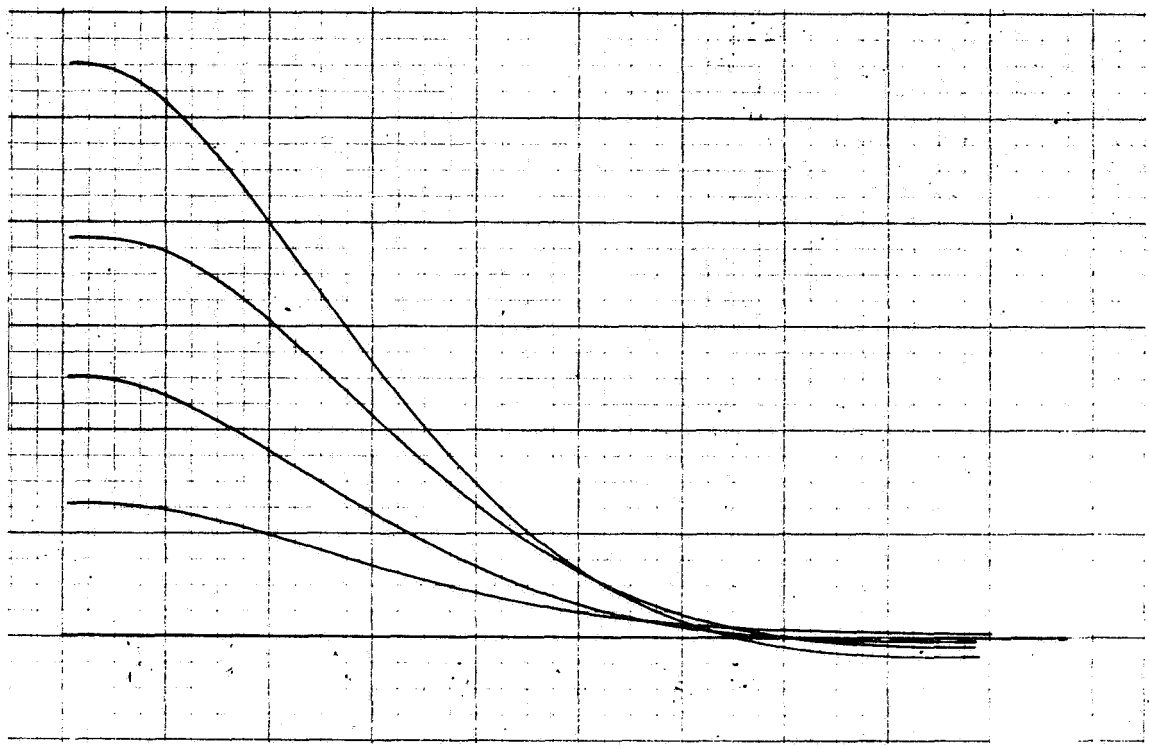

Run 3

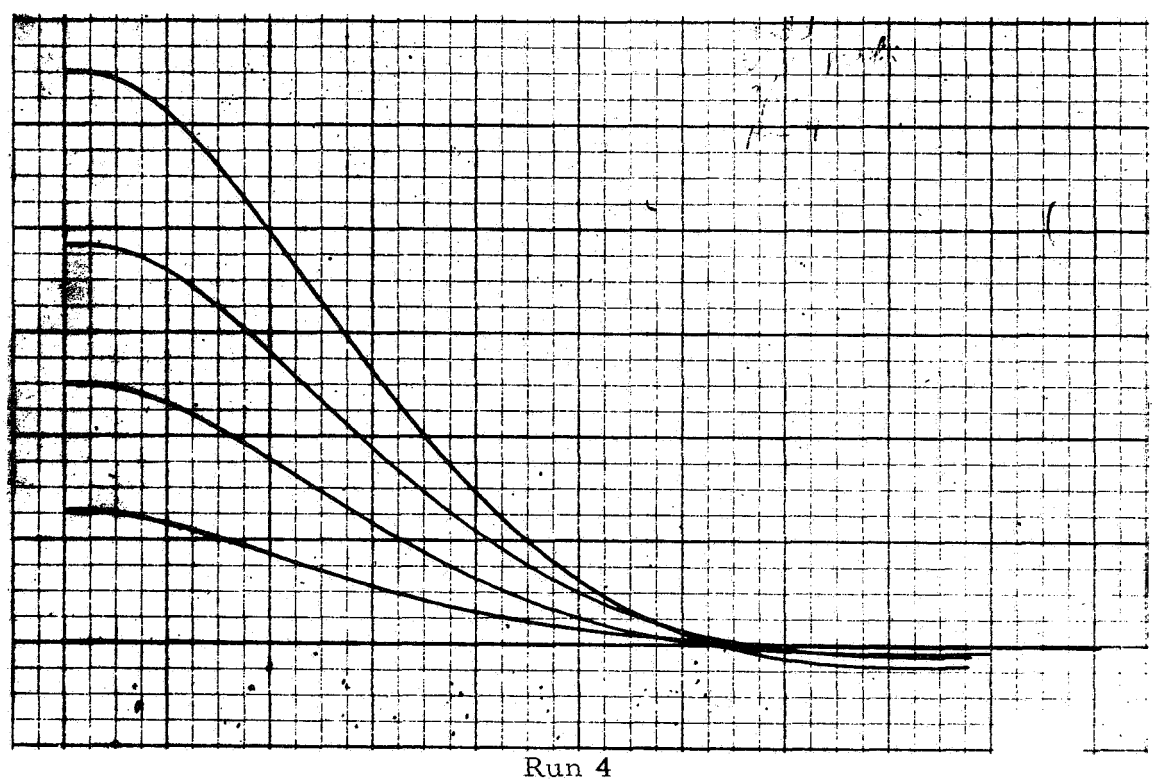

Run 4

Figure A-19. (Cont)

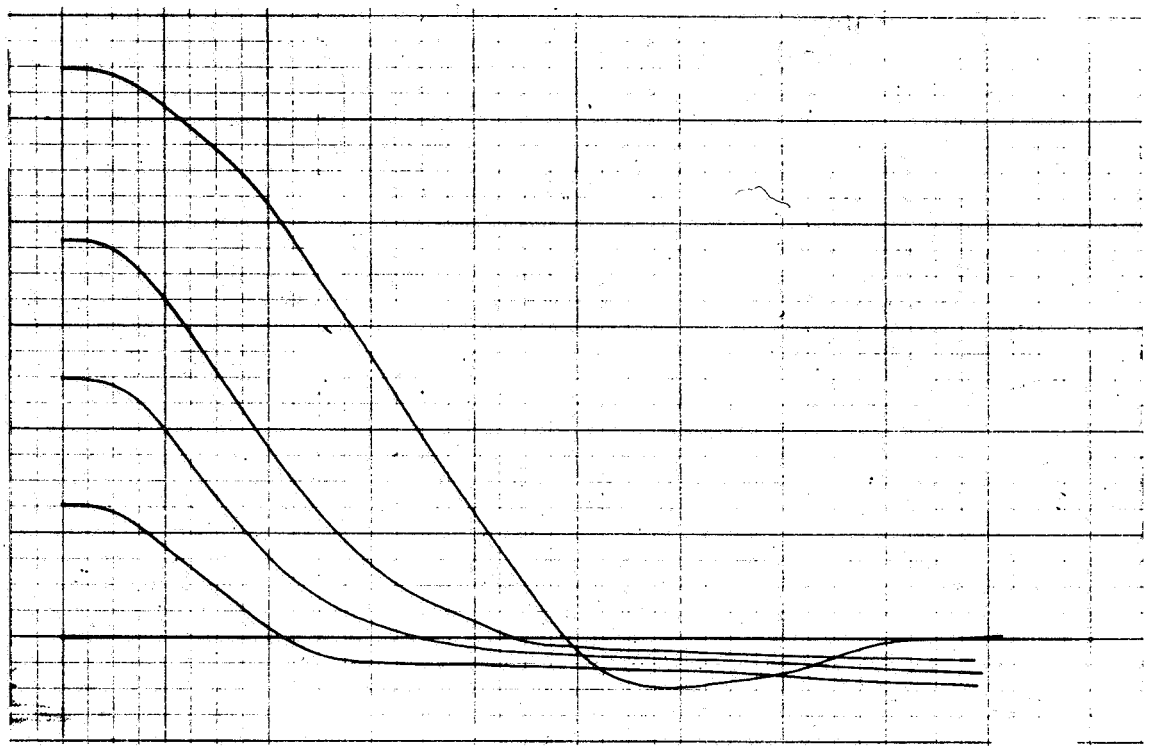

Run 1

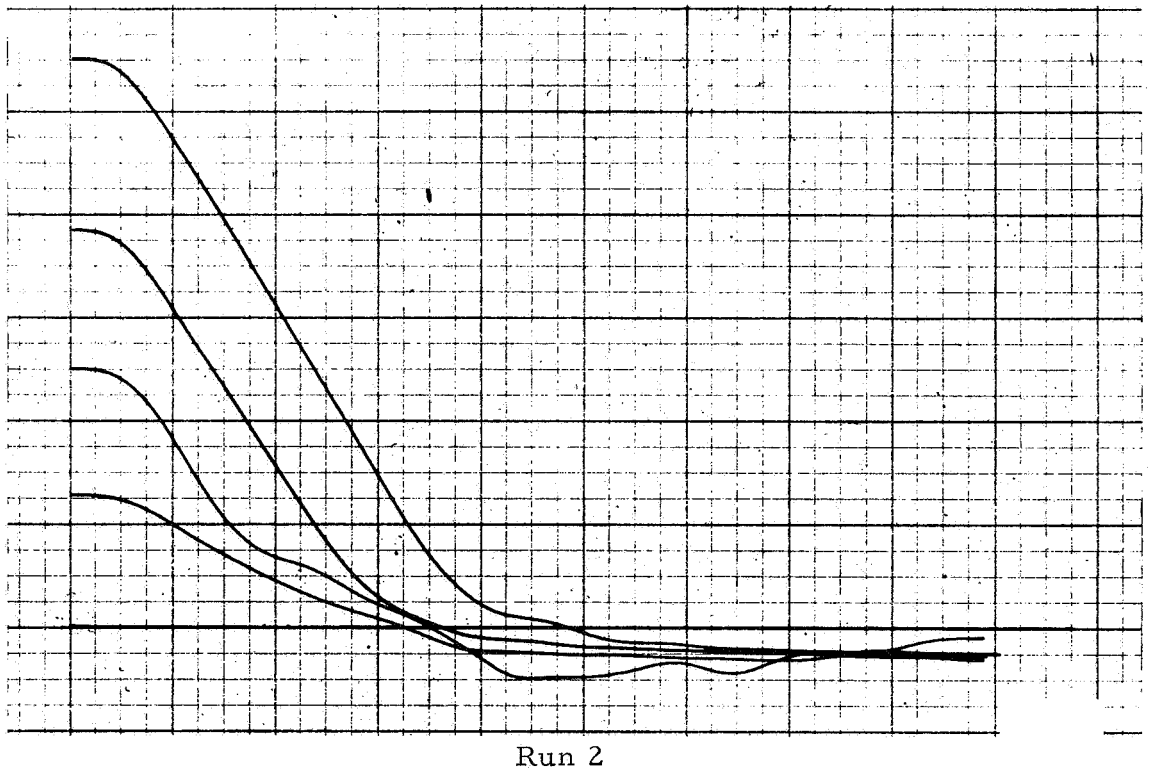

Run 2

Figure A-20. Subject 5 - Conventional

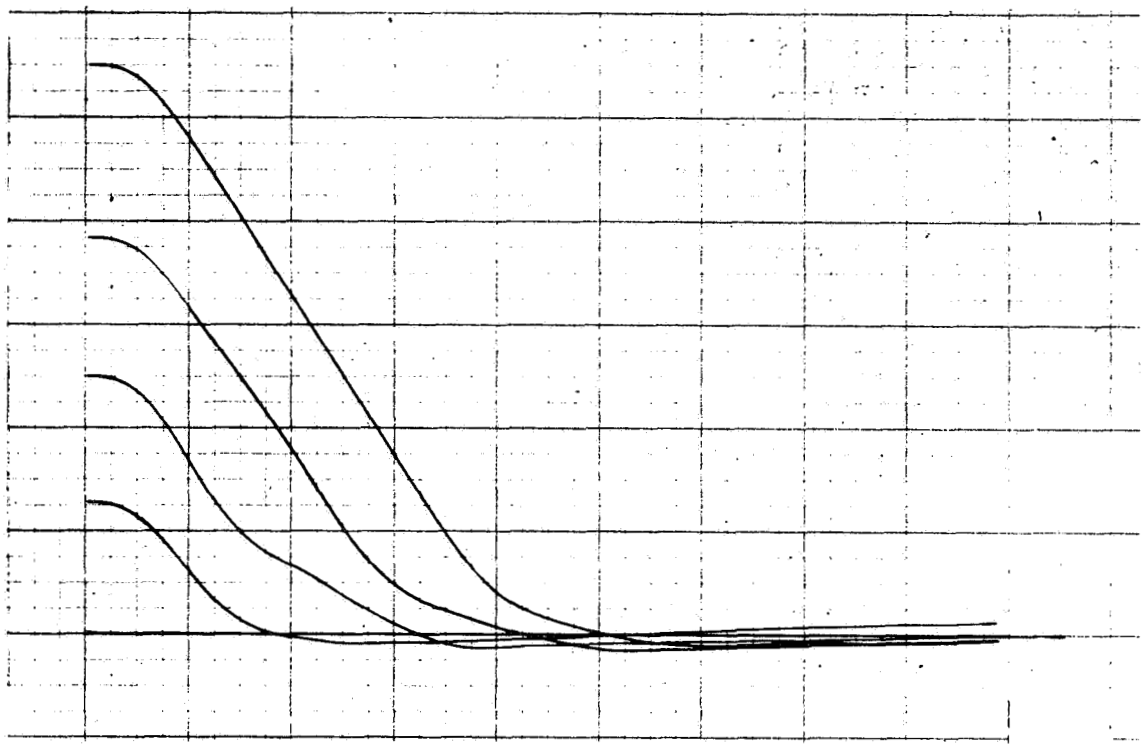

Run 3

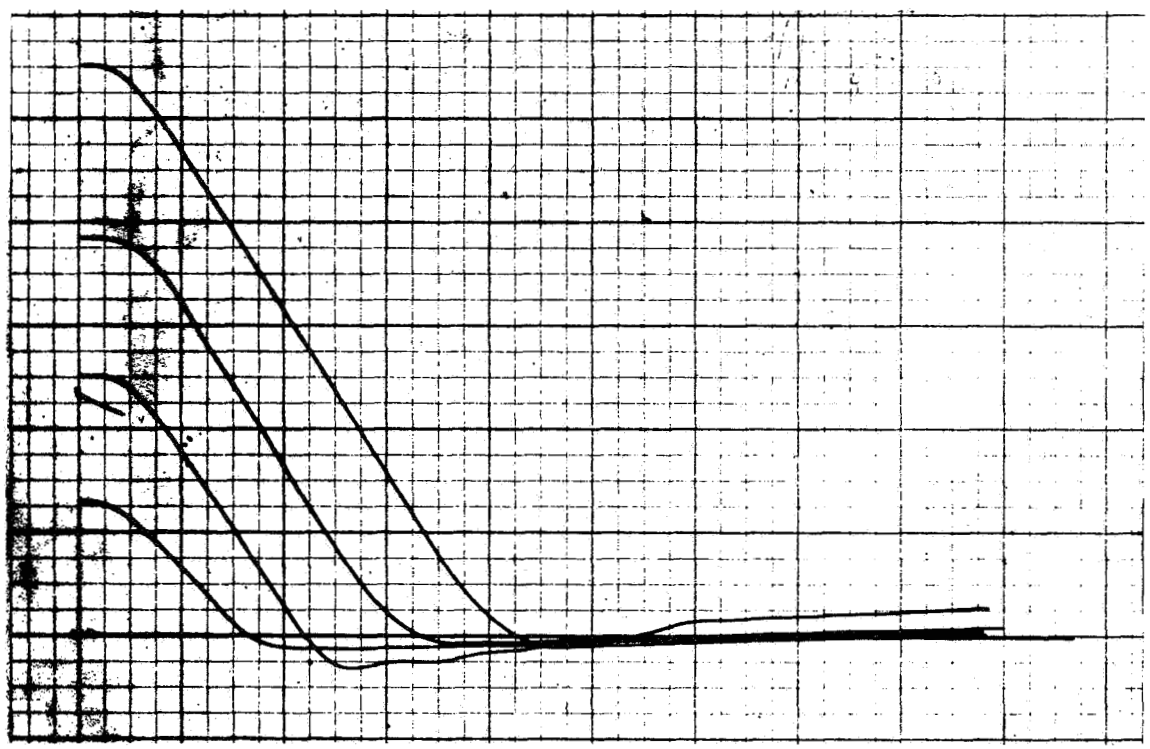

Run 4

Figure A-20. (Cont)

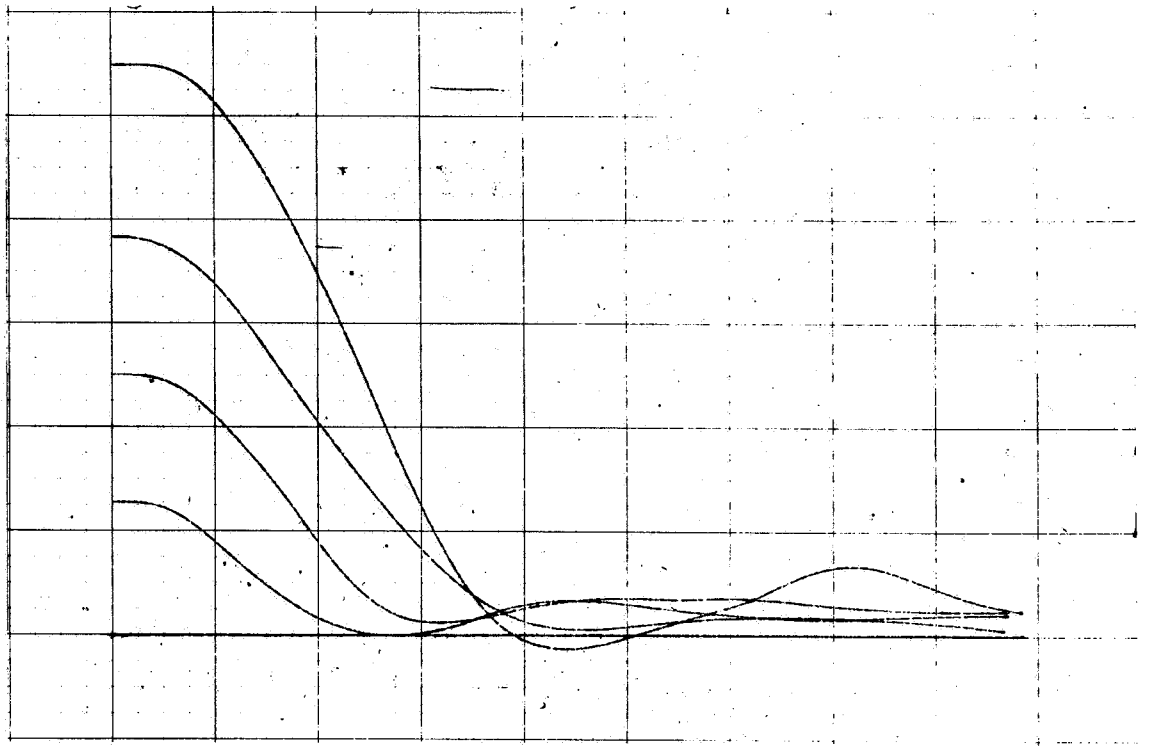

Run 1

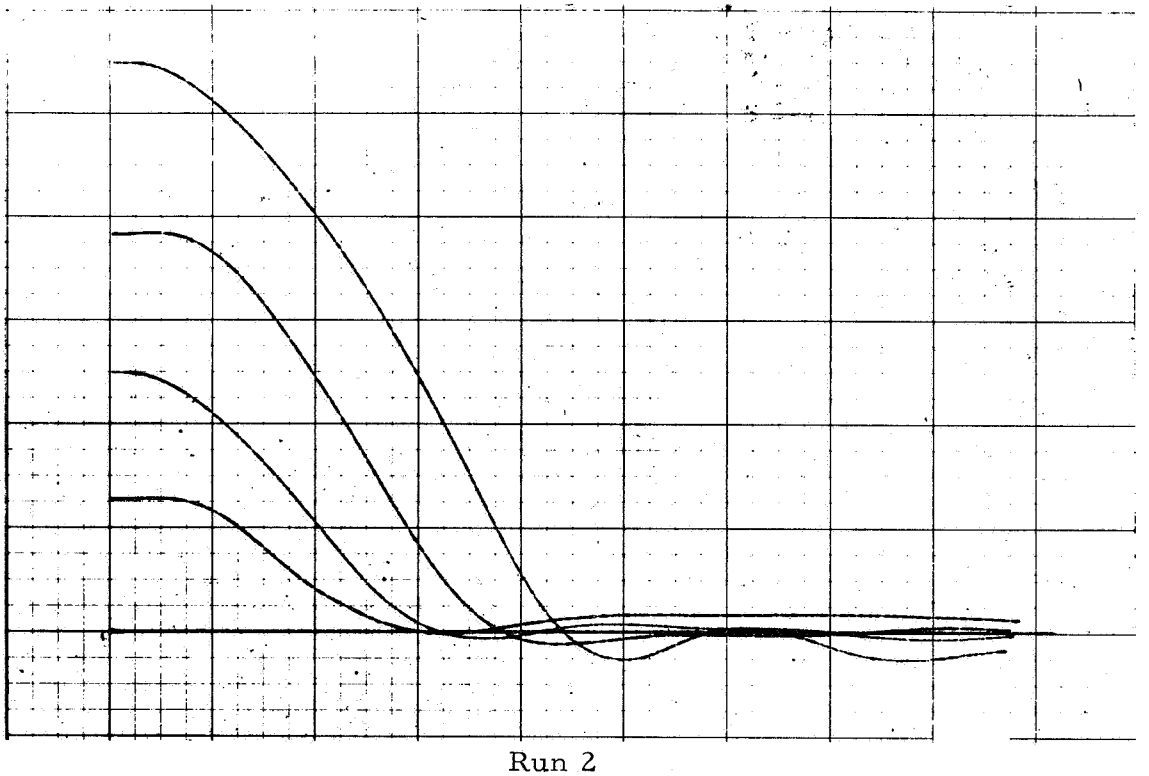

Run 2

Figure A-21. Subject 6 - 5 Seconds

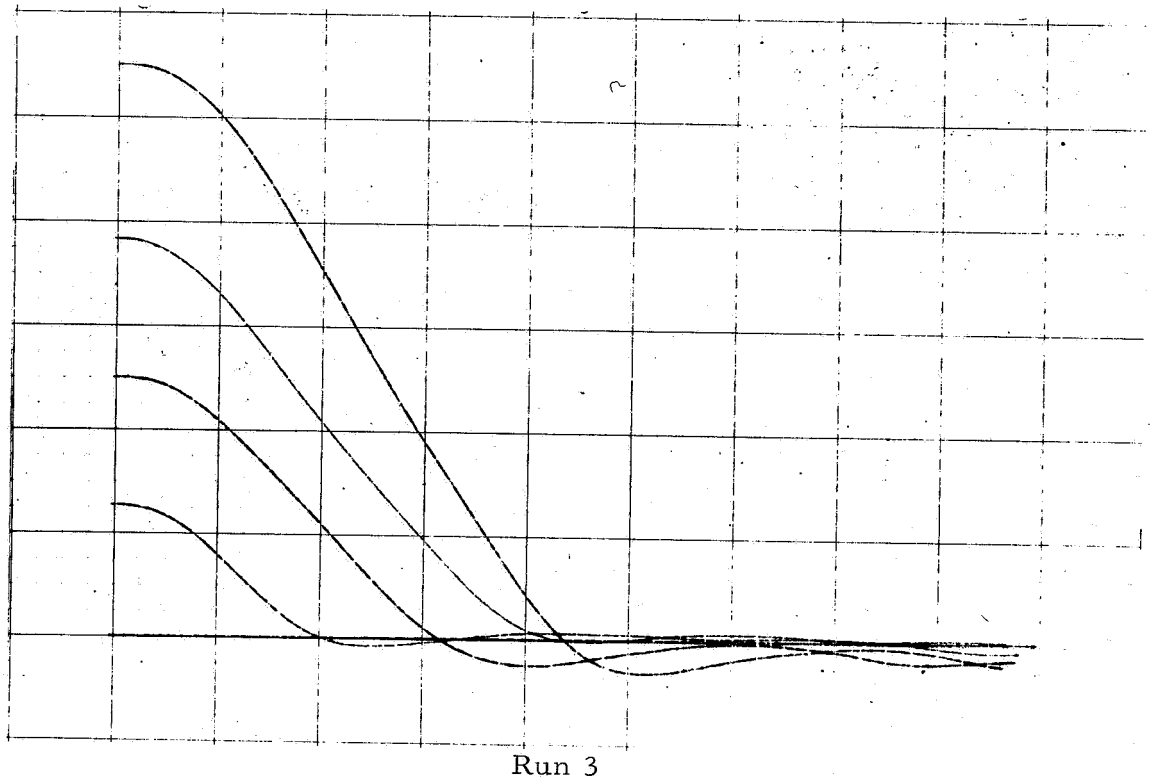

Run 3

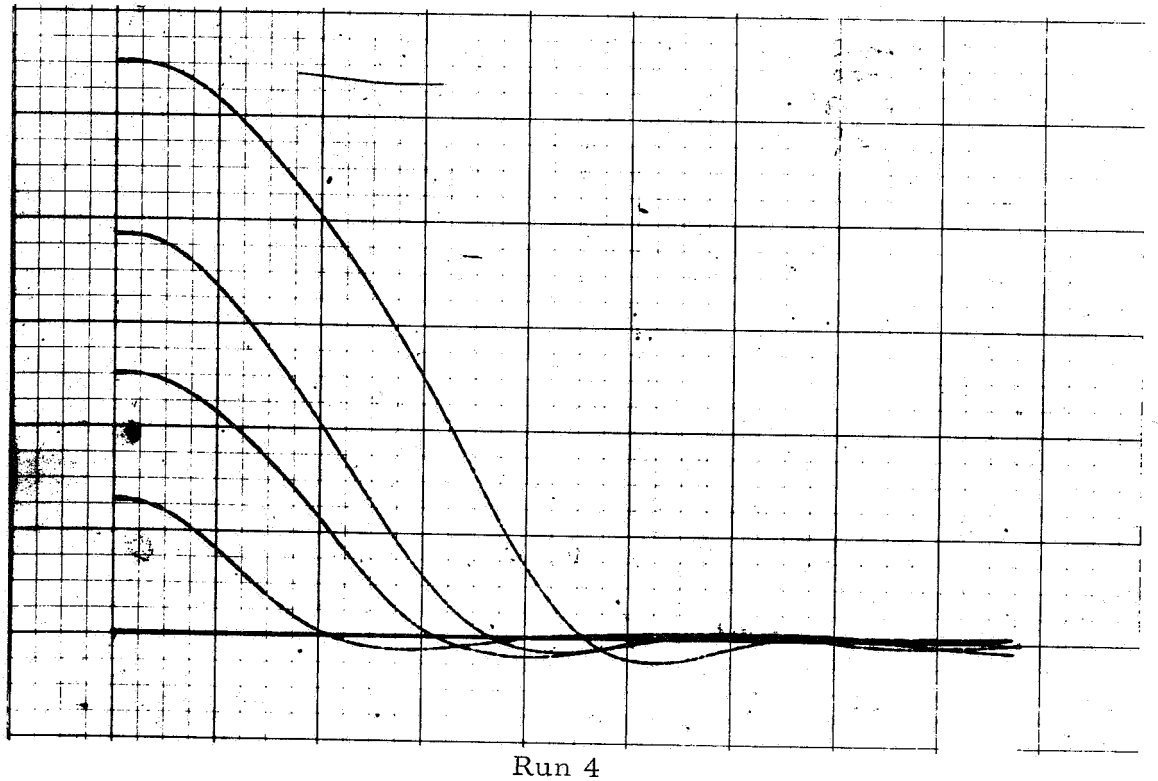

Run 4

Figure A-21. (Cont)

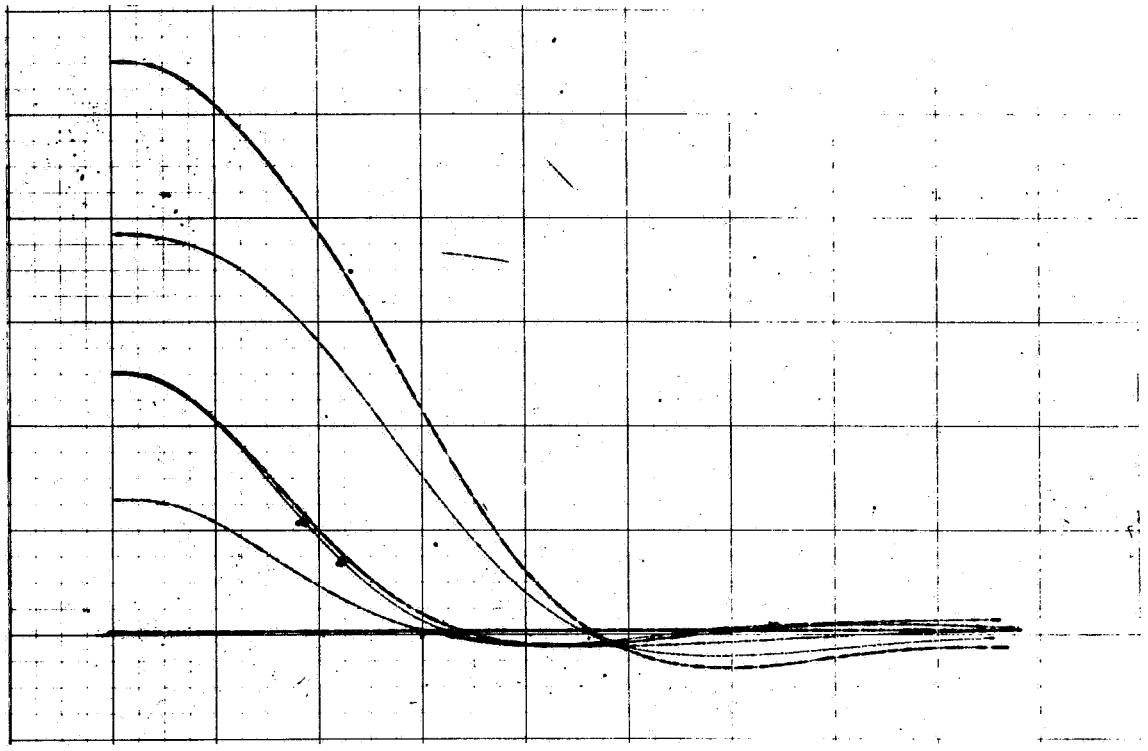

Run 1

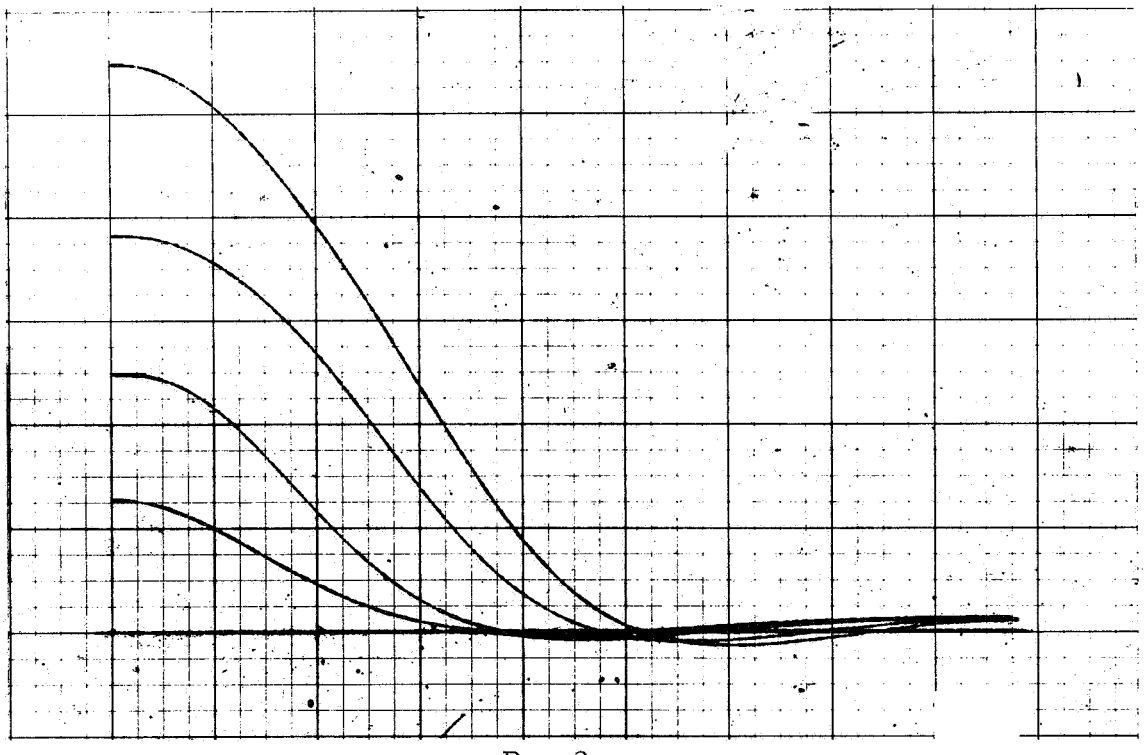

Run 2

Figure A-22. Subject 6 - 10 Seconds

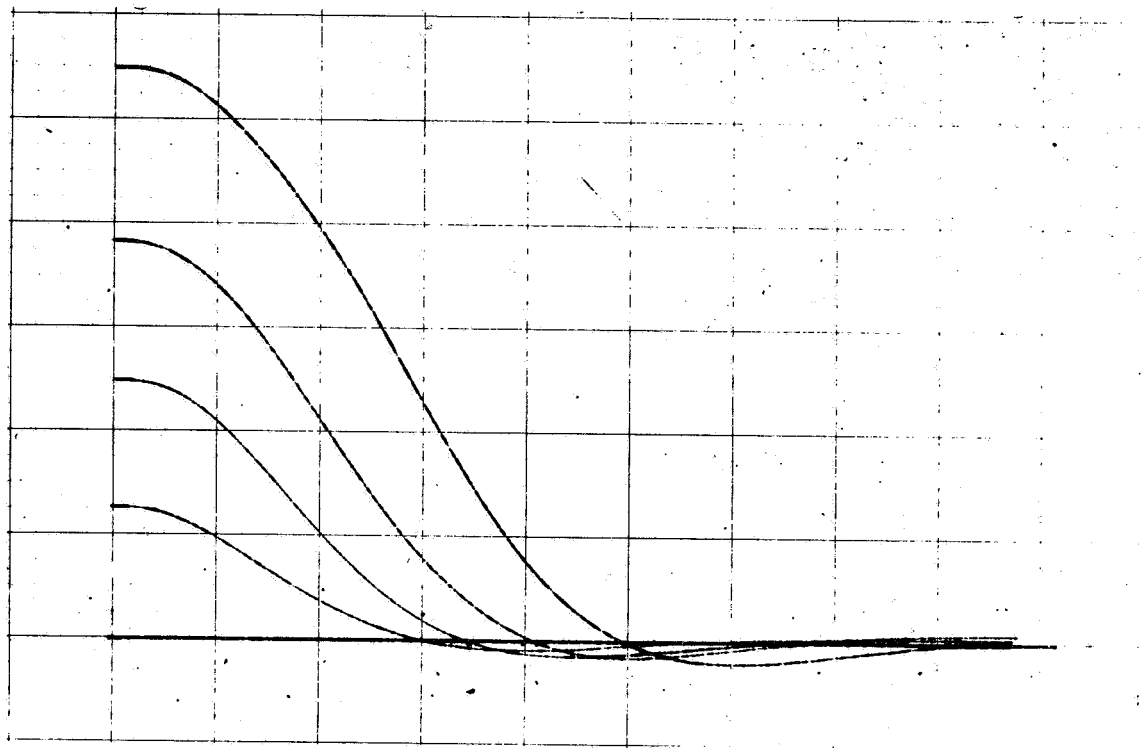

Run 3

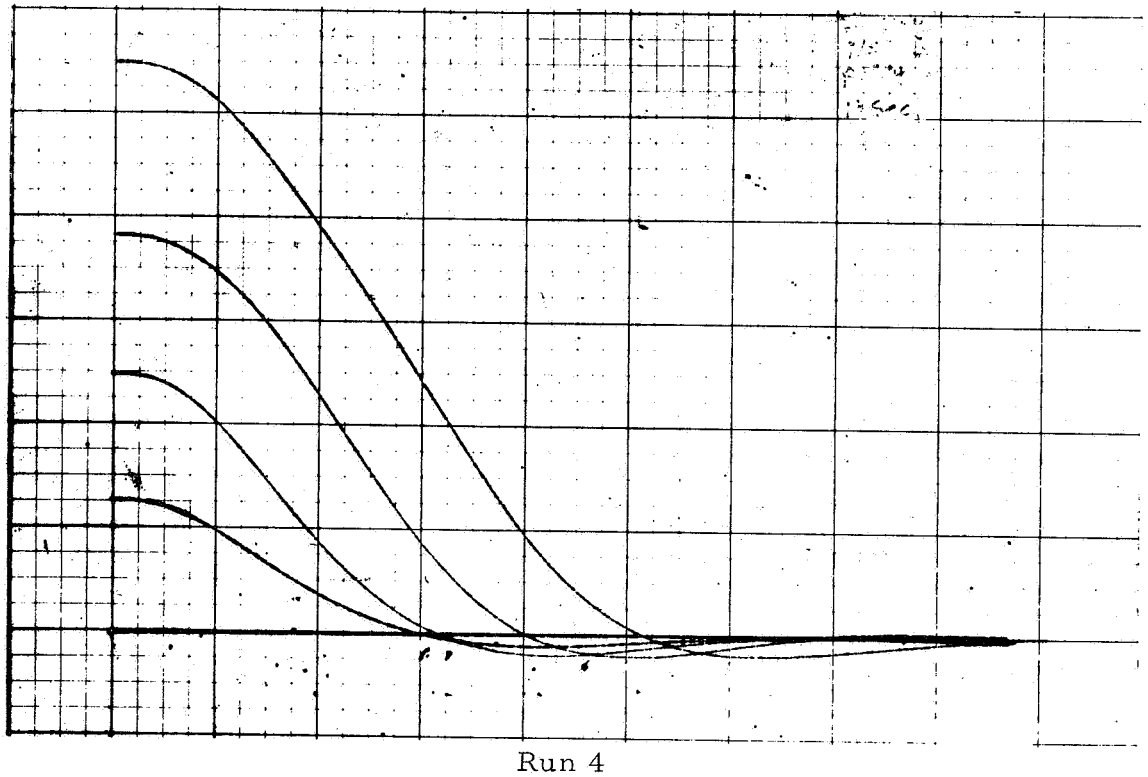

Run 4

Figure A-22. (Cont)

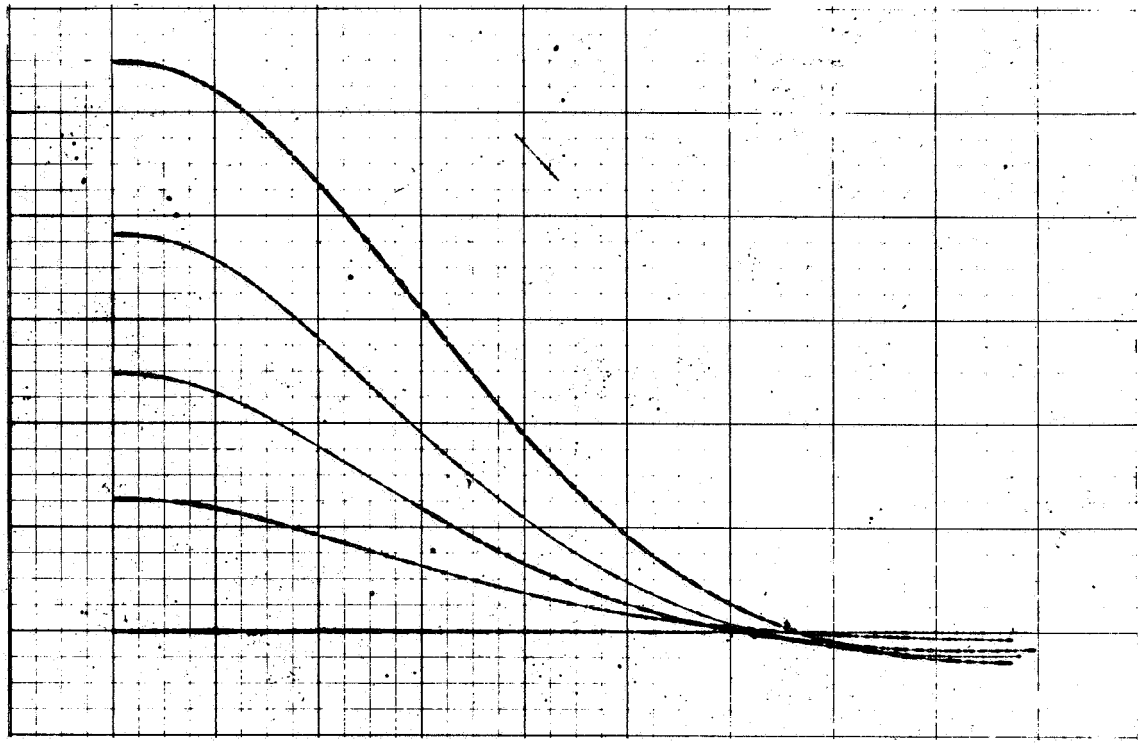

Run 1

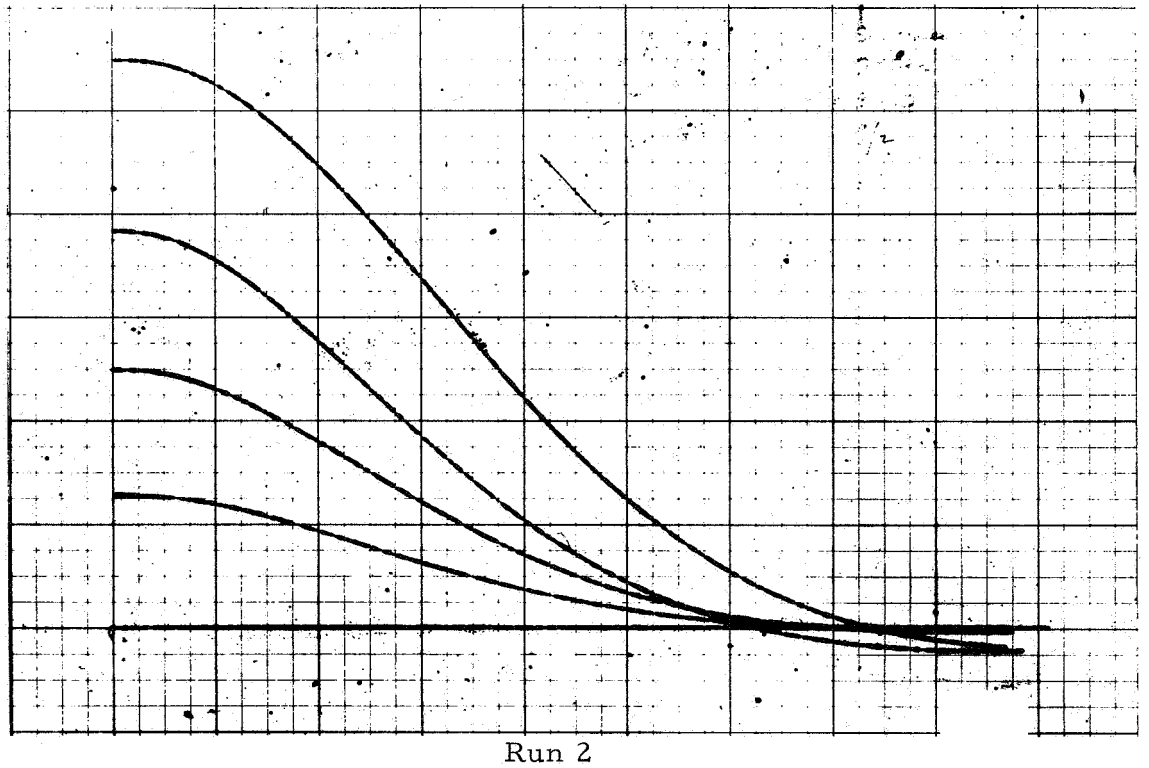

Run 2

Figure A-23. Subject 6 - 20 Seconds

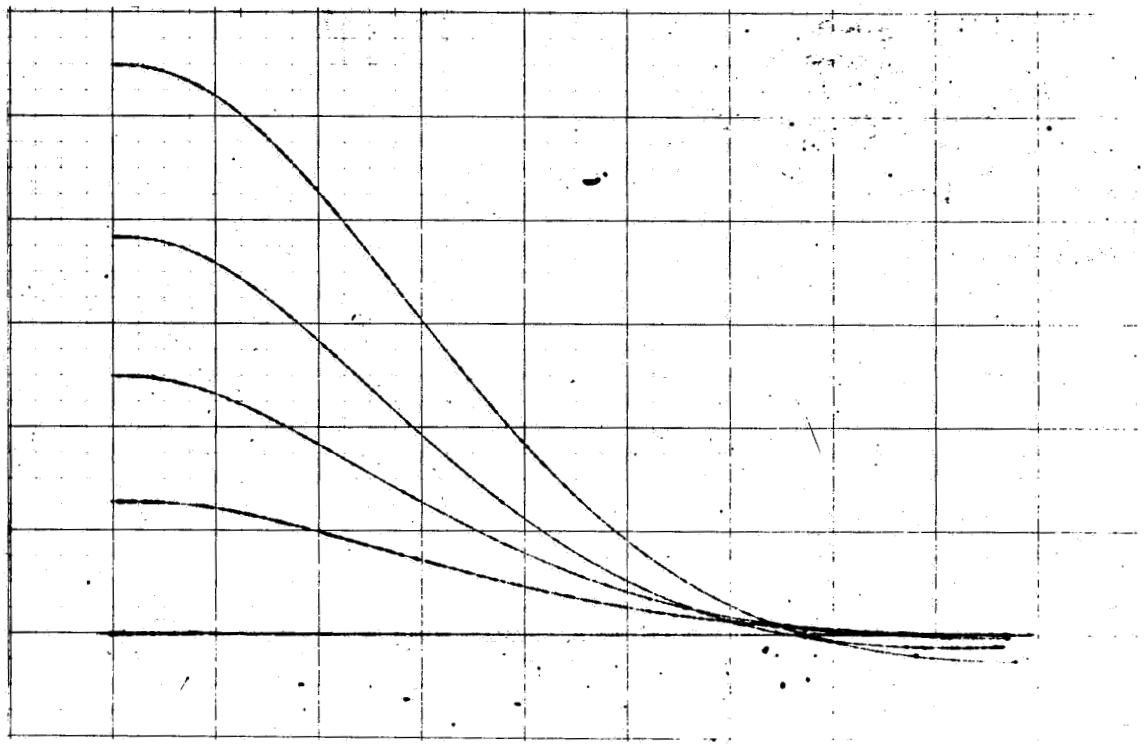

Run 3

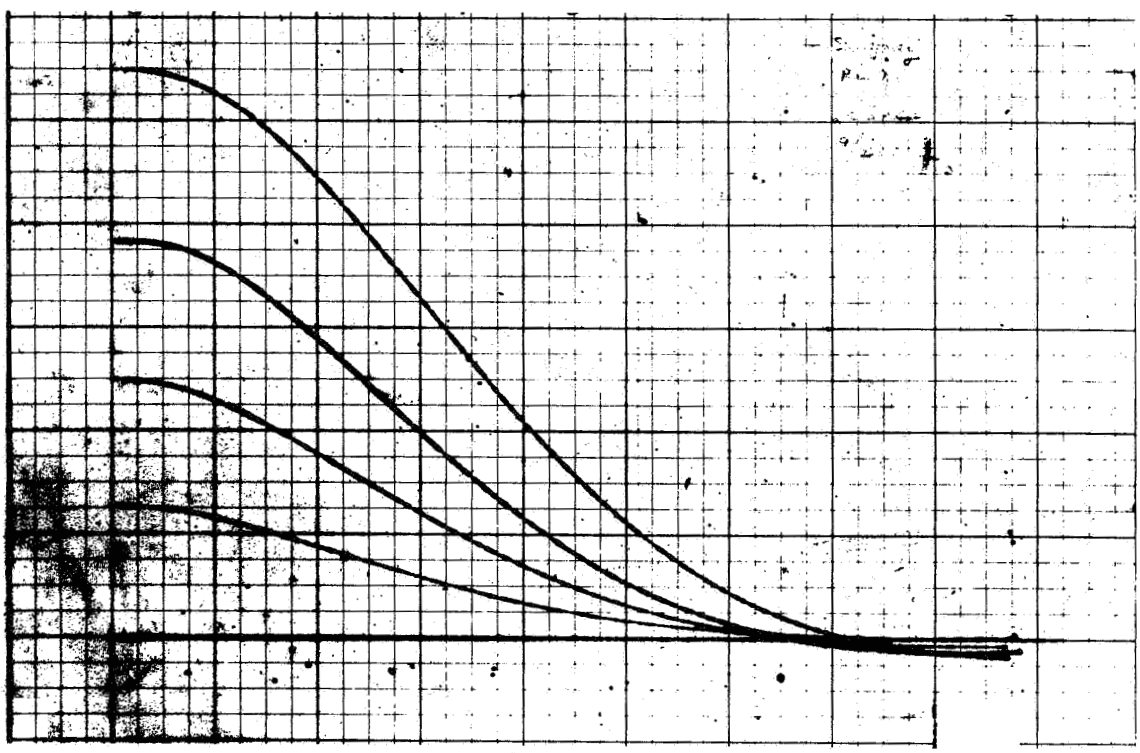

Run 4

Figure A-23. (Cont)

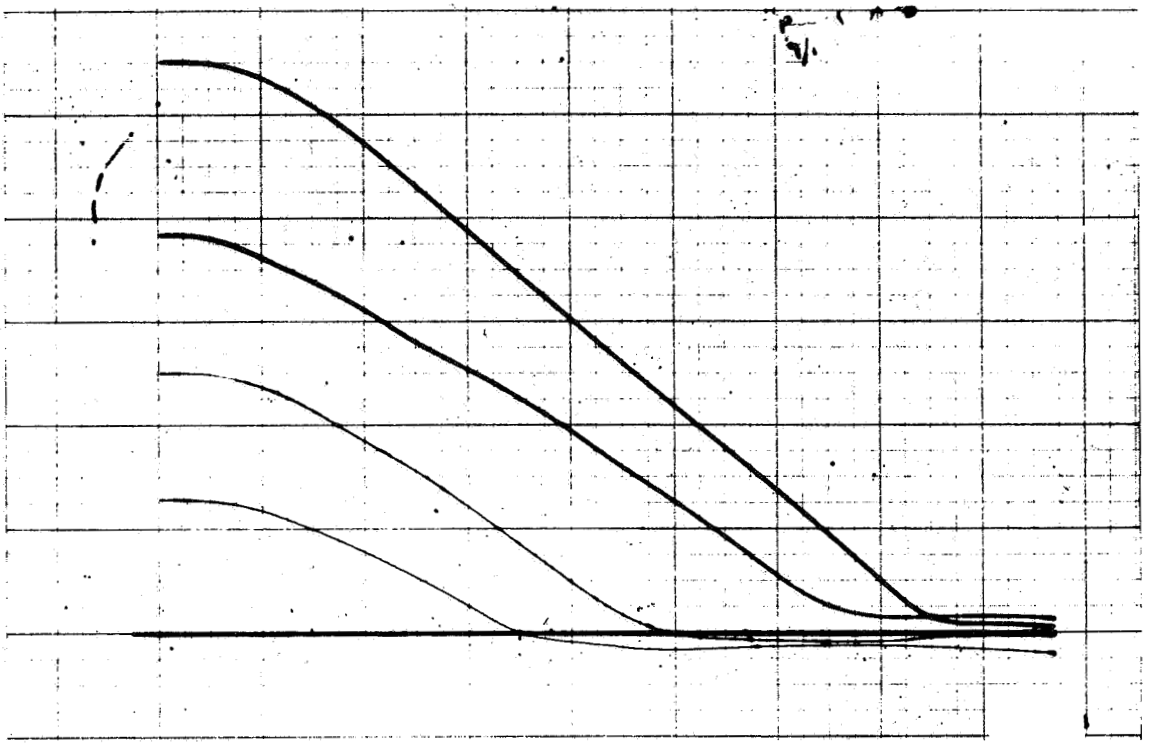

Run 1

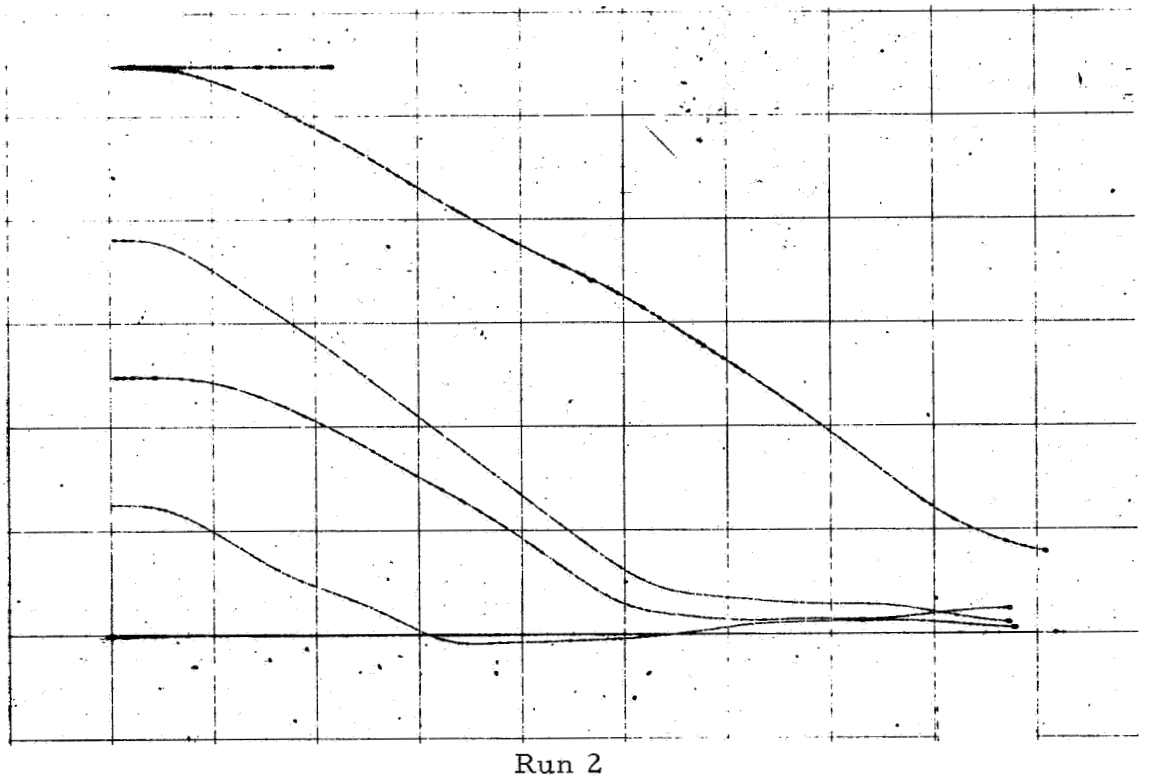

Run 2

Figure A-24. Subject 6 - Conventional

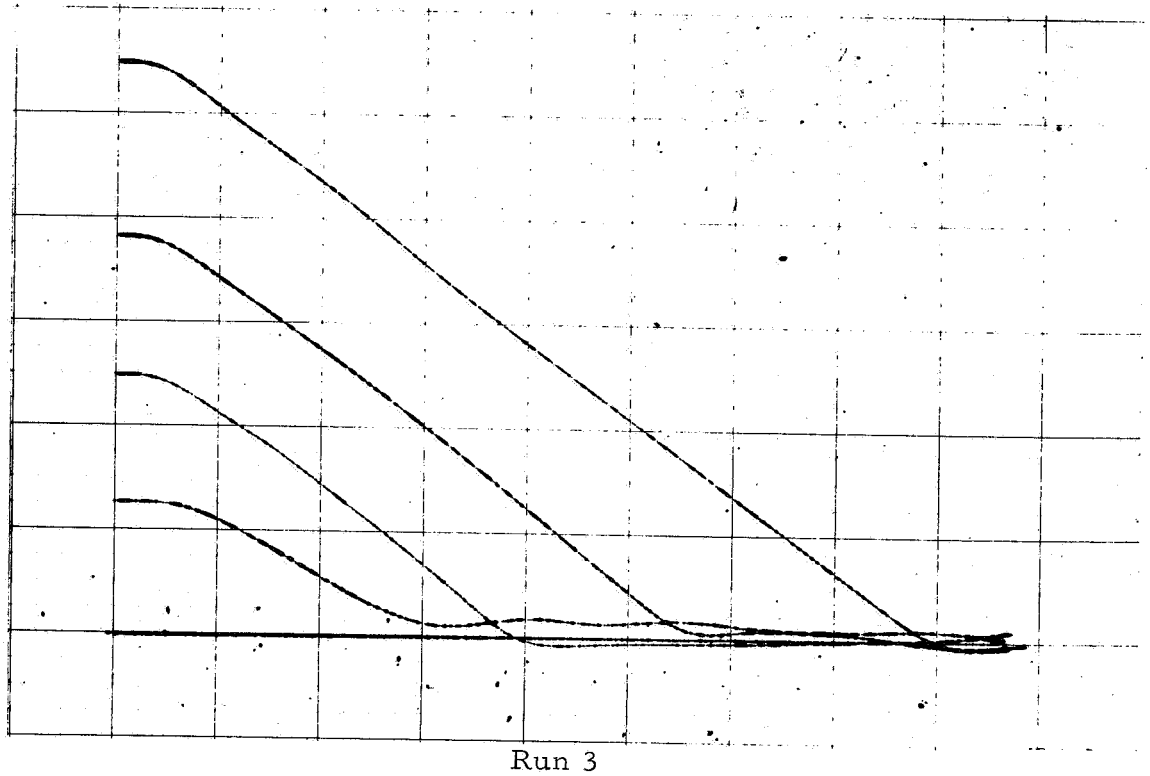

Run 3

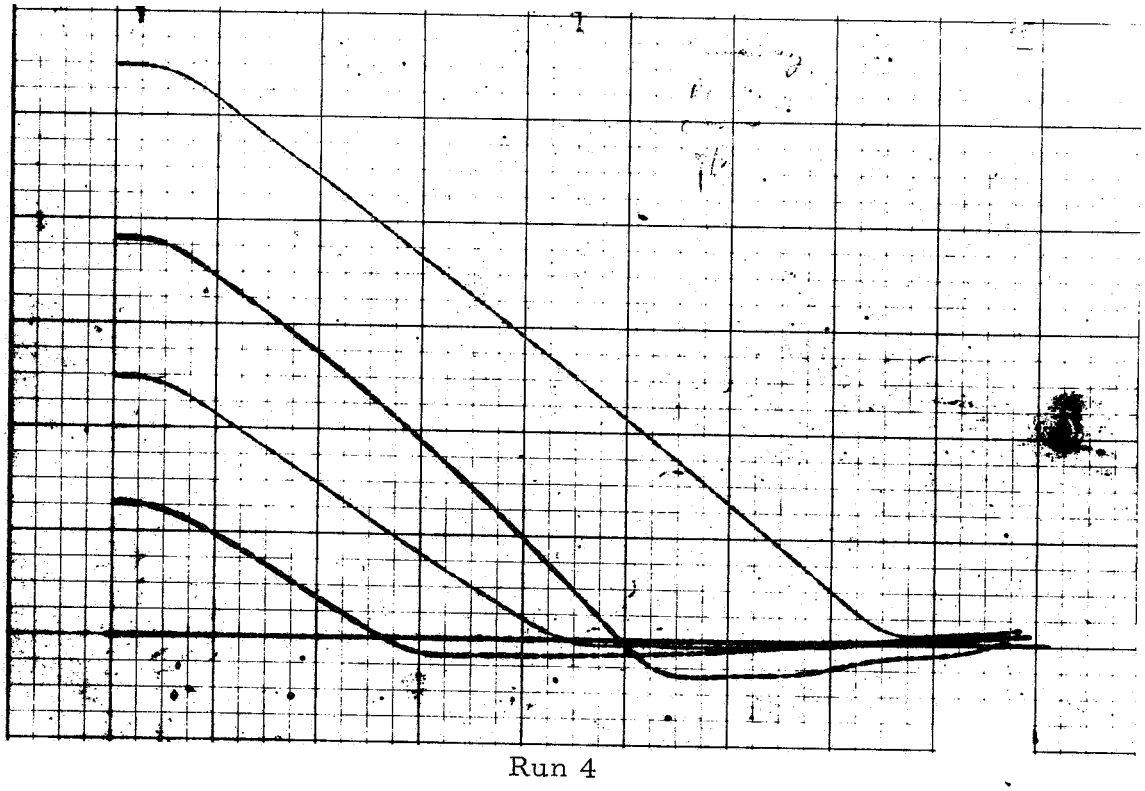

Run 4

Figure A-24. (Cont)